Amplitudes for Black Holes

Matteo Sergola

Doctor of Philosophy
The University of Edinburgh
2023

Lay Summary

In popular culture, black holes (BH) are often surrounded by an aura of intricacy and mystery. This is to some extent justified. Their beautiful mathematical and physical properties have stimulated a wealth of research and discoveries, with some questions still left unanswered. On the other hand, a potato can be a much more complicated object in terms of degrees of freedom: this is because black holes are also very constrained objects. If we study their classical behaviour in long-range scattering problems, then they turn out to be more similar to elementary point particles, meaning that we can describe them with a handful of parameters.

The recent experimental detection of gravitational waves (GW) has started a new era of astronomical observations, and a great source of the signal is released by black hole mergers. These incredibly powerful processes release an enormous amount of energy in the form of gravitational waves. However, we were only able to measure this type of radiation just over a few years ago for the first time: the GW signals that we observe on earth reach us with a minuscule amplitude. Nonetheless, interferometers are becoming more and more advanced, with a new generation of systems starting to operate over the next few years. As a consequence, state-of-the-art detections will call for an even better analytic characterisation and theoretical understanding of waveform templates.

It is in this scenario that this thesis fits in. Here, we will describe our small contribution to classical black hole scattering through the lenses of quantum mechanics. In fact, we will be able to compute classical gravity observables starting from quantum matrix elements, and by taking the limit $\hbar \to 0$ of gauge theory amplitudes. This will allow us to show how efficient and applicable particle perturbation theory is, and at the same time to unveil new structures and simplifications that occur in the classical limit of gravity amplitudes.

Abstract

In recent years the double copy has provided a bridge between scattering amplitudes and gravitational interactions, allowing physicists to perform computations once unthinkable. Its strength relies on borrowing perturbative (much easier) results from gauge theories, and extracting classical results from quantum amplitudes. Recently, the gravitational two-body problem, central for the blooming field of gravitational wave physics, is being scrutinized under the light of such duality. In this thesis we work towards understanding how the double copy can help us compute classical gravity observables through the so-called "KMOC formalism". This is a framework that has already received great interest from both the gravitational waves and the amplitude community, since it focuses directly on the computation of physical observables (for instance, without resorting to a Hamiltonian) allowing for a deeper understanding of underlying structures present in the classical limit of amplitudes.

Declaration

I declare that this thesis was composed by myself, that the work contained herein is my own except where explicitly stated otherwise in the text, and that this work has not been submitted for any other degree or professional qualification except as specified. The results of chapters 3, 4, 5 were produced in collaboration and appear in the following

Chapter 3

[1]: R. Monteiro, D. O'Connell, D. Peinador Veiga and M. Sergola, *Classical solutions and their double copy in split signature*, *JHEP* **05** (2021) 268, [`2012.11190`].

[2]: R. Monteiro, S. Nagy, D. O'Connell, D. Peinador Veiga and M. Sergola, *NS-NS Spacetimes from Amplitudes*, *JHEP* **06** (2022) 021, [`2112.08336`].

Chapter 4

[3]: A. Elkhidir, D. O'Connell, M. Sergola and I. A. Vazquez-Holm, *Radiation and Reaction at One Loop*, `2303.06211`.

Chapter 5

[4]: A. Cristofoli, R. Gonzo, N. Moynihan, D. O'Connell, A. Ross, M. Sergola and C. D. White, *The Uncertainty Principle and Classical Amplitudes*, `2112.07556`.

Further article

As a Ph.D. student, I have also been one of the authors of

[5]: G. Menezes and M. Sergola, *NLO deflections for spinning particles and Kerr black holes*, *JHEP* **10** (2022) 105, [2205.11701],

which is not directly presented in this thesis.

(Matteo Sergola, March 2023)

Acknowledgements

First, I would like to thank my supervisor Donal O'Connell. Donal is an inspiring scientist with great insight. Not only that, he is also an incredibly nice and down to earth guy: I never felt too stupid asking him silly questions. It is mostly thanks to him that I have become a better physicist, and if sometimes I speak with a slight Irish accent.

I would also like to thank all my collaborators: Asaad, Andrea, Ingrid, Riccardo, Ricardo, David, Silvia, Alasdair, Nathan, Chris, Gabriel, Justin, Stefano, John-Joseph, Ben, Andrés, Graham, Josh, Paolo, Lucile and Tim. I am probably forgetting someone but please don't be mad... I really enjoy doing physics with you all guys!

Then, I would like to thank all my office mates: Emmet, Conor, Alasdair (wow double thanks for you Alasdair!) and Jérémy. We really were the best office. Steal... ahem "borrowing" the sofa from the Higgs Centre was Jérémy's idea, not mine.

Also, I couldn't have done this without the support of my family (thank you for sending me proper Italian food) and friends, so many great thanks to you as well!

Finally, thanks to my true muse and inspiration: Briosa. Thank you for showing me how physics and art really are the same thing. You are the ultimate blend of pure maths, coffee and love.

I acknowledge the financial support under the Principal's Career Development Scholarship from the University of Edinburgh and the School of Physics and Astronomy.

Contents

Chapter 1

Foreword

In this thesis we will study classical aspects of black holes through the use of gauge theory amplitudes. At a superficial glance, these two topics may appear unrelated. Quantum field theory (QFT) describes weak, strong and electromagnetic (EM) interactions within the standard model, while gravity dictates the dynamics of the cosmos and spacetime itself. It would then seem that amplitudes are tools confined to the realm of collider physics, but this is not the case. In fact, recent years have seen an incredible surge of research concerning amplitudes applications to gravity [4, 6–33]. This remarkable body of work has been prompted by the recent revolutionary observations of gravitational waves (GW) [34–68], made by the LIGO-Virgo-KAGRA collaboration [69–73]. Scattering amplitudes can indeed be used to describe gravitating bodies in a variety of methods: they can be used to compute interaction potentials [6, 34, 35], deflected angles [5, 49, 50], EFT Lagrangians [36–39, 74, 75], bound state observables [8, 57–59, 76] and radiated waveforms [3, 33, 77–79]. New generations of gravitational wave observatories will work at higher signal-to-noise ratios, thus calling for more advanced analytic templates [80–83].

Luckily, at this point in time, particle physicists have developed a powerful arsenal of theoretical instruments that are usually applied to the calculation of challenging multiloop processes. Some of the most important tools are generalized unitarity, recursion relations, differential equations of Feynman integrals and integration by parts techniques [84–91]. All this technology can be efficiently re-applied to gravity. In fact, this poses an exciting new challenge to particle theorists: to compute cutting-edge gravity observables using amplitudes and QFT technology.

Indeed, some of these state of the state-of-the-art expressions have already been determined using scattering amplitudes [92].

However, there is another important reason for looking at classical GR, and black holes, through the lens of scattering amplitudes: the double copy. The double copy correspondence is a ground-breaking computational algorithm which allows us to compute graviton amplitudes from knowledge of gauge theory ones. This is done via a precise algorithm which instructs us to "square" YM amplitudes in order to generate gravity ones. This duality was first discovered in string theory as a tree-level relationship between open and closed string amplitudes in [93]. Recently, this correspondence was given new and more powerful light by Bern, Carrasco and Johansson [94] who deepened its scope and explored loop applications.

It is obvious then the double copy provides an entirely new way to look at gravitational processes, which is very different from the standard geometric way to study Einstein's equations. A crucial advantage of this duality resides in its extraordinary efficiency when compared to usual gravity perturbations. By looking at much simpler YM perturbation theory, theorists are able to push calculations to an accuracy level which was unthinkable before.

Even more, the double copy duality has been further extended beyond perturbative treatment to exact solutions of Einstein's field equations, first expored in [95]. This second formulation however, applies to solutions of general relativity which admit the so called "Kerr-Schild" (KS) decomposition, it is purely classical and holds to complete metric solutions. On the other hand, the BCJ double copy applies to quantum scattering amplitudes, which are computed perturbatively. This raises the question of whether the double copy is a fundamental property of nature or not. In fact, a definitive mathematical proof of the BCJ duality to all orders is still missing, and it is in general hard to make connection between the BCJ and the KS double copy. Nonetheless, a vast amount of high-loop calculations have been performed and support the conjecture with evidence.

Thus, we have a direct link between gravity and gauge theory at the level of scattering amplitudes. However, amplitudes are quantum mechanical in nature so a procedure for extracting the classical part has to be developed. In recent years, one framework that have received considerable attention is the so-called "KMOC" formalism, after Kosower, Maybee and O'Connell [49, 50]. Their idea is to use amplitudes in a region where the correspondence regime can be applied and quantum effects can be easily isolated. In this way one can compute classical observables as expectation values of hermitian operators taken between suitable semiclassical states. If certain reasonable classical conditions are met, one is able to extract the classical limit of an amplitude by reinstating $\hbar$ and performing an expansion around it.

In this way one is able to focus directly on the computation of physical, on-shell, quantities without the needing to resort to off-shell quantities (such as an interaction potential). In turn, this allows for a deeper understanding of underlying structures present in the classical limit of amplitudes and at the same time we can make use of all the existing amplitude tools.

An important advantage of the KMOC formalism is its applicability. Indeed, one can compute a great variety of observables such as: scattering angles, momentum deflections, spin precessions and memory effects. Furthermore, within this framework the core principles of unitary evolution and conservation laws are implemented naturally from the beginning. This implies that both conservative and non-conservative (i.e. radiative) effects can be computed [3, 4, 96].

In fact, the KMOC formalism was originally conceived with GW observables in mind. From this perspective, a gravitational perturbation produced by two scattering black holes is characterised by computing the expectation value of Riemann's tensor in a quantum sense and then taking its classical limit. The curvature tensor is often referred to as "waveform" in this case. The scalar components of this, in the long-range limit, are often called "Newman-Penrose" scalars [97, 98]. They are the quantities directly measured in interferometric observations and of interest to numerical relativists [99]. These analytical templates, computed in a KMOC way, turn out to be essentially Fourier transforms of scattering amplitudes. Furthermore, we will argue that classical waveforms are extremely interesting objects for yet another reason: they can be seen as expectation values of coherent states. This makes sense classically: coherent states saturate Heisenberg's uncertainty bound, re-summing infinitely many light/gravity modes into one classical state. However, from the amplitude side, we will see how coherence implies non-trivial structures and new recursions.

In this work we will thus investigate different aspects revolving around the fascinating topics of the gravitational two-body problem employing scattering amplitudes, the double copy and the KMOC formalism.

1.0.1 Summary

This thesis is structured as follows. In chapter 2 we introduce the necessary technical tools of on-shell classical observables, in preparation for the thesis main body. We begin with a discussion of waveforms and GR solutions in chapter 3, where we study these through a certain spacetime continuation called "split signature". Then, we extend our findings to waveforms with support in Minkowski spacetime, at one loop, in chapter 4. Here, to better interpret the physics, we divide waveform amplitude kernels into real and imaginary parts. Then, in chapter 5, we propose a general coherent and eikonal state structure in Minkowski, dictated by classical factorisation. This will allow us to discover an infinity of classical relations and factorisation properties between amplitudes. Finally, we conclude in chapter 6.

1.0.2 Miscellaneous conventions

Before moving onto a more technical overview, we find it useful to outline below few conventions.

Throughout the rest of this thesis we write covariant vectors as $x^\mu = (x^0, x^i) = (t, \mathbf{x})$ and work with mostly minus signature $(+1, -1, -1, -1)$, or $(+1, +1, -1, -1)$ in the split signature chapter. Fourier transforms are defined by

$$f(x) = \int \frac{\mathrm{d}^n q}{(2\pi)^n} e^{-iq\cdot x} \tilde{f}(q), \qquad \tilde{f}(q) = \int \mathrm{d}^n x \, e^{iq\cdot x} f(x), \tag{1.1}$$

and we will consistently hide powers of 2π via

$$\hat{\mathrm{d}}^n q \equiv \frac{\mathrm{d}^n q}{(2\pi)^n}, \qquad \hat{\delta}^{(n)}(q) \equiv (2\pi)^n \delta^{(n)}(q). \tag{1.2}$$

Furthermore, we find it convenient to define Lorentz invariant phase space delta functions and measures through

$$\delta_\Phi(p_1 - p_2) \equiv 2E_{p_1} \hat{\delta}^{(3)}(\mathbf{p}_1 - \mathbf{p}_2), \quad \mathrm{d}\Phi(p) \equiv \hat{\mathrm{d}}^4 p \, \hat{\delta}(p^2 - m^2) \Theta(p^0), \tag{1.3}$$

with $E_p = \sqrt{\mathbf{p}^2 + m^2}$. For the states we take

$$|p\rangle \equiv a^\dagger(p)|0\rangle, \qquad [a(p_1), a^\dagger(p_2)] = \delta_\Phi(p_1 - p_2), \tag{1.4}$$

we indicate tensor products as

$$|p_1, p_2 \cdots p_n\rangle \equiv |p_1\rangle \otimes |p_2\rangle \otimes \cdots |p_n\rangle, \tag{1.5}$$

and products of measures similarly

$$\mathrm{d}\Phi(p_1, p_2 \cdots p_n) \equiv \mathrm{d}\Phi(p_1)\mathrm{d}\Phi(p_2) \cdots \mathrm{d}\Phi(p_n). \tag{1.6}$$

We set $c = 1$ but keep $\hbar \neq 1$ unless otherwise stated. We also choose $\epsilon_{0123} = 1$. For a given tensor we (anti)symmetrize without normalising

$$u^{(\mu}v^{\nu)} \equiv u^\mu v^\nu + u^\nu v^\mu, \quad u^{[\mu}v^{\nu]} \equiv u^\mu v^\nu - u^\nu v^\mu, \tag{1.7}$$

and so on for higher ranks. Finally, this is our choice of phase for the sum over diagrams

$$i\mathcal{A}\text{mplitude } \hat{\delta}^{(4)}(p_{tot}) = \sum \text{Feynman diagrams.} \tag{1.8}$$

In gravity we take the coupling to be $\kappa = \sqrt{32\pi G}$. Another choice of convention we adopt is to take incoming momenta of initial states to be ingoing and final momenta to be outgoing. Thus

$$p^\mu_{tot} = \sum_{n\in\, in} p^\mu_n - \sum_{m\in\, out} p^\mu_m = 0. \tag{1.9}$$

Split signature spinor conventions are given their own section in the appendix A.1.

Chapter 2

Overview of preliminary topics

In this chapter we gather some of the necessary existing knowledge that will be needed for the research presented here. As we outlined, our original work builds upon few important elements: the KMOC formalism, the double copy, waveforms and coherent states. Let us discuss these starting from the KMOC framework.

2.1 KMOC: Observables from Amplitudes

The KMOC formalism [49] is a framework for extracting classical observables from quantum-mechanical amplitudes. The core intuition of the authors was to exploit the correspondence principle: any classical observable can be seen as some classical limit of a quantum expectation value. We will better explain what we mean by "classical limit" soon, but for now the reader can think of it as a $\hbar \to 0$ limit. Obviously, not every quantum matrix element is well behaved classically, so we will have to understand what exactly characterises $\hbar \to 0$.

To this end, we find it illuminating to present the KMOC framework through a textbook example: relativistic Rutherford scattering in classical electrodynamics. Let us then begin from the classical side of the story. Here, the two scattering particles are scalars with charges Q_1, Q_2 and masses m_1, m_2. Furthermore, we take the two bodies to be initially well separated by a space-like vector b^μ. After the particles have interacted, one finds that the bodies (without loss of generality we focus on particle one) will come out deflected by a certain amount. This deflection can be computed perturbatively[1] at each order in the coupling. For instance, one straightforward way to do this is to solve the Maxwell equations of motion

$$m_1 \frac{\mathrm{d}p_1^\mu}{\mathrm{d}\tau} = Q_1 F_{12}^{\mu\nu}(x) p_{1\nu} \tag{2.1}$$

iteratively. Above, the Lorentz force field strength $F_{12}^{\mu\nu}$ is sourced by particle "two" and causes the other one to deviate. In the end one finds that the four-momentum changes by the following amount, [49]

$$\Delta p_1^\mu = p_{1,\text{out}}^\mu - p_{1,\text{in}}^\mu = \frac{Q_1 Q_2}{2\pi} \frac{\gamma}{\sqrt{1-\gamma^2}} \frac{b^\mu}{-b^2} + \mathcal{O}((Q_1 Q_2)^2). \tag{2.2}$$

Above, $\gamma^{-1} = \sqrt{1-\beta^2}$ is the usual Lorentz factor, $\beta = |\mathbf{v}|$ is the relative velocity and $\Delta p_2^\mu = -\Delta p_1^\mu$ in the COM frame.

At this point our goal is to reproduce (2.2) using quantum amplitudes and the correspondence principle. First of all, it is somewhat intuitively clear that amplitudes (or some limit of them) could be used to solve the equations of motion. In fact, these entail quantum-mechanical evolution through the unitary S-matrix operator $S = 1 + iT$

$$i\mathcal{A}(p_1 \cdots p_m \to p_1' \cdots p_n') \hat{\delta}^{(4)}(p_1 + \cdots + p_m - p_1' - \cdots - p_n') = \langle p_1' \cdots p_n' | iT | p_1 \cdots p_m \rangle. \tag{2.3}$$

For Rutherford scattering specifically, we will have to focus on $2 \to 2$ scattering (as will be clear soon). This is actually a general property of conservative processes. Indeed, later we will see how radiative observables need $2 \to 3$ amplitudes: different phenomena may (in principle) require different multiplicities.

Subsequently, we have to choose a way to model classical point particles. We do so by employing a 2-particle tensor state. This reads in Fourier space

$$|\psi\rangle = \int \mathrm{d}\Phi(p_1, p_2) \phi_b(p_1, p_2) |p_1, p_2\rangle, \tag{2.4}$$

specifying the initial state of the system in the Heisenberg picture. Here, $|p_1, p_2\rangle$ are plane wave momentum eigenstates and ϕ_b is the wavefunction of the system. The latter deserves some scrutiny.

[1] Actually, if we neglect radiation, this problem can be solved analytically to all orders [100] but for the purposes of our narrative we want to think of it in terms of a perturbative expansion.

Given our goal to set up a scattering problem which well describes a classical one, it is clear that we have to make some appropriate assumptions on the wavepackets. We can begin by taking the two particles to be separated at past infinity by an impact parameter b^μ. We then write

$$\phi_b(p_1,p_2) = \phi_1(p_1)\phi_2(p_2)e^{\frac{ib\cdot p_1}{\hbar}} = \phi(p_1,p_2)e^{\frac{ib\cdot p_1}{\hbar}}, \qquad \int \mathrm{d}\Phi(p_i)|\phi_i(p_i)|^2 = 1, \quad (2.5)$$

where the second equation is a normalization condition. For what we are concerned with, the distance $b = \sqrt{-b^\mu b_\mu}$ is typically very large although this is not the only length at play. In fact, there are two more scales: the Compton length λ_c and the characteristic spread of the wavefunction l_w. In [49] it was argued that if the following set of "Goldilocks" inequalities are satisfied

$$\lambda_c \ll l_w \ll \sqrt{-b^2}, \quad (2.6)$$

then one expects that matrix elements taken on the state (2.4) will exhibit classical behavior. Let us interpret such conditions. The first inequality $\lambda_c \ll l_w$ tells us that the wavepacket widths are such that the point particle description is valid: $\phi_i(p_i)$ is a wavefunction peaked around the classical value of momenta $p^\mu \approx mu^\mu$, where u^μ is a four velocity. The second one $l_w \ll \sqrt{-b^2}$ guarantees that the wavefunctions are initially distant enough such that no overlap occurs (which is what we look for in long range scattering). Finally $\lambda_c \ll \sqrt{-b^2}$ is best interpreted in terms of the classical radius of the particle, which in electrodynamics and gravity are, respectively

$$r_s = \left(\frac{Q^2}{4\pi m}, \quad 2Gm\right). \quad (2.7)$$

Thus the final inequality determines that the following parameters are small

$$\frac{Q^2}{4\pi m b}, \quad \frac{2Gm}{b}, \quad (2.8)$$

which renders amplitudes good tools for computing observables in a series of powers of (2.8). This perturbation scheme is known as "Post-Minkowskian" (PM) approximation, and it is a weak field framework whose zeroth order corresponds to special relativity. We showed that the third goldilock inequality implies good behaviour (convergence) of the PM perturbation series. Although beyond the scope of this thesis, it would be certainly interesting to study what happens when we relax the other two inequalities while keeping this last one to hold.

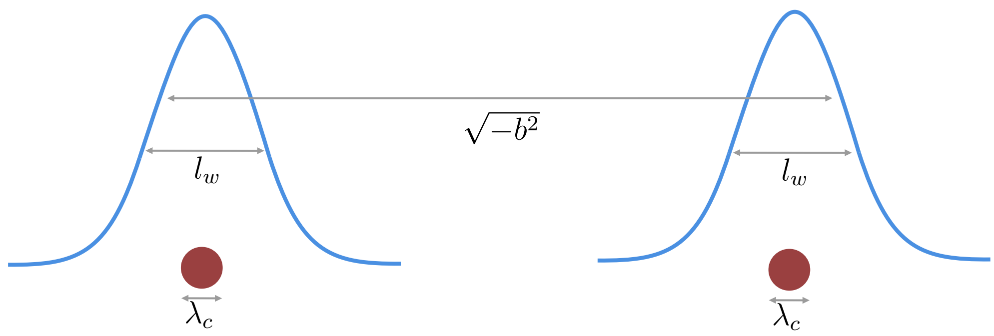

Figure 2.1 *A pictorial representation of the Goldilocks inequalities* (2.6).

It is important to stress that other computational frameworks are available in classical GR. For instance, another very powerful method is the "Post-Newtonian" (PN) expansion. There, the fields can be strong but velocities are small and one expands in powers of $v/c \sim GM/(rc^2) \ll 1$. However, this is not unrelated to the PM framework: each relativistic PM expression can always be re-expanded for small velocities and compared to its analogue PN one.

Let us go back to the momentum deflection observable. With these assumptions of classicality in mind, we can proceed to set up the observable Δp^μ as a matrix element. We can write this quantum mechanically as the difference between the time-evolved momentum operator of particle one (subtracted by its initial value) taken on the state (2.4)

$$\Delta p_1^\mu = \langle\psi|S^\dagger P_1^\mu S|\psi\rangle - \langle\psi|P_1^\mu|\psi\rangle. \tag{2.9}$$

Here the momentum operator of particle one is defined as usual through its action on momentum states

$$P_1^\mu|p_1, p_2\rangle = p_1^\mu|p_1, p_2\rangle. \tag{2.10}$$

Next we can be further rewrite (2.9) using $S = 1 + iT$, so

$$\Delta p_1^\mu = \langle\psi|[P_1^\mu, iT]|\psi\rangle + \langle\psi|T^\dagger P_1^\mu T|\psi\rangle \approx \langle\psi|[P_1^\mu, iT]|\psi\rangle. \tag{2.11}$$

Where for now we are working at first order in T (leading order in perturbation theory), although we will be back to $\mathcal{O}(T^\dagger T)$ corrections later. Now, plugging in the formulae for the initial states we obtain

$$\Delta p_1^\mu = \int \mathrm{d}\Phi(p_1, p_2, p_1', p_2')\phi(p_1, p_2)\phi^*(p_1', p_2')e^{ib\cdot(p_1-p_1')/\hbar}(p_1 - p_1')^\mu \\ \times \hat{\delta}^{(4)}(p_1 + p_2 - p_1' - p_2')\mathcal{A}(p_1, p_2 \to p_1', p_2'), \tag{2.12}$$

where we have expanded the modes of $\langle\psi|$ with primed variables and the modes of the ket with unprimed ones. To further simplify our expression we introduce a change of variables, and write primed variables in terms of a massless mode mismatch q_i:

$$p_i' = p_i + q_i. \tag{2.13}$$

Which in turns allows us to rewrite the two of the phase space measures as q_i integrals

$$\mathrm{d}\Phi(p_i + q_i) = \hat{\mathrm{d}}^4 q_i\, \hat{\delta}(2p_i \cdot q_i + q_1^2)\Theta(p_1^0 + q_i^0), \tag{2.14}$$

with the four-fold momentum conservation delta simply enforcing $q_1^\mu + q_2^\mu = 0$.

In order to proceed, we have to now re-introduce powers of $\hbar$. These can enter in two ways: in the couplings which must be rescaled by $g \to g/\sqrt{\hbar}$ and in massless momenta. These are to be interpreted classically in terms of wavelength vectors times $\hbar$: $q^\mu \to \hbar\bar{q}^\mu$. After doing so, we have to perform a Laurent series as $\hbar \to 0$. With this in mind, we can carry out few simplifications in (2.12)

$$\begin{aligned}\Delta p_1^\mu = \hbar^3 &\int \mathrm{d}\Phi(p_1, p_2)\phi(p_1, p_2)\phi^*(p_1 + \hbar\bar{q}_1, p_2 + \hbar\bar{q}_2) \\ &\times \int \hat{\mathrm{d}}^4\bar{q}_1\hat{\mathrm{d}}^4\bar{q}_2\hat{\delta}(2p_1 \cdot \bar{q}_1 + \hbar\bar{q}_1^2)\hat{\delta}(2p_2 \cdot \bar{q}_2 + \hbar\bar{q}_2^2)e^{-ib\cdot\bar{q}_1} \\ &\quad \times \bar{q}_1^\mu\mathcal{A}(p_1, p_2 \to p_1 + \hbar\bar{q}_1, p_2 + \hbar\bar{q}_2)\hat{\delta}^{(4)}(\bar{q}_1 + \bar{q}_2) \\ &\approx \hbar^3 \int \mathrm{d}\Phi(p_1, p_2)|\phi(p_1, p_2)|^2 \int \hat{\mathrm{d}}^4\bar{q}_1\hat{\mathrm{d}}^4\bar{q}_2\hat{\delta}(2p_1 \cdot \bar{q}_1)\hat{\delta}(2p_2 \cdot \bar{q}_2)e^{-ib\cdot\bar{q}_1} \\ &\quad \times \bar{q}_1^\mu\mathcal{A}(p_1, p_2 \to p_1 + \hbar\bar{q}_1, p_2 + \hbar\bar{q}_2)\hat{\delta}^{(4)}(\bar{q}_1 + \bar{q}_2),\end{aligned} \tag{2.15}$$

where in the second equality we have approximated $\phi(p_i + \hbar\bar{q}_i) \approx \phi(p_i)$ and dropped q-corrections inside on-shell measures

$$\hat{\delta}(2p_i \cdot \bar{q}_i + \hbar\bar{q}_i^2)\Theta(p_i^0 + \hbar\bar{q}_i^0) \approx \hat{\delta}(2p_i \cdot \bar{q}_i)\Theta(p_i^0). \tag{2.16}$$

In the future, it will be convenient to employ the following piece of notation

$$\left\langle\!\!\left\langle f(p_1,p_2) \right\rangle\!\!\right\rangle \equiv \int \mathrm{d}\Phi(p_1,p_2)|\phi(p_1,p_2)|^2 f(p_1,p_2), \tag{2.17}$$

which indicates an on-shell average over initial states.

Note that at this stage (2.15) is a very general expression which can be used to compute deflections of any theory, depending on what amplitude is inserted. Then let us specialise to quantum scalar electrodynamics, this is the theory needed to reproduce Rutherford scattering of spinless particles. In our case the four-point amplitude is obtained from the Feynman rules of scalar QED with Lagrangian

$$\mathcal{L} = -\frac{1}{4}F^{\mu\nu}F_{\mu\nu} + \sum_{i=1,2}\left(D_i^\mu \Phi_i^\dagger D_{i\mu}\Phi_i - m_i\Phi_i^\dagger\Phi_i\right), \quad D_i^\mu = \partial^\mu + iQ_iA^\mu, \tag{2.18}$$

which gives the tree level amplitude

$$i\mathcal{A}(p_1,p_2 \to p_1+\hbar\bar{q}_1, p_2+\hbar\bar{q}_2) = i\frac{Q_1Q_2}{\hbar}\frac{4p_1\cdot p_2 + \hbar^2\bar{q}_1^2}{\hbar^2\bar{q}_1^2}. \tag{2.19}$$

The expression above makes us already appreciate how amplitudes generally have a non-homogeneus dependence on $\hbar$. This means that care must be taken in Laurent expanding these expressions. We observe now that the leading piece in $\hbar$ above exactly cancels the prefactor in equation (2.15)! We get, integrating out the momentum conserving delta by setting $q_1^\mu = q^\mu = -q_2^\mu$

$$\Delta p_1^\mu = \left\langle\!\!\left\langle \int \hat{\mathrm{d}}^4\bar{q}\,\hat{\delta}(2p_1\cdot\bar{q})\hat{\delta}(2p_2\cdot\bar{q})e^{-ib\cdot\bar{q}} iQ_1Q_2\frac{4p_1\cdot p_2}{\bar{q}^2}\bar{q}^\mu \right\rangle\!\!\right\rangle. \tag{2.20}$$

At this point the wavefunction average can be carried out. As it is expected when the wavepackets are well peaked around their classical value, this average simply sets the values of massive momenta to be

$$p_i^\mu = m_i u_i^\mu, \tag{2.21}$$

where u_i is a timelike four velocity vector. We finally obtain

$$\Delta p_1^\mu = iQ_1Q_2\int \hat{\mathrm{d}}^4\bar{q}\,\hat{\delta}(u_1\cdot\bar{q})\hat{\delta}(u_2\cdot\bar{q})e^{-ib\cdot\bar{q}}\frac{u_1\cdot u_2}{\bar{q}^2}\bar{q}^\mu, \tag{2.22}$$

telling us that the deflection experienced by the particle is a Fourier transform (constrained to the plane of scattering by delta functions) in impact parameter space of the t-channel pole $1/q^2$. To this end, let us observe an important point which will be used profusely in later chapters: in (2.19) we have neglected the quantum contribution $\mathcal{A} \sim (q^2)^0$, which is also an analytic contact term. This is intuitive: we do not expect such contributions to enter long range interactions. Even more, had we kept this term we would have gotten, from performing the Fourier transform, a contribution which is local in position space $\sim \delta^2(\mathbf{b})$. However, the impact parameter is not zero by definition so this term integrate to zero from having no support.

Finally, to show the equivalence between (2.22) and (2.2) we need to perform the $\bar{q}$ integral, this is easily done in a frame where

$$u_1^\mu = \gamma(1,0,0,\beta), \quad u_2^\mu = (1,0,0,0), \tag{2.23}$$

one finds [49]

$$\Delta p_1^\mu = \frac{iQ_1Q_2}{\beta\gamma} \int \hat{\mathrm{d}}^2\bar{\mathbf{q}}\, e^{i\mathbf{b}\cdot\bar{\mathbf{q}}} \frac{\gamma}{-\bar{\mathbf{q}}^2}(0,\bar{q}_x,\bar{q}_y,0) = \frac{Q_1Q_2}{2\pi}\frac{\gamma}{\sqrt{\gamma^2-1}}\frac{\hat{\mathbf{b}}}{\mathbf{b}^2}, \tag{2.24}$$

which is indeed (2.2) (recall that $\beta\gamma = \sqrt{\gamma^2-1}$). We give below a graphical description of the scattering process

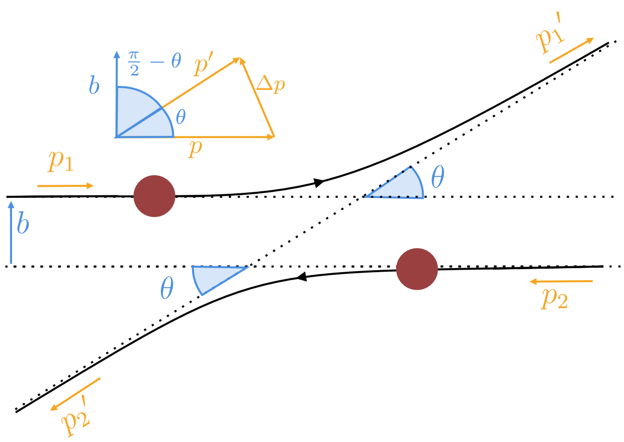

Figure 2.2 *Particle scattering in the center of mass.*

Note that the scattering angle is readily derived from the knowledge of Δp^μ from contracting with b. The geometry is such that one has

$$\sin\frac{\theta}{2} = \frac{|\Delta\mathbf{p}_1|}{2|\mathbf{p}_1|} = \frac{-\Delta p_1 \cdot \hat{b}}{2m_1\sqrt{\gamma^2-1}}. \tag{2.25}$$

We believe this derivation efficiently shows how amplitudes nicely pack classical data and how to extract it. Even though we illustrated how KMOC works through a specific example, it will soon be clear that the steps we took can be adapted to a great number of phenomena and to different theories. For instance, we will soon see how classical radiation can be computed in the next sections. The algorithm for computing observables will always be the same: we express an observable as an quantum expectation value on the states (2.4), and then we consider its classical limit reinstating powers of $\hbar$. Of course, different technical challenges may arise in each situations and will have to be tackled accordingly.

One obvious difficulty will be presented by loops, which arise at higher order computations. Indeed, perturbation theory in the sense of the PM expansion of (2.8) corresponds precisely to taking into account classical loops. Curiously, it is often believed that loops in QFT are always quantum but this is incorrect [101]. As we will see in the main body of this work, having massive propagators inside loops has the effect of generating classical non-linear contributions.

To this end, let us then investigate the structure of the next-to-leading (NLO) momentum deflection. In fact, above in (2.11) we neglected the $\mathcal{O}(T^\dagger T)$ cut term, but what happens if we keep this in? As such, at one loop both contributions to (2.11) will be needed: one is a linear in T and another one involves the product $T^\dagger T$. The linear one-loop term will simply be

$$\begin{aligned}\Delta p_1^\mu &\to I^\mu_{(1)}\\ &= \hbar^3 \left\langle\!\!\left\langle \int \hat{\mathrm{d}}^4\bar{q}\,\hat{\delta}(2p_1\cdot\bar{q})\hat{\delta}(2p_2\cdot\bar{q})e^{-ib\cdot\bar{q}}\bar{q}^\mu \mathcal{A}^{1Loop}(p_1,p_2\to p_1+\hbar\bar{q},p_2-\hbar\bar{q})\right\rangle\!\!\right\rangle,\end{aligned} \tag{2.26}$$

where $\mathcal{A}^{1Loop}$ is the classical one loop amplitude. However, now we have an additional contribution which happens to be a cut of a one-loop amplitude, or an integral of two tree-level amplitudes weighted by on-shell delta functions. This is treated in the same manner of the first term, except that we have to insert a complete set of states to resolve the cut. One arrives at

$$
\begin{aligned}
\Delta p_1^\mu \to I_{(2)}^\mu &= \langle\psi|T^\dagger P_1^\mu T|\psi\rangle = \sum_X \int \mathrm{d}\Phi(\tilde{p}_1,\tilde{p}_2)\langle\psi|T^\dagger P_1^\mu|\tilde{p}_1,\tilde{p}_2,X\rangle\langle\tilde{p}_1,\tilde{p}_2,X|T|\psi\rangle \\
&\approx -i\hbar^5 \left\langle\!\!\left\langle \int \hat{\mathrm{d}}^4\bar{q}\,\hat{\delta}(2p_1\cdot\bar{q})\hat{\delta}(2p_2\cdot\bar{q})e^{-ib\cdot\bar{q}} \int \hat{\mathrm{d}}^4\bar{\ell}\,\hat{\delta}(2p_1\cdot\bar{\ell})\hat{\delta}(2p_2\cdot\bar{\ell})\bar{\ell}^\mu \right.\right. \\
&\left.\left. \times\, \mathcal{A}^{tree}(p_1,p_2\to p_1+\hbar\bar{\ell},p_2-\hbar\bar{\ell})\mathcal{A}^{tree}(p_1+\hbar\bar{\ell},p_2-\hbar\bar{\ell}\to p_1+\hbar\bar{q},p_2-\hbar\bar{q}) \right\rangle\!\!\right\rangle,
\end{aligned}
\tag{2.27}
$$

having neglected the quantum corrections inside $\hat{\delta}(p_i\cdot\bar{\ell})$. These cuts come from the intermediate on-shell states, which we have expanded in a similar fashion to what was done in (2.13) as $\tilde{p}_i = p_i + \hbar\bar{\ell}$. We note that above, X is a set of states (both a discrete or continuum) that can in principle run inside the cut. At this order, the only term which survives in the completeness relation is the one which generates the product of tree amplitudes above. Meaning that we have really used

$$
1 \approx \int \mathrm{d}\Phi(\tilde{p}_1,\tilde{p}_2)|\tilde{p}_1,\tilde{p}_2\rangle\langle\tilde{p}_1,\tilde{p}_2|. \tag{2.28}
$$

Thus, we have learnt that at one loop Δp is composed of a “pure” one-loop amplitude part subtracted by a cut. This is indeed a very general structure of any higher order observable and it will be investigated, in two different ways, throughout chapter 4 and 5. In the latter, we will also interpret these cuts in terms of dissipative forces and momentum conservation. Furthermore, in chapter 5 we will derive the NLO deflection $I_{(1)}^\mu + I_{(2)}^\mu$ for classical Einstein gravity, and in chapter 4 for electrodynamics.

Let us comment on a few more things. As we explained loops introduce further difficulties, amongst the most obvious ones are the actual extraction of the one loop classical amplitude and its loop integration. Typically, these steps are tackled with modern QFT and amplitude technology: IBP identities, dimensional regularization, on-shell techniques, unitarity and double copy (if doing gravity). But there is another subtlety which comes up. In contrast to the tree level computation, at one loop one finds that the leading $\hbar$ behaviour of the observable is not classical, but is proportional to a singular term $\hbar^{-1}$ [5, 49]. Similarly, at two loops one encounters both $\hbar^{-2}$ and $\hbar^{-1}$ singularities, and so on at higher orders. These terms have to cancel in the physical observable and are usually referred to as “superclassical” terms. Currently, there is no formal proof that these singularities vanish at all orders, although it has been verified in each occasion. Efficient treatment of superclassical terms is in fact an important aspect, which we deal with in both chapters 4 and 5.

2.2 A Practical Double Copy Interlude

In this section we want to describe how gravity can be studied using amplitudes and the double copy. The double copy is a correspondence between gravity and gauge theory, proposed in [94, 102] but which first appeared in the stringy tree-level incarnation of [93]. This is a perturbative duality which relates "squares" of YM amplitudes to gravity ones. In its most common form, the BCJ double copy starts from considering an n-point L-loop YM amplitude $\mathcal{A}_{n,L}$ and writing it as a sum over cubic diagrams

$$i\mathcal{A}_{n,L} = i^{L+1} g^{n-2+2L} \sum_{i\in\Gamma} \int \prod_{j=1}^{L} \hat{\mathrm{d}}^4 \ell_j \frac{n_i c_i}{d_i}. \tag{2.29}$$

In this formula, the denominators d_i contain all relevant products of propagators at each order, and the n_i are (gauge dependent) kinematic factors associated with the i-th graph. These can be Lorentz invariant products of polarization tensors, loop and external momenta. Finally, c_i are colour factors dressing each vertex with products of Lie group structure constants. BCJ duality (or color-kinematics duality) conjectures that for each color Jacobi identity obeyed by c_i, there exists at least one set of kinematic numerators n_i that satisfies the same relation. For instance if $c_\alpha \pm c_\beta \pm c_\gamma = 0$, exploiting gauge redundancy, we can always find numerators such that $n_\alpha \pm n_\beta \pm n_\gamma = 0$. Needless to say, the BCJ choice of n_i numerators is not always manifest nor easy to find, but once implemented the double copy states that

$$i\mathcal{M}_{n,L} = -i^{L+1} \left(\frac{\kappa}{2}\right)^{n-2+2L} \sum_{i\in\Gamma} \int \prod_{j=1}^{L} \hat{\mathrm{d}}^4 \ell_j \frac{n_i \tilde{n}_i}{d_i}, \tag{2.30}$$

is an n-point L-loop gravity amplitude with $\kappa = \sqrt{32\pi G}$, and graviton field $h_{\mu\nu}$ defined by [2] $g_{\mu\nu} = \eta_{\mu\nu} + \kappa\, h_{\mu\nu}$. In the above expression $\tilde{n}_i$ may be a distinct set of YM-numerators satisfying colour-kinematics duality. The choice of n and $\tilde{n}$ determines the resulting gravity theory. For instance if

[2] One can choose different parametrizations, for instance one can decide to expand around flat space not $g_{\mu\nu}$ but $\sqrt{-g}g_{\mu\nu}$, in this thesis we stick with the first choice.

both numerators correspond to pure non-supersymmetric Yang-Mills (YM), the theory yielding amplitudes (2.30) is general relativity coupled to a 2-form field and a dilaton. These modes correspond to breaking the tensor product $A_\mu \otimes \tilde{A}_\nu = h_{(\mu\nu)} \oplus B_{[\mu\nu]} \oplus \phi$ into irreps. They are the modes one finds in the low energy limit of string theory. In fact as already hinted at, at tree level the double copy can be tracked down to the KLT relations between open and closed strings [103]. Note that if one is interested in pure Einstein gravity spurious modes have to be removed, this can be laborious but can be done in different ways [48, 104–106]. Even so, it is obvious that this remarkable duality brings a great deal of efficiency and simplifications, since gauge theories are typically much easier to deal with than gravity ones.

Let us see how the double copy works with another instructive example. We have just seen how Rutherford scattering is described by (a classical limit of) the scalar QED amplitude (2.19). Why not obtain Newton scattering in a similar fashion then? As we will see, this problem will be characterised by a four-point scalar amplitude, the difference is that the interaction between massive states will be mediated by a graviton. First, in light of the double copy, it is useful to rethink the QED amplitude in therms of tree level unitarity. This allows us to construct amplitudes from knowledge of their lower order sub-amplitudes. In this case there is only one channel (the t-channel) so we can write

$$i\mathcal{A}(p_1, p_2 \to p_1+q, p_2-q) = \frac{i}{q^2} \sum_\eta \mathcal{A}(p_1 \to p_1+q, q^\eta)\mathcal{A}^*(p_2 \to p_2-q, q^\eta). \quad (2.31)$$

We see that on the RHS we have a product of on-shell three level amplitudes with a photon emission

$$i\mathcal{A}(p_1 \to p_1 + q, q^\eta) = iQ_1(2p_1 + q) \cdot \varepsilon_\eta(q). \quad (2.32)$$

Is is obvious that (2.31) yields (2.19) after summing over intermediate physical states using the usual quantum-mechanical completeness relation

$$\sum_\eta \varepsilon^\mu_\eta \varepsilon^{*\nu}_\eta = -\left(\eta^{\mu\nu} - \frac{q^{(\mu}k^{\nu)}}{q \cdot k} + q^2 \frac{k^\mu k^\nu}{(k \cdot q)^2}\right). \quad (2.33)$$

Here however, we are entitled to drop any q or k-dependent terms since they vanish on the support of the integration.

In this tree level example, we can apply a double copy prescription in a very simple, KLT-like, manner without having to consider non-Abelian color coefficients. Putting aside couplings for now, the double copy dictates squaring the numerator while leaving the propagator fixed, effectively implying

$$p_i \cdot \varepsilon_\eta(\bar{q}) \to (p_i \cdot \varepsilon_\eta(\bar{q}))^2 = e_\eta^{\mu\nu} p_{i\mu} p_{i\nu}, \tag{2.34}$$

having already discarded the quantum, q dependent, contribution[3]. The RHS of the equation above is exactly the three-point scalar-graviton vertex, where gravity degrees of freedom are simply described by tensoring light polarization vectors

$$e_\eta^{\mu\nu}(\bar{q}) = \varepsilon_\eta^\mu(\bar{q}) \varepsilon_\eta^\mu(\bar{q}). \tag{2.35}$$

Observe that this is traceless and symmetric due to $\varepsilon_\eta^2 = 0$. The simple step (2.34), together with the replacement prescription for the coupling constants [94, 107]

$$Q \to \frac{\kappa}{2}, \qquad \kappa = \sqrt{32\pi G}, \tag{2.36}$$

allows us to immediately obtain

$$\begin{aligned} i\mathcal{M}(p_1, p_2 \to p_1 + \hbar\bar{q}, p_2 - \hbar\bar{q}) &= \left(\frac{\kappa}{2\sqrt{\hbar}}\right)^2 \frac{i}{\hbar^2 \bar{q}^2} \sum_\eta (p_1 \cdot \varepsilon_\eta(\bar{q}))^2 (p_2 \cdot \varepsilon_\eta^*(\bar{q}))^2 \\ &= \frac{\kappa^2}{4} \frac{i}{\hbar^3 \bar{q}^2} p_{1\mu} p_{1\nu} p_{2\rho} p_{2\sigma} \sum_\eta \varepsilon_\eta^\mu \varepsilon_\eta^{*\nu} \varepsilon_\eta^\rho \varepsilon_\eta^{*\sigma}, \end{aligned} \tag{2.37}$$

being the four point gravitational amplitude of two massive scalars exchanging a graviton.

[3] Also note that $\varepsilon^\mu(q) = \varepsilon^\mu(\bar{q})$, since polarizations only depend on the direction.

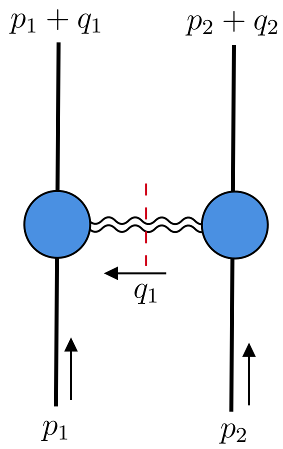

Figure 2.3 *Cut needed for the calculation of the gravitational deflection* Δp.

In the case under study, we can restrict to Einstein gravity explicitly. Any spurious dilaton term can be in fact projected out by summing over physical states only[4] (traceless and symmetric). Then, the helicity summation yields the well known expression of the completeness relation in gravity

$$\sum_{\eta} \varepsilon^{\mu}_{\eta} \varepsilon^{*\nu}_{\eta} \varepsilon^{\rho}_{\eta} \varepsilon^{*\sigma}_{\eta} = \frac{1}{2} \left(\eta^{\mu\rho} \eta^{\nu\sigma} + \eta^{\mu\sigma} \eta^{\nu\rho} - \eta^{\mu\nu} \eta^{\rho\sigma} \right) + (q - \text{terms}), \tag{2.38}$$

where we also note that, just like in gauge theory, any gauge dependent q-term above can be dropped: these will be plugged inside the expression (2.15) and contracted with at leas one p^{μ}, but $p_i \cdot \bar{q} = 0$. Thus, the classical piece reads

$$i\mathcal{M}(p_1, p_2 \to p_1 + \hbar\bar{q}, p_2 - \hbar\bar{q}) = \frac{\kappa^2}{8} \frac{i}{\hbar^3 \bar{q}^2} \left(2(p_1 \cdot p_2)^2 - p_1^2 p_2^2 \right), \tag{2.39}$$

which is all we need to obtain the momentum deflection by black holes scattering off each other. To this end, one proceeds exactly as in (2.20) and (2.21), integrating out the wavefunctions to set $p_i^{\mu} = m_i u_i^{\mu}$. The interpretation of the initial wavepacket (2.4) is different here: these now describe black holes in their point particle approximation. The $\mathcal{O}(G)$ momentum deflection formula finally

[4]Had we simply squared the numerator of (2.19) we would have obtained $\mathcal{M} \sim (p_1 \cdot p_2)^2/q^2$ which includes a spurious dilaton mode. This is subtracted by the last term in (2.38): $-\eta^{\mu\nu}\eta^{\rho\sigma}/2$.

reads

$$
\begin{aligned}
\Delta p_1^\mu &= \frac{i\kappa^2\, m_1 m_2}{8}\int \hat{\mathrm{d}}^4\bar{q}\,\hat{\delta}(u_1\cdot\bar{q})\hat{\delta}(u_2\cdot\bar{q})e^{-ib\cdot\bar{q}}\frac{\bar{q}^\mu}{\bar{q}^2}(2\gamma^2-1) \\
&= \frac{\kappa^2\, m_1 m_2}{8}\frac{b^\mu}{2\pi b^2}\frac{2\gamma^2-1}{\sqrt{\gamma^2-1}} = 2G\, m_1 m_2 \frac{b^\mu}{b^2}\frac{2\gamma^2-1}{\sqrt{\gamma^2-1}}.
\end{aligned}
\tag{2.40}
$$

It is worth commenting on our result. We managed to derive the (relativistically corrected) Newton momentum deflection starting from just electrodynamics! This was both fascinating and efficient. In fact, although in this specific tree-level example Feynman rules wouldn't have been too bad to deal with, at higher loops standard diagrammatic methods become soon inefficient. It is here that the double copy shows its incredible advantage over usual methods. It is however worth noting that at higher orders the extraction of pure Einstein gravity can still be trickier. In our example we were able to insert an explicit sum over physical states, but at higher loops things are more involved. Then, one can either insert a physical sum, but may encounter many diagrams, or construct BCJ numerators (as in (2.30)) but may have to subtract spurious states (axions and dilatons). Although these procedures can be laborious, at higher perturbative orders the double copy still remains the only way to go in most cases, having already provided us with many spectacular calculations [108]. This explains why modern amplitude methods are particularly well suited for GR calculations.

We would like to stress how this surprising squaring algorithm was not only useful, but also largely unexpected at the level of the Lagrangian. There is no hint of a spin-2 field in (2.18), nor of this striking correspondence. This is indeed a general feature of the double copy: its origin at the Lagrangian level is often quite mysterious. Nonetheless, partial results on its interpretation as a hidden "kinematic symmetry" of the equation of motions have been investigated [109, 110] and may soon clarify the physical origin of the duality. On the other hand this correspondence is usually manifest at the amplitude level. In fact, that the classical gravity amplitude $\mathcal{M}\sim(2\gamma^2-1)/q^2$ is some kinematic square of $\mathcal{A}\sim\gamma/q^2$ is very easy to see, at least in this simple case. If one expresses Lorentz factors using a rapidity variable ϕ we would find[5]

$$
\cosh\phi = \gamma, \qquad \cosh 2\phi = 2\gamma^2 - 1. \tag{2.41}
$$

So, the gravity amplitude is obtained by doubling the rapidity variable $\phi\to 2\phi$

[5] Not to be confused with any scalar field!

which is another instance of the double copy[6], first observed in [90, 107].

We will see in all the upcoming chapters how the double copy reverberates in different forms. For instance in chapter 3 we will study how the simple tree level amplitudes (2.34) source QED and GR waveforms in split-signature space times. This analytic continuation is needed because, strictly speaking, three-point tree-level amplitudes can only be on-shell in Minkowski if they are zero.[7] Instead in chapter 4 we will see how a double copy involving Compton amplitudes describes radiation reaction and gravitational self force.

However, before we move onto waveforms we would like to give a brief review of another kind of double copy: the Kerr-Schild (KS) double copy. In contrast to the BCJ/KLT duality, this double copy is non perturbative (in the sense that the duality is manifest at all orders in the chare or Newton's constant), and applies to purely classical solutions of GR and gauge theory which can be recasted in a KS form. This was first discovered by Monteiro, White and O'Connell in [95].

As a start, we begin by introducing Kerr-Schild coordinates, which are most often employed in the context of gravity [111]. There exists a special class of solutions of the *full* Einstein field equations (EFE) which admit the following choice of coordinates

$$g_{\mu\nu}(x) = \eta_{\mu\nu} + \phi(x) k_\mu(x) k_\nu(x), \tag{2.42}$$

such solutions are referred to as "KS" spacetimes. Above, ϕ and k_μ are a space-time dependent scalar and vector with the crucial properties

$$k^\mu k^\nu \eta_{\mu\nu} = 0 = k^\mu k^\nu g_{\mu\nu}, \quad \eta_{\alpha\beta} k^\alpha \partial^\beta k^\mu = 0. \tag{2.43}$$

This means that k_μ is null and geodesic with respect to the flat space metric, which is then used to contract indices. These simple but powerful properties imply that

$$g^{\mu\nu}(x) = \eta^{\mu\nu} - \phi(x) k^\mu(x) k^\nu(x), \quad \sqrt{-g(x)} = 1 \tag{2.44}$$

hold everywhere as exact statements. Another striking consequence of (2.43) is that KS coordinates linearise Einstein's field equations fully: the (mixed-index) Ricci tensor $R^\mu{}_\nu$ is linear in the metric $h_{\mu\nu}$. One immediate consequence of this is that (2.42) is a full solution of the EFE, even if its form is reminiscent of the

[6] The denominator $\sqrt{\gamma^2 - 1} = \sinh\phi$ in the final result is instead coming from a Jacobian factor in the q integral.

[7] Another way to get around this issue is to complexify momenta, which we have tacitly done in (2.31) and (2.37): our three-point subamblitudes would otherwise be trivial.

one of a perturbation. We can further observe that if we define a vector

$$A^\mu(x) = \phi(x)k^\mu(x), \tag{2.45}$$

then the vacuum EFE imply that A^μ satisfies the YM equations of motion [95]. Doing so allows us to construct a gauge theory for the gauge potential $\phi(x)k^\mu(x)$. For further developments on the KS double copy see [1, 2, 5, 42, 44, 48, 98, 105, 112–173].

In fact, these observations led the authors of [95] to introduce a classical correspondence relating solutions of the EFE to gauge theory ones, in a purely classical and nonperturbative fashion. Luckily, many important curved spacetimes admit a choice of KS coordinates and can indeed be related to YM accordingly. Among some of them we find Schwarzschild and Kerr-Newmann metrics, together with different shock-wave and gravitational-wave solutions.

Although this is a duality between gauge theory and gravity, it appears evidently different from the perturbative one of [94]. However, in chapter 3 we will show how, following [1], the BCJ and the KS double copy are actually the same thing! This result is another fascinating consequence of split-signature spacetimes, together with a suitable choice of boundary conditions.

2.3 Waveforms and Coherent States of Radiation

In this final part of the introduction we present an introduction to two other cardinal aspects of the thesis: waveforms and coherent states. As we will see, both these topics play an essential role in classical *radiative* observables, which are of particular interest to the field of gravitational waves. As before, we study them adopting the KMOC formalism. In this case, the observables which compute radiation are curvature fields [4, 33, 174]. We will then be interested in computing Maxwell's tensor (in electrodynamics) and the Riemann curvature (in gravity).

It is useful to understand electrodynamics first, so let us do that. Consider the second quantized field strength

$$\mathbb{F}^{\mu\nu}(x) = -i\sum_{\eta=\pm}\int \mathrm{d}\Phi(k)\hbar^{-\frac{3}{2}}\left(a_\eta(k)k^{[\mu}\varepsilon_\eta^{\nu]}e^{-i\frac{k\cdot x}{\hbar}} - a_\eta^\dagger(k)k^{[\mu}\varepsilon_\eta^{*\nu]}e^{i\frac{k\cdot x}{\hbar}}\right). \tag{2.46}$$

We want to measure its expectation value in the future assuming the past boundary condition

$$a_\eta(k)|\psi\rangle = 0, \tag{2.47}$$

i.e. no radiation was present in the far past. Evolving this field operator with the S-matrix we then obtain

$$F^{\mu\nu} \equiv \langle\psi|S^\dagger \mathbb{F}^{\mu\nu} S|\psi\rangle = 2\,\mathrm{Re}\, i\langle\psi|\mathbb{F}^{\mu\nu}T|\psi\rangle + \langle\psi|T^\dagger \mathbb{F}^{\mu\nu}T|\psi\rangle\,. \tag{2.48}$$

As before, let us work at leading order which allows us to approximate

$$F^{\mu\nu}(x) \simeq 2\,\mathrm{Re}\, i\langle\psi|\mathbb{F}^{\mu\nu}(x)T|\psi\rangle. \tag{2.49}$$

Substituting the initial semiclassical state (2.4), the expectation value becomes

$$\begin{aligned} F^{\mu\nu}(x) =& 2\hbar^{-\frac{3}{2}}\,\mathrm{Re}\sum_\eta \int \mathrm{d}\Phi(k)\,\langle\psi|a_\eta(k)T|\psi\rangle\, k^{[\mu}\varepsilon_\eta^{\nu]}\, e^{-i\frac{k\cdot x}{\hbar}} \\ =& 2\hbar^{-\frac{3}{2}}\,\mathrm{Re}\sum_\eta \int \mathrm{d}\Phi(p_1', p_2', p_1, p_2, k)\,\phi^*(p_1', p_2)\phi(p_1, p_2)\; e^{-ik\cdot x/\hbar} e^{i(p_1-p_1')\cdot b/\hbar} \\ & \times \langle p_1', p_2'|a_\eta(k)T|p_1, p_2\rangle\, k^{[\mu}\varepsilon_\eta^{\nu]}, \end{aligned} \tag{2.50}$$

where we see the appearance of a five-point amplitude with a massless external state, describing the emission of a photon

$$\langle p_1', p_2', k|iT|p_1, p_2\rangle = i\mathcal{A}(p_1, p_2 \to p_1', p_2', k^\eta)\hat{\delta}^{(4)}(p_1 + p_2 - p_1' - p_2' - k). \tag{2.51}$$

Next, we would like to simplify this expression for the field strength in the classical approximation. We can do this using the same change of variables (2.15)

$$p_i' = p_i + q_i = p_i + \hbar\bar{q}_i. \tag{2.52}$$

We note again that the classical approximation is valid when the scales in our problem satisfy $x \gg l_w \gg \lambda_c$. This means that when working in Fourier space, we require that $k \ll 1/l_w \ll m$ (where k is a massless momentum, sometimes referred to as "messenger"). It is only when these inequalities are satisfied that our classical expressions are valid. Thus, we assume that the integrals appearing in the equation above are defined (e.g. with cutoffs) so that these inequalities are satisfied. For instance, taking advantage of such an approximation, we can ignore the shift k in the wave function $\phi(p+q) \simeq \phi(p)$, because this shift is small on the scale $1/l_w$ of the wave function.

At this point, it is also useful to introduce a wavenumber $\bar{k}$ associated with the momentum k by $k = \hbar\bar{k}$. Making use of (2.14) we then have

$$\begin{aligned} F^{\mu\nu}(x) =& 2\hbar^{7/2}\,\mathrm{Re}\sum_\eta \left\langle\!\!\left\langle \int \mathrm{d}\Phi(\bar{k}) e^{-i\bar{k}\cdot x} \int \hat{\mathrm{d}}^4\bar{q}_1 \hat{\mathrm{d}}^4\bar{q}_2 \hat{\delta}(2p_1\cdot q_1)\hat{\delta}(2p_2\cdot q_2) e^{-ib\cdot\bar{q}_1} \right.\right. \\ & \left.\left. \times\, \mathcal{A}(p_1, p_2 \to p_1 + \hbar\bar{q}_1, p_2 + \hbar\bar{q}_2, \bar{k}^\eta)\, \bar{k}^{[\mu}\varepsilon_\eta^{\nu]}\hat{\delta}^{(4)}(\bar{q}_1 + \bar{q}_2 + \bar{k}) \right\rangle\!\!\right\rangle. \end{aligned} \tag{2.53}$$

This important expression will be useful below and throughout the rest of the thesis. Let us consider gravity now.

The derivation of the analogous gravity expression for the Riemann tensor follows in exactly the same manner. This just involves more spacetime indices

$$\begin{aligned} R^{\mu\nu\rho\sigma}(x) =& 2\hbar^{7/2}\,\mathrm{Re}\,\frac{i\kappa}{2}\sum_\eta \left\langle\!\!\left\langle \int \mathrm{d}\Phi(\bar{k}) e^{-i\bar{k}\cdot x} \int \hat{\mathrm{d}}^4\bar{q}_1 \hat{\mathrm{d}}^4\bar{q}_2 \hat{\delta}(2p_1\cdot q_1)\hat{\delta}(2p_2\cdot q_2) e^{-ib\cdot\bar{q}_1} \right.\right. \\ & \left.\left. \times\, \mathcal{M}(p_1, p_2 \to p_1 + \hbar\bar{q}_1, p_2 + \hbar\bar{q}_2, \bar{k}^\eta)\, \bar{k}^{[\mu}\varepsilon_\eta^{\nu]}\bar{k}^{[\rho}\varepsilon_\eta^{\sigma]}\hat{\delta}^{(4)}(\bar{q}_1 + \bar{q}_2 + \bar{k}) \right\rangle\!\!\right\rangle. \end{aligned} \tag{2.54}$$

This expression is again obtained by second-quantizing the graviton potential $\mathbb{h}_{\mu\nu}$ and by taking its derivatives via

$$g_{\mu\nu}(x) = \eta_{\mu\nu} + h_{\mu\nu}(x), \quad R^{\mu\nu\rho\sigma} = \frac{\kappa}{2}(\partial^\sigma\partial^{[\mu}h^{\nu]\rho} - \partial^\rho\partial^{[\mu}h^{\nu]\sigma}). \tag{2.55}$$

To be precise, gravitational radiation should be characterised by the components of the Weyl tensor; this is a version of the Riemann one with traces removed. However, these two are equal in empty space [175] so we won't make a distinction. In fact, one can immediately verify that all the traces vanish in (2.54). Furthermore, we observe that for all our purposes we can drop any non linear curvature elements, since the typical distances we are interested in are astronomical. As a consequence, any $R_{\mu\nu\rho\sigma} \sim \Gamma_{\mu\nu\lambda}\Gamma^\lambda{}_{\rho\sigma} \sim 1/r^2$ will always be suppressed.

A few comments on formulae (2.53) and (2.54) are in order. First of all, their double copy structure is evident: the gravity curvature field is a tensored square of the electrodynamic one [98]. Roughly, the field integral kernels are related by

$$\mathcal{A}\ k^{[\mu}\varepsilon^{\nu]} \to (\mathcal{A}\ k^{[\mu}\varepsilon^{\nu]})^{\otimes 2} \sim (\mathcal{A})^2\ k^{[\mu}\varepsilon^{\nu]}k^{[\rho}\varepsilon^{\sigma]} \sim \mathcal{M}\ k^{[\mu}\varepsilon^{\nu]}k^{[\rho}\varepsilon^{\sigma]}. \tag{2.56}$$

Secondly, we see that the leading order amplitude governing the emission of radiation is a five point amplitude. We will see explicit expressions for these amplitudes in the chapter 4 at one loop, while the tree-level one were examined in [33, 48].

Even so, one might still wonder to what extent the five-point $\mathcal{A}_5$ is the most "fundamental" building block which describes radiation. We believe this is not the case. As such, in (2.34) we already showed how the elementary building block of the four-point amplitude really was the three-point vertex between two massive particles and a massless messenger $(p \cdot \varepsilon)^n$, $n = 1, 2$. However, there is one extra difficulty which prevents us now from pursuing the same logic here. In our previous Δp^μ examples, the emitted boson $\varepsilon^\mu(q)$ was only necessary to build the four-point amplitude. There, this is eventually "integrated" out in the sum over states. For this reason, in that case we could think of the three-point tree-level amplitudes as analytically continued to complex momenta: they could be taken on-shell without vanishing, yet no external state was complex in the final expression. Indeed, for the three legs of the $p \cdot \varepsilon$ vertex to be *all* on shell we have to require

$$p \cdot k = 0 \ \text{ and } \ \ k^2 = 0. \tag{2.57}$$

For *real* kinematics this implies that $k^0 = 0$ and $|\mathbf{k}| = 0$, leaving no space for invariants in Minkowski spacetime. For this reason, if we considered a *single* initial massive particle

$$|\psi\rangle = \int \mathrm{d}\Phi(p)\phi(p)|p\rangle \tag{2.58}$$

sourcing a curvature field, we would find[8] the curvature to be linear in the on-shell vertex $p \cdot \varepsilon$. This quantity would be either zero on-shell, *or* would describe complex physical radiation. We will see how this can be avoided by working in a different signature of spacetime in chapter 3. There, we will consider a metric of signature $\eta^{\mu\nu} = \mathrm{diag}(+1, +1, -1, -1)$, which we call *split* signature. Doing so will allow us to have both on-shell three-point kinematics *and* real variables. Importantly, the latter condition guarantees well defined reality conditions of the radiative observables $F^{\mu\nu}$, $R^{\mu\nu\rho\sigma}$. Again, this is not at all guaranteed if we

[8]As we will see this is because in this case $\langle\psi|S^\dagger \mathbb{F}^{\mu\nu} S|\psi\rangle \sim \langle p'|aT|p\rangle$ is a three-point amplitude.

complexify momenta, thus obscuring the physical picture of the problem.

Let us now move to a final key ingredient to the characterisation of classical waveforms: coherence [4, 33]. Let us consider EM in this introduction. We want to compare the field operator $\mathbb{F}^{\mu\nu}(x)$ (2.46) to the textbook expression for the classical Maxwell field strength. The latter reads

$$F_{cl}^{\mu\nu}(x) = -i \sum_{\eta=\pm} \int \mathrm{d}\Phi(\bar{k}) \left(\alpha_\eta(\bar{k}) \bar{k}^{[\mu} \varepsilon_\eta^{\nu]} e^{-i\bar{k}\cdot x} - \alpha_\eta^\dagger(\bar{k}) \bar{k}^{[\mu} \varepsilon_\eta^{*\nu]} e^{i\bar{k}\cdot x} \right) , \tag{2.59}$$

where the $\alpha_\eta(\bar{k})$ are here simple Fourier modes. What is a straightforward way to get $F_{cl}^{\mu\nu}$ from its operator cousin? The coherent state defined by

$$|\alpha\rangle \equiv \mathcal{N}_\alpha^{-1} \exp\left[\sum_\eta \int \mathrm{d}\Phi(\bar{k}) \alpha_\eta(\bar{k}) a_\eta^\dagger(\bar{k}) \right] |0\rangle, \tag{2.60}$$

is the answer. Here, $\mathcal{N}_\alpha$ is a normalization easily computed to be

$$\mathcal{N}_\alpha = \exp\left[\frac{1}{2} \sum_\eta \int \mathrm{d}\Phi(\bar{k}) |\alpha_\eta(\bar{k})|^2 \right] . \tag{2.61}$$

The state (2.60) is such that the following important operator identities are obeyed

$$a_\eta(\bar{k})|\alpha\rangle = \alpha_\eta(\bar{k})|\alpha\rangle, \qquad \langle\alpha|a_\eta^\dagger(\bar{k}) = \langle\alpha|\alpha_\eta^*(\bar{k}). \tag{2.62}$$

A simple way to remember these is to think of the action $a_\eta|\alpha\rangle$ as a functional derivative with respect to the creation operator, and vice-versa. Thanks to these relations we can elucidate the physical significance of (2.60), which is made clear by sandwiching $\mathbb{F}^{\mu\nu}$ on these states. In fact, a simple application of (2.62) and of the Baker-Campbell-Hausdorff identity yields the remarkable relations

$$\langle\alpha|\mathbb{F}^{\mu\nu}(x)|\alpha\rangle = F_{cl}^{\mu\nu}(x) + \mathcal{O}(\hbar), \tag{2.63}$$

together with

$$\langle\alpha|\mathbb{F}^{\mu\nu}(x)\mathbb{F}^{\rho\sigma}(y)|\alpha\rangle = F_{cl}^{\mu\nu}(x) F_{cl}^{\rho\sigma}(y) + \mathcal{O}(\hbar). \tag{2.64}$$

This means that coherent states are the massless equivalents of the semiclassical KMOC states (2.4)! Here, the function representing the Fourier transform of the beam of light $\alpha_\eta(\bar{k})$ plays the role of the wavefunction $\phi_i(p_i)$. Thus we have learnt that by summing over an infinite amount of exponentiated light modes (each weighted by $\alpha(\bar{k})$) we are able to reproduce classical electromagnetic light. This is the main property of coherent states, first unveiled by Glauber in his seminal work [176]. Moreover, in the classical limit, coherence further assures us that products c-numbers commute (see (2.64)), as they should.

In [33] coherent states were first[9] used within the KMOC formalism to describe massless initial states; and it was shown how one is able to rightly reproduce with them classical light scattering, such as Thomson scattering. In this thesis we will push this idea even further: we will employ coherent states to describe scattered radiation of the outgoing state. We will first see this in a split signature scenario and then in Minkowski space in chapter 5. This will allow us to interpret the waveforms (2.53) and (2.54) (and the one-loop ones of chapter 4) as an expectation value of a coherent state whose parameter function is a five (or three) point amplitude

$$\alpha_\eta(\bar{k}) \sim \mathcal{A}(p_1, p_2 \to p_1 + \hbar\bar{q}_1, p_2 + \hbar\bar{q}_2, \bar{k}^\eta). \tag{2.65}$$

Eventually, this will lead to investigate whether the action of the classical S-matrix fully re-sums itself into a coherent state exponential. To this end, we will often refer to the coherent state parameter $\alpha_\eta(k)$ as "waveshape", especially in chapters 4 and 5. We will also show in chapter 5 how conservative effects also exponentiate into an eikonal phase, this will be instead characterised by a four-point amplitude.

Another fascinating aspect we will investigate is what the exponential structure can tell us about classical amplitudes and the hierarchies among themselves. Interestingly, we will find that once we assume coherence, the classical factorization property (2.64) will yield an infinity of nontrivial factorization relations for classical amplitudes. For instance, at one loop, having a coherent state predicts that the five-point one-loop amplitude factorizes into a product of a five-point and a four-point tree. We will be able to explicitly verify this in two instances, in both chapters 4 and 5.

Finally let us quickly comment on the gravitational coherent state. This will be defined analogously and (2.63), (2.64) will hold after changing: $\mathbb{F}^{\mu\nu} \to \mathbb{R}^{\mu\nu\rho\sigma}$ and $F^{\mu\nu}_{cl} \to R^{\mu\nu\rho\sigma}_{cl}$. In gravity we will see that the coherent state parameter will be specified by the gravitational five-point amplitude

$$\alpha_\eta(\bar{k}) \sim \mathcal{M}(p_1, p_2 \to p_1 + \hbar\bar{q}_1, p_2 + \hbar\bar{q}_2, \bar{k}^\eta), \tag{2.66}$$

[9] Here we are interested in coherent states of radiation, but these can also be employed to describe classical color particles [20] and classical high-spin states [51].

with an on-shell graviton state. The classical limit of this tree-level amplitude was first computed in [48], so we will investigate its structure at NLO in chapter 4.

Chapter 3

Split Signature Solutions and the Double Copy

3.1 Introduction

Three-point scattering amplitudes are the building blocks in our modern approach to computing interactions between particles in quantum field theory. Using BCFW [91] and generalised unitarity [88, 89], it is possible to construct the complete S-matrix for Yang-Mills theory and (up to ultraviolet divergences) for general relativity from their respective three-point amplitudes. These amplitudes are gauge invariant and beautifully simple objects, completely specified by the helicities of the massless gluons and gravitons [177]. This basic simplicity carries over to the case of massive particles, for any spin [178]. But in spite of all these virtues, three-point amplitudes have a peculiarity: they do not exist in Minkowski space. As for any n-point amplitude, the external particles involved in a three-point amplitude must all be on shell. But there is no solution to the on-shell conditions in Minkowski space for three particles with different momenta (which are not complex).

It should be evident by now that the tools of quantum field theory have deep implications for classical physics. Certain amplitudes are closely connected with specific classical concepts: for example, the four-point amplitude between massive particles in gravity is closely related to the classical potential [179, 180]. But the three-point amplitude has so far received no classical interpretation, because it is not present in Minkowski space.

Of course, the fact that the three-point amplitude vanishes in Minkowski space is no obstacle for the programme of determining more complicated amplitudes. BCFW taught us a simple trick: we analytically continue the momenta so that the on-shell conditions *do* have a solution. We can take the momenta to be complex-valued, or else continue to a spacetime with metric signature $(+,+,-,-)$.[1] This second option has some conceptual virtues: we can choose real momenta and polarisation vectors; the spinor variables we frequently use exist and are real; the chirality properties in a four-dimensional manifold with this split signature mean that the two types of spinors are independent.

Another virtue of a real spacetime with signature $(+,+,-,-)$ is that real classical equations exist in this spacetime and their solutions can be studied. In this chapter, we find a classical interpretation for the three-point amplitude in a split-signature spacetime: it computes the Newman-Penrose scalars [97] (a spinorial version of the curvature of the field) for the classical solution that is generated by the massive particle in the amplitude. For example, the three-point amplitude between a massive scalar and a gauge boson computes the electromagnetic field strength of a static point charge in split signature. In gravity, the three-point amplitude between a massive scalar and a graviton computes the Weyl spinor of the split-signature analogue of the Schwarzschild solution. Solutions in split signature which are determined by three-point amplitudes are, from the perspective of scattering amplitudes, the simplest non-trivial classical solutions.

The Newman-Penrose (NP) formalism can be illuminated by taking a spinorial approach to field theory. The Lorentz group in split signature is locally isomorphic to $\mathrm{SL}(2,\mathbb{R}) \times \mathrm{SL}(2,\mathbb{R})$, and the spinorial representations of $\mathrm{SO}(2,2)$ are the (real) two-dimensional fundamental representations of each $\mathrm{SL}(2,\mathbb{R})$ factor. In electrodynamics, for example, we can pass from the tensorial field strength $F_{\mu\nu}(x)$ to a spinorial equivalent known as the Maxwell spinor $\phi_{\alpha\beta}(x)$. This is obtained by contracting the Lorentz indices of $F_{\mu\nu}(x)$ with matrices $\sigma^{\mu\nu}{}_{\alpha\beta}$ which are proportional to the Lorentz generators in the spinor representation (that is, the $\sigma^{\mu\nu}{}_{\alpha\beta}$ generate one of the $\mathrm{SL}(2,\mathbb{R})$ subgroups of the Lorentz group). We have

$$\phi_{\alpha\beta}(x) = \sigma^{\mu\nu}{}_{\alpha\beta} F_{\mu\nu}(x)\,. \tag{3.1}$$

In split signature, the Maxwell spinor is a real quantity, symmetric in its

[1] In our conventions, the $(+)$-directions are timelike and the $(-)$-directions are spacelike.

spinor indices. There is a second Maxwell spinor associated with the spinor representation of the other chirality:

$$\tilde{\phi}_{\dot{\alpha}\dot{\beta}}(x) = \tilde{\sigma}^{\mu\nu}{}_{\dot{\alpha}\dot{\beta}} F_{\mu\nu}(x)\,, \tag{3.2}$$

where $\tilde{\sigma}^{\mu\nu}{}_{\dot{\alpha}\dot{\beta}}$ are again proportional to the Lorentz generators, but now of the other "antichiral" $\mathrm{SL}(2,\mathbb{R})$ subgroup.

To obtain Newman-Penrose scalars, we expand the Maxwell spinor (and its antichiral friend) on a basis of spinors. Let us consider the Maxwell spinor due to some localised source, such as a point-like charge. Solving the field equations with a retarded boundary condition, we can introduce spinors at any spacetime point by taking the light-cone direction k from the charge to the point. Using the notation of spinor-helicity, the vector k is also the bispinor $|k\rangle[k|$. To complete the basis of (chiral) spinors, we choose another spinor $|n\rangle$. Now we may write out the Maxwell spinor in this basis:[2]

$$\phi_{\alpha\beta}(x) = \phi_0(x)|n\rangle_\alpha|n\rangle_\beta - \,\phi_1(x)|k\rangle_{(\alpha}|n\rangle_{\beta)} + \phi_2(x)|k\rangle_\alpha|k\rangle_\beta\,. \tag{3.3}$$

The three scalar fields $\phi_i(x)$ are Newman-Penrose scalars. There are three more NP scalars in the antichiral field strength: these are the six different components of the field strength. In split signature, all the quantities in (3.3) are real, and the chiral quantities are independent from the antichiral ones.

In gravity, the story is very similar. We pass from the Weyl curvature $W_{\mu\nu\rho\sigma}(x)$ (via a frame) to a Weyl spinor $\Psi_{\alpha\beta\gamma\delta}(x)$, which is real and completely symmetric in its four spinor indices. Expanding the Weyl spinor on our basis of spinors, we encounter five real NP scalars, namely

$$\begin{aligned}\Psi_{\alpha\beta\gamma\delta}(x) = \Psi_0(x)|n\rangle_\alpha|n\rangle_\beta|n\rangle_\gamma|n\rangle_\delta - \frac{1}{6}\,\Psi_1(x)|k\rangle_{(\alpha}|n\rangle_\beta|n\rangle_\gamma|n\rangle_{\delta)} \\ + \frac{1}{4}\,\Psi_2(x)|k\rangle_{(\alpha}|k\rangle_\beta|n\rangle_\gamma|n\rangle_{\delta)} - \frac{1}{6}\,\Psi_3(x)|k\rangle_{(\alpha}|k\rangle_\beta|k\rangle_\gamma|n\rangle_{\delta)} \\ + \Psi_4(x)|k\rangle_\alpha|k\rangle_\beta|k\rangle_\gamma|k\rangle_\delta\,.\end{aligned} \tag{3.4}$$

Together with their compatriots in the antichiral Weyl spinor $\tilde{\Psi}$, these are the ten real components of the Weyl tensor.

In Minkowski space, the NP scalars have an important property known as peeling

[2]Details of our notation can be found in appendix A.1. For later convenience, our (anti)symmetrisation symbols do not include the $1/n!$ factor.

[97, 181]. This is a hierarchy in their fall-off with large distance r between the observer and the localised source. In electrodynamics, we have

$$\begin{aligned} \phi_0(x) &= \phi_0^1(\bar{x})\,\frac{1}{r^3} + \mathcal{O}(1/r^4)\,, \\ \phi_1(x) &= \phi_1^1(\bar{x})\,\frac{1}{r^2} + \mathcal{O}(1/r^3)\,, \\ \phi_2(x) &= \phi_2^1(\bar{x})\,\frac{1}{r^1} + \mathcal{O}(1/r^2)\,, \end{aligned} \tag{3.5}$$

where $\bar{x}$ denotes non-radial dependence. Thus, the scalar $\phi_2(x)$ is the dominant component of the field at large distances: it describes the asymptotic radiation field. Meanwhile, $\phi_1(x)$ is Coulombic. In gravity, the situation is very similar:

$$\begin{aligned} \Psi_0(x) &= \Psi_0^1(\bar{x})\,\frac{1}{r^5} + \mathcal{O}(1/r^6)\,, \\ \Psi_1(x) &= \Psi_1^1(\bar{x})\,\frac{1}{r^4} + \mathcal{O}(1/r^5)\,, \\ \Psi_2(x) &= \Psi_2^1(\bar{x})\,\frac{1}{r^3} + \mathcal{O}(1/r^4)\,, \\ \Psi_3(x) &= \Psi_3^1(\bar{x})\,\frac{1}{r^2} + \mathcal{O}(1/r^3)\,, \\ \Psi_4(x) &= \Psi_4^1(\bar{x})\,\frac{1}{r^1} + \mathcal{O}(1/r^2)\,. \end{aligned} \tag{3.6}$$

Asymptotic gravitational radiation is described by $\Psi_4(x)$, while $\Psi_2(x)$ describes a potential-type contribution, as in Schwarzschild. We will see aspects of this structure in our split-signature examples.

The double copy relation between scattering amplitudes in gravity and in Yang-Mills theory [94, 102, 103, 182] is quite a surprise from the classical geometric perspective on general relativity: geometrically, there seems to be little hint that gravity is some kind of “square” of Yang-Mills theory. In recent years, it has been clear that some aspects of gravity are analogues of aspects of gauge theory (or, in simple settings, of electrodynamics), and the application of the double copy to classical solutions in recent years has provided a unified understanding to several such analogies [42, 44, 48, 95, 98, 105, 110, 112–124, 126–131, 138, 139, 143–145, 147, 148, 151–156, 165, 168, 169, 183–188]. For instance, the structure of the gravitational Newman-Penrose scalars is evidently analogous to that of the electromagnetic NP scalars. This is particularly clear for special classes of solutions, such as the Petrov type N class, which has only $\Psi_4 \neq 0$ for an appropriate choice of spinor basis. Then the Weyl spinor is simply

$$\Psi_{\alpha\beta\gamma\delta}(x) = \Psi_4(x)|k\rangle_\alpha|k\rangle_\beta|k\rangle_\gamma|k\rangle_\delta\,. \tag{3.7}$$

In electrodynamics, we can consider a similar situation where the Maxwell spinor is simply

$$\phi_{\alpha\beta}(x) = \phi_2(x)|k\rangle_\alpha|k\rangle_\beta\,. \tag{3.8}$$

Roughly speaking, type N spacetimes look like two copies of purely radiative electromagnetic solutions. A more careful analysis led to a sharp proposal of an exact "Weyl" double copy for special classes of solutions [98], where the Maxwell and Weyl spinors are related by

$$\Psi_{\alpha\beta\gamma\delta}(x) = \frac{1}{S(x)}\phi_{(\alpha\beta}(x)\phi_{\gamma\delta)}(x)\,. \tag{3.9}$$

Here, $S(x)$ is a scalar field satisfying the (flat space) wave equation. The proposal was first proven for vacuum solutions of type D, which have only $\Psi_2 \neq 0$, but has also been studied for vacuum solutions of type N [128]; see [129] for the relation to the twistor correspondence in the linearised case. In split signature, we will show that the double copy relation between the three-point amplitudes in gauge theory and gravity directly relates the Newman-Penrose scalars of the Coulomb charge and the Schwarzschild solution at linearised level. This relation between the Newman-Penrose scalars in gauge theory and gravity is directly expressed in the on-shell momentum space formalism of [49], but the translation to position space for these particular solutions precisely reproduces the Weyl double copy (3.9).

At the quantum level, it is natural to expect that the Coulomb field or the Schwarzschild field should be described by a coherent state. For instance, in the Schwarzschild case, the metric would be given by the expectation value of the all-order metric quantum operator on the coherent state (this operator would include all higher-order perturbative terms). We show that the coherent state is uniquely described by the relevant three-point amplitude. This is a gauge-invariant characterisation of the classical field. Thus, both the field strengths and the coherent state are determined by the same data. This is satisfying: classically, knowledge of the field strength is complete knowledge of the field, so it should be that one can determine the coherent state from the field strength. Indeed, this is the case. The structure of the coherent state we encounter is strongly reminiscent of the eikonal exponentiation which is receiving renewed attention in the context of the dialog between scattering amplitudes and classical physics. It is exactly this structure which will be presented in the final chapter of the thesis, this time in Minkowski space. From this point of view then, split signatures act as a guiding compass eventually yielding to a Minkowski generalisation.

Our results concerning the classical double copy have direct implications for Lorentzian signature. Indeed, as we will see, the Newman-Penrose scalars we construct have a close Lorentzian analogue. The Coulombic $\phi_1(x)$ and the Schwarzschild-like $\Psi_2(x)$ that we compute from our coherent states in split signature are essentially trivial analytic continuations of their Minkowski-space counterparts.

The double copy between Coulomb and Schwarzschild is expected to be exact, but our methods based on amplitudes are perturbative. To go beyond perturbation theory, we use the Kerr-Schild double copy [95] to find the exact classical metric set up by our static particle, subject to the precise boundary conditions we impose in split signature. We believe that this example is the first time that the double copy has been used to find a novel exact solution in gravity. While we could in principle obtain the exact solution using purely gravitational methods, some care would be required to ensure that the correct boundary conditions are imposed at non-linear level. Using the Kerr-Schild double copy, the boundary conditions in gravity are trivially imported from those of the 'single copy' gauge theory solution.

In the final part of the chapter, we will present a more general double copy and coherent state to source solutions which correspond to NS-NS gravity. This is a classical $\mathcal{N} = 0$ supergravity solution of the EFE involving dilaton and axions. We will find that simple QED amplitudes will not be enough to source such extra field, thus naturally leading us to the inclusion of extra couplings: spin and magnetic charge.

This part of the thesis is organised as follows. In section 3.2, we explain how to compute electromagnetic and gravitational field strengths using the methods of quantum field theory, making direct contact with three-point amplitudes. We also discuss the corresponding coherent states. We point out a double copy between the Maxwell and Weyl spinors in momentum space, induced directly by the corresponding amplitudes. Building on this observation in section 3.3, we determine the nature of the double copy in position space by performing integrals over on-shell momentum space. We recover the Weyl double copy, thereby directly connecting the Weyl form of the classical double copy to scattering amplitudes. In section 3.4, we use a Kerr-Schild Ansatz to determine the exact spacetime metric in the gravitational context. The implications of our split-signature results for Minkowski space are described in section 3.5. An extended "mixed" double copy is then described in 3.6, showing how classical gravity solutions involving dilatons and axions can also be characterised by simple three-point amplitudes. Finally, the discussion contains a summary of our results with an overview of some of their implications. We provide a detailed exposition of our choice of retarded Green's function for split signature in the appendix, together with a brief recap of Riemann-Cartan gravity.

3.2 Classical Solutions from Three-Point Amplitudes

To connect three-point amplitudes to Newman-Penrose scalars, all that is needed is a direct computation using the methods of quantum field theory. The first order of business, then, is to define the quantum fields we use in split signature. In the following chapter we stick to $D = 4$ since spinor variables are not so easy to extend to arbitrary dimensions, it would be certainly fascinating to explore our results in higher D.

Given that our spacetime has two time directions, which we will denote as t^1 and t^2, there are two notions of energy. Correspondingly, the choice of vacuum is not unique. Much of the interesting physics we exploit actually arises from this non-uniqueness. For our force-carrying "messenger" particles (photons or gravitons), we impose the condition that the fields are in a vacuum state for $t^1 \to -\infty$. The corresponding mode expansion of the field operator in the electromagnetic case is then[3]

$$\mathbb{A}^\mu(x) = \sum_{\eta=\pm} \int \mathrm{d}\Phi(k)\, \hbar^{-\frac{1}{2}} \left(a_\eta(k)\varepsilon_\eta^\mu(k) e^{-i\frac{k\cdot x}{\hbar}} + a_\eta^\dagger(k)\varepsilon_\eta^\mu(k) e^{i\frac{k\cdot x}{\hbar}} \right), \tag{3.10}$$

where the position and momentum are given by $x = (t^1, t^2, \mathbf{x})$ and $k = (E^1, E^2, \mathbf{k})$,

[3]The notation is that $(a_\eta(k))^\dagger \equiv a_\eta^\dagger(k)$. Notice that the helicity polarisation vectors are real in split signature. Also polarization vectors are taken real here, see the appendix as well: $\varepsilon_\eta^{*\mu} = \varepsilon_\eta^\mu$.

while the measure is now

$$\mathrm{d}\Phi(k) = \hat{\mathrm{d}}^4 k\, \hat{\delta}(k^2)\Theta(E^1)\,. \tag{3.11}$$

The sum is over the helicity η. Notice that we have retained factors of $\hbar$; it will be reassuring to check that these factors drop out for classical quantities. The theta function ensures that quanta created around the vacuum have momenta directed into the future with respect to t^1; in other words, they have positive energy with respect to this choice of time direction.

We also introduce a scalar particle which will be our source. In order for our calculation to be in the regime of validity of the classical approximation, we place our particle in a wave packet of the type discussed in detail in reference [49], or in the introduction. We will discuss the properties of these wave packets in more detail shortly. For now, note simply that the wave packet is such that the uncertainties in the position and the momentum of our source are small. We will treat this scalar particle as a probe.

To benefit from the unusual possibilities of a split-signature spacetime, we choose the expectation value of the probe's momentum to be $\langle p^\mu \rangle = m\, u^\mu = m\,(0,1,0,0)$. Thus, the particle's worldline can be chosen to be the t^2 axis. As a probe particle, we will not need a field operator for this state. Here, it is enough to define the state itself:

$$|\psi\rangle = \int \mathrm{d}\Phi(p)\, \phi(p)\, |p\rangle, \quad \mathrm{d}\Phi(p) = \hat{\mathrm{d}}^4 p\, \hat{\delta}(p^2 - m^2)\Theta(E_2)\,, \tag{3.12}$$

where the wave function $\phi(p)$ is sharply-peaked around the momentum $p^\mu = m u^\mu$. Note that in this case the theta function[4] enforces positive energy along t^2. For brevity of notation, we left it implied that a measure $\mathrm{d}\Phi(p)$ involves a factor $\Theta(E_2)$ while a measure $\mathrm{d}\Phi(k)$ involves $\Theta(E^1) = \Theta(E_1)$.

3.2.1 The electromagnetic case

Now, let us investigate the electromagnetic field set up by endowing our probe with a charge Q. For large negative t^1 we have chosen a trivial electromagnetic field. To characterise the field for other times t^1 we must perform a computation.

[4]We write $\Theta(E_2)$ rather than $\Theta(E^2)$ to emphasise that the second component of the momentum vector is constrained, avoiding confusion with a squared energy. Recall that $E_2 = E^2$ in our conventions.

As we will see, the result is non-trivial.

We evolve the state along t^1 with

$$|\psi_{\text{out}}\rangle = \lim_{t^1\to\infty} U(-t^1, t^1)|\psi\rangle = S|\psi\rangle, \tag{3.13}$$

and we measure the expectation value of the quantum operator

$$\mathbb{F}^{\mu\nu}(x) = -i\sum_{\eta=\pm}\int \mathrm{d}\Phi(k)\hbar^{-\frac{3}{2}}\left(a_\eta(k)k^{[\mu}\varepsilon_\eta^{\nu]}e^{-i\frac{k\cdot x}{\hbar}} - a_\eta^\dagger(k)k^{[\mu}\varepsilon_\eta^{\nu]}e^{i\frac{k\cdot x}{\hbar}}\right). \tag{3.14}$$

While the scattering picture may suggest that we reproduce the electromagnetic field only for large positive t^1, in fact we reproduce the field for any time t^1 much larger than any time scale characteristic of the scattering. In our case, the largest spacetime length associated with the scattering is the size of the wave packet of the source particle (the Compton wavelength of the particle is very small compared to the size of the wave packet, as we saw in the introduction).

Defining the T matrix via $S = 1 + iT$, we find that this expectation value[5] is

$$F^{\mu\nu} \equiv \langle\psi|S^\dagger\mathbb{F}^{\mu\nu}S|\psi\rangle = 2\,\mathrm{Re}\,i\langle\psi|\mathbb{F}^{\mu\nu}T|\psi\rangle + \langle\psi|T^\dagger\mathbb{F}^{\mu\nu}T|\psi\rangle\,. \tag{3.15}$$

Notice that we imposed

$$\langle\psi|\mathbb{F}^{\mu\nu}|\psi\rangle = 0\,, \tag{3.16}$$

which holds because of our boundary conditions (there are no photons in the initial state).

In the Minkowski case, the expectation value of the field of a static massive charge is of course the Coulomb field, and can be computed exactly. In our split-signature case the expectation value, although less familiar, is evidently some sort of analytic continuation of Coulomb. We will determine the field to all orders of perturbation theory below. Before doing so, however, it is instructive to recompute the leading order field strength at this order, closely following the methods of section 2.3.

At leading order in perturbation theory, we can approximate

$$F^{\mu\nu}(x) \simeq 2\,\mathrm{Re}\,i\langle\psi|\mathbb{F}^{\mu\nu}(x)T|\psi\rangle. \tag{3.17}$$

[5]Note that we have dropped the cl subscript used in the introduction $F^{\mu\nu}_{cl} \to F^{\mu\nu}$.

Inserting the explicit initial state of equation (3.12), the expectation value becomes

$$
\begin{aligned}
F^{\mu\nu}(x) &= 2\hbar^{-\frac{3}{2}}\,\mathrm{Re}\sum_\eta \int \mathrm{d}\Phi(k)\,\langle\psi|a_\eta(k)T|\psi\rangle\,k^{[\mu}\varepsilon_\eta^{\nu]}\,e^{-i\frac{k\cdot x}{\hbar}} \\
&= 2\hbar^{-\frac{3}{2}}\,\mathrm{Re}\sum_\eta \int \mathrm{d}\Phi(k)\mathrm{d}\Phi(p')\mathrm{d}\Phi(p)\,\phi^*(p')\phi(p)\,\langle p'|a_\eta(k)T|p\rangle\,k^{[\mu}\varepsilon_\eta^{\nu]}\,e^{-i\frac{k\cdot x}{\hbar}}\,.
\end{aligned}
\tag{3.18}
$$

Expanding the matrix element $\langle p'|a_\eta(k)T|p\rangle$ appearing in equation (3.18) in terms of a three-point amplitude and the momentum-conserving delta function, we can equivalently write

$$
\begin{aligned}
F^{\mu\nu}(x) = 2\hbar^{-\frac{3}{2}}\,\mathrm{Re}\sum_\eta \int \mathrm{d}\Phi(k)\mathrm{d}\Phi(p)\,\Theta(E^2+k^2)\hat{\delta}(2p\cdot k+k^2) \\
\times\,\phi^*(p)\phi(p+k)\,\mathcal{A}^{(3)}_{-\eta}(k)\,k^{[\mu}\varepsilon_\eta^{\nu]}\,e^{-ik\cdot x/\hbar}\,.
\end{aligned}
\tag{3.19}
$$

where $\mathcal{A}^{(3)}_\eta(k)$ is the three-point scattering amplitude for the process shown in figure 3.1. The helicity labels of our amplitudes are for incoming messengers; since our photons are outgoing, we encounter the amplitude for the opposite helicity $-\eta$.

This expression for the field strength simplifies in the classical approximation, as argued in the introduction. Introducing wavenumbers, we obtain

$$
F^{\mu\nu}(x) = 2\,\mathrm{Re}\sum_\eta \int \mathrm{d}\Phi(\bar{k})\mathrm{d}\Phi(p)\,|\phi(p)|^2\,\hat{\delta}(2p\cdot\bar{k}+\hbar\bar{k}^2)\sqrt{\hbar}\mathcal{A}^{(3)}_{-\eta}(\bar{k})\,\bar{k}^{[\mu}\varepsilon_\eta^{\nu]}\,e^{-i\bar{k}\cdot x}\,.
\tag{3.20}
$$

Now, the wave function is sharply-peaked about an average (classical) momentum mu^μ. The integral of this sharply-peaked function over the amplitude, which is smooth near the peak momentum, sets the momenta appearing in the amplitude to mu^μ, and at the same time will broaden the explicit delta function. We can therefore drop the $\hbar\bar{k}^2$ shift in the delta function, arriving at

$$
F^{\mu\nu}(x) = \frac{1}{m}\,\mathrm{Re}\sum_\eta \int \mathrm{d}\Phi(\bar{k})\,\hat{\delta}(u\cdot\bar{k})\,\sqrt{\hbar}\,\mathcal{A}^{(3)}_{-\eta}(\bar{k})\,\bar{k}^{[\mu}\varepsilon_\eta^{\nu]}\,e^{-i\bar{k}\cdot x}\,.
\tag{3.21}
$$

Notice that the field strength is given by the scattering amplitude, up to a universal (theory independent) integration and essential kinematic factors.

For our static charge in electromagnetism, the amplitude is the three-point scalar

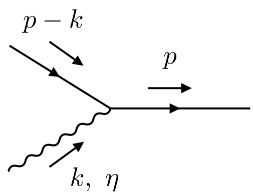

Figure 3.1 *The three-point electromagnetic amplitude. Notice that the photon with polarization η is incoming.*

QED vertex,

$$\begin{aligned}\mathcal{A}_-^{(3)}(k) &= -2\frac{Q}{\sqrt{\hbar}}\,p\cdot\varepsilon_-(k) = \sqrt{2}m\,\frac{Q}{\sqrt{\hbar}}\frac{1}{X}, \qquad \frac{1}{X} := -\sqrt{2}u\cdot\varepsilon_-,\\ \mathcal{A}_+^{(3)}(k) &= -2\frac{Q}{\sqrt{\hbar}}\,p\cdot\varepsilon_+(k) = -\sqrt{2}m\,\frac{Q}{\sqrt{\hbar}}X, \qquad X := \sqrt{2}u\cdot\varepsilon_+,\end{aligned} \tag{3.22}$$

where we have written $\mathcal{A}$ in terms of the kinematics-dependent X-factor introduced in [178].[6] We observe that $XX^{-1} = -2u_\mu u_\nu \varepsilon_+^\mu \varepsilon_-^\nu = 1$. Notice that the amplitude depends on k only through the polarisation vector $\varepsilon_\eta(k)$: it therefore does not depend on whether we treat k as a momentum or as a wave vector.

Taking the factor $1/\sqrt{\hbar}$ in the amplitude into account, we see that the $\hbar$ dependence of equation (3.21) reassuringly drops out. This is obviously consistent with the computation of a classical quantity. Since all factors of $\hbar$ will similarly disappear for classical quantities in the remainder of the chapter, we will henceforth set $\hbar = 1$, restoring it only when necessary.

Our expressions simplify further if we pass from the field strength tensor to the associated spinorial quantity, the Maxwell spinor defined in equation (3.1), which we reproduce here for convenience:

$$\phi_{\alpha\beta}(x) = \sigma^{\mu\nu}{}_{\alpha\beta}F_{\mu\nu}(x)\,. \tag{3.23}$$

The $\sigma^{\mu\nu}$ matrices are symmetric on their spinor indices α and β. These matrices project two-forms onto their self-dual parts,[7] and are proportional to the generators of $\mathrm{SL}(2,\mathbb{R})$. (Details of our spinor conventions are given in appendix A.1.) In view of the fact that the $\sigma^{\mu\nu}$ matrices matrices are real (as are their antichiral counterparts $\tilde{\sigma}^{\mu\nu}$), we can write the expectation value of the

[6]We use the notation X for this factor rather than x to avoid confusion with the position x.
[7]In our nomenclature, a two-form F is self-dual if $*F = F$, and anti-self-dual if $*F = -F$.

Maxwell spinor as

$$\begin{aligned}\phi_{\alpha\beta}(x) &= \frac{1}{m}\,\mathrm{Re}\sum_{\eta}\int \mathrm{d}\Phi(k)\,\hat{\delta}(u\cdot k)\,\sigma_{\mu\nu\,\alpha\beta}\,k^{[\mu}\varepsilon_{\eta}^{\nu]}\,e^{-ik\cdot x}\,\mathcal{A}^{(3)}_{-\eta}(k)\\ &= -\frac{\sqrt{2}}{m}\,\mathrm{Re}\int \mathrm{d}\Phi(k)\,\hat{\delta}(u\cdot k)\,|k\rangle_{\alpha}|k\rangle_{\beta}\,e^{-ik\cdot x}\,\mathcal{A}^{(3)}_{+}(k)\,,\end{aligned} \tag{3.24}$$

where we have used the fact that a negative helicity plane wave has a self-dual field strength (equation (A.14)), while a positive helicity plane wave has an anti-self-dual field strength (equation (A.15)). For the other chirality, we similarly find

$$\tilde{\phi}_{\dot{\alpha}\dot{\beta}}(x) = +\frac{\sqrt{2}}{m}\,\mathrm{Re}\int \mathrm{d}\Phi(k)\,\hat{\delta}(u\cdot k)\,[k|_{\dot{\alpha}}[k|_{\dot{\beta}}\,e^{-ik\cdot x}\,\mathcal{A}^{(3)}_{-}(k)\,. \tag{3.25}$$

Thus, the two helicity amplitudes correspond directly to the two different chiralities of Maxwell spinor. In split signature, these spinorial field strengths are real (as is evident in the particular case of our expressions) and independent. We will focus on the chiral case of $\phi_{\alpha\beta}$ below, though the story for $\tilde{\phi}_{\dot{\alpha}\dot{\beta}}$ is completely parallel.

More concretely, we can evaluate the field strength by inserting the standard expressions (3.22) for the amplitude. The Maxwell spinor becomes simply

$$\phi_{\alpha\beta}(x) = 2\,Q\,\mathrm{Re}\int \mathrm{d}\Phi(k)\,\hat{\delta}(u\cdot k)\,|k\rangle_{\alpha}|k\rangle_{\beta}\,e^{-ik\cdot x}\,X\,. \tag{3.26}$$

In other words, the spinorial field strength is in essence an on-shell Fourier transform of the unique kinematic factor X.

3.2.2 The coherent state

In the previous section, we found the classical electromagnetic field produced by a static source. Even in split signature, it is reasonable to expect that this field should be very simple, so it is a little unsatisfying that we performed a perturbative approximation along the way, at equation (3.17). Fortunately, it is not hard to determine the final quantum state to all orders in the perturbative coupling Q. We only compute the classical approximation to the field, which (in this particular electromagnetic case) means that we should restrict to tree-level amplitudes. The diagrams are shown in figure 3.2.

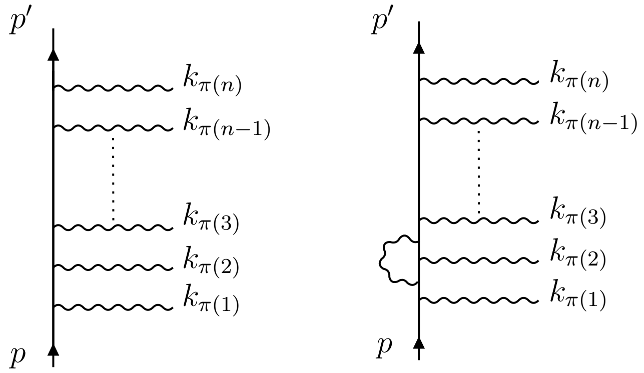

Figure 3.2 *Diagrams of the form shown on the left contribute to the radiation field to all orders in the coupling, but leading classical order. Loop effects, as shown in the diagram on the right, are quantum corrections.*

In fact, the final state of the electromagnetic field is coherent:

$$S|\psi\rangle = \frac{1}{\mathcal{N}} \int \mathrm{d}\Phi(p)\phi(p) \exp\left[\sum_{\eta} \int \mathrm{d}\Phi(k)\, \hat{\delta}(2p\cdot k)\, i\mathcal{A}^{(3)}_{-\eta}(k)\, a^{\dagger}_{\eta}(k)\right] |p\rangle\,, \quad (3.27)$$

where $\mathcal{N}$ is a normalisation factor ensuring that $\langle\psi|S^{\dagger}S|\psi\rangle = 1$. The exponential structure of the state captures the intuition that the outgoing field contains a great many photons. It is also consistent with the intuition that coherent states are the natural description of classical wave phenomena in quantum field theory.[8] The coherence of the state could also be demonstrated by taking advantage of the linear coupling between the gauge field A_μ and a massive probe source worldline, so it comes as no surprise. However, it is satisfying to see that the state is completely controlled by the on-shell three-point amplitude.

To see how the exponentiation in (3.27) comes about in our approach, we expand the S matrix acting on our initial state as

$$S|\psi\rangle = \frac{1}{\mathcal{N}}(1 + iT_3 + iT_4 + \cdots)|\psi\rangle\,, \quad (3.28)$$

[8]More discussion of coherent states, amplitudes and classicality is in [33].

where the T_n are defined by

$$T_{n+2} = \frac{1}{n!} \sum_{\eta_1,\ldots,\eta_n} \int \mathrm{d}\Phi(p')\mathrm{d}\Phi(p) \prod_{i=1}^{n} \mathrm{d}\Phi(k_i)\, \mathcal{A}^{(n+2)}_{-\eta_1,\ldots,-\eta_n}(p \to p', k_1 \cdots k_n)$$
$$\times\, \hat{\delta}^4 \left(p - p' - \sum k_i\right) a^\dagger_{\eta_1}(k_1) \cdots a^\dagger_{\eta_n}(k_n)\, a^\dagger(p') a(p)\,. \tag{3.29}$$

That is, the T_{n+2} are projections of the transition matrix T onto final states with n photons, in addition to the massive particle. We denote the creation and annihilation operators for the massive scalar state by $a^\dagger(p')$ and $a(p)$, respectively, as opposed to the photon creation operators $a^\dagger_{\eta_i}(k_i)$. Note that we include precisely one creation and one annihilation operator for our scalar, which is consistent with treating it as a probe source. We omit all terms in T_{n+2} containing photon annihilation operators since these would annihilate the initial state $|\psi\rangle$. The factor $n!$ in equation (3.29) is a symmetry factor associated with n identical photons in the final state.

We begin by computing the action of T_3 and T_4 on $|\psi\rangle$ explicitly. It will then be a small step to the general case and the exponential structure. First, the case of T_3 is straightforward:

$$\begin{aligned} iT_3|\psi\rangle &= \sum_\eta \int \mathrm{d}\Phi(p')\mathrm{d}\Phi(p)\mathrm{d}\Phi(k)\, \phi(p)\, i\mathcal{A}^{(3)}_{-\eta}(k)|p', k^\eta\rangle\, \hat{\delta}^4\left(p - p' - k\right) \\ &= \sum_\eta \int \mathrm{d}\Phi(p)\mathrm{d}\Phi(k)\, \phi(p+k)\, \Theta(E^2 + k^2)\hat{\delta}(2p\cdot k)\, i\mathcal{A}^{(3)}_{-\eta}(k)|p, k^\eta\rangle\,, \end{aligned} \tag{3.30}$$

where, in the second line, we integrated over p with the help of a four-fold delta function, and we relabelled p' to p. As we saw for the field strength, this expression simplifies when we compute in the domain of validity of the classical approximation. We find

$$iT_3|\psi\rangle = \sum_\eta \int \mathrm{d}\Phi(p)\mathrm{d}\Phi(k)\, \varphi(p)\, \hat{\delta}(2p\cdot k)\, i\mathcal{A}^{(3)}_{-\eta}(k)\, a^\dagger_\eta(k)|p\rangle\,. \tag{3.31}$$

Comparing to the form for the coherent state we advertised in equation (3.27), we now see how the exponent can begin to emerge.

The four-point case requires a little more work on the actual amplitude. Working at the textbook level of Feynman diagrams (using the notation in figure 3.3), we

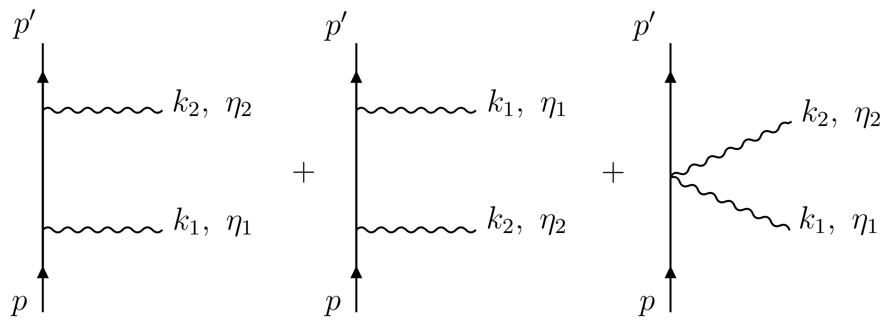

Figure 3.3 *The familiar Feynman diagrams for the four point scalar QED amplitude. In this figure, the photons are outgoing.*

find

$$i\mathcal{A}^{(4)} = -iQ^2\frac{4p\cdot\varepsilon_{-\eta_1}(k_1)\,p'\cdot\varepsilon_{-\eta_2}(k_2)}{2k_1\cdot p+i\epsilon}+iQ^2\frac{4p\cdot\varepsilon_{-\eta_2}(k_2)\,p'\cdot\varepsilon_{-\eta_1}(k_1)}{2k_1\cdot p'-i\epsilon} + 2iQ^2\varepsilon_{-\eta_1}(k_1)\cdot\varepsilon_{-\eta_2}(k_2)\,. \tag{3.32}$$

Now, of these three terms the last is suppressed relative to the other two in the classical approximation. The suppression factor is of order $p\cdot k/m^2$, which is of order the energy of a single photon in units of the mass of the particle. (Equivalently, the suppression factor is $\hbar\bar{k}/m$, where $\bar{k}$ is a typical component of the wave vector of the photon. From this perspective, the contact term is explicitly down by a factor $\hbar$.) We therefore neglect the contact diagram. In terms of a more modern unitarity-based construction of the amplitude, this means that we can simply "sew" three-point amplitudes to compute the dominant part of the four-point amplitude relevant for this computation.[9]

We can make this sewing completely manifest in our four-point amplitude by writing

$$k_1\cdot p' = k_1\cdot p + \mathcal{O}(\hbar)\,, \qquad p'\cdot\varepsilon(k) = p\cdot\varepsilon(k)+\mathcal{O}(\hbar)\,, \tag{3.33}$$

and neglecting the $\hbar$ corrections. (In dimensionless terms, these corrections are again suppressed by factors of the photon energy over the particle mass.) It is

[9]It may be worth emphasising that a one-loop computation of a classical observable such as the impulse also involves the four-point tree amplitude. But in that case the contact term is absolutely necessary to recover the correct classical result, and in fact the terms we are concentrating on cancel.

then a matter of algebra to see that

$$\begin{aligned} i\mathcal{A}^{(4)} &= \hat{\delta}(2p\cdot k_1)\,(-2iQ\,p\cdot\varepsilon_{-\eta_1}(k_1))(-2iQ\,p\cdot\varepsilon_{-\eta_2}(k_2)) \\ &= \hat{\delta}(2p\cdot k_1)\,i\mathcal{A}^{(3)}_{-\eta_1}(k_1)\,i\mathcal{A}^{(3)}_{-\eta_2}(k_2)\,. \end{aligned} \tag{3.34}$$

We picked up a delta function from the sum of two propagators. It is perhaps worth pausing to note that the two photon emissions are completely uncorrelated from one another.

Now we can compute the action of T_4 on our initial state. Using the definition (3.29) of T_4 and the fact that

$$a(p)|\psi\rangle = \phi(p)|0\rangle\,, \tag{3.35}$$

we find

$$\begin{aligned} iT_4|\psi\rangle = \frac{1}{2}\sum_{\eta_1,\eta_2}\int \mathrm{d}\Phi(p')\mathrm{d}\Phi(p)\mathrm{d}\Phi(k_1)\mathrm{d}\Phi(k_2)\,\phi(p)\,i\mathcal{A}^{(4)}_{-\eta_1,-\eta_2}(p\to p',k_1^{\eta_1}k_2^{\eta_2}) \\ \times\,\hat{\delta}^4(p-p'-k_1-k_2)|p'\,k_1^{\eta_1}k_2^{\eta_2}\rangle\,. \end{aligned} \tag{3.36}$$

The integration over the momentum p is trivial using the explicit four-fold delta function. The measure $\mathrm{d}\Phi(p)$ contains a theta function, requiring that the E^2 component of $p'+k_1+k_2$ is positive. Since the $d\Phi(p')$ measure already requires the relevant energy of p' to be positive, and the photon energies are small compared to the mass, we can ignore this theta function. We also encounter the wave function evaluated at $p'+k_1+k_2$; since the photon energies are small compared to the width of the wave function, we may approximate as before $\phi(p'+k_1+k_2)\simeq\phi(p')$. Finally, $\mathrm{d}\Phi(p)$ contains a delta function requiring

$$p^2 = (p'+k_1+k_2)^2 = m^2\,. \tag{3.37}$$

Since $p'^2 = m^2$, this becomes a factor

$$\hat{\delta}(2p'\cdot(k_1+k_2)+(k_1+k_2)^2)$$

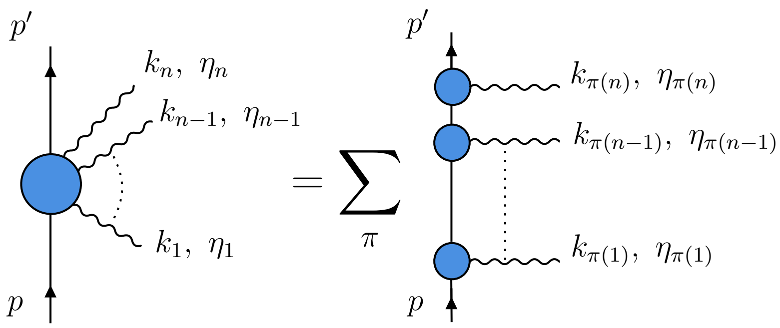

Figure 3.4 *The dominant term in the $n+2$ point amplitude can be obtained by sewing n three-point amplitudes. The full amplitude is obtained by summing over permutations π of the n outgoing photon lines.*

in $T_4|\psi\rangle$. Once again, we may neglect this shift of the delta function, finding

$$iT_4|\psi\rangle = \frac{1}{2}\sum_{\eta_1,\eta_2}\int \mathrm{d}\Phi(p)\mathrm{d}\Phi(k_1)\mathrm{d}\Phi(k_2)\,\phi(p)\,i\mathcal{A}^{(4)}_{-\eta_1,-\eta_2}(p+k_1+k_2\to p, k_1k_2)$$
$$\times\,\hat{\delta}(2p\cdot(k_1+k_2))|p\,k_1^{\eta_1}k_2^{\eta_2}\rangle\,, \tag{3.38}$$

where we relabelled the momentum p' to p. Now we may use our result (3.34) for the four-point amplitude, arriving at

$$\begin{aligned}iT_4|\psi\rangle &= \frac{1}{2}\sum_{\eta_1,\eta_2}\int \mathrm{d}\Phi(p)\mathrm{d}\Phi(k_1)\mathrm{d}\Phi(k_2)\,\phi(p)\,\hat{\delta}(2p\cdot k_1)\hat{\delta}(2p\cdot k_2)\\ &\qquad\qquad\times\, i\mathcal{A}^{(3)}_{-\eta_1}(k_1)\,i\mathcal{A}^{(3)}_{-\eta_2}(k_2)|p\,k_1^{\eta_1}k_2^{\eta_2}\rangle\\ &= \frac{1}{2}\int \mathrm{d}\Phi(p)\,\phi(p)\left(\sum_\eta\int \mathrm{d}\Phi(k)\hat{\delta}(2p\cdot k)i\mathcal{A}^{(3)}_{-\eta}(k)a^\dagger_\eta(k)\right)^2|p\rangle\,,\end{aligned} \tag{3.39}$$

consistent with the exponential structure of the coherent state in equation (3.27).

Now we turn to the general term, evaluating $T_{n+2}|\psi\rangle$. We can make use of the knowledge gained from the four-point example, including the fact that the leading term in the $(n+2)$-point amplitude can be obtained by sewing n three-point amplitudes. We must nevertheless sum over permutations of the external photon momenta as shown in figure 3.4. The dominant term in the amplitude is

$$i\mathcal{A}^{(n+2)} = \left(\prod_{i=1}^{n} i\mathcal{A}^{(3)}_{-\eta_i}(k_i)\right) \sum_{\pi} \frac{i}{2p\cdot k_{\pi(1)} + i\epsilon} \frac{i}{2p\cdot (k_{\pi(1)} + k_{\pi(2)}) + i\epsilon} \cdots \\ \times \frac{i}{2p\cdot (k_{\pi(1)} + k_{\pi(2)} + \cdots k_{\pi(n-1)}) + i\epsilon} \,. \tag{3.40}$$

The sum is over permutations π of the n final-state photons.

At four points, the sum over sewings led to a delta function, and the same happens here. We can state the result most simply at the level of $T_{n+2}|\psi\rangle$, which can be written as

$$iT_{n+2}|\psi\rangle = \frac{1}{n!} \sum_{\eta_1,\ldots,\eta_n} \int \mathrm{d}\Phi(p) \prod_{i=1}^{n} \mathrm{d}\Phi(k_i)\, \phi(p)\, \hat{\delta}\left(2p\cdot \sum_{j=1}^{n} k_j\right) i\mathcal{A}^{(n+2)}\, |p\; k_1^{\eta_1} \cdots k_n^{\eta_n}\rangle \,, \tag{3.41}$$

using the properties of the wave function, and neglecting terms suppressed in the classical region. We may now simplify the sum in equation (3.40) using the result

$$\hat{\delta}\left(\sum_{i=1}^{n} \omega_i\right) \sum_{\pi} \frac{i}{\omega_{\pi(1)} + i\epsilon} \frac{i}{\omega_{\pi(1)} + \omega_{\pi(2)} + i\epsilon} \cdots \frac{i}{\omega_{\pi(1)} + \omega_{\pi(2)} + \cdots \omega_{\pi(n-1)} + i\epsilon} \\ = \hat{\delta}(\omega_1)\hat{\delta}(\omega_2)\cdots\hat{\delta}(\omega_n) \,. \tag{3.42}$$

This result, which is an on-shell analogue of the eikonal identity, is proven (for example) in appendix A of reference [168]. We find that

$$iT_{n+2}|\psi\rangle = \frac{1}{n!} \int \mathrm{d}\Phi(p)\, \phi(p) \left(\sum_{\eta} \int \mathrm{d}\Phi(k)\, \hat{\delta}(2p\cdot k)\, i\mathcal{A}^{(3)}_{-\eta}(k)\, a^{\dagger}_{\eta}(k)\right)^{n} |p\rangle \,. \tag{3.43}$$

Performing the sum over n, we confirm the exponential structure of the state in equation (3.27).

What about the normalisation factor of the coherent state (3.27)? As usual, to ensure a correct normalisation we need to include disconnected vacuum bubble diagrams. It is simpler to demand that the factor $\mathcal{N}$ appearing in equation (3.27) is such that $S^{\dagger}S = 1$, and this is the procedure we adopt.

Now that we have seen that the final state is indeed given by equation (3.27), let us return to the evaluation of the expectation value of the field strength. The computation is simplified when we recall that (as usual for a coherent state) the annihilation operator acts as a derivative on the state:

$$
\begin{aligned}
a_\eta(k)S|\psi\rangle &= \hat{\delta}(2p\cdot k)\, i\mathcal{A}^{(3)}_{-\eta}(k)\, S|\psi\rangle \\
&= \frac{\delta}{\delta a^\dagger_\eta(k)} S|\psi\rangle\,.
\end{aligned}
\tag{3.44}
$$

The field strength is therefore

$$
\begin{aligned}
\langle\psi|S^\dagger\, \mathbb{F}^{\mu\nu}(x)\, S|\psi\rangle &= -2\,\mathrm{Re}\, i \sum_\eta \int \mathrm{d}\Phi(k)\, \langle\psi|S^\dagger\, a_\eta(k)\, S|\psi\rangle\, k^{[\mu}\varepsilon^{\nu]}_\eta\, e^{-ik\cdot x} \\
&= \frac{1}{m}\,\mathrm{Re} \sum_\eta \int \mathrm{d}\Phi(k)\, \hat{\delta}(u\cdot k)\mathcal{A}^{(3)}_{-\eta}(k)\, k^{[\mu}\varepsilon^{\nu]}_\eta\, e^{-ik\cdot x}\,.
\end{aligned}
\tag{3.45}
$$

Notice that this agrees with our previous expression, equation (3.21), which we now see is correct to all orders in the classical limit. Similarly, the Maxwell spinor is

$$
\begin{aligned}
\langle\psi|S^\dagger\, \phi_{\alpha\beta}(x)\, S|\psi\rangle &= -\frac{\sqrt{2}}{m}\,\mathrm{Re} \int \mathrm{d}\Phi(k)\, \hat{\delta}(u\cdot k)\, |k\rangle_\alpha |k\rangle_\beta\, e^{-ik\cdot x} \mathcal{A}^{(3)}_{+}(k) \\
&= 2\,Q\,\mathrm{Re} \int \mathrm{d}\Phi(k)\, \hat{\delta}(u\cdot k)\, |k\rangle_\alpha |k\rangle_\beta\, e^{-ik\cdot x}\, X\,,
\end{aligned}
\tag{3.46}
$$

in agreement with our earlier equations (3.24) and (3.26).

It is worth pausing to comment on this agreement. Classically, the field strength fully characterises the (electromagnetic) radiation field. We are using a quantum-mechanical formalism, but we now see that it is still true that knowledge of the field strength is also knowledge of the full state of the electromagnetic field, once we add the extra piece of information that this state is coherent. Mathematically, the field strength operator essentially differentiates the exponential form of the coherent state once, pulling down the parameter of the state. The structure of this computation is strongly reminiscent of eikonal methods which have also been of interest as a method of connecting classical field theory to scattering amplitudes [6, 13, 14, 66, 189–207]. We will get back to such methods in the final chapter.

3.2.3 The gravitational case and the momentum-space Weyl double copy

We have seen that a coherent state, equation (3.27), beautifully captures the radiation field in the electromagnetic case. What about gravity?

Graviton self-interactions could spoil the exponentiation present in electromagnetism. Clearly there are additional diagrams in gravity, for example at four points we could encounter the diagram

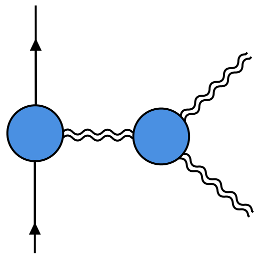

which involves a graviton three-point interaction. However, self-interactions of gravitons are suppressed compared to the dominant diagram

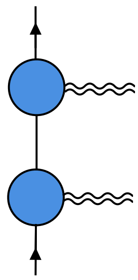

where the gravitons connect directly to the massive line. The reason is simply that the graviton self-interaction involves powers of the momenta of the gravitons, while the coupling to the massive line involves the particle mass. Since the particle mass is large compared to the graviton momenta, we may neglect graviton self-interactions. We may also neglect contact vertices (as in electromagnetism) for the same reason.

This does not mean that all self-interactions of the gravitational field are eliminated. The metric quantum operator has a perturbative expansion which includes these self-interactions. The expectation value of this all-order operator on our coherent state reproduces the classical metric. Notice that the coherent state is gauge invariant, while the quantum operator may not be (in quantum gravity, only asymptotic observables may be associated with gauge-invariant operators). This procedure would allow us to perturbatively construct the Schwarzschild metric, along the lines of [25, 208, 209] but in a manifestly on-shell formalism; see also [36] for an alternative approach based on an intermediate matching with an effective theory of sources coupled to gravitons.

The computation of the final state $S|\psi\rangle$ proceeds in the gravitational case precisely as in the electromagnetic case. Writing the gravitational three-point amplitude as $\mathcal{M}^{(3)}$, we find that

$$S|\psi\rangle = \frac{1}{\mathcal{N}}\int \mathrm{d}\Phi(p)\phi(p) \exp\left[\sum_\eta \int \mathrm{d}\Phi(k)\, \hat{\delta}(2p\cdot k)\, i\mathcal{M}^{(3)}_{-\eta}(k)\, a^\dagger_\eta(k)\right]|p\rangle\,, \quad (3.47)$$

where once more $\mathcal{N}$ is a normalisation factor.

We can now compute the gravitational field strength in the classical limit. We place an observer far from the source; then the gravitational field is weak, and we can work in the formalism of linearised quantum gravity. The graviton field operator is

$$\mathbb{h}^{\mu\nu}(x) = 2\,\mathrm{Re}\sum_\eta \int \mathrm{d}\Phi(k)\, a_\eta(k)\varepsilon^\mu_\eta(k)\varepsilon^\nu_\eta(k)\, e^{-ik\cdot x}\,, \quad (3.48)$$

where we have written the polarisation tensor of a graviton as the outer product of polarisation vectors $\varepsilon^\mu_\eta(k)$. The Weyl tensor $W_{\mu\nu\rho\sigma}(x)$ in empty space equals the curvature tensor $R_{\mu\nu\rho\sigma}(x)$, which in linearized gravity is

$$R^{\mu\nu\rho\sigma}(x) = \frac{\kappa}{2}\left(\partial^\sigma\partial^{[\mu}h^{\nu]\rho} + \partial^\rho\partial^{[\nu}h^{\mu]\sigma}\right)\,. \quad (3.49)$$

Thus, the Weyl tensor operator is

$$\mathbb{W}^{\mu\nu\rho\sigma}(x) = \kappa\,\mathrm{Re}\sum_\eta \int \mathrm{d}\Phi(k)\, a_\eta(k)\varepsilon^{[\mu}_\eta(k)k^{\nu]}\varepsilon^{[\rho}_\eta(k)k^{\sigma]}\, e^{-ik\cdot x}\,. \quad (3.50)$$

It is now very easy to compute the expectation value of the Weyl tensor, taking advantage once again of the fact that the action of $a_\eta(k)$ on the coherent state is the same as a functional derivative with respect to the creation operator:

$$\begin{aligned} W^{\mu\nu\rho\sigma}(x) &\equiv \langle\psi|S^\dagger\, \mathbb{W}^{\mu\nu\rho\sigma}(x)\, S|\psi\rangle \\ &= \kappa\,\mathrm{Re}\sum_\eta \int \mathrm{d}\Phi(k)\, \hat{\delta}(2p\cdot k)\, i\mathcal{M}^{(3)}_{-\eta}(k)\, \varepsilon^{[\mu}_\eta(k)k^{\nu]}\varepsilon^{[\rho}_\eta(k)k^{\sigma]}\, e^{-ik\cdot x}\,. \end{aligned} \quad (3.51)$$

The expectation value of the Weyl spinor is obtained by contracting with $\sigma^{\mu\nu}$ matrices, leading to

$$\langle\psi|S^\dagger\,\Psi_{\alpha\beta\gamma\delta}(x)\,S|\psi\rangle = 2\kappa\,\mathrm{Re}\int \mathrm{d}\Phi(k)\,\hat{\delta}(2p\cdot k)\,i\mathcal{M}_+^{(3)}(k)\,|k\rangle_\alpha|k\rangle_\beta|k\rangle_\gamma|k\rangle_\delta\,e^{-ik\cdot x}\,. \tag{3.52}$$

This expression for the Weyl tensor is very interesting from the perspective of the double copy. Comparing to the Maxwell spinor (3.46), note that the amplitudes $\mathcal{A}_+^{(3)}(k)$ and $\mathcal{M}_+^{(3)}(k)$ are related by the double copy. Let us define momentum-space versions of the Maxwell and Weyl spinors by

$$\begin{aligned}\phi_{\alpha\beta}(x) &= -\,\mathrm{Re}\int \mathrm{d}\Phi(k)\,\hat{\delta}(2p\cdot k)\,\phi_{\alpha\beta}(k)\,e^{-ik\cdot x}\,,\\ \Psi_{\alpha\beta\gamma\delta}(x) &= \kappa\,\mathrm{Re}\int \mathrm{d}\Phi(k)\,\hat{\delta}(2p\cdot k)\,\Psi_{\alpha\beta\gamma\delta}(k)\,e^{-ik\cdot x}\,,\end{aligned} \tag{3.53}$$

so that

$$\begin{aligned}\phi_{\alpha\beta}(k) &= 2\sqrt{2}\,|k\rangle_\alpha|k\rangle_\beta\,\mathcal{A}_+^{(3)}(k)\,,\\ \Psi_{\alpha\beta\gamma\delta}(k) &= 2|k\rangle_\alpha|k\rangle_\beta|k\rangle_\gamma|k\rangle_\delta\,i\mathcal{M}_+^{(3)}(k)\,.\end{aligned} \tag{3.54}$$

Let us also consider the scalar field theory analogue,

$$S(x) = \mathrm{Re}\int \mathrm{d}\Phi(k)\,\hat{\delta}(2p\cdot k)\,S(k)\,e^{-ik\cdot x}\,, \tag{3.55}$$

where the three-point amplitude $iS(k)$ is a real constant. Notice that $S(x)$ manifestly satisfies the wave equation; more precisely, it is the Green's function, as we shall see later. With this scalar counterpart in hand, we obtain an on-shell momentum-space analogue of the position-space Weyl double copy (3.9),

$$\Psi_{\alpha\beta\gamma\delta}(k) = \frac{1}{S(k)}\phi_{(\alpha\beta}(k)\phi_{\gamma\delta)}(k)\,, \tag{3.56}$$

which follows from the double copy relating the three-point amplitudes in gauge theory and in gravity.

We will verify in the next section the position-space version of the expression above, i.e. after performing the on-shell momentum integrals in (3.53). These integrals affect the algebraic structure of the spinors. Notice that the momentum-space Weyl and Maxwell spinors are of type N, if we use the analogue of the position-space characterisation of Weyl spinors. This is consistent with the intuition that the on-shell three-point amplitudes describe radiation of messengers. However, there is something of a puzzle: the field strength of a point charge should have a Coulomb term, and a point mass should have a type D Schwarzschild term. In fact, these terms are present in the Weyl (3.52) and Maxwell (3.46) spinors. They emerge when we perform the Fourier integrals to determine the position-space form of the field strength spinors, as we now show.

3.3 The Position-Space Fields and Weyl Double Copy

In the previous section, we saw that quantum field theory relates the Maxwell and Weyl spinors for a static charge and mass, respectively, by the double copy, at least in Fourier space. We would like to express these quantities in position space. In fact, it is not hard to perform the Fourier integrals to arrive at explicit expressions in position space, where the double copy will still be manifest.

3.3.1 The Maxwell spinor in position space

We will discuss the case of electrodynamics explicitly. Starting from the field strength expectation, equation (3.45), we insert the explicit scalar QED three-point amplitudes to find

$$\begin{aligned} F^{\mu\nu}(x) &\equiv \langle\psi|S^\dagger\, \mathbb{F}^{\mu\nu}(x)\, S|\psi\rangle \\ &= -2Q\,\mathrm{Re}\sum_\eta \int \mathrm{d}\Phi(k)\,\hat{\delta}(k\cdot u)\, e^{-ik\cdot x}\, k^{[\mu}\varepsilon_\eta^{\nu]}\, \varepsilon_{-\eta}\cdot u\,. \end{aligned} \tag{3.57}$$

This expression simplifies if we resolve the proper velocity onto a Newman-Penrose-like basis of vectors given by k^μ, $\varepsilon_\pm^\mu$ and a gauge choice n^μ, such that $k\cdot n \neq 0$ while $n\cdot\varepsilon_\pm = 0$. Since $k\cdot u = 0$ on the support of the integration, the velocity is

$$u^\mu = \frac{u\cdot n}{k\cdot n}\, k^\mu - \varepsilon_-\cdot u\, \varepsilon_+^\mu - \varepsilon_+\cdot u\, \varepsilon_-^\mu\,. \tag{3.58}$$

Consequently, the field strength is given by the simple formula

$$F^{\mu\nu}(x) = 2Q\,\mathrm{Re}\int \mathrm{d}\Phi(k)\,\hat{\delta}(k\cdot u)\, e^{-ik\cdot x}\, k^{[\mu}u^{\nu]}\,. \tag{3.59}$$

Before we perform any integrations, let us pause to interpret this formula. Note that we may write

$$F^{\mu\nu}(x) = 2Q\partial^{[\mu}u^{\nu]}\,\mathrm{Re}\,i\int \mathrm{d}\Phi(k)\,\hat{\delta}(k\cdot u)\,e^{-ik\cdot x}\,. \tag{3.60}$$

We recognise the definition of the field strength as the (antisymmetrised) derivative of the gauge potential,

$$A^{\mu}(x) = \mathrm{Re}\,2iQ\,u^{\mu}\int \mathrm{d}\Phi(k)\,\hat{\delta}(k\cdot u)\,e^{-ik\cdot x}\,. \tag{3.61}$$

To interpret this formula, it's worth briefly digressing to discuss our situation from a classical perspective.

Consider solving the Maxwell equation with a static point charge

$$\partial_{\mu}F^{\mu\nu}(x) = \int d\tau\,Qu^{\nu}\,\delta^4(x-u\tau)\,, \tag{3.62}$$

where $u^{\mu} = (0,1,0,0)$, with the boundary condition that the electromagnetic field vanishes for $t^1 < 0$. Choosing Lorenz gauge, we can write the solution as a familiar Fourier integral:

$$A^{\mu}(x) = -\int \hat{\mathrm{d}}^4k\,\hat{\delta}(k\cdot u)\,e^{-ik\cdot x}\frac{1}{k^2}Qu^{\mu}\,. \tag{3.63}$$

As usual, we need to define the k integral taking our boundary conditions into account. These boundary conditions are also familiar: they are just traditional retarded boundary conditions. The only novelty lies in the signature of the metric. But even the unfamiliar pattern of signs in split signature disappears for the problem at hand, because of the factor

$$\hat{\delta}(k\cdot u) = \hat{\delta}(k_2)$$

in the measure. Consequently, the second component of the wave vector k^{μ} is guaranteed to be zero. We end up with an integral of Minkowskian type, but in $1+2$ dimensions. This is a consequence of translation invariance in the t^2 direction.

Treating the k integration as a contour integral, the only poles in the integration of equation (3.63) occur when

$$(k^1)^2 = \mathbf{k}^2\,, \tag{3.64}$$

where $\mathbf{k} = (k^3, k^4)$ are the spatial components of the wave vector. Taking the sign of the exponent in equation (3.63) into account, retarded boundary conditions are obtained by displacing the poles below the real axis:

$$\frac{1}{k^2} \to \frac{1}{k_{\rm ret}^2} = \frac{1}{(k^1 + i\epsilon)^2 + (k^2)^2 - (k^3)^2 - (k^4)^2}\,, \tag{3.65}$$

while advanced boundary conditions correspond to

$$\frac{1}{k^2} \to \frac{1}{k_{\rm adv}^2} = \frac{1}{(k^1 - i\epsilon)^2 + (k^2)^2 - (k^3)^2 - (k^4)^2}\,. \tag{3.66}$$

Notice that

$$\frac{1}{k_{\rm ret}^2} - \frac{1}{k_{\rm adv}^2} = \frac{1}{k^2 + i(k^1)\epsilon} - \frac{1}{k^2 - i(k^1)\epsilon} \quad = -i\,\mathrm{sign}(k^1)\hat{\delta}(k^2)\,, \tag{3.67}$$

where, in the first equality, we have written (k^1) for the first component of the 4-vector k and have freely rescaled ϵ by positive quantities (as is conventional, we take $\epsilon \to 0$ from above at the end of our calculation).

Returning to the gauge field of equation (3.63), we have

$$\begin{aligned} A^\mu(x) &= -\int \hat{\mathrm{d}}^4 k\, \hat{\delta}(k\cdot u)\, e^{-ik\cdot x} \left(-i\,\mathrm{sign}(k^1)\hat{\delta}(k^2) + \frac{1}{k_{\rm adv}^2}\right) Q u^\mu \\ &= i\int \hat{\mathrm{d}}^4 k\, \hat{\delta}(k\cdot u)\, e^{-ik\cdot x}\ \mathrm{sign}(k^1)\hat{\delta}(k^2)\, Q u^\mu \\ &= i\int \mathrm{d}\Phi(k)\, \hat{\delta}(k\cdot u)\, Q u^\mu \left(e^{-ik\cdot x} - e^{ik\cdot x}\right)\,. \end{aligned} \tag{3.68}$$

We dropped the advanced term because, with our boundary conditions, the position x has positive t^1. But equation (3.68) is just the result we found from the quantum expectation (3.61). Thus, our quantum mechanical methods are computing the complete gauge field, as expected.

Given that we have made contact with a classical situation, we can use classical intuition to perform the Fourier integrals. The integrals to be performed in equation (3.63) are the same as the integrals in the computation of the retarded Green's function in 1 + 2 dimensions. We discuss this Green's function in appendix A.2. We find

$$A^\mu(x) = \frac{Q u^\mu}{2\pi}\Theta(t^1)\frac{\Theta(x^2 - (x\cdot u)^2)}{\sqrt{x^2 - (x\cdot u)^2}}\,. \tag{3.69}$$

In many respects, this result is familiar: it is just the usual 1/'distance' fall-off. There is no other possibility: the dimensional analysis requires this behaviour with distance. The key new feature in split signature is the theta function $\Theta(x^2 - (x \cdot u)^2)$. To see why, let's differentiate to compute the field strength, which is[10]

$$F^{\mu\nu}(x) = -\frac{Q\,\Theta(t^1)\,x^{[\mu}u^{\nu]}}{2\pi(x^2 - (x \cdot u)^2)^{1/2}} \left(\frac{\Theta(x^2 - (x \cdot u)^2)}{x^2 - (x \cdot u)^2} - 2\,\delta\big(x^2 - (x \cdot u)^2\big) \right) . \tag{3.70}$$

The term involving the $\Theta(x^2 - (x \cdot u)^2)$ is the familiar Coulomb field. However, there is an additional δ function describing the impulsive radiation field when the charge "appears" from the point of view of the observer. Although the radiation field looks very singular classically, this should not really trouble us: the delta function distribution is only present in the approximation that the source wave function is treated as of zero size. In reality, this wave function must have some spatial size l_w (see (2.6)), and the delta function will be broadened into a smooth function when this width is taken into account.

It will also be interesting to investigate the Maxwell spinor generated by our set up, especially when comparing to the Weyl spinor in the gravitational case. First, let's break up our field strength into two terms,

$$F_{\mu\nu}(x) = F^{(1)}_{\mu\nu}(x) + F^{(2)}_{\mu\nu}(x)\,, \tag{3.71}$$

where

$$\begin{aligned} F^{(1)}_{\mu\nu}(x) &= -\frac{Q\,\Theta(t^1)\,x_{[\mu}u_{\nu]}}{2\pi(x^2 - (x \cdot u)^2)^{3/2}}\Theta(x^2 - (x \cdot u)^2)\,, \\ F^{(2)}_{\mu\nu}(x) &= \frac{Q\,\Theta(t^1)\,x_{[\mu}u_{\nu]}}{\pi(x^2 - (x \cdot u)^2)^{1/2}}\delta(x^2 - (x \cdot u)^2)\,. \end{aligned} \tag{3.72}$$

It's natural to define the "radial distance" (i.e. its analogue under analytic continuation)

$$\rho^2 = x^2 - (x \cdot u)^2 \tag{3.73}$$

and the associated vector

$$K_\mu = x_\mu - (x \cdot u)u_\mu\,. \tag{3.74}$$

The Maxwell spinor $\phi^{(1)}_{\alpha\beta}(x)$ associated with the Coulombic field strength $F^{(1)}$ is[11]

[10] We assume that the point x is not on the worldline of the source particle, so we drop a term in the field strength involving $\delta(t^1)\Theta(x^2 - (x \cdot u)^2)$, which is only non-vanishing on this worldline.

[11] Here, $\phi^{(1)}_{\alpha\beta}$ corresponds to the middle term on the right-hand side of (3.3). Likewise, $\phi^{(2)}_{\alpha\beta}$

$$\phi^{(1)}_{\alpha\beta}(x) = -\frac{Q\Theta(t^1)}{2\pi\rho^3}\sigma^{\mu\nu}{}_{\alpha\beta}K_{[\mu}u_{\nu]}\Theta(\rho^2)\,. \tag{3.75}$$

Meanwhile, on the support of the delta function factor in $F^{(2)}$, the vector K_μ becomes null. Furthermore, a simple computation shows that, in general,

$$K\cdot u = 0\,. \tag{3.76}$$

Therefore, we may erect a Newman-Penrose basis using the vector K, an arbitrary gauge choice, and two "polarisation" vectors $\varepsilon_\pm(K)$ which can be taken to be the standard spinor-helicity vectors associated with the "on-shell momentum" K; these are defined explicitly in equation (A.12). In this basis we may once again decompose the proper velocity using the obvious analogue of equation (3.58). It follows that the Maxwell spinor is

$$\phi^{(2)}_{\alpha\beta}(x) = \frac{Q}{\pi\,\rho}\,\Theta(t^1)\,X\,|K\rangle_\alpha|K\rangle_\beta\,\delta(\rho^2)\,. \tag{3.77}$$

Evidently, $\phi^{(2)}_{\alpha\beta}(x)$ has the structure expected for the radiative part of the field strength. We will encounter an analogous situation in gravity.

3.3.2 The Weyl spinor and the double copy in position space

We can perform the Fourier integrals for gravity in exact analogy with the electromagnetic case. Beginning from the Weyl tensor (3.51), we insert the explicit amplitudes

$$\mathcal{M}^{(3)}_\eta(k) = -\kappa\,m^2(u\cdot\varepsilon_\eta(k))^2 \tag{3.78}$$

to find that

$$\begin{aligned}W^{\mu\nu\rho\sigma}(x) = -\operatorname{Re} i\kappa^2 m^2\int \mathrm{d}\Phi(k)\,\hat{\delta}(2k\cdot p)\,e^{-ik\cdot x}\Big[&(\varepsilon_+\cdot u)^2 k^{[\mu}\varepsilon_-^{\nu]}k^{[\rho}\varepsilon_-^{\sigma]}\\ &+(\varepsilon_-\cdot u)^2 k^{[\mu}\varepsilon_+^{\nu]}k^{[\rho}\varepsilon_+^{\sigma]}\Big]\,.\end{aligned} \tag{3.79}$$

Again, this expression is easily interpreted in the classical theory. We define the metric perturbation by

$$g_{\mu\nu} = \eta_{\mu\nu} + \kappa h_{\mu\nu}\,. \tag{3.80}$$

further below corresponds to the last term in (3.3).

By solving the linearised Einstein equation in De Donder gauge, we find that the metric perturbation is

$$h_{\mu\nu}(x) = -2\,\mathrm{Re}\, i\kappa m^2 \int \mathrm{d}\Phi(k)\,\hat{\delta}(2k\cdot p)\, e^{-ik\cdot x}\left(u_\mu u_\nu - \frac{1}{2}\eta_{\mu\nu}\right) . \tag{3.81}$$

The Riemann tensor (3.49) is explicitly

$$R^{\mu\nu\rho\sigma}(x) = \mathrm{Re}\, i\kappa^2 m^2 \int \mathrm{d}\Phi(k)\,\hat{\delta}(2k\cdot p)\, e^{-ik\cdot x}\left(k^{[\mu}u^{\nu]}k^{[\sigma}u^{\rho]} - \frac{1}{2}k^{[\mu}\eta^{\nu][\rho}k^{\sigma]}\right) . \tag{3.82}$$

It is not obvious in this form that the traces of the Riemann tensor vanish. Of course, they must do so since our observer at x is in empty space. In fact, it is possible to simplify the tensor structure of this Riemann tensor by resolving the vector u onto the Newman-Penrose-like basis of k, $\epsilon_\pm(k)$ and n as in equation (3.58). The flat metric tensor in this basis is

$$\eta^{\mu\nu} = \frac{1}{k\cdot n}k^{(\mu}n^{\nu)} - \varepsilon_+^{(\mu}\varepsilon_-^{\nu)} . \tag{3.83}$$

It follows that

$$k^{[\mu}\eta^{\nu][\rho}k^{\sigma]} = -k^{[\mu}\varepsilon_+^{\nu]}\varepsilon_-^{[\rho}k^{\sigma]} - k^{[\mu}\varepsilon_-^{\nu]}\varepsilon_+^{[\rho}k^{\sigma]} , \tag{3.84}$$

while the other tensor structure in the Riemann tensor simplifies to

$$\begin{aligned} k^{[\mu}u^{\nu]}k^{[\sigma}u^{\rho]} = (\varepsilon_+\cdot u)^2 k^{[\mu}\varepsilon_-^{\nu]}k^{[\sigma}\varepsilon_-^{\rho]} + (\varepsilon_-\cdot u)^2 k^{[\mu}\varepsilon_+^{\nu]}k^{[\sigma}\varepsilon_+^{\rho]} \\ - \frac{1}{2}k^{[\mu}\varepsilon_-^{\nu]}k^{[\sigma}\varepsilon_+^{\rho]} - \frac{1}{2}k^{[\mu}\varepsilon_+^{\nu]}k^{[\sigma}\varepsilon_-^{\rho]} . \end{aligned} \tag{3.85}$$

Combining, the Riemann tensor manifestly has no traces and we recover the Weyl tensor of equation (3.155).

Now it is easy to perform the Fourier integrals, for example at the level of the metric perturbation, which yields

$$h_{\mu\nu}(x) = -\frac{\kappa m}{4\pi}\Theta(t^1)\frac{\Theta(x^2-(x\cdot u)^2)}{\sqrt{x^2-(x\cdot u)^2}}\left(u_\mu u_\nu - \frac{1}{2}\eta_{\mu\nu}\right) . \tag{3.86}$$

The expectation value of the (linearised) Weyl tensor can be computed by differentiation. There are various terms, depending on whether derivatives act on the delta functions or the $1/\rho$ fall-off factors. Analogously to (3.71), we can write the Weyl tensor as

$$W_{\mu\nu\rho\sigma} = W^{(2)}_{\mu\nu\rho\sigma} + W^{(3)}_{\mu\nu\rho\sigma} + W^{(4)}_{\mu\nu\rho\sigma} , \tag{3.87}$$

with

$$W^{(2)}_{\mu\nu\rho\sigma} = \frac{3\kappa^2\, m\, \Theta(t^1)\, \Theta(\rho^2)}{32\pi\, \rho^5}\; w_{\mu\nu\rho\sigma}\,, \tag{3.88}$$

$$W^{(3)}_{\mu\nu\rho\sigma} = -\frac{\kappa^2\, m\, \Theta(t^1)\, \delta(\rho^2)}{8\pi\, \rho^3}\; w_{\mu\nu\rho\sigma}\,, \tag{3.89}$$

$$W^{(4)}_{\mu\nu\rho\sigma} = \frac{\kappa^2\, m\, \Theta(t^1)\, \delta'(\rho^2)}{8\pi \rho}\; w_{\mu\nu\rho\sigma}\,, \tag{3.90}$$

where

$$w^{\,\mu\nu}{}_{\rho\sigma} = 4\, K^{[\mu} u^{\nu]} K_{[\rho} u_{\sigma]} + 2\, K^{[\mu} \delta^{\nu]}_{[\rho} K_{\sigma]} + 2\, \rho^2\, u^{[\mu} \delta^{\nu]}_{[\rho} u_{\sigma]} + \frac{2\rho^2}{3} \delta^{[\mu}_{[\rho}\, \delta^{\nu]}_{\sigma]}\,. \tag{3.91}$$

The corresponding Weyl spinor is

$$\Psi_{\alpha\beta\gamma\delta} = \Psi^{(2)}_{\alpha\beta\gamma\delta} + \Psi^{(3)}_{\alpha\beta\gamma\delta} + \Psi^{(4)}_{\alpha\beta\gamma\delta}\,, \quad \text{with} \quad \Psi^{(i)}_{\alpha\beta\gamma\delta} = W^{(i)}_{\mu\nu\rho\sigma} \sigma^{\mu\nu}_{\alpha\beta} \sigma^{\mu\nu}_{\gamma\delta}\,. \tag{3.92}$$

If we now compare these expressions with the ones for the Maxwell spinor obtained in the previous subsection, we find the position-space double copy relations

$$\frac{\Theta(\rho^2)\, \Theta(t^1)}{2\pi\, \rho}\, \Psi^{(2)}_{\alpha\beta\gamma\delta} = \frac{3\kappa^2\, m}{4 \cdot 4!\, Q^2} \phi^{(1)}_{(\alpha\beta} \phi^{(1)}_{\gamma\delta)}\,, \tag{3.93}$$

$$\frac{\Theta(\rho^2)\, \Theta(t^1)}{2\pi\, \rho}\, \Psi^{(3)}_{\alpha\beta\gamma\delta} = \frac{\kappa^2\, m}{2 \cdot 4!\, Q^2} \phi^{(1)}_{(\alpha\beta} \phi^{(2)}_{\gamma\delta)}\,, \tag{3.94}$$

$$\frac{\delta^2(\rho^2)\, \Theta(t^1)}{2\pi\, \rho}\, \Psi^{(4)}_{\alpha\beta\gamma\delta} = \frac{\kappa^2\, m\, \delta'(\rho^2)}{4 \cdot 4!\, Q^2} \phi^{(2)}_{(\alpha\beta} \phi^{(2)}_{\gamma\delta)}\,. \tag{3.95}$$

Notice that, in the first two lines, the relation (3.9) is satisfied with

$$S(x) = \frac{\Theta(t_1) \Theta(\rho^2)}{2\pi\, \rho}\,,$$

up to numerical factors. The clearest example is that of $\Psi^{(2)}_{\alpha\beta\gamma\delta}$, which is the only one that has support in the interior of the future light-cone, as opposed to just the future light-cone itself. Hence, it satisfies on its own the Bianchi identity in that region. Indeed, its analytic continuation is the linearised Weyl tensor of the Lorentzian Schwarzschild solution, in the same way that the term $F^{(1)}_{\mu\nu}$ in (3.71) is associated to the Coulomb solution. Therefore, the terms corresponding to the interior of the light-cone satisfy the position space Weyl double copy for type D solutions, equation (3.9), as discussed for the Lorentzian solutions in [98].

The spinors $\Psi^{(3)}_{\alpha\beta\gamma\delta}$ and $\Psi^{(4)}_{\alpha\beta\gamma\delta}$ are distributional, and supported only on the future light-cone, where K_μ is null. Analogously to (3.77), they are both proportional to $|K\rangle_\alpha|K\rangle_\beta|K\rangle_\gamma|K\rangle_\delta$.[12] They look very singular, and they do not satisfy the Bianchi identity on their own on the light-cone, since this identity receives contributions from the three terms. Nevertheless, a type of double copy is still evident in position space, satisfying the expectation of the type N position-space Weyl double copy [128]. In fact, this follows from (3.56), when the on-shell momentum integrands of (3.53) are evaluated only at $k_\mu \propto K_\mu$.

3.4 The Kerr-Schild Double Copy and the Exact Metric

In the previous sections, we computed the linearised metric and curvature generated by a massive particle. It is actually straightforward for us to compute the exact metric. To do so, we exploit the Kerr-Schild double copy presented in the introduction. As a reminder of the Kerr-Schild double copy, recall that, in the case of Lorentzian $(1,3)$ signature, we start with a Green's function

$$\Phi^{(L)} = \frac{1}{4\pi\sqrt{x^2+y^2+z^2}}\,, \tag{3.96}$$

satisfying

$$-(\partial_x^2+\partial_y^2+\partial_z^2)\,\Phi^{(L)} = \delta(x)\delta(y)\delta(z)\,. \tag{3.97}$$

The Coulomb solution is

$$A^{(L)} = Q\,\Phi^{(L)}\,\mathrm{d}t\,, \tag{3.98}$$

or in "Kerr-Schild" gauge,

$$\begin{aligned} A^{(L,KS)} &= Q\,\Phi^{(L)}\,\mathrm{d}t - \frac{Q}{4\pi}\,\mathrm{d}\log\frac{\sqrt{x^2+y^2+z^2}}{r_0} = Q\,\Phi^{(L)}\,L^{(L)}\,, \\ L^{(L)} &= \mathrm{d}t - \frac{x\mathrm{d}x+y\mathrm{d}y+z\mathrm{d}z}{\sqrt{x^2+y^2+z^2}}\,, \end{aligned} \tag{3.99}$$

where $K^{(L)}$ is null and r_0 is a constant needed for dimensional purposes.

[12] Notice that $\phi^{(1)}_{\alpha\beta}$ degenerates on the light-cone (its principal rank-1 spinors coincide), and it becomes proportional to $\phi^{(2)}_{\alpha\beta}$.

The (vacuum) double copy of this solution is the Schwarzschild solution, which can be written in Kerr-Schild coordinates as

$$\mathrm{d}s^2_{(L)} = \mathrm{d}t^2 - \mathrm{d}x^2 - \mathrm{d}y^2 - \mathrm{d}z^2 - \frac{\kappa^2 m}{4}\,\Phi^{(L)}\,L^{(L)}L^{(L)}\,. \tag{3.100}$$

It can also be written in static coordinates as

$$\mathrm{d}s^2_{(L)} = \left(1 - \frac{\kappa^2 m}{4}\,\Phi^{(L)}\right)\mathrm{d}t'^2 - \mathrm{d}x^2 - \mathrm{d}y^2 - \mathrm{d}z^2 - \frac{\frac{\kappa^2 m}{4}\,\Phi^{(L)}}{1 - \frac{\kappa^2 m}{4}\,\Phi^{(L)}}\frac{(x\mathrm{d}x + y\mathrm{d}y + z\mathrm{d}z)^2}{x^2+y^2+z^2}\,, \tag{3.101}$$

with

$$\mathrm{d}t' = \mathrm{d}t + \frac{\frac{\kappa^2 m}{4}\,\Phi^{(L)}}{1 - \frac{\kappa^2 m}{4}\,\Phi^{(L)}}\,\frac{x\mathrm{d}x + y\mathrm{d}y + z\mathrm{d}z}{\sqrt{x^2+y^2+z^2}}\,. \tag{3.102}$$

The commonly-seen Schwarzschild coordinates are obtained by changing from rectangular to spherical coordinates,

$$\mathrm{d}s^2_{(L)} = \left(1 - \frac{\kappa^2 m}{4}\,\Phi^{(L)}\right)\mathrm{d}t'^2 - \frac{\mathrm{d}r^2}{1 - \frac{\kappa^2 m}{4}\,\Phi^{(L)}} - r^2(\mathrm{d}\theta^2 + \sin^2\theta\,\mathrm{d}\phi^2)\,, \tag{3.103}$$

with $r = \sqrt{x^2+y^2+z^2}$ and $\Phi^{(L)} = (4\pi r)^{-1}$.

Following the same steps as in the Lorentzian case, let us consider the case of split signature discussed in previous sections. As we saw earlier (and as is discussed in appendix A.2), the retarded Green's function is

$$\Phi = \frac{\Theta(t_1 - \sqrt{x^2+y^2})}{2\pi\sqrt{t_1^2 - x^2 - y^2}} = \Theta(t_1 - \sqrt{x^2+y^2})\,\hat{\Phi}\,, \tag{3.104}$$

satisfying

$$(\partial^2_{t_1} - \partial^2_x - \partial^2_y)\,\Phi = \delta(t_1)\delta(x)\delta(y)\,. \tag{3.105}$$

The causal boundary condition breaks the t_1 parity. There are major differences with respect to the Lorentzian Green's function, including the singularity structure. The Lorentzian Green's function is singular only at the origin — the locus of the delta-function source. The split-signature Green's function is singular along the future light-cone, even though it is only sourced at the origin of the light-cone. This singularity, both via the denominator and via the discontinuity of the step function, requires some care but, as was seen previously, presents no difficulty in Fourier space.

The associated gauge field is

$$A = Q\,\Phi\,\mathrm{d}t_2\,. \tag{3.106}$$

We can now try to proceed to obtain the "Kerr-Schild" gauge, but two apparent difficulties arise. The first is that a complex gauge transformation is required for the gauge field to be null. This is acceptable as a means to obtain a gravity solution in complex Kerr-Schild form, but which can be made real by a complex diffeomorphism.[13] The second difference is more subtle and is related to the breaking of t^1 time reversal symmetry: the Green's function is not solely a function of $t_1^2 - x^2 - y^2$. Let us proceed in the region $t_1 > \sqrt{x^2+y^2}$, strictly inside the future (3D) light-cone, since the subtlety only affects the light-cone. Then we can obtain the complex 'Kerr-Schild' gauge,

$$\begin{aligned} t_1 > \sqrt{x^2+y^2}\ :\quad A^{(KS)} &= Q\,\hat{\Phi}\,\mathrm{d}t_2 - \frac{Q}{2\pi i}\,\mathrm{d}\log\frac{\sqrt{t_1^2-x^2-y^2}}{r_0} = Q\,\hat{\Phi}\,L\,,\\ L &= \mathrm{d}t_2 + i\,\frac{t_1\mathrm{d}t_1 - x\mathrm{d}x - y\mathrm{d}y}{\sqrt{t_1^2-x^2-y^2}}\,. \end{aligned} \tag{3.107}$$

The exact gravity solution, in complex Kerr-Schild coordinates, is then given as

$$t_1 > \sqrt{x^2+y^2}\ :\quad \mathrm{d}s^2 = \mathrm{d}t_2^2 + \mathrm{d}t_1^2 - \mathrm{d}x^2 - \mathrm{d}y^2 - \frac{\kappa^2 m}{4}\,\hat{\Phi}\,L\,L\,. \tag{3.108}$$

It can be expressed in terms of real coordinates as

$$\begin{aligned} &t_1 > \sqrt{x^2+y^2}\ :\\ &\mathrm{d}s^2 = \left(1 - \frac{\kappa^2 m}{4}\,\hat{\Phi}\right)\mathrm{d}t_2'^{\,2} + \mathrm{d}t_1^2 - \mathrm{d}x^2 - \mathrm{d}y^2 + \frac{\frac{\kappa^2 m}{4}\,\hat{\Phi}}{1-\frac{\kappa^2 m}{4}\,\hat{\Phi}}\,\frac{(t_1\mathrm{d}t_1 - x\mathrm{d}x - y\mathrm{d}y)^2}{t_1^2-x^2-y^2}\,, \end{aligned} \tag{3.109}$$

using

$$\mathrm{d}t_2' = \mathrm{d}t_2 - i\,\frac{\frac{\kappa^2 m}{4}\,\hat{\Phi}}{1-\frac{\kappa^2 m}{4}\,\hat{\Phi}}\,\frac{t_1\mathrm{d}t_1 - x\mathrm{d}x - y\mathrm{d}y}{\sqrt{t_1^2-x^2-y^2}}\,. \tag{3.110}$$

[13]In what regards complexification, this situation is analogous to the double copy interpretation of the Taub-NUT solution from the dyon, and more generally of generic type D vacuum solutions.

Now it is clear how to extend the solution beyond $t_1 > \sqrt{x^2+y^2}$,

$$\mathrm{d}s^2 = \left(1 - \frac{\kappa^2 m}{4}\,\Phi\right)\mathrm{d}t_2'^{\,2} + \mathrm{d}t_1^2 - \mathrm{d}x^2 - \mathrm{d}y^2 + \frac{\frac{\kappa^2 m}{4}\,\Phi}{1-\frac{\kappa^2 m}{4}\,\Phi}\,\frac{(t_1\mathrm{d}t_1 - x\mathrm{d}x - y\mathrm{d}y)^2}{t_1^2 - x^2 - y^2}\,. \tag{3.111}$$

This gives us the final answer of the exact gravity solution.[14] To check its consistency with the previous linearised result, we can put (3.109) in de Donder gauge. This can be done by applying the diffeomorphism generated by

$$\xi = \frac{\kappa^2\, m}{16\pi}\,\mathrm{d}\,\log\frac{\sqrt{t_1^2-x^2-y^2}}{r_0} = \frac{\kappa^2\, m}{8}\,\hat{\Phi}\,(t_1\mathrm{d}t_1 - x\,\mathrm{d}x - y\,\mathrm{d}y)\ . \tag{3.114}$$

The resulting linearised metric is

$$h_{\mu\nu} = -\frac{\kappa\, m}{2}\hat{\Phi}\left(u_\mu u_\nu - \frac{1}{2}\eta_{\mu\nu}\right)\ . \tag{3.115}$$

Once again, this result is valid inside the lightcone. If we wish to extend it outside, we can replace $\hat{\Phi}$ by Φ, recovering (3.86).

3.5 Analytic Continuation to Lorentzian Signature

The discussions above focus on split signature, but there are direct implications for Lorentzian signature, via analytic continuation.

Let us compare again the Green's functions. In the split-signature case, we chose boundary conditions such that the Green's function is

$$\Phi = \frac{\Theta(t_1 - \sqrt{x^2+y^2})}{2\pi\sqrt{t_1^2-x^2-y^2}}\,, \tag{3.116}$$

[14] We could also write the line element in coordinates analogous to the Schwarzschild spherical coordinates, but would have to split into spacetime regions. Inside the light-cone, with $\chi = \sqrt{t_1^2-x^2-y^2}$ and $\hat{\Phi} = (2\pi\chi)^{-1}$, we pick $t_1 = \chi\cosh\psi$ inside the future light-cone and $t_1 = -\chi\cosh\psi$ inside the past light-cone, obtaining

$$t_1^2 > x^2+y^2\ :\quad \mathrm{d}s^2 = \left(1-\frac{\kappa^2 m}{4}\,\Theta(t_1)\hat{\Phi}\right)\mathrm{d}t_2'^{\,2} + \frac{d\chi^2}{1-\frac{\kappa^2 m}{4}\,\Theta(t_1)\hat{\Phi}} - \chi^2(d\psi^2 + \sinh^2\psi\, d\phi^2)\,. \tag{3.112}$$

Outside the light-cone, with $\tilde{\chi} = \sqrt{x^2+y^2-t_1^2}$, we can write

$$t_1^2 < x^2+y^2\ :\quad \mathrm{d}s^2 = \mathrm{d}t_2'^{\,2} - d\tilde{\chi}^2 + \tilde{\chi}^2(-d\tilde{\psi}^2 + \sin^2\tilde{\psi}\, d\phi^2)\,. \tag{3.113}$$

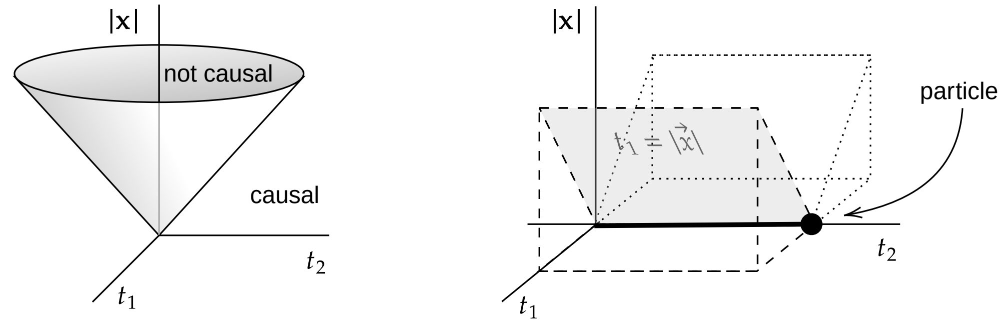

Figure 3.5 *The left image shows the 4D light-cone in split signature. The "inner" part of the cone contains all the events that are not causally connected to the vertex, whereas the events in the "exterior" can be reached by causal curves. On the right, the diagram shows the support of the Green's function for our choice of t_1-retarded boundary conditions. The point particle trajectory is represented by the thick line moving along the t_2 axis. The shaded surface is $t_1 - |\mathbf{x}| = 0$, which contains the radiation. The dashed lines enclose the region where the retarded Green's function is non-zero, i.e. the t_1-future of the particle. The dotted volume is the t_1-past of the particle.*

satisfying

$$(\partial_{t_1}^2 - \partial_x^2 - \partial_y^2)\,\Phi = \delta(t_1)\delta(x)\delta(y)\,. \tag{3.117}$$

Since we have the 3D wave operator, we made a choice that exhibits causality in the subspace $\{t_1, x, y\}$ by picking the retarded Green's function. This is shown in figure 3.5, where the support of the retarded Green's function is represented as a dashed volume.

We could have picked a t_1-symmetric Green's function, which is perhaps more natural from the point of view of analytic continuation to Lorentzian spacetime. With the latter choice, we would have

$$\Phi_{t_1\mathrm{sym}} = \frac{\Theta(t_1^2 - x^2 - y^2)}{4\pi\sqrt{t_1^2 - x^2 - y^2}}\ . \tag{3.118}$$

This follows from the fact that equation (3.117) is satisfied by both the retarded Green's function (3.116), which is supported on the future light cone, and the advanced Green's function, obtained from (3.116) by the substitution $t_1 - \sqrt{x^2+y^2} \to t_1 + \sqrt{x^2+y^2}$ in the argument of the theta function. Then $\Phi_{t_1\mathrm{sym}}$ is the average of the retarded and advanced Green's functions and has support on the dashed and dotted volumes in figure 3.5.[15]

[15]We could also have chosen the Green's function to be $\Theta(x^2+y^2-t_1^2)/(4\pi\sqrt{x^2+y^2-t_1^2})$,

Now, if we perform an analytic continuation to the Lorentzian case via $t_1 \to iz$, we obtain $-i\Phi^{(L)}$, with

$$\Phi^{(L)} = \frac{1}{4\pi\sqrt{x^2+y^2+z^2}} \tag{3.119}$$

satisfying

$$-(\partial_x^2+\partial_y^2+\partial_z^2)\,\Phi^{(L)} = \delta(x)\delta(y)\delta(z)\,. \tag{3.120}$$

From this Green's function, we can construct solutions in electromagnetism and in gravity, and they obviously correspond to the Coulomb and Schwarzschild solutions, respectively. Therefore, the discussions above concerning the description of solutions in terms of scattering amplitudes and the origin of the classical double copy from the double copy of scattering amplitudes extend to the Lorentzian case. The three-point scattering amplitudes that underlie those discussions would then be supported on complex kinematics.

3.6 Non-diagonal double copies: NS-NS fields

As a final application of our set up we want to now study how the double copy can source the following extra fields: dilatons and axions. In fact, in general the duality will not only generate pure Einstein gravity, but more general NS-NS gravity. Besides the graviton, this theory includes a scalar field ϕ, the dilaton, and a two-form field $B_{\mu\nu}$ known as the B-field or the Kalb-Ramond field. A complete classical double copy map should include all three fields on its gravitational side. Examples of such maps have been found using double field theory, both for certain exact solutions [116, 130, 161, 162, 185] and for perturbative solutions [210, 211]. In all these studies, the map is written in terms of fields, in contrast to the Weyl double copy, where the map relates curvatures, which are gauge invariant at the linearised level.

We will address this challenge by investigating a generalised curvature that packages all the NS-NS fields in geometric degrees of freedom, and show how this is sourced by a "non-diagonal" type of double copy. On the amplitude side we will also endow amplitude with both magnetic and spin charges. These new couplings, at tree-level-three-point, will be incorporated by exponential phases

which is acausal from the 3D perspective, but for which the analytic continuation below seems perhaps more straightforward.

according to [23, 107].

Let us go back to the classical geometric side of the story for a moment. In the appendix A.3 we have summarised the main geometric aspects relevant to this section. For the main purpose of this section, we will only need to know how the Riemann tensor packages the new NS-NS data. This is sometimes referred to as "fat" Riemann or generalised curvature field. In what follows, we will restrict to linearised fields. Then, the curvature can be now written as

$$\begin{aligned}\mathfrak{R}_{\mu\nu}{}^{\rho\sigma} &= -\frac{\kappa}{2}\left(\partial_{[\mu}\partial^{[\rho}h_{\nu]}{}^{\sigma]} - \delta_{[\mu}{}^{[\rho}\partial_{\nu]}\partial^{\sigma]}\phi - \partial_{[\mu}\partial^{[\rho}B_{\nu]}{}^{\sigma]}\right)\\ &= -\frac{\kappa}{2}\left(\partial_{[\mu}\partial^{[\rho}h_{\nu]}{}^{\sigma]} - \delta_{[\mu}{}^{[\rho}\partial_{\nu]}\partial^{\sigma]}\phi + \epsilon^{\rho\sigma\lambda}{}_{[\mu}\partial_{\nu]}\partial_{\lambda}\sigma\right)\end{aligned} \tag{3.121}$$

Note that the second expression follows from dualisation in $d = 4$:

$$H_{\mu\nu\rho} = \partial_{[\mu}B_{\nu\rho]} = -\epsilon_{\mu\nu\rho\sigma}\partial^{\sigma}\sigma \ , \tag{3.122}$$

allowing us to characterise the B-field as a scalar.

Soon, we will see how the different products of gauge theory amplitudes are associated to the different components of the generalised curvature. To this end, we will work in $d = 4$ where it is convenient to use the spinor-helicity formalism for the amplitudes. The relation between the amplitudes and the generalised curvature is, therefore, much clearer if we also express the latter spinorially. Thus, we decompose the generalised Riemann tensor as

$$\begin{aligned}\mathfrak{R}_{\alpha\dot{\alpha}\beta\dot{\beta}\gamma\dot{\gamma}\delta\dot{\delta}} &= \mathbf{X}_{\alpha\beta\gamma\delta}\,\epsilon_{\dot{\alpha}\dot{\beta}}\,\epsilon_{\dot{\gamma}\dot{\delta}} + \tilde{\mathbf{X}}_{\dot{\alpha}\dot{\beta}\dot{\gamma}\dot{\delta}}\,\epsilon_{\alpha\beta}\,\epsilon_{\gamma\delta}\\ &\quad + \mathbf{\Phi}_{\alpha\beta\dot{\gamma}\dot{\delta}}\,\epsilon_{\dot{\alpha}\dot{\beta}}\,\epsilon_{\gamma\delta} + \tilde{\mathbf{\Phi}}_{\dot{\alpha}\dot{\beta}\gamma\delta}\,\epsilon_{\alpha\beta}\,\epsilon_{\dot{\gamma}\dot{\delta}} \ ,\end{aligned} \tag{3.123}$$

where we use the bold typeface in order to distinguish the spinors from those of $R_{\mu\nu\rho\sigma}$.

At linearised level, we can compare the right-hand side of (3.123) to the right-hand side of (3.121): the first line of the former corresponds to the graviton contribution, whereas the second line corresponds to contributions from combinations of the dilaton and the axion (which is the single degree of freedom of the B-field in $d = 4$). Our next step is to characterise these components through amplitudes. In this part of the chapter, our emphasis will be more on the gravity side than the gauge theory.

3.6.1 NS-NS fields from Amplitudes

Here, the main ingredient will be the following double copy map

$$\mathcal{M}_{\eta_L \eta_R} = -\frac{\kappa}{4\,Q^2}\, c_{\eta_L \eta_R}\, \mathcal{A}^{(L)}_{\eta_L}\, \mathcal{A}^{(R)}_{\eta_R}\ , \tag{3.124}$$

where there are four choices for (η_L, η_R):

$$(+,+)\,, \quad (-,-)\,, \quad (+,-)\,, \quad (-,+)\,. \tag{3.125}$$

These correspond, respectively, to the gravity field being: positive-helicity graviton, negative-helicity graviton, complex scalar (dilaton and axion), and conjugate complex scalar. In general, we allow for four distinct couplings $c_{\eta_L \eta_R}$ of our massive particle to these gravity fields. Any choice of these couplings will lead to a linearised gravity solution. In practice, we will be most interested in the case where the particle couples equally to the two chiralities, in which case we take $c_{++} = c_{--}$ and $c_{+-} = c_{-+}$.

Consider the following mode expansion of the fat Riemann operator

$$\mathfrak{R}^{\mu\nu\rho\sigma} = \kappa\ \mathrm{Re} \int \mathrm{d}\Phi(k) \left[\sum_{\eta_L \eta_R} a_{\eta_L \eta_R}\, \varepsilon^{[\mu}_{\eta_L}(k) k^{\nu]} \varepsilon^{[\rho}_{\eta_R}(k) k^{\sigma]} \right] e^{-ik\cdot x}\ . \tag{3.126}$$

The operator version of the linearised spinor coefficients are computed by contracting with the sigma matrices as before [212], except now we have more possibilities

$$\mathbf{X}_{\alpha\beta\gamma\delta} = \sigma^{\mu\nu}{}_{\alpha\beta} \sigma^{\rho\sigma}{}_{\gamma\delta}\, \mathfrak{R}_{\mu\nu\rho\sigma}\ , \qquad \tilde{\mathbf{X}}_{\dot\alpha\dot\beta\dot\gamma\dot\delta} = \tilde\sigma^{\mu\nu}{}_{\dot\alpha\dot\beta} \tilde\sigma^{\rho\sigma}{}_{\dot\gamma\dot\delta}\, \mathfrak{R}_{\mu\nu\rho\sigma}\ , \tag{3.127}$$

$$\mathbf{\Phi}_{\alpha\beta\dot\gamma\dot\delta} = \sigma^{\mu\nu}{}_{AB} \tilde\sigma^{\rho\sigma}{}_{\dot\gamma\dot\delta}\, \mathfrak{R}_{\mu\nu\rho\sigma}\ , \qquad \tilde{\mathbf{\Phi}}_{\dot\alpha\dot\beta\gamma\delta} = \tilde\sigma^{\mu\nu}{}_{\dot\alpha\dot\beta} \sigma^{\rho\sigma}{}_{\gamma\delta}\, \mathfrak{R}_{\mu\nu\rho\sigma}\ . \tag{3.128}$$

The resulting spinors are

$$\mathbf{X}_{\alpha\beta\gamma\delta} = \kappa \ \mathrm{Re}\ 2 \int \mathrm{d}\Phi(k)\ a_{--}|k\rangle_\alpha |k\rangle_\beta |k\rangle_\gamma |k\rangle_\delta \, e^{-ik\cdot x} \ , \tag{3.129}$$

$$\tilde{\mathbf{X}}_{\dot\alpha\dot\beta\dot\gamma\dot\delta} = \kappa \ \mathrm{Re}\ 2 \int \mathrm{d}\Phi(k)\ a_{++}[k|_{\dot\alpha}[k|_{\dot\beta}[k|_{\dot\gamma}[k|_{\dot\delta} \, e^{-ik\cdot x} \ , \tag{3.130}$$

$$\mathbf{\Phi}_{AB\dot\gamma\dot\delta} = -\kappa \ \mathrm{Re}\, 2 \int \mathrm{d}\Phi(k)\ a_{-+}\, |k\rangle_\alpha |k\rangle_\beta |_{\dot\gamma}[k|_{\dot\delta} \, e^{-ik\cdot x} \ , \tag{3.131}$$

$$\tilde{\mathbf{\Phi}}_{\dot\alpha\dot\beta\gamma\delta} = -\kappa \ \mathrm{Re}\, 2 \int \mathrm{d}\Phi(k)\ a_{+-}\, [k|_{\dot\alpha}[k|_{\dot\beta}|k\rangle_\gamma |k\rangle_\delta \, e^{-ik\cdot x} \ . \tag{3.132}$$

In order to link these objects to the amplitudes (3.124), we would like to use the equivalent of the coherent state for the NS-NS fields. This is easily generalized from (3.47) as

$$\begin{aligned} S|\psi\rangle = \frac{1}{\mathcal{N}} \int \mathrm{d}\Phi(p)\varphi(p) \exp\Bigg[\int \mathrm{d}\Phi(k)\, i\, \hat\delta(2p\cdot k) \\ \times \left(\sum_{\eta_L\eta_R} \mathcal{M}_{-\eta_L,-\eta_R}(k)\, a^\dagger_{\eta_L\eta_R}(k) \right) \Bigg] |p\rangle \, . \end{aligned} \tag{3.133}$$

Hence, we conclude that

$$\begin{aligned} a_{\eta_L\eta_R}(k) S|\psi\rangle &= \hat\delta(2p\cdot k)\, i\mathcal{M}_{-\eta_L,-\eta_R}(k)\, S|\psi\rangle \\ &= \frac{\delta}{\delta a^\dagger_{\eta_L\eta_R}(k)} S|\psi\rangle \, . \end{aligned} \tag{3.134}$$

Equation (3.134) implies that we can easily exchange annihilation operators for amplitudes inside expectation values, so that we find

$$\mathfrak{R}^{\mu\nu\rho\sigma}(x) = \kappa \ \mathrm{Re}\ i \int \mathrm{d}\Phi(k)\hat\delta(2k\cdot p) \Bigg[\sum_\eta \mathcal{M}_{-\eta_L,-\eta_R}\, \varepsilon^{[\mu}_{\eta_L}(k) k^{\nu]} \varepsilon^{[\rho}_{\eta_R}(k) k^{\sigma]} \Bigg] e^{-ik\cdot x} \, . \tag{3.135}$$

The same can be done in the spinor coefficients. The application of the map

(3.124) results in

$$\mathbf{X}_{\alpha\beta\gamma\delta} = -\frac{\kappa^2 c_{++}}{2Q^2}\,\mathrm{Re}\; i \int \mathrm{d}\Phi(k)\hat{\delta}(2p\cdot k)\,\mathcal{A}_+^{(L)}\mathcal{A}_+^{(R)}\;|k\rangle_\alpha|k\rangle_\beta|k\rangle_\gamma|k\rangle_\delta\, e^{-ik\cdot x}\;, \tag{3.136}$$

$$\tilde{\mathbf{X}}_{\dot\alpha\dot\beta\dot\gamma\dot\delta} = -\frac{\kappa^2 c_{--}}{2Q^2}\,\mathrm{Re}\; i \int \mathrm{d}\Phi(k)\hat{\delta}(2p\cdot k)\,\mathcal{A}_-^{(L)}\mathcal{A}_-^{(R)}\;[k|_{\dot\alpha}[k|_{\dot\beta}[k|_{\dot\gamma}[k|_{\dot\delta}\, e^{-ik\cdot x}\;, \tag{3.137}$$

$$\mathbf{\Phi}_{\alpha\beta\dot\gamma\dot\delta} = +\frac{\kappa^2 c_{+-}}{2\,Q^2}\,\mathrm{Re}\, i \int \mathrm{d}\Phi(k)\hat{\delta}(2p\cdot k)\,\mathcal{A}_+^{(L)}\mathcal{A}_-^{(R)}\;|k\rangle_\alpha|k\rangle_\beta[k|_{\dot\gamma}[k|_{\dot\delta}\, e^{-ik\cdot x}\;, \tag{3.138}$$

$$\tilde{\mathbf{\Phi}}_{\dot\alpha\dot\beta\gamma\delta} = +\frac{\kappa^2 c_{-+}}{2\,Q^2}\,\mathrm{Re}\, i \int \mathrm{d}\Phi(k)\hat{\delta}(2p\cdot k)\,\mathcal{A}_-^{(L)}\mathcal{A}_+^{(R)}\;[k|_{\dot\alpha}[k|_{\dot\beta}|k\rangle_\gamma|k\rangle_\delta\, e^{-ik\cdot x}\;. \tag{3.139}$$

The above expressions make it clear that every quadratic term in the amplitudes sources a different component of the spinorial curvature. We note that the double copy structure is remarkably explicit when all fields are expressed in a spinorial way.

Let us specify the amplitudes now. In earlier sections, we constructed gravity starting from the most basic amplitude in QED for a static point particle. Now, we will generalise this amplitude to allow for magnetic charge and classical spin. In fact, as we will soon see, a non trivial axion field can only be sourced if there is an additional degree of freedom in the gauge amplitude.

The magnetic charge will be achieved by an electromagnetic duality rotation, which transforms the amplitudes as [23, 213]

$$\mathcal{A}_\eta(k) \to \mathcal{A}_\eta(k)\, e^{\theta\,\eta}\;, \tag{3.140}$$

Notice that the rotation parameter has been continued from Lorentzian space $\theta \to -i\theta$ as well.[16] Angular momentum can be induced by a Newman-Janis shift [107, 214]. It acts on the amplitudes as

$$\mathcal{A}_\eta(k) \to \mathcal{A}_\eta(k)\, e^{i\,\eta\,k\cdot a}\;. \tag{3.141}$$

[16] This can be justified by noting that the stress energy tensor has to be invariant under duality transformations.

The vector a^μ is related to the classical angular momentum. It will be taken to lie along the Wick rotated coordinate: $a^\mu = (a, 0, 0, 0)$. Consequently, the Lorentzian exponent $-\eta\, k \cdot a$ has been analytically continued to split signature as $i\,\eta\, k\cdot a$. Neither of these transformations obstructs the exponentiation leading to the coherent state already derived.

Inspired by this we, consider the gauge amplitudes

$$\begin{aligned}\mathcal{A}^{(L)}_\eta &= -2Q(p\cdot\varepsilon_\eta)e^{\eta(\theta_L+ik\cdot a_L)},\\ \mathcal{A}^{(R)}_\eta &= -2Q(p\cdot\varepsilon_\eta)e^{\eta(\theta_R+ik\cdot a_R)},\end{aligned}\tag{3.142}$$

which under the double copy map imply that, for the spinors above

$$\begin{aligned}\mathbf{X}_{\alpha\beta\gamma\delta}(x) &= e^{\bar\theta}\mathbf{X}^{\text{JNW}}_{\alpha\beta\gamma\delta}(x-\bar a)\ ,\\ \tilde{\mathbf{X}}_{\dot\alpha\dot\beta\dot\gamma\dot\delta}(x) &= e^{-\bar\theta}\tilde{\mathbf{X}}^{\text{JNW}}_{\dot\alpha\dot\beta\dot\gamma\dot\delta}(x+\bar a)\ ,\\ \mathbf{\Phi}_{\alpha\beta\dot\gamma\dot\delta}(x) &= e^{\Delta\theta}\mathbf{\Phi}^{\text{JNW}}_{\alpha\beta\dot\gamma\dot\delta}(x-\Delta a)\ ,\\ \tilde{\mathbf{\Phi}}_{\dot\alpha\dot\beta\gamma\delta}(x) &= e^{-\Delta\theta}\tilde{\mathbf{\Phi}}^{\text{JNW}}_{\dot\alpha\dot\beta\gamma\delta}(x+\Delta a)\ ,\end{aligned}\tag{3.143}$$

where we have defined

$$\bar\theta := \theta_L + \theta_R\ , \qquad \Delta\theta := \theta_L - \theta_R\ ,\tag{3.144}$$

$$\bar a := a_L + a_R, \qquad \Delta a := a_L - a_R\,.\tag{3.145}$$

The superscript JNW refers to the solution where both single copies are Coulomb.

In fact, in the previous work [105, 123, 185], it was argued that the most general real spacetime that can be interpreted as a double copy of the Coulomb solution is the solution discovered by Janis, Newman and Winicour (JNW) [215]. The JNW solution has two parameters: mass (‘graviton parameter’) and dilaton parameter; Schwarzschild is the case with vanishing dilaton parameter. In the framework we present here, the two parameters arise from the linear combination of the real graviton field, such that $(\eta_L, \eta_R) = (\pm1, \pm1)$, and the real dilaton field with vanishing axion, $(\eta_L, \eta_R) = (\pm1, \mp1)$.

Notice that, at linearised level, the first two spinors in (3.143) match those of the Schwarzschild solution. The various parameters are elegantly distributed over the different spinors. The parameter $\bar{a}$ corresponds to the spin of Kerr, and appears as expected via the Newman-Janis shift, while $\bar{\theta}$ corresponds to the split-signature version of the rotation between the mass and the NUT parameter; together, these two parameters correspond to the Kerr-Taub-NUT solution [23]. The parameters Δa and $\Delta\theta$ correspond, respectively, to a novel type of Newman-Janis shift for the axion and dilaton, and to the standard axion-dilaton supergravity duality transformation.

The spinorial language is better fitted for displaying the double copy, but it is instructive to think about the dilaton and axion further. We can map (3.135) to the field degrees of freedom using (3.121), together with the mode expansions of the fields

$$\mathbb{h}^{\mu\nu}(x) = 2\ \mathrm{Re} \sum_{\eta} \int \mathrm{d}\Phi(k) a_{\eta\eta}(k) \varepsilon_{\eta}^{\mu}(k) \varepsilon_{\eta}^{\nu}(k)\, e^{-ik\cdot x}\ , \tag{3.146}$$

$$\phi(x) = 2\ \mathrm{Re} \int \mathrm{d}\Phi(k)\, a_{\phi}(k)\, e^{-ik\cdot x}\ , \tag{3.147}$$

$$\mathbb{B}^{\mu\nu}(x) = 2\ \mathrm{Re} \int \mathrm{d}\Phi(k)\, a_{B}(k) \left(\varepsilon_{+}^{\mu}(k) \varepsilon_{-}^{\nu}(k) - \varepsilon_{-}^{\mu}(k) \varepsilon_{+}^{\nu}(k) \right)\, e^{-ik\cdot x}\ . \tag{3.148}$$

Substituting in (3.121) implies that (3.135) can be re-expressed as

$$\begin{aligned} \mathfrak{R}^{\mu\nu\rho\sigma}(x) = \kappa\ \mathrm{Re} \int \mathrm{d}\Phi(k) \Bigg[& \sum_{\eta} a_{\eta} \varepsilon_{\eta}^{[\mu}(k) k^{\nu]} \varepsilon_{\eta}^{[\rho}(k) k^{\sigma]} \\ & + a_{\phi}\, k^{[\mu} \eta^{\nu][\rho} k^{\sigma]} + a_{B}\, k^{[\mu} (\varepsilon_{+}^{\nu]} \varepsilon_{-}^{[\rho} - \varepsilon_{-}^{\nu]} \varepsilon_{+}^{[\rho}) k^{\sigma]} \Bigg] e^{-ik\cdot x}\ . \end{aligned} \tag{3.149}$$

The first term in the second line of (3.149) needs simplification. This is achieved by expanding the flat metric in terms of the null tetrad

$$k^{[\mu} \eta^{\nu][\rho} k^{\sigma]} = -k^{[\mu} \varepsilon_{+}^{\nu]} \varepsilon_{-}^{[\rho} k^{\sigma]} - k^{[\mu} \varepsilon_{-}^{\nu]} \varepsilon_{+}^{[\rho} k^{\sigma]}\,. \tag{3.150}$$

Comparison to (3.126) then implies the following relations between annihilation operators

$$\begin{aligned} a_{++} &= a_{+}\ , \qquad & a_{-+} &= a_{\phi} + a_{B}\ , \\ a_{--} &= a_{-}\ , \qquad & a_{-+} &= a_{\phi} - a_{B}\ , \end{aligned} \tag{3.151}$$

and hence the corresponding relation for amplitudes

$$\begin{aligned}
\mathcal{M}_{\eta\eta} &= -\frac{\kappa}{4\,Q^2}\, c_{\eta\eta}\, \mathcal{A}_\eta^{(L)}\, \mathcal{A}_\eta^{(R)} \ , \\
\mathcal{M}_\phi &= -\frac{\kappa}{4\,Q^2}\, \frac{1}{2} \left(c_{+-} \mathcal{A}_+^{(L)} \mathcal{A}_-^{(R)} + c_{-+} \mathcal{A}_-^{(L)} \mathcal{A}_+^{(R)} \right) \ , \\
\mathcal{M}_B &= -\frac{\kappa}{4\,Q^2}\, \frac{1}{2} \left(c_{+-} \mathcal{A}_+^{(L)} \mathcal{A}_-^{(R)} - c_{-+} \mathcal{A}_-^{(L)} \mathcal{A}_+^{(R)} \right) \ .
\end{aligned} \tag{3.152}$$

In the next sections this prescription will be put into practice to compute the classical fields. In the following we will restrict to the case $c_{++} = c_{--}$ and $c_{+-} = c_{-+}$ since these solutions naturally continue to real solutions in Minkowski signature.

3.6.2 Duality rotation

We will now turn to a concrete example. Consider left and right amplitudes that differ in their EM duality angle,

$$\begin{aligned}
\mathcal{A}_\eta^{(L)} &= -2Q(p\cdot\varepsilon_\eta) e^{\theta_L \eta}, \\
\mathcal{A}_\eta^{(R)} &= -2Q(p\cdot\varepsilon_\eta) e^{\theta_R \eta},
\end{aligned} \tag{3.153}$$

the effect of this difference will be the existence of a rotation between dilaton and axion. The double copied amplitudes are obtained by applying the map (3.152),

$$\begin{aligned}
\mathcal{M}_\eta &= -c_{++}\kappa\, m^2 (u\cdot\varepsilon_\eta)^2\, e^{\bar{\theta}\eta} \ , \\
\mathcal{M}_\phi &= \frac{\kappa\, c_{+-}}{2} p^2 \, \cosh\Delta\theta = \frac{\tilde{c}\, m}{2} \, \cosh\Delta\theta \ , \\
\mathcal{M}_B &= \frac{\kappa\, c_{+-}}{2} p^2 \, \sinh\Delta\theta = \frac{\tilde{c}\, m}{2} \, \sinh\Delta\theta \ ,
\end{aligned} \tag{3.154}$$

where we have defined $\tilde{c} = \kappa\, c_{+-}\, m$. To test the effect of the rotation on the metric, let us compute the transformed Weyl tensor,

$$\begin{aligned}
W^{\mu\nu\rho\sigma}(x) = -\operatorname{Re} i\kappa^2\, c_{++}\, m^2 \int \mathrm{d}\Phi(k)\, \hat{\delta}(2k\cdot p)\, e^{-ik\cdot x} \Big[&(\varepsilon_+\cdot u)^2 k^{[\mu}\varepsilon_-^{\nu]} k^{[\rho}\varepsilon_-^{\sigma]}\, e^{\bar{\theta}} \\
&+ (\varepsilon_-\cdot u)^2 k^{[\mu}\varepsilon_+^{\nu]} k^{[\rho}\varepsilon_+^{\sigma]}\, e^{-\bar{\theta}} \Big] \ .
\end{aligned} \tag{3.155}$$

A little algebra shows that this can be rewritten as

$$
\begin{aligned}
&W^{\mu\nu\rho\sigma}(x) = -\,\mathrm{Re}\, i\kappa^2\, c_{++}\, m^2 \int \mathrm{d}\Phi(k)\, \hat{\delta}(2k\cdot p)\, e^{-ik\cdot x} \\
&\times \left[\cosh\bar{\theta}\left(k^{[\mu}u^{\nu]}k^{[\rho}u^{\sigma]} + \frac{1}{2}k^{[\mu}\eta^{\nu][\rho}k^{\sigma]}\right) - \frac{1}{2}\sinh\bar{\theta}\,\epsilon^{\mu\nu\tau\lambda}\left(k_{[\tau}u_{\lambda]}k^{[\rho}u^{\sigma]} + \frac{1}{2}k_{[\tau}\delta^{[\rho}_{\lambda]}k^{\sigma]}\right)\right] .
\end{aligned}
\tag{3.156}
$$

The first term, with the hyperbolic cosine, corresponds to the Schwarzschild solution, expression (3.26) of [1], which we will denote $W^{\mu\nu\rho\sigma}_{\text{Schw.}}$. Making use of this notation leads to the compact result

$$
W^{\mu\nu\rho\sigma} = \cosh\bar{\theta}\; W^{\mu\nu\rho\sigma}_{\text{Schw.}} - \sinh\bar{\theta}\,\frac{1}{2}\epsilon^{\mu\nu\tau\lambda}\; W^{\text{Schw.}\;\rho\sigma}_{\quad\tau\lambda} . \tag{3.157}
$$

The second term represents the dual of $W_{\text{Schw.}}$, in analogy with electromagnetic duality. We conclude that the angle $\bar{\theta}$ indeed rotates the mass and the NUT charge of the solution [121, 213].

The Weyl tensor we have computed represents the graviton degrees of freedom in $\mathfrak{R}^{\mu\nu\rho\sigma}$. The next step is to obtain the classical expectation value of the dilaton and axion degrees of freedom. Instead of computing the corresponding components of $\mathfrak{R}^{\mu\nu\rho\sigma}$, we will obtain the field profiles ϕ and σ directly.

Let us start with the classical expectation value of the dilaton field, $\phi = \langle\psi|S^\dagger\phi S|\psi\rangle$. We use the field operator (3.147), exponentiation of the coherent state (3.133) with the amplitude given in (3.154). The result is

$$
\phi(x) = \tilde{c}\, m\, \cosh\Delta\theta\;\; \mathrm{Re}\, i \int \mathrm{d}\Phi(k)\, \hat{\delta}(2p\cdot k) e^{-ik\cdot x} . \tag{3.158}
$$

Performing the integration (see the appendix A.2), we obtain

$$
\phi(x) = \tilde{c}\, \cosh\Delta\theta\; \frac{\Theta(\rho^2)}{8\pi}\,\frac{1}{\rho} . \tag{3.159}
$$

We will now tackle the axion field. Recalling (3.148) and taking a derivative, we quickly find

$$
H_{\mu\nu\rho}(x) = \frac{1}{2}\partial_{[\mu}B_{\nu\rho]}(x) = \frac{\tilde{c}}{2}\,\sinh\Delta\theta\,\mathrm{Re}\int \mathrm{d}\Phi(k)\hat{\delta}(u\cdot k)k_{[\mu}\varepsilon^+_\nu\varepsilon^-_{\rho]}\, e^{-ik\cdot x} . \tag{3.160}
$$

At this stage, it is very helpful to note that

$$
\epsilon^{\mu\nu\rho\sigma}k_{[\nu}\varepsilon^+_\rho\varepsilon^-_{\sigma]} = k^{[\mu}n^\nu\varepsilon^\rho_+\varepsilon^{\sigma]}_- k_{[\nu}\varepsilon^+_\rho\varepsilon^-_{\sigma]} = -3!\, k^\mu , \tag{3.161}
$$

having expressed the Levi-Civita in a convenient basis $\epsilon^{\mu\nu\rho\sigma} = k^{[\mu} n^{\nu} \varepsilon_{+}^{\rho} \varepsilon_{-}^{\sigma]}$. Hence,

$$
\begin{aligned}
\Rightarrow \epsilon^{\mu\nu\rho\sigma} H_{\nu\rho\sigma}(x) &= -3\,\tilde{c}\,\sinh\Delta\theta\ \mathrm{Re}\int \mathrm{d}\Phi(k)\,\hat{\delta}(k\cdot u)\,k^{\mu}\,e^{-ik\cdot x} \\
&= -3\,\tilde{c}\,\sinh\Delta\theta\,\partial^{\mu}\left(\frac{\Theta(\rho^2)}{4\pi}\,\frac{1}{\rho}\right) \ .
\end{aligned}
\tag{3.162}
$$

This expression provides direct information on the axion σ. To see how, note from equation (A.40), expanded to leading order, that the relation between H and σ is simply

$$
H_{\mu\nu\rho} = -\epsilon_{\mu\nu\rho\sigma}\,\partial^{\sigma}\sigma \Rightarrow \epsilon^{\mu\nu\rho\sigma} H_{\nu\rho\sigma} = -3!\,\partial^{\mu}\sigma \ . \tag{3.163}
$$

Comparing with the previous expression, we find

$$
\sigma(x) = \tilde{c}\,\sinh\Delta\theta\,\frac{\Theta(\rho^2)}{8\pi}\,\frac{1}{\rho} \ , \tag{3.164}
$$

which vanishes if $\Delta\theta \to 0$.

3.6.3 Newman-Janis shift

Now we turn our attention to the spin parameter. Just as we did in the previous section, we can use the prescription (3.124) to source an axion and a dilaton. However, we now consider products of gauge theory amplitudes with different spins

$$
\begin{aligned}
\mathcal{A}_{\eta}^{(L)} &= -2Q(p\cdot\varepsilon_{\eta})e^{i\,\eta\,a_L\cdot k}, \\
\mathcal{A}_{\eta}^{(R)} &= -2Q(p\cdot\varepsilon_{\eta})e^{i\,\eta\,a_R\cdot k}.
\end{aligned}
\tag{3.165}
$$

These yield the following gravity amplitudes

$$
\begin{aligned}
\mathcal{M}_{\eta} &= -\kappa\,c_{++}\,m^2(u\cdot\varepsilon_{\eta})^2\,e^{i\,\eta\,\bar{a}\cdot k} \ , \\
\mathcal{M}_{\phi} &= \frac{\tilde{c}\,m}{2}\ \cos(\Delta a\cdot k) \ , \\
\mathcal{M}_{B} &= \frac{\tilde{c}\,m}{2}\ \sin(\Delta a\cdot k) \ .
\end{aligned}
\tag{3.166}
$$

Once more, the graviton components of the fat curvature tensor found in (3.135) reduce to the Weyl tensor

$$
W^{\mu\nu\rho\sigma}(x) = \kappa\,c_{++}\ \mathrm{Re}\ i\int \mathrm{d}\Phi(k)\hat{\delta}(2k\cdot p)e^{-ik\cdot x}\sum_{\eta}\mathcal{M}_{\eta}\varepsilon_{-\eta}^{[\mu}k^{\nu]}\varepsilon_{-\eta}^{[\rho}k^{\sigma]}e^{i\eta k\cdot\bar{a}}. \tag{3.167}
$$

It is not difficult to see that this matches the classical computation with a spinning source. The linearised EOMs are, writing $g_{\mu\nu}(x) = \eta_{\mu\nu} + \kappa\, h_{\mu\nu}(x)$

$$\partial^2 h^{\mu\nu}(x) = -\kappa\, \mathsf{P}^{\mu\nu}{}_{\alpha\beta} T^{\alpha\beta}(x), \qquad \mathsf{P}^{\mu\nu}{}_{\alpha\beta} = \frac{1}{4}\delta^{(\mu}{}_{(\alpha}\delta^{\nu)}{}_{\beta)} - \frac{1}{2}\eta^{\mu\nu}\eta_{\alpha\beta}, \tag{3.168}$$

with the following stress-energy tensor for Kerr [214, 216]

$$T^{\mu\nu}(x) = m \int \mathrm{d}\tau\, u^{(\mu} \exp(\bar{a} * \partial)^{\nu)}{}_{\rho} u^{\rho} \delta^{(4)}(x - u\tau)\,, \tag{3.169}$$

where we defined $(\bar{a} * \partial)_{\mu\nu} = \epsilon_{\mu\nu\rho\sigma}\bar{a}^{\rho}\partial^{\sigma}$. Solving (3.168) with the usual boundary conditions, we find the linearised metric

$$\begin{aligned} h^{\mu\nu}(x) &= -\kappa m^2 \mathrm{Re}\, i \int \mathrm{d}\Phi(k) \hat{\delta}(p\cdot k) e^{-ik\cdot x}\, \mathsf{P}^{\mu\nu}{}_{\alpha\beta}\, u^{(\alpha} \exp(-i\bar{a} * k)^{\beta)}{}_{\rho} u^{\rho} \\ &= -\kappa m^2 \mathrm{Re}\, i \int \mathrm{d}\Phi(k) \hat{\delta}(p\cdot k) e^{-ik\cdot x} \left[\left(u^{\mu}u^{\nu} - \frac{1}{2}\eta^{\mu\nu} \right) \cos(\bar{a}\cdot k) \right. \\ &\qquad\qquad \left. - \frac{i}{2} u^{(\mu}\epsilon^{\nu)}(\bar{a}, k, u)\, \frac{\sin(\bar{a}\cdot k)}{\bar{a}\cdot k} \right], \end{aligned} \tag{3.170}$$

from which the curvature can be computed. After some tedious but straightforward algebra one finds

$$W^{\mu\nu\rho\sigma}(x) = -\kappa^2 m^2 \mathrm{Re}\, i \sum_{\eta} \int \mathrm{d}\Phi(k) \hat{\delta}(2p\cdot k) e^{-ik\cdot x} (\varepsilon_{\eta}\cdot u)^2 k^{[\mu}\varepsilon^{\nu]}_{-\eta} k^{[\rho}\varepsilon^{\sigma]}_{-\eta} e^{i\eta k\cdot\bar{a}}. \tag{3.171}$$

The result matches the one we obtained from amplitudes upon setting $c_{++} = 1$.

For the dilaton and the axion, the calculations are formally analogous to the ones outlined in 3.6.2, except that now we have momentum dependent trigonometric functions which characterise the spin mixing. We find for the dilaton

$$\begin{aligned} \phi(x) &= \frac{\tilde{c}}{2}\, \mathrm{Re}\, i \int \mathrm{d}\Phi(k)\, \hat{\delta}(u\cdot k) e^{-ik\cdot x} \cos(\Delta a\cdot k) \\ &= \frac{\tilde{c}}{8} \left(S_{\Delta a,0}(x) + S_{-\Delta a,0}(x) \right), \end{aligned} \tag{3.172}$$

where the scalar potential is a straightforward extension of the one in (3.55)

$$\begin{aligned} S_{a,\theta}(x) &:= 2\,\mathrm{Re}\, i \int \mathrm{d}\Phi(k)\hat{\delta}(k\cdot u)\, e^{-i\,k\cdot(x-a)}e^{\theta} \\ &= \frac{e^{\theta}}{2\pi}\,\frac{\Theta((t_1-a)^2-r^2)}{\sqrt{(t_1-a)^2-r^2}} = e^{\theta}S_{0,0}(x-a). \end{aligned} \tag{3.173}$$

The axion is instead given by

$$\epsilon^{\mu\nu\rho\sigma}H_{\nu\rho\sigma}(x) = -3\,\tilde{c}\,\partial^{\mu}\,\mathrm{Re}\, i \int \mathrm{d}\Phi(k)\,\hat{\delta}(k\cdot u)\, e^{-ik\cdot x}\sin(\Delta a\cdot k), \tag{3.174}$$

telling us that the scalar σ is at leading order

$$\begin{aligned} \sigma(x) &= \frac{\tilde{c}}{2}\,\mathrm{Re}\, i \int \mathrm{d}\Phi(k)\,\hat{\delta}(u\cdot k)e^{-ik\cdot x}\sin(\Delta a\cdot k) \\ &= \frac{\tilde{c}}{8}\left(S_{\Delta a,0}(x) - S_{-\Delta a,0}(x)\right), \end{aligned} \tag{3.175}$$

which is again vanishing in the spinless limit.

3.6.4 Comparison with known solutions

The linearised solution obtained in section 3.6.2 corresponds to an axi-dilaton Taub-NUT black hole. This solution is known exactly; see (17), (19) in [217]. It is interesting to check that our results agree with the linearisation of the known solution. There, dilaton and axion are given as[17]

$$e^{-\phi} = (1+\epsilon^2)\frac{\Lambda^{\delta}}{\epsilon^2\Lambda^{2\delta}+1}\,, \qquad \sigma = \frac{\epsilon(\Lambda^{2\delta}-1)}{\epsilon^2\Lambda^{2\delta}+1}\,, \tag{3.176}$$

where

$$\Lambda = 1 - \frac{R_0}{R}\,,$$

$\delta\, R_0$ is the charge of the dilaton and ϵ is a duality rotation parameter between dilaton and axion. Notice that R is the (3,1) signature equivalent of ρ. At linearised level, the fields decouple and the metric is equivalent to Taub-NUT. Expanding at linear order the other fields and defining $\epsilon = -\tan\frac{\Delta\theta}{2}$, we find

$$\phi = \cos\Delta\theta\,\frac{\delta\, R_0}{R}\,, \qquad \sigma = \sin\Delta\theta\,\frac{\delta\, R_0}{R}\,. \tag{3.177}$$

[17] Ignoring factors of $\sqrt{3}$ that can be absorbed into δ at linear order..

Our solution (3.159), (3.164) agrees with this up to an overall constant ($\tilde{c} = 16\pi\,\delta\,R_0$). Then, $\Delta\theta$ is just the parameter inside $\mathrm{SL}(2,\mathbb{R})$ that generates linear rotations between dilaton and axion.

In the special case where $\theta_L = \theta_R$ both single copies are identical, and we have no mixing: $\Delta\theta = 0$. From (3.154), we see that this implies that the axion will vanish, leaving a linearised solution that would be the equivalent to Taub-NUT plus the dilaton. In [217], this corresponds to (17) and (18).

On the contrary, if $\theta_R = -\theta_L$, $\bar{\theta}$ vanishes and the resulting metric has vanishing NUT charge. The result is a linearised Schwarzschild metric plus axion plus dilaton, corresponding to the linearisation of (10) and (13) in [217].

When both rotation angles are zero, both the NUT charge and axion vanish. We are left with a linearised JNW solution.

The solutions considered in section 3.6.3 involving spin are not so well understood in the literature. There have been attempts to apply a Newman-Janis shift to the JNW solution, with the prospects of obtaining a spinning generalisation. However, these claimed generalisations fail to satisfy the Einstein-dilaton equations of motion [218]. Although linear, our solution might help to find a satisfactory generalisation of the JNW metric with spin.

3.7 Discussion

Let us summarise the results gathered in this chapter. We used the building block of the on-shell approach to scattering amplitudes, the three-point amplitude, to study classical solutions in electromagnetism and in gravity. The three-point amplitudes studied correspond to the emission of a messenger (photon or graviton) by a charged/massive particle, and the classical solutions are precisely the solutions sourced by the massive particle. In order for the three-point amplitude to be non-trivial, we worked with a split-signature spacetime. The alternative would have been to consider complexified momenta in Lorentzian signature, as often done in the scattering amplitudes literature, but we found the split-signature choice more straightforward, given that relevant quantities like spinors are real. Moreover, split signature is interesting in its own right, particularly regarding boundary conditions and the meaning of causality. We discussed how our results are related via analytic continuation to Lorentzian signature.

Building on the KMOC formalism [49], we used the three-point amplitude to determine the coherent state generated by the massive particle, which is associated to the split-signature versions of the Coulomb and Schwarzschild solutions, for electromagnetism and gravity respectively. We described how to extract from that a classical field, namely via the expectation value of a quantum operator on the coherent state, in the classical limit. As operators, we considered the 'curvatures': the field strength in electromagnetism and the spacetime curvature in vacuum (Weyl or Riemann, as they match in vacuum). These are gauge-invariant quantities (for gravity, in the linearised approximation). We found that the vacuum expectation value of these curvatures is an on-shell Fourier transform of the corresponding three-point amplitudes. This is easier to verify when we express the curvatures in terms of spinors, namely the Maxwell and Weyl spinors.

The expressions we obtained for the Maxwell and Weyl spinors exhibit a Weyl-type classical double copy in on-shell momentum space, which follows directly from the double copy of the three-point scattering amplitudes. We then showed that this leads to the previously known Weyl double copy in position space, which applies to certain algebraically special classes of solutions [98, 128].

Then, we also used the Kerr-Schild-type classical double copy to obtain the exact gravity solution, rather than the linearised one. This is, to our knowledge, the first use of the classical double copy to write down a novel solution: the split-signature version of Schwarzschild. Although this could also have been achieved by analytic continuation of the Lorentzian Schwarzschild solution, with due attention paid to the split-signature boundary conditions, it was easier for us to use the classical double copy given that the split-signature boundary conditions were directly related to those in gauge theory.

Finally, building upon knowledge gathered from the Coulomb-Schwarzschild correspondence, we generalised our double copy map to source new types of fields: axions and dilatons. These are obtained from more general gauge theory amplitudes which involve additional magnetic and spin couplings. Although now the classical spinor fields correspond to more complicated gravity solutions, the underlying philosophy remains the same: the fundamental building block in $(2,2)$ is still the simple three-point tree-level gauge theory amplitude. Furthermore, the Weyl double copy structure continues to be straightforward at the spinorial level, confirming the power of on-shell variables.

The domain of applicability of the classical double copy is a natural question. Although many previous results support these ideas, we have provided here the ultimate connection to the double copy of scattering amplitudes. The Weyl double copy in on-shell momentum space *is* the amplitudes double copy.

This discussion brings the end of the chapter and at a good point to start the next one. Indeed, we will now focus on NLO waveforms, this time in Minkowski space signature.

Chapter 4

One-Loop Waveforms: Radiation and Reaction

4.1 Introduction

Gravitational waveforms sourced by compact binary coalescence events are now the basic physical observable in precision studies of General Relativity. As we argued in the introduction, these waveforms are closely related to the Riemann curvature: in the transverse traceless gauge, the waveform's second derivative is a curvature component.

In this chapter, we will make heavy use of generalised unitarity [88, 89] to study these objects. This method allows us to construct loop-level scattering amplitudes from tree amplitudes. We can further combine the double copy and generalised unitarity, effectively building the dynamical information necessary for gravitational waveforms from tree amplitudes in Yang-Mills theory. The union of generalised unitarity and the double copy has already proven very fruitful in the study of General Relativity, and provides a fresh perspective on the relativistic two-body problem [4–33, 51, 74, 75, 96, 219–229].

We make use of a method for constructing radiation fields from amplitudes which has been developed in recent years [8, 33, 42, 44, 49, 137, 174, 230]. Similarly to the previous chapter, the basic idea is to use a quantum-mechanical language to describe the event; the physical observable to be computed becomes the expectation value of the Riemann curvature (this time in $(3,1)$ signature). As we will see, the formalism is general and can be applied to field strengths in a variety of theories: electromagnetism, Yang-Mills theory, and gravity.

In this chapter, we build on previous work which studied scattering encounters between classical, point-like objects at leading order (LO) [33, 44, 48, 49, 137]. We describe the structure of field strength observables at next-to-leading order (NLO) in terms of scattering amplitudes. As we have hinted at in the introductory section 2.1, the structure of on-shell observables is remarkably simple. These are always made of two types of contributions: one which is linear in the amplitude and another one with cuts of amplitudes. We will see this here as well, applied to waveforms. At NLO, these will turn out to be associated with the real and imaginary parts of a one-loop five-point amplitude (the latter being related to cuts). We will see that the imaginary part has the classical interpretation of the portion of radiation emitted by an object accelerating under its own self-field. That is, the imaginary part arises as a consequence of radiation reaction at one loop order. This radiation from radiation-reaction is determined by Compton amplitudes in electrodynamics, YM theory, and in gravity. Our treatment makes it clear that this aspect of radiation reaction double-copies in a straightforward manner at NLO.

We begin in section 4.2 with a discussion the general structure of field-strength observables at NLO before describing some technical simplifications we can take advantage of at this order in section 4.3. After those preliminaries, we dive into the main computations of the chapter. First, in section 4.4, we determine the radiation at one loop which is associated with the real part of the scattering amplitude. This part of the radiation field is classically associated with essentially conservative forces (eg the Lorentz force in electromagnetism). Then, we inspect the role of the imaginary part in section 4.5. This will turn out to be related to radiation reaction and dissipative forces. Finally, we address infrared divergences in 4.6 and then we conclude.

4.2 Field strengths from amplitudes

Our goal is to compute the radiation field generated by a scattering event involving two point-like classical objects using the methods of scattering amplitudes. The basic observable of interest is the field strength (in electrodynamics and YM theory) or the Riemann curvature (in gravity), both of which are very similar in structure; we will refer to both generically as "field strengths". In this section, we explain how to determine these field strengths from scattering amplitudes at next-to-leading order accuracy. We begin with a short review of the connection between amplitudes and observables, focusing on the case of the field strength.

4.2.1 States and observables

Field strengths, as observables in themselves, were first discussed from the perspective of amplitudes in references [1, 33] and were recently reviewed in [231, 232]. Amplitudes are quantum-mechanical objects, so we must start by specifying an initial quantum state which happens to be in the domain of validity of the classical approximation. If we also arrange initial conditions so that we may rely on the classical approximation throughout the scattering event, the equivalence principle guarantees that the quantum treatment will agree with a classical treatment up to small quantum corrections which we systematically drop. As in the previous chapter, we will follow the notation of KMOC closely below.

We choose our initial state to be the usual two-particle one

$$|\psi\rangle = \int \mathrm{d}\Phi(p_1, p_2)\, \phi_b(p_1, p_2)|p_1, p_2\rangle\,, \tag{4.1}$$

with

$$\phi_b(p_1, p_2) \equiv e^{ib_1\cdot p_1} e^{ib_2\cdot p_2} \phi_1(p_1)\phi_2(p_2)\,, \tag{4.2}$$

being a sharply-peaked wavefunction on classical momenta values. The two-particle wavefunction in equation (4.2) displaces particle i by a distance b_i relative to an origin; then the impact parameter is $b_{12} = b_1 - b_2$.

Our basic task is to compute the future expectation value of a field strength operator. In Yang-Mills theory, the relevant operator is the field strength tensor

$$\mathbb{F}^a_{\mu\nu} = \partial_\mu \mathbb{A}^a_\nu - \partial_\nu \mathbb{A}^a_\mu + g f^{abc} \mathbb{A}^b_\mu \mathbb{A}^c_\nu\,. \tag{4.3}$$

There is one immediate simplification from working in the far-field limit. In the far field, the expectation value of the Yang-Mills potential $\mathbb{A}(x)$ is inversely proportional to the large radius r between the observer and the scattering event. We will only be interested in this leading $1/r$ behaviour. As a result we may replace the full non-Abelian field strength with its abelianised version:

$$\mathbb{F}^a_{\mu\nu} \simeq \partial_\mu \mathbb{A}^a_\nu - \partial_\nu \mathbb{A}^a_\mu \,. \tag{4.4}$$

In gravity, we are only interested in the expectation value of the linearised Riemann tensor for the same reason. It may be worth emphasising that there is still non-linear (non-Abelian) dynamics in the core of spacetime.

The state in the far future is $S|\psi\rangle$ since the S matrix is the all-time evolution operator. Placing our detector at a position x near lightlike future infinity, the observable of interest to us in Yang-Mills theory is

$$F^a_{\mu\nu}(x) \equiv \langle\psi|S^\dagger \mathbb{F}^a_{\mu\nu}(x) S|\psi\rangle \,. \tag{4.5}$$

As we did before, we connect with scattering amplitudes using the mode expansion for the quantum field $\mathbb{A}^a_\mu$:

$$\mathbb{A}^a_\mu(x) = \sum_\eta \int \mathrm{d}\Phi(k) \left[\varepsilon^\eta_\mu(k) a^a_\eta(k) e^{-ik\cdot x} + \text{h.c.}\right] \,, \tag{4.6}$$

so that

$$F^a_{\mu\nu}(x) = 2\,\mathrm{Re} \sum_\eta \int \mathrm{d}\Phi(k) \left[-ik_{[\mu}\varepsilon^\eta_{\nu]}(k) \langle\psi|S^\dagger a^a_\eta(k) S|\psi\rangle e^{-ik\cdot x}\right] \,. \tag{4.7}$$

Most of our focus in this chapter will be on the computation of $\langle\psi|S^\dagger a^a_\eta(k) S|\psi\rangle$. Once this quantity is known, an explicit expression for the field strength can be found by integration.

In gravity, defining the curvature expectation

$$R_{\mu\nu\rho\sigma}(x) \equiv \langle\psi|S^\dagger \mathbb{R}_{\mu\nu\rho\sigma}(x) S|\psi\rangle \,, \tag{4.8}$$

it similarly follows that

$$R_{\mu\nu\rho\sigma}(x) = \kappa\,\mathrm{Re} \sum_\eta \int \mathrm{d}\Phi(k) \left[k_{[\mu}\varepsilon^\eta_{\nu]}(k) k_{[\rho}\varepsilon^\eta_{\sigma]}(k) \langle\psi|S^\dagger a_\eta(k) S|\psi\rangle e^{-ik\cdot x}\right] \,. \tag{4.9}$$

We have introduced the annihilation operator $a_\eta(k)$ of a graviton state with helicity η and momentum k. As in gauge theory, the key dynamical quantity to be determined is $\langle\psi|S^\dagger a^a_\eta(k) S|\psi\rangle$.

The field strength of equation (4.7) and the curvature (4.9) both involve an integration over the phase space of a massless particle. At large distances, this integral can be reduced to a one-dimensional Fourier transform using standard methods (see [231, 232] for a recent review). Writing the observation coordinate as $x = (x^0, \boldsymbol{x})$ and introducing the retarded time $u = x^0 - |\boldsymbol{x}|$, the results are

$$F^a_{\mu\nu}(x) = \frac{-1}{4\pi|\boldsymbol{x}|} 2\,\mathrm{Re} \int_0^\infty \hat{\mathrm{d}}\omega\, e^{-i\omega u} \sum_\eta k_{[\mu}\varepsilon^\eta_{\nu]}(k)\, \langle\psi|S^\dagger a^a_\eta(k) S|\psi\rangle\,, \tag{4.10}$$

in Yang-Mills theory, and

$$R_{\mu\nu\rho\sigma}(x) = \frac{-\kappa}{4\pi|\boldsymbol{x}|} \mathrm{Re} \int_0^\infty \hat{\mathrm{d}}\omega\, e^{-i\omega u} \sum_\eta ik_{[\mu}\varepsilon^\eta_{\nu]}(k) k_{[\rho}\varepsilon^\eta_{\sigma]}(k)\, \langle\psi|S^\dagger a_\eta(k) S|\psi\rangle\,, \tag{4.11}$$

in gravity. Note that in both integrals (4.10) and (4.11) the momentum of the messenger reads $k^\mu = \omega(1, \hat{\mathbf{x}})$.

In terms of amplitudes and quantum field theory, then, the object we need to compute is

$$\alpha_\eta(k) \equiv \langle\psi|S^\dagger a_\eta(k) S|\psi\rangle\,, \tag{4.12}$$

where $a_\eta(k)$ is an annihilation operator for the relevant field. We will refer to this quantity as the "waveshape", since it is the parameter describing the coherent state of radiation which has the same field strength as given in equation (4.7). The connection between amplitudes, coherent states and radiation will be the topic of the next chapter.

Having discussed the general connection between amplitudes and field strengths, let us now understand how to construct the waveshape from perturbative scattering amplitudes.

One obvious way to proceed is simply to extend the KMOC framework, as previously done. We compute the matrix element by expanding $S = 1 + iT$. This immediately leads to the leading order expression

$$\alpha_\eta(k) = \int \mathrm{d}\Phi(p_1', p_2', p_1, p_2)\, \phi_b^*(p_1', p_2')\phi_b(p_1, p_2)\hat{\delta}^D(p_{\mathrm{tot}})\, i\mathcal{A}_{5,0}(p_1, p_2 \to p_1', p_2', k_\eta)\,, \tag{4.13}$$

where we are adopting the notation that $\mathcal{A}_{n,L}$ is an n point, L loop amplitude. The waveshape is slightly more involved at one loop (order g^5), where we encounter two terms

$$\alpha_\eta(k) = \int \mathrm{d}\Phi(p_1', p_2', p_1, p_2)\, \phi_b^*(p_1', p_2')\phi_b(p_1, p_2)\hat{\delta}^D(p_{\mathrm{tot}})\, \Big(i\mathcal{A}_{5,1}(p_1, p_2 \to p_1', p_2', k_\eta) + \int \mathrm{d}\Phi(\tilde{p}_1, \tilde{p}_2)\hat{\delta}^D(\tilde{p}_{\mathrm{tot}})\mathcal{A}_{5,0}(p_1, p_2 \to \tilde{p}_1, \tilde{p}_2, k_\eta)\mathcal{A}_{4,0}^*(\tilde{p}_1, \tilde{p}_2 \to p_1', p_2') \Big)\,, \tag{4.14}$$

with the delta functions imposing the usual conservation of energy and momentum

$$p_{\mathrm{tot}} = p_1 + p_2 - p_1' - p_2' - k = 0, \quad \tilde{p}_{\mathrm{tot}} = \tilde{p}_1 + \tilde{p}_2 - p_1' - p_2' = 0, \tag{4.15}$$

for external states and across the cut.

It is easy to see that the structure of the one-loop waveshape (4.14) is indeed very similar to the impulse described in the intoduction chapter [49]: one sums (i times) the one-loop amplitude and the specific cut shown in equation (4.14). However, here we find it to be very useful to rearrange the observable in a form which clarifies the physics while also simplifying aspects of the computation.

4.2.2 Real and imaginary parts

One clue that there is another way of constructing the observable is the fact that the two terms in (4.14), instruct us to sum i times the amplitude and the cut of the amplitude. The Cutkowski rules however tell us that cuts arise from imaginary parts of amplitudes, it is clear that the combination $i\mathcal{A} + \mathrm{Cut}\mathcal{A}$ in (4.14) is effectively *removing* an imaginary part of the one-loop amplitude then. However, it is natural to ask whether the the cut in equation (4.14) gives the complete imaginary part of the amplitude or just a contribution of it: we will indeed find that other cuts can be taken. To make this clear we will soon proceed with a better rearrangement for the waveshape than the one given in (4.14).

The usefulness of real and imaginary parts of amplitudes in the construction of KMOC-style classical observables was first emphasised in reference [32] which studied the impulse in classical scattering. The authors found that classically-singular terms[1] are absent in the real part of the amplitude, while singular terms did appear in the imaginary part. These classically-singular terms cancelled

[1]These terms involve inverse powers of $\hbar$ and must cancel in observables. They are sometimes known as “superclassical” or “hyperclassical” terms.

among the different contributions to the imaginary part. We will soon find an analogous phenomenon in the waveshape.

Real and imaginary parts of amplitudes are intimately connected to unitarity of the S matrix. To separate these parts of the amplitude, we first use $S = 1 + iT$ and the unitarity relation

$$-i(T - T^\dagger) = T^\dagger T \tag{4.16}$$

to write the waveshape (4.12) as

$$\begin{aligned} \alpha_\eta(k) &= \frac{1}{2}\langle\psi| ia_\eta(k)\,(T + T^\dagger) - ia_\eta(k)\,T^\dagger T + 2T^\dagger\, a_\eta(k) T|\psi\rangle \\ &= \frac{1}{2}\langle\psi| ia_\eta(k)\,(T + T^\dagger) - [a_\eta(k), T^\dagger]\,T + T^\dagger\,[a_\eta(k), T]|\psi\rangle\,. \end{aligned} \tag{4.17}$$

The first of these terms involves the combination $(T+T^\dagger)/2$; up to a momentum-conserving delta function, this is the "real" part of the amplitude. It can be evaluated by cutting one internal propagator, and replacing all others by principal value prescriptions as we discuss below in section 4.3.4.

The other terms involve cuts of the amplitude and are therefore linked to its imaginary part.

Because the cuts involve two T matrices (one conjugated), and we work at order g^5, it follows that we need one insertion of a g^2 tree amplitude and a g^3 tree amplitude. There is a short list of possible amplitudes: at order g^2, we encounter four-point amplitudes involving four scalars, Compton-type amplitudes with two scalars and two messengers, or four messenger amplitudes. At order g^5 we simply dress the order g^2 amplitudes with one additional messenger. Furthermore, the commutator $[a_\eta(k), T]$ vanishes unless the corresponding amplitude contains at least one outgoing messenger.

Let us first consider the term

$$\begin{aligned} \alpha_\eta(k) &\supset \frac{1}{2}\langle\psi|T^\dagger\,[a_\eta(k), T]|\psi\rangle \\ &= \frac{1}{2}\int \mathrm{d}\Phi(p_1', p_2', p_1, p_2)\phi_b^*(p_1', p_2')\phi_b(p_1, p_2)\,\langle p_1', p_2'|T^\dagger\,[a_\eta(k), T]|p_1, p_2\rangle\,. \end{aligned} \tag{4.18}$$

The T matrix here acts on the incoming two-scalar state, and (because of the commutator) must involve at least one outgoing messenger. The only possibility in our list of order g^2 and g^3 amplitudes is the $2 \to 3$ amplitude involving radiation of one messenger as the two scalars scatter. Similarly $\langle p_1', p_2'|T^\dagger$ must evaluate to the four-point four-scalar amplitude as the only order g^2 amplitude with two final-state scalars. Thus[2],

$$\langle p_1', p_2'|T^\dagger[a_\eta(k), T]|p_1, p_2\rangle =$$

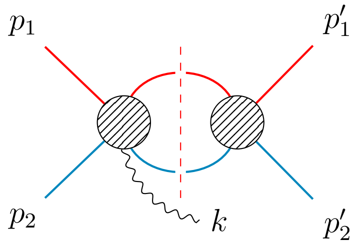

$$. \tag{4.19}$$

Now we turn to the final structure in our new formulation (4.17) of the waveshape, namely

$$\begin{aligned}\alpha_\eta(k) &\supset -\frac{1}{2}\langle\psi|[a_\eta(k), T^\dagger]\,T|\psi\rangle \\ &= -\frac{1}{2}\int \mathrm{d}\Phi(p_1', p_2', p_1, p_2)\phi_b^*(p_1', p_2')\phi_b(p_1, p_2)\,\langle p_1', p_2'|[a_\eta(k), T^\dagger]\,T|p_1, p_2\rangle\,.\end{aligned} \tag{4.20}$$

First, consider the action of T on the initial state $|p_1, p_2\rangle$. There are two possibilities on our list of g^2 and g^3 trees: the $2 \to 2$ four scalar scattering amplitude, or the $2 \to 3$ five-point amplitude involving four scalars and an outgoing messenger. Considering first the order g^2 possibility, the remaining factor $\langle p_1', p_2'|[a_\eta(k), T^\dagger]$ must be the order g^3 $2 \to 3$ five-point amplitude. On the other hand, if the T matrix contributes as the $2 \to 3$ five-point amplitude then we must extract an order g^2 amplitude from $[a_\eta(k), T^\dagger]$. The only order g^2 amplitude with one final messenger that we can insert here is the Compton

[2]Throughout this chapter, we adopt the convention of drawing massive particle lines as solid lines. We will always indicate particle 1 with a red line and particle 2 with a blue one.

amplitude. That is,

$$\langle p_1', p_2'|[a_\eta(k), T^\dagger]\, T|p_1, p_2\rangle =$$

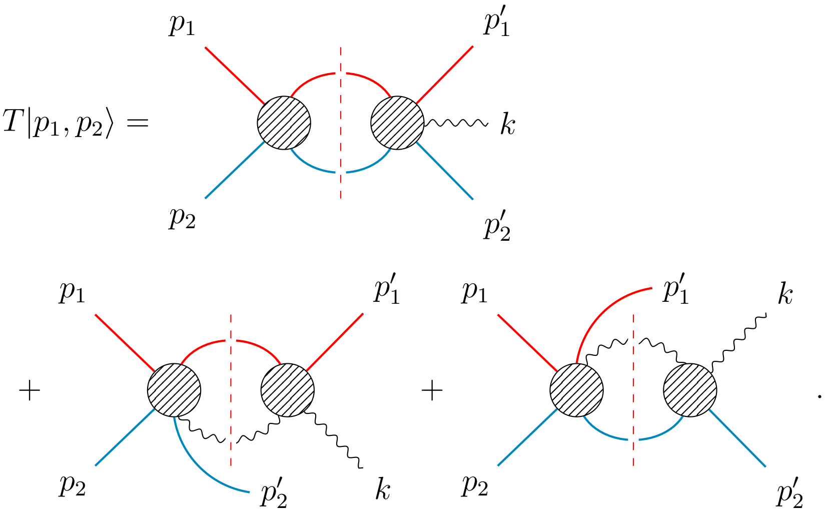

(4.21)

The presence of Compton amplitudes in this cut is significant. In fact, we will see that in the classical limit it is *only* these cuts which survive.

4.3 Technical simplifications

Given that the KMOC formalism is a "quantum-first" framework, the full quantum structure of the waveshape $\alpha_\eta(k)$ could also be constructed from amplitudes using this formalism. While there are may be many interesting aspects of the quantum-mechanical case (for instance the computation of quantum corrections to coherent states), the focus on this thesis is on the classical waveshape. Obviously the classical case is simpler than the full quantum case, and we now wish to discuss the details and the simplifications we can take advantage of to simplify our work. More specifically, we are interested in the classical limit of small angle scattering, or the "post-Minkowski" expansion in the gravitational context. This is the relativistically covariant perturbative expansion of classical quantities which we introduced in (2.8).

4.3.1 Classical LO waveshape and heavy-particle crossing

We have seen the on-loop structure of the waveshape in (4.14) but let us go back to the LO term for a moment. The waveshape (4.13) can be written at leading order as

$$\alpha_\eta(k) = \int \mathrm{d}\Phi(p_1', p_2', p_1, p_2)\, \phi^*(p_1', p_2')\phi(p_1, p_2)\, e^{ib_1\cdot(p_1-p_1')}e^{ib_2\cdot(p_2-p_2')} \\ \times i\mathcal{A}_{5,0}(p_1, p_2 \to p_1', p_2', k_\eta)\, \hat{\delta}^D(p_1' + p_2' + k - p_1 - p_2). \tag{4.22}$$

Again, let's simplify this expression in the classical limit. This will allow us to learn something new about the tree waveshape.

First, write the "outgoing" momenta[3] as usual

$$p_i' = p_i + q_i\,. \tag{4.23}$$

The momenta q_i are messenger momenta, satisfying[4] $k = -q_1 - q_2$. Applying the classical considerations presented in the introduction chapters, the waveshape can be simplified down to

$$\alpha_\eta(k) = \int \mathrm{d}\Phi(p_1, p_2)\hat{\mathrm{d}}^D q_1 \hat{\mathrm{d}}^D q_2\, \hat{\delta}(2p_1\cdot q_1)\hat{\delta}(2p_2\cdot q_2)\, |\phi(p_1, p_2)|^2\, e^{-ib_1\cdot q_1}e^{-ib_2\cdot q_2} \\ \times i\mathcal{A}'^{*}_{5,0}(p_1, p_2 \to p_1 + q_1, p_2 + q_2, k_\eta)\, \hat{\delta}^D(k + q_1 + q_2)\,. \tag{4.24}$$

On the other hand, returning to equation (4.22) and instead setting

$$p_i = p_i' - q_i\,, \tag{4.25}$$

we find, using the same logic,

$$\alpha_\eta(k) = \int \mathrm{d}\Phi(p_1', p_2')\hat{\mathrm{d}}^D q_1 \hat{\mathrm{d}}^D q_2\, \hat{\delta}(2p_1'\cdot q_1)\hat{\delta}(2p_2'\cdot q_2)\, |\phi(p_1', p_2')|^2\, e^{-ib_1\cdot q_1}e^{-ib_2\cdot q_2} \\ \times i\mathcal{A}_{5,0}(p_1' - q_1, p_2' - q_2 \to p_1', p_2', k_\eta)\, \hat{\delta}^D(k + q_1 + q_2)\,. \tag{4.26}$$

There is nothing stopping us from dropping the primes in this equation, since p_i' are simply variables of integration.

Comparing equations (4.24) and (4.26), the only difference is in the details of the momentum dependence in the tree amplitude. The wavefunction is unspecified; we have only used properties it must have in the classical limit. We conclude that

[3]As our observable is an expectation value, the apparent in and out states are both in states. Nevertheless it can be convenient at times to think of the primed momenta as outgoing.

[4]Sometimes, in the next chapter 5 we may use instead $k = q_1 + q_2$.

$$\mathcal{A}_{5,0}(p_1, p_2 \to p_1 + q_1, p_2 + q_2, k_\eta) = \mathcal{A}_{5,0}(p_1 - q_1, p_2 - q_2 \to p_1, p_2, k_\eta)\,. \quad (4.27)$$

This expression can only hold for the classical "fragment" of the amplitude, in the sense of reference [4] (see next chapter): at tree level, the classical fragment is simply the dominant term in the classical Laurent expansion. An alternative perspective is that this crossing relation follows from the scale separation between the heavy-mass scale m_1 and m_2 in the momenta of the scalar particles, and the light scale of order q in the messengers.

The result, then, is a kind of crossing relation valid for heavy particle effective theories.[5] It essentially allows us to cross the messenger momentum leaving the large particle momentum untouched. We will find this result is very useful below. It is straightforward to check this heavy-particle crossing relation in explicit examples: the QED amplitude is visible in equation 5.46 of reference [49] while the gravitational five point case is written in equation 4.21 of reference [48]. In both cases, heavy-particle crossing is achieved by eliminating the momentum k in favour of $q_1 + q_2$, and then replacing $q_i \to -q_i$. This has the effect of replacing $p_i + q_i$ with the desired $p_i - q_i$ without clashing with the relation between k and the q_i (this relation does not pick up a sign in the crossing).

Returning to the waveshape, we shall write

$$\alpha_\eta(k) = \left\langle\!\!\left\langle \int \hat{\mathrm{d}}^D q_1 \hat{\mathrm{d}}^D q_2 \, \hat{\delta}(2p_1 \cdot q_1)\hat{\delta}(2p_2 \cdot q_2)\, e^{-ib_1 \cdot q_1} e^{-ib_2 \cdot q_2} \, (\cdots) \right\rangle\!\!\right\rangle \quad (4.28)$$

at LO and NLO. Here the dots signify a general integrand, made of amplitudes and cuts. The large angle brackets remind us that the result must be integrated against the wavefunctions. However, once the integrand has been fully simplified in the classical limit, in particular to cancel terms involving singular powers of $\hbar$, the integrand is smooth on the scale of the wavepacket. As before, we take the wavepacket size to zero, so that the wavepacket integral simply localises the incoming momenta p_i on their classical values.

[5] In fact, recently EFT/HEFT approaches have shown prominent results and applications. Inspired by the success of heavy-quark effective theory [233–237], the HEFT approach implements the classical limit as a large mass limit. For more on these see [15, 60, 74, 74, 75, 75, 225, 238].

4.3.2 Vanishing cuts

Earlier, we advertised that certain cuts which contribute to the full quantum waveshape cancel in the classical waveshape. We are now in a position to show this in detail. The result of this subsection is that

$$\int \mathrm{d}\Phi(p_1', p_2', p_1, p_2)\, \phi^*(p_1', p_2')\phi(p_1, p_2)\, e^{ib_1\cdot(p_1-p_1')}e^{ib_2\cdot(p_2-p_2')}\,\hat{\delta}^D(p_1'+p_2'+k-p_1-p_2)$$

$\times \Big[$ 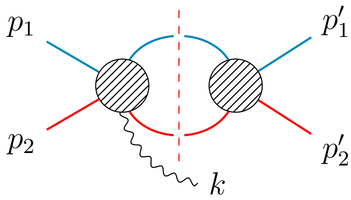

$-$ 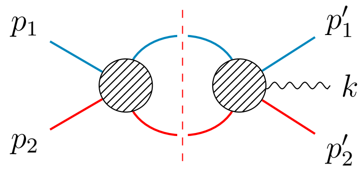

$\Big] = 0\,.$ (4.29)

In other words, these two cuts make no contribution to the classical waveshape. This cancellation can be interpreted as the cancellation of classically-singular ("superclassical") terms which occur in the five point one-loop amplitude. The result can be seen as a generalisation of the removal of iterated trees in an exponentiated form of the amplitude along the lines of the eikonal or radial action at four points (we will see this more in detail soon in the next chapter).

To see how the cancellation works, we adjust the initial and final states under the integral signs to reach

$$\int \mathrm{d}\Phi(p_1, p_2, p_1+q_1, p_2+q_2)\, |\phi(p_1, p_2)|^2\, e^{-ib_1\cdot q_1}e^{-ib_2\cdot q_2}\,\hat{\delta}^D(k+q_1+q_2)$$

$\times \Big[$ 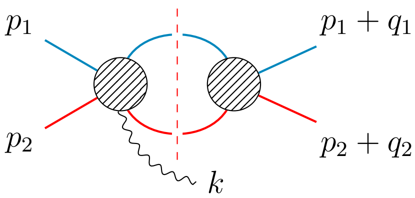

$-$ 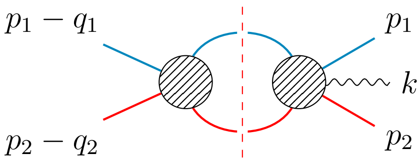

$\Big]\,.$ (4.30)

Writing out the cut, this becomes

$$\begin{aligned}
\Bigg\langle\!\!\Bigg\langle \int &\hat{\mathrm{d}}^D q_1 \hat{\mathrm{d}}^D q_2\, \hat{\delta}(2p_1\cdot q_1)\hat{\delta}(2p_2\cdot q_2)\hat{\delta}^D(k+q_1+q_2)\, e^{-ib_1\cdot q_1} e^{-ib_2\cdot q_2} \\
&\times \int \hat{\mathrm{d}}^D \ell_1 \hat{\mathrm{d}}^D \ell_2\, \hat{\delta}(2p_1\cdot \ell_1)\hat{\delta}(2p_2\cdot \ell_2)\, \hat{\delta}^D(\ell_1+\ell_2+k) \\
&[\mathcal{A}_{5,0}(p_1,p_2\to p_1+\ell_1,p_2+\ell_2,k)\mathcal{A}_{4,0}(p_1+\ell_1,p_2+\ell_2\to p_1+q_1,p_2+q_2) \\
&\; - \mathcal{A}_{4,0}(p_1-q_1,p_2-q_2\to p_1-\ell_1,p_2-\ell_2)\mathcal{A}_{5,0}(p_1-\ell_1,p_2-\ell_2\to p_1,p_2,k)] \Bigg\rangle\!\!\Bigg\rangle\,.
\end{aligned} \tag{4.31}$$

Using heavy-particle crossing, the two five point trees are shown to be equal. As for the four point trees, one could use a result analogous to this crossing to show that they match. Alternatively, it is a simple point that these trees only depend on the t-channel Mandelstam variable, which is the same in both terms, times the point-particle data. Thus, we conclude that the result vanishes.

4.3.3 Vanishing integrals

In our one-loop computations, we will encounter topologies including pentagons, boxes, triangles etc. Here we largely work at the level of the integrand. Nevertheless it is very useful to simplify our integrand by dropping terms which integrate to zero.

The situation with loop integrals in the classical limit at four-points at one and two loops is very well understood and is thoroughly discussed for example in references [8, 14]. There are some similarities between four and five points. For example, we note that

$$\int \hat{\mathrm{d}}^D \ell \frac{(\ell-q_1)^2}{\ell^2(\ell-q_1)^2(p_1\cdot\ell)(p_2\cdot\ell)} = 0\,. \tag{4.32}$$

One viewpoint is that this occurs because the integral is scaleless in dimensional regulation. An alternative viewpoint is that the integral is irrelevant classically with any choice of regulator because it leads to a contact term connecting the two point-like particles. These contact terms are only non-vanishing outside the domain of validity of the classical theory when the two particles are spatially separated by less than their Compton wavelength.

As another example, consider the integral

$$\begin{aligned}\int \hat{\mathrm{d}}^D\ell \frac{\ell^2}{\ell^2(\ell-q_1)^2(p_1\cdot\ell)(p_2\cdot\ell)} &= \int \hat{\mathrm{d}}^D\ell \frac{1}{(\ell-q_1)^2(p_1\cdot\ell)(p_2\cdot\ell)} \\ &= \int \hat{\mathrm{d}}^D\ell \frac{1}{\ell^2(p_1\cdot\ell)(p_2\cdot(\ell+q_1))}\,.\end{aligned} \tag{4.33}$$

In the second step, we simply set $\ell' = \ell - q_1$, and then dropped the prime. We also set $p_1\cdot q_1 = 0$, assuming that the $\hbar$-suppressed correction term of order q_1^2 could be neglected. This integral is *not* scaleless: indeed, there is a scale $p_2\cdot q_1 = -p_2\cdot k$ in the integral. Nevertheless we may still drop this integral:

$$\int \hat{\mathrm{d}}^D\ell \frac{\ell^2}{\ell^2(\ell-q_1)^2(p_1\cdot\ell)(p_2\cdot\ell)} = \frac{1}{m_1m_2}\int \hat{\mathrm{d}}^D\ell \frac{1}{\ell^2(u_1\cdot\ell)(u_2\cdot(\ell-k))} \to 0\,. \tag{4.34}$$

Again, the reason is that, since the integral is analytic in q_1, after carrying out the on-shell the Fourier transform integrals in (4.28) it leads to a contact term in b-space. Note that care must be taken in the context of eg pentagon diagrams with three massless internal propagators; pinching one of these need not necessarily lead to a vanishing contact term.

4.3.4 Real parts from single cuts and principal values

Let us now return to the waveform, and look in more detail at the term containing the real part of the amplitude:

$$\begin{aligned}\alpha_\eta(k)|_1 &\equiv \frac{1}{2}\langle\psi|ia_\eta(k)\,(T+T^\dagger)|\psi\rangle \\ &= \frac{1}{2}\int \mathrm{d}\Phi(p_1',p_2',p_1,p_2)\,\phi_b^*(p_1',p_2')\phi_b(p_1,p_2)\,i\langle p_1',p_2',k_\eta|T+T^\dagger|p_1,p_2\rangle\,.\end{aligned} \tag{4.35}$$

The matrix element appearing here can be expressed in terms of amplitudes as

$$\langle p_1',p_2',k_\eta|T+T^\dagger|p_1,p_2\rangle = \left(\mathcal{A}_{5,0}+\mathcal{A}'^{*}_{5,0}\right)\,\hat{\delta}^D(p_1+p_2-p_1'-p_2'-k)\,, \tag{4.36}$$

where the five-point tree amplitudes are more explicitly

$$\begin{aligned}\mathcal{A}_{5,0} &\equiv \mathcal{A}(p_1,p_2\to p_1',p_2',k_\eta)\,,\\ \mathcal{A}'_{5,0} &\equiv \mathcal{A}(p_1',p_2',k_{-\eta}\to p_1,p_2)\,.\end{aligned} \tag{4.37}$$

Notice that the initial and final states are swapped in $\mathcal{A}'_{5,0}$ relative to $\mathcal{A}_{5,0}$. The close relationship between the conjugated amplitude $\mathcal{A}'^{*}_{5,0}$ and the amplitude $\mathcal{A}_{5,0}$ is discussed in many quantum field theory textbooks, though the focus in typically on the imaginary part $i(\mathcal{A}_{5,0} - \mathcal{A}'^{*}_{5,0})$ because of its relevance to unitarity (see, for example, [239–242] for helpful discussions in this particular context). Because the real part $\mathcal{A}_{5,0} + \mathcal{A}'^{*}_{5,0}$ is relevant to us, it is worth giving an example to see how the combination works.

We consider a one-loop diagram contributing to the amplitude $\mathcal{A}_{5,0}$ in Yang-Mills theory:

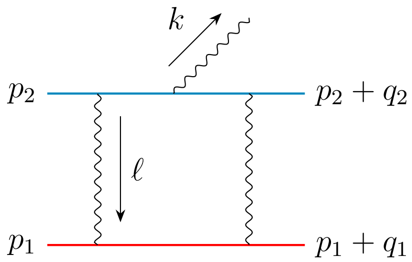

$$= g^5 \mathcal{C} \int \hat{\mathrm{d}}^D \ell \, N P \, . \tag{4.38}$$

This diagram depends on a color factor $\mathcal{C}$, a kinematic numerator N and a propagator structure P. The Feynman rules lead to

$$\begin{aligned} P^{-1} &= (\ell^2 + i\epsilon)[(q_1 - \ell)^2 + i\epsilon][(p_1 + \ell)^2 - m_1^2 + i\epsilon][(p_2 - \ell)^2 - m_2^2 + i\epsilon] \\ &\qquad \times [(p_2 - \ell - k)^2 - m_2^2 + i\epsilon] \, , \\ N &= \varepsilon^*_\eta \cdot (2p_2 - 2\ell)(2p_1 + \ell) \cdot (2p_2 - \ell)(2p_1 + \ell + q_1) \cdot (2p_2 - \ell + q_1 + 2q_2) \, . \end{aligned} \tag{4.39}$$

Note the appearance of the (possibly complex) polarisation vector ε^*_h. To describe the color factor, we suppose the initial color of particle i is specified by a color vector χ_i, while another vector χ'_i defines the final color. Let us further suppose that the outgoing gluon has adjoint color a. Then we have

$$\mathcal{C} = \bar{\chi}'_1 \cdot T_1^b \cdot T_1^c \cdot \chi_1 \, \bar{\chi}'_2 \cdot T_2^b \cdot T_2^a \cdot T_2^b \cdot \chi_2 \, . \tag{4.40}$$

The contribution of this diagram to the amplitude is

$$\mathcal{A}_{5,0} \supset -i g^5 \mathcal{C} \int \hat{\mathrm{d}}^D \ell \, N P \, , \tag{4.41}$$

since (in our conventions) the Feynman rules evaluate to i times the amplitude[6].

As the initial and final states are interchanged in $\mathcal{A}'_{5,0}$, we instead encounter the

[6]This is consistent with $S = 1 + iT$, and the convention that, for example, the tree four-point amplitude in $\lambda\phi^4/4!$ theory is λ.

diagram

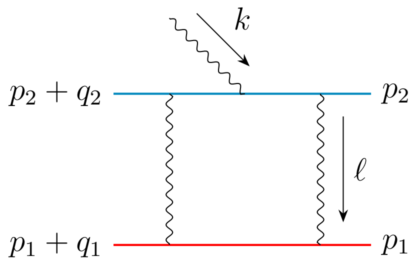

$$= g^5 \mathcal{C}' \int \hat{\mathrm{d}}^D \ell \, N' P' \,. \tag{4.42}$$

The color factor, numerator and propagators are now

$$\begin{aligned}
P'^{-1} &= (\ell^2 + i\epsilon)[(q_1 - \ell)^2 + i\epsilon][(p_1 + \ell)^2 - m_1^2 + i\epsilon][(p_2 - \ell)^2 - m_2^2 + i\epsilon] \\
&\qquad\qquad\qquad\qquad \times [(p_2 - \ell - k)^2 - m_2^2 + i\epsilon] \,, \\
N' &= \varepsilon_\eta \cdot (2p_2 - 2\ell)(2p_1 + \ell) \cdot (2p_2 - \ell)(2p_1 + \ell q_1) \cdot (2p_2 - \ell + q_1 + 2q_2) \,, \\
\mathcal{C}' &= \bar{\chi}_1 \cdot T_1^c \cdot T_1^b \cdot \chi_1' \, \bar{\chi}_2 \cdot T_2^c \cdot T_2^a \cdot T_2^b \cdot \chi_2' \,.
\end{aligned} \tag{4.43}$$

It is important that N' is the complex conjugate of N, and $\mathcal{C}'$ is the complex conjugate of $\mathcal{C}$ while the propagator structures are equal: $P = P'$. As a consequence, we can write

$$\mathcal{A}'^{*}_{5,0} \supset i g^5 \mathcal{C} \int \hat{\mathrm{d}}^D \ell \, N P^* \,. \tag{4.44}$$

This is a general fact: the one-loop Feynman diagrams contributing to $\mathcal{A}'^{*}_{5,0}$ can be obtained from the diagrams for $\mathcal{A}_{5,0}$ by (i) changing the overall sign, and (ii) replacing the $i\epsilon$ prescription in propagators by $-i\epsilon$. For the two diagrams at hand, we have

$$\begin{aligned}
\mathcal{A}_{5,0}(p_1, p_2 \to p_1', p_2', k_\eta) + \mathcal{A}'^{*}_{5,0}(p_1', p_2', k_{-\eta} \to p_1, p_2) &\supset g^5 \mathcal{C} \int \hat{\mathrm{d}}^D \ell \, N \, [-i(P - P^*)] \\
&= 2 g^5 \mathcal{C} \int \hat{\mathrm{d}}^D \ell \, N \, \mathrm{Im} \, P \,.
\end{aligned} \tag{4.45}$$

The general conclusion is that

$$\begin{aligned}
\alpha_\eta(k)|_1 = \int \mathrm{d}\Phi(p_1', p_2', p_1, p_2) \, \phi_b^*(p_1', p_2') \phi_b(p_1, p_2) \, \hat{\delta}^D(p_1 + p_2 - p_1' - p_2' - k) \\
\times i \, \mathrm{Im}_{\text{prop}} \, \mathcal{A}_{5,0}(p_1, p_2 \to p_1', p_2', k_\eta) \,.
\end{aligned} \tag{4.46}$$

The instruction $\mathrm{Im}_{\text{prop}}$ tells us to take the imaginary part of the propagator structure of the amplitudes. Alternatively, we can think of this instruction as the imaginary part of the amplitude, treating colour factors and polarisation vectors as real quantities.

It is very natural to obtain the imaginary part of the propagator structure using

$$\frac{1}{p^2 - m^2 + i\epsilon} = \mathrm{PV}\left(\frac{1}{p^2 - m^2}\right) - \frac{i}{2}\hat{\delta}(p^2 - m^2)\,, \tag{4.47}$$

where PV is the principal value[7]. The delta function here is equivalent to cutting a single particle. By counting powers of i, it is clear that the imaginary part of our propagator structure is obtained by cutting an odd number of propagators. (This contrasts with the usual unitarity cuts at one loop which involve cutting two propagators, we will see how these cuts are related to different phenomena in a later section. These will give imaginary part *of the waveshape* instead.)

Our diagrams contain five propagators, so in principle there are imaginary parts when we cut one, three or five propagators. However, three point amplitudes have no support in Minkowski space — so there is no need to consider cutting five propagators. It is also easy to see that cutting three propagators necessarily leads to one three-point amplitude. Thus our imaginary parts necessarily arise from single cuts; all other propagators are then to be evaluated with the principal-value pole prescription. It is worth emphasising that this pole prescription appears naturally from general considerations.

4.4 Radiation

In this chapter we discuss the complete real part of the QED and QCD waveshape in detail at the level of their integrand. As we will see, taking the real part of the one-loop amplitude corresponds to isolating "conservative" contributions in radiative fields. By that we mean all radiation which is caused by one particle accelerating in the Lorentz/geodesic fields of the second one. That is, the forces acting on the particle are conservative, and (classically) omit the self-field of the particle. We return to these intrinsically dissipative self-force corrections to the radiation field in the next chapter of this manuscript. It may be worth commenting that the factor of i between the real and imaginary parts of the waveshape is itself a signal of time-reversal violation.

We begin with electrodynamics. The waveshape in QED is remarkably simple yet it is physically interesting and closely connected to more complicated radiation

[7]In the closed time-path (Schwinger-Keldysh) approach to computing expectation values in field theory, the $T^\dagger$ matrix arises from the part of the contour which goes "backwards" in time.

fields. This is why we find it is useful to discuss it in detail. Indeed, the QED waveshape computes well-defined parts of the QCD waveshape, associated with specific ordered amplitudes. We will discuss how QED is embedded in QCD in more detail later.

4.4.1 QED

We are now at a good place to compute the QED waveshape. At NLO, this is fifth order in the coupling. But in electrodynamics we are free to give our two particles different charges Q_1 and Q_2, and correspondingly the five coupling powers in the NLO waveshape can be decomposed into four different charge sectors: $Q_1Q_2^4$, $Q_1^2Q_2^3$, $Q_1^3Q_2^2$, and $Q_1^4Q_2$. (There can be no terms of order Q_1^5 or Q_2^5 since at least one photon must connect the two particles for radiation to occur.) In the language of scattering amplitudes, the one-loop five-point amplitude in QED can be decomposed into four different partial amplitudes corresponding to these four charge sectors. There are really only two independent partial amplitudes to compute, which we can take to be the $Q_1^2Q_2^3$ and $Q_1Q_2^4$ amplitudes. The $Q_1^3Q_2^2$ and $Q_1^4Q_2$ partial amplitudes can be recovered by interchanging particles 1 and 2.

In this section, we start with the $Q_1^2Q_2^3$ partial amplitude. In order to show how this waveshape can be extracted most simply, it is convenient to digress briefly on a related computation: the impulse at next-to-leading order.

NLO impulse

The impulse at NLO involves a one-loop four-point amplitude. This amplitude has real and imaginary parts, which play rather different roles in the observable. In particular, at one loop, the real part controls the scattering angle, while the imaginary part ensures that the on-shell condition is satisfied. Here it is most relevant to focus on the contribution of the real part of the amplitude to the observable, so we define

$$\Delta p_1^\mu|_{\text{real}} \equiv \int \mathrm{d}^D q\, \hat{\delta}(2p_1 \cdot q)\hat{\delta}(2p_2 \cdot q_2)\, iq^\mu\, e^{-iq\cdot b}\, \mathrm{Re}\, \mathcal{A}_{4,1}(p_1, p_2 \to p_1 + q, p_2 - q)\,. \tag{4.48}$$

One-loop four-point amplitudes involve at most four propagators. In this case, two of those propagators involve photons while the other two are associated with the massive particles with momenta p_1 or p_2. The real part of the amplitude arises by replacing a propagator with the corresponding delta function: this places one line on shell, effectively performing a single cut of the amplitude. First, we consider the result of placing the propagator for line 2 on shell. Diagrammatically, we must then consider

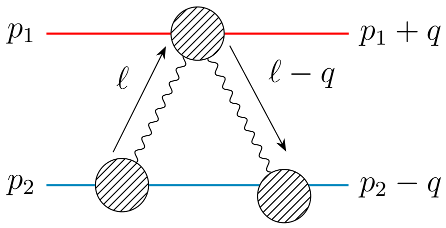

$$. \tag{4.49}$$

The contribution of this diagram to the amplitude is

$$\mathrm{Re}\,\mathcal{A}_{4,1}|_{p_2} = \int \hat{\mathrm{d}}^D\ell \frac{1}{\ell^2(\ell-q)^2}\frac{1}{2}\hat{\delta}(2p_2\cdot\ell)N(\ell)\,, \tag{4.50}$$

where $N(\ell)$ is a numerator function we must fix.

We fix the numerator by cutting all the propagators in the diagram: we have explicitly cut the massive propagator, and any terms in $N(\ell)$ which are proportional to ℓ^2 or $(\ell-q)^2$ integrate to zero. In other words we can take each of the blobs in the diagram to be on-shell amplitudes, so that

$$N(\ell) = \sum_{\text{helicities}} \mathcal{A}_{3,0}(p_2,\ell)\mathcal{A}_{4,0}(p_1,\ell,\ell-q)\mathcal{A}_{3,0}(p_2-\ell,\ell-q)\,. \tag{4.51}$$

In D dimensions, the helicity sum is straightforward using formal polarisation vectors. Let us write the polarisation vector for a photon of momentum k and gauge q as $\varepsilon(k;q)$. If we choose the gauge to be $q = p_1$, then the Compton amplitude[8] appearing in the cut is

$$\mathcal{A}_{4,0}(p_1,\ell,\ell-q) = 2Q_1^2\,\varepsilon(\ell,p_1)\cdot\varepsilon^*(\ell-q,p_1)\,. \tag{4.52}$$

The three-point amplitudes are trivially obtained from

$$\mathcal{A}_{3,0}(p_2,\ell) = 2Q_2\,\varepsilon(\ell,p_1)\cdot p_2\,. \tag{4.53}$$

[8]The reader will/might have noticed the frequent appearance of Compton amplitudes in this chapter. These are in fact extremely important in waveforms computations and will play a crucial role when including spin effects: here the role of spin is still not completely understood due to the appearance of spurious poles for high spin terms. For more on this see [243–247].

To perform the helicity sum, we only need the completeness relation which, in case of a massive gauge vector, is

$$\sum_{\text{helicities}} \varepsilon^\mu(k,q)\varepsilon^{\nu*}(k,q) = -\left(\eta^{\mu\nu} - \frac{k^\mu q^\nu + k^\nu q^\mu}{k\cdot q} + q^2\frac{k^\mu k^\nu}{(k\cdot q)^2}\right) . \tag{4.54}$$

This summation involves products of a polarisation vector and its conjugate. As usual in generalised unitarity, this structure naturally arises in the product of amplitudes appearing in the diagram (4.49) because a photon connecting two amplitudes must be outgoing with respect to one amplitude and incoming with respect to the other.

It then follows that the numerator is

$$N(\ell) = 8Q_1^2Q_2^2\left(m_2^2 + \frac{(p_1\cdot p_2)^2}{(p_1\cdot \ell)^2}\ell\cdot(\ell-q)\right) . \tag{4.55}$$

As a result, the contribution to the observable is

$$\begin{aligned}\Delta p_1^\mu|_{\text{real},p_2} = \frac{iQ_1^2Q_2^2}{2}&\int \mathrm{d}^D q\, \hat\delta(u_1\cdot q)\hat\delta(u_2\cdot q_2)\, q^\mu\, e^{-iq\cdot b}\\ &\times\int \frac{\hat{\mathrm{d}}^D\ell}{\ell^2(\ell-q)^2}\frac{\hat\delta(u_2\cdot\ell)}{m_1}\left(1+\frac{(u_1\cdot u_2)^2}{(u_1\cdot\ell)^2}\ell\cdot(\ell-q)\right) ,\end{aligned} \tag{4.56}$$

where we used the proper velocities $u_i = p_i/m_i$.

The contribution from cutting the massive propagator with incoming momentum p_1 can be obtained from equation (4.56) by symmetrising on particles 1 and 2. By summing these two contributions we find agreement with the impulse given in equation 5.38 of reference [49][9].

In this way, we reproduce the one-loop impulse in a very straightforward manner. However we did so by cutting only the massive propagators, omitting possible cuts of the massless photon propagators. These cuts do not contribute to the classical impulse. Indeed, from a purely classical perspective the messengers are Fourier transforms of the Coulomb field, and therefore can transport no energy in the rest frame of the source. Thus, they cannot go on shell. From the perspective of amplitudes and cuts, one can show that when one of the messenger lines are cut the resulting amplitude is suppressed by a power of $\hbar$. (This involves choosing a specific gauge for the polarisation objects of the messengers and a remaining

[9] Terms in that equation 5.38 which involve derivatives of delta functions arise from the imaginary part of the amplitude when included correctly in the observable.

cancellation among Feynman diagrams.) We shall omit this class of cuts in the following discussion for the same reason.

Lorentz impulse: heavy mass

We now turn to the radiation at order $Q_1^2 Q_2^3$. Classically, this radiation results from the acceleration of particle 2 due to the Lorentz force in the field of particle 1. To determine the radiation field we recycle much of the computation of the impulse.

As in the case of the impulse above, we do not cut internal photon lines (the internal photons are both potential modes.) We focus first on the contribution arising by cutting line 1, leading to the diagram

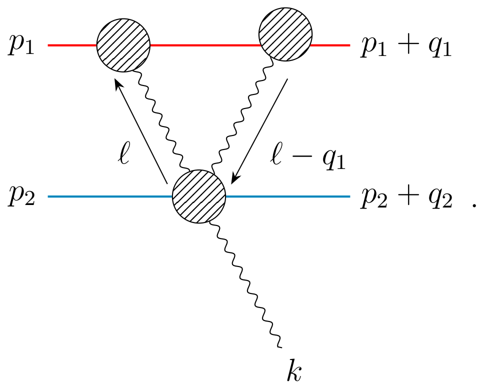

. (4.57)

We will soon see that this diagram gives the dominant contribution to the waveshape when the mass m_1 of particle 1 is large. Its contribution to the amplitude can be computed in a manner which is almost identical to the impulse. The main novelty relative to our discussion of the impulse is the appearance of a five-point tree amplitude:

$i\mathcal{A}_{5,0} =$ 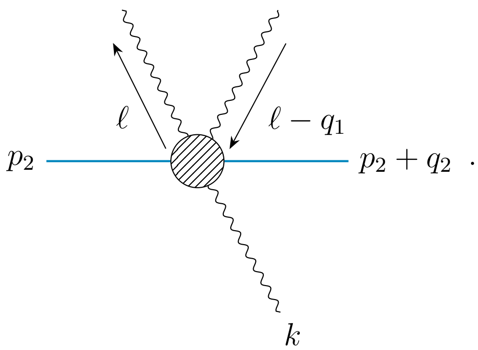

. (4.58)

If we choose the gauge of both polarisation vectors to be p_2, there are only three possible Feynman diagrams leading to a compact and (for our purposes) convenient expression for the amplitude:

$$\mathcal{A}_{5,0} = -4Q_2^3 \left[\frac{\varepsilon^*(\ell)\cdot\varepsilon(\ell-q_1)\,\varepsilon^*(k)\cdot q_1}{2p_2\cdot q_1} - \frac{\varepsilon^*(\ell)\cdot\varepsilon^*(k)\,\varepsilon(\ell-q_1)\cdot q_2}{2p_2\cdot(\ell-q_1)} \right. \\ \left. + \frac{\varepsilon(\ell-q_1)\cdot\varepsilon^*(k)\,\varepsilon^*(\ell)\cdot q_2}{2p_2\cdot\ell} \right] . \tag{4.59}$$

Notice that the second and third terms are related by swapping the momenta ℓ and $q_1 - \ell$. This is a symmetry of the rest of the diagram (4.57), so these last two terms in the five-point tree make an identical contribution in the cut. We do not indicate the helicity of the polarisation vectors: this information washes out in the completeness relation (since each polarisation vector in the product of amplitudes is multiplied by its conjugate polarisation).

To determine the contribution of the cut (4.57) to the real part of the one-loop amplitude, we must sum the product of the five-point tree (4.59) and two three-point amplitudes over helicities. The helicity sum can be performed using the completeness relation of equation (4.54). Because the last two terms in the five-point tree (4.59) make an identical contribution to the cut, there are only two different polarisation sums to consider. The first term in equation (4.59) leads to the sum

$$\sum_{\text{helicities}} p_1\cdot\varepsilon(\ell)\,p_1\cdot\varepsilon^*(\ell-q_1)\frac{\varepsilon^*(\ell)\cdot\varepsilon(\ell-q_1)\,\varepsilon^*(k)\cdot q_1}{2p_2\cdot q_1} \\ = \left(m_1^2 + \frac{\ell\cdot(\ell-q_1)(p_1\cdot p_2)^2}{p_2\cdot\ell\,p_2\cdot(\ell-q_1)}\right)\frac{\varepsilon^*(k)\cdot q_1}{2p_2\cdot q_1} . \tag{4.60}$$

Notice that this term — specifically, the part appearing in brackets — bears a strong structural similarity with the numerator which appeared in the impulse, equation (4.55). The relationship between radiation and the impulse is an example of the "memory" effect, encountered here at the level of the one-loop integrand.

The second class of polarisation sum to be performed is

$$\sum_{\text{helicities}} p_1\cdot\varepsilon(\ell)\,p_1\cdot\varepsilon^*(\ell-q_1)\frac{\varepsilon(\ell-q_1)\cdot\varepsilon^*(k)\,\varepsilon^*(\ell)\cdot q_2}{2p_2\cdot\ell} \\ = \left(p_1\cdot q_2 + \frac{p_1\cdot p_2\,\ell\cdot q_2}{p_2\cdot\ell}\right)\left(p_1\cdot\varepsilon^*(k) - \frac{p_1\cdot p_2}{p_2\cdot(\ell-q_1)}(\ell-q_1)\cdot\varepsilon^*(k)\right)\frac{1}{2p_2\cdot\ell} . \tag{4.61}$$

Putting these together, diagram (4.57) leads to terms in the one-loop five-point amplitude given by

$$\mathcal{A}_{5,1} = -4Q_1^2Q_2^3 \int \frac{\hat{\mathrm{d}}^D\ell}{\ell^2(\ell-q_1)^2} \frac{1}{p_1\cdot\ell + i\epsilon} \left[\left(m_1^2 + \frac{\ell\cdot(\ell-q_1)(p_1\cdot p_2)^2}{p_2\cdot\ell\, p_2\cdot(\ell-q_1)} \right) \frac{\varepsilon^*(k)\cdot q_1}{p_2\cdot q_1} \right.$$
$$\left. + \left(p_1\cdot q_2 + \frac{p_1\cdot p_2\, \ell\cdot q_2}{p_2\cdot\ell} \right) \left(p_1\cdot\varepsilon^*(k) - \frac{p_1\cdot p_2}{p_2\cdot(\ell-q_1)}(\ell-q_1)\cdot\varepsilon^*(k) \right) \frac{2}{p_2\cdot\ell} \right] + \cdots, \tag{4.62}$$

where the ellipsis indicates terms not captured by the cut.

The contribution of this part of the amplitude to the waveshape involves taking the imaginary part of the explicit massive propagator. Including the rest of the structure of the waveshape, we find

$$\alpha_\eta(k)|_1 = \frac{iQ_1^2Q_2^3}{2m_1m_2} \int \hat{\mathrm{d}}^4q_1\hat{\mathrm{d}}^4q_2\, \hat{\delta}(q_1\cdot u_1)\hat{\delta}(q_2\cdot u_2)\hat{\delta}^D(q_1+q_2+k)e^{-iq_1\cdot b_1}e^{-iq_2\cdot b_2}$$
$$\times \int \frac{\hat{\mathrm{d}}^4\ell}{\ell^2(\ell-q_1)^2}\hat{\delta}(p_1\cdot\ell) \left[\left(m_1^2 + \frac{\ell\cdot(\ell-q_1)(p_1\cdot p_2)^2}{p_2\cdot\ell\, p_2\cdot(\ell-q_1)} \right) \frac{\varepsilon^*(k)\cdot q_1}{p_2\cdot q_1} \right.$$
$$+ \left(p_1\cdot\varepsilon^*(k) - \frac{p_1\cdot p_2}{p_2\cdot(\ell-q_1)}(\ell-q_1)\cdot\varepsilon^*(k) \right) \frac{2p_1\cdot q_2}{p_2\cdot\ell}$$
$$\left. + \left(p_1\cdot\varepsilon^*(k) - \frac{p_1\cdot p_2}{p_2\cdot(\ell-q_1)}(\ell-q_1)\cdot\varepsilon^*(k) \right) \frac{2p_1\cdot p_2\, \ell\cdot q_2}{(p_2\cdot\ell)^2} \right]. \tag{4.63}$$

To see how this term scales with the masses of the particles, scale the masses out from the momenta via $p_i = m_iu_i$. It is then clear that this part of the waveshape is proportional to $m_1^0m_2^{-2}$ so that, as we advertised above, this cut corresponds to the radiation emitted in the large m_1 limit.

Lorentz impulse: symmetric mass

The remaining single-particle cuts at order $Q_1^2 Q_2^3$ are proportional to $1/(m_1 m_2)$. The cut diagrams are:

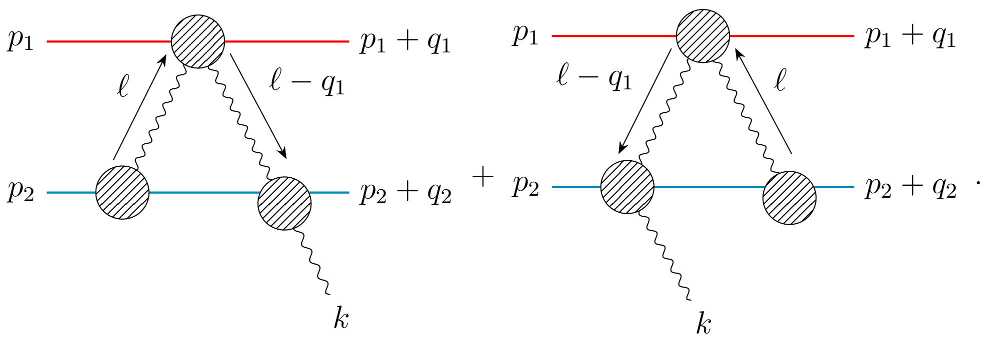

(4.64)

This topology can easily be determined using the methods discussed above; the only (slight) novelty is that the two Compton amplitudes which appear are most simply evaluated in terms of polarisation vectors in different gauges. Both diagrams make an equal contribution to the waveform so we may study only the first diagram.

The contribution of this diagram to the one-loop five-point amplitude can be written as

$$i\mathcal{A}_{5,1}^B = -i \int \frac{\hat{\mathrm{d}}^D \ell}{\ell^2 (\ell - q_1)^2} \frac{1}{-2p_2 \cdot \ell + i\epsilon} K^B \,, \tag{4.65}$$

where K^B is the evaluation of the cut, namely

$$iK^B = -8iQ_1^2 Q_2^3 \sum_{\text{helicities}} p_2 \cdot \varepsilon^*(\ell)\, \varepsilon(\ell, p_1) \cdot \varepsilon^*(\ell - q_1, p_1)\, \varepsilon(\ell - q_1, p_2) \cdot \varepsilon^*(k, p_2) \,. \tag{4.66}$$

We have introduced the notation $\varepsilon(k, p)$ for the polarisation vectors corresponding to a photon with momentum k in gauge p. Note that we used different gauges for the polarisation vectors in different tree Compton amplitudes in the cut. However, it is an easy matter to change the gauge, and in particular we find it convenient to write

$$\varepsilon^\mu(\ell - q_1, p_1) = \varepsilon^\mu(\ell - q_1, p_2) - (\ell - q_1)^\mu \frac{p_1 \cdot \varepsilon(\ell - q_1, p_2)}{p_1 \cdot \ell} \,. \tag{4.67}$$

The helicity sum can then be performed in D dimensions straightforwardly. The contribution of the cut to the waveform is

$$\begin{aligned}\frac{iQ_1^2Q_2^3}{m_1m_2}\int \hat{\mathrm{d}}^Dq_1\hat{\mathrm{d}}^Dq_2\,\hat{\delta}(q_1\cdot u_1)\hat{\delta}(q_2\cdot u_2)\hat{\delta}^D(q_1+q_2+k)\,e^{-iq_1\cdot b_1}e^{-iq_2\cdot b_2}\\ \times\int \hat{\mathrm{d}}^D\ell\frac{\hat{\delta}(u_2\cdot\ell)}{\ell^2(\ell-q_1)^2}K^B\,.\end{aligned} \tag{4.68}$$

where the quantity K^B, which is directly proportional to the polarisation sum, is

$$\begin{aligned}K^B=&\frac{1}{(u_1\cdot\ell)^2}\Bigg[u_1\cdot\varepsilon^*(k,p_2)\,(u_1\cdot\ell\,u_2\cdot q_1-u_1\cdot u_2\,\ell\cdot q_1)\\&+(\ell-q_1)\cdot\varepsilon^*(k,p_2)\left(u_1\cdot u_2\,u_1\cdot\ell-\frac{(u_1\cdot u_2)^2\ell\cdot q_1}{u_2\cdot q_1}+\frac{(u_1\cdot\ell)^2}{u_2\cdot q_1}\right)\\&-\ell\cdot\varepsilon^*(k,p_2)\,u_1\cdot u_2\,u_1\cdot\ell\Bigg]\,.\end{aligned} \tag{4.69}$$

It is straightforward to recover $Q_1^3Q_2^2$ terms in the waveshape by swapping the particle labels 1 and 2. The $Q_1^4Q_2$ and $Q_1Q_2^4$ partial waveshapes are described below.

We have tested these results in a number of ways. Firstly, we have compared our expressions to the one-loop five-point Yang-Mills amplitudes presented in [26]. We also compared with the work of Shen [137], who iterated the classical equations to this order.

4.4.2 QCD

Let us move to Yang-Mills at this point, and analyse some of the main features of the waveshape in QCD. For the purposes of this chapter, the main difference between QED and Yang-Mills amplitudes is the handling of color degrees of freedom. In fact, now the waveshape will also include various color-dependent factors which enter diagram vertices. Here, we choose to represent the massive scalars and gluons in our problem in the fundamental T^a_{ij} and adjoint f^{abc} representation of the color group, respectively. Overall, our treatment of classical color follows [20].

Our strategy is to proceed in the usual way, by exploiting the following gauge theory structure

$$\begin{gathered} [T^a, T^b]_{ij} = f^{abc} T^c_{ij}, \\ f^{dac} f^{cbe} - f^{dbc} f^{cae} = f^{abc} f^{dce}, \end{gathered} \tag{4.70}$$

to organise and expand our amplitudes (or cuts thereof) in a color basis, and focus on each gauge invariant sector independently.

Schematically, the one-loop amplitude can be expanded in a basis of color coefficients

$\mathcal{A}_{5,1}(p_1 \ldots k) = \mathcal{C}\Big($ 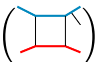 $\Big) A_1 + \mathcal{C}\Big($ 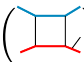 $\Big) A_2$

$+\, \mathcal{C}\Big($ 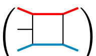 $\Big) A_3 + \mathcal{C}\Big($ 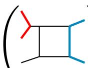 $\Big) A_4 + \mathcal{C}\Big($ 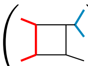 $\Big) A_5 + \cdots,$ (4.71)

where A_i is the partial amplitude corresponding to the color factor C_i, and the expression in the ellipsis includes quantum corrections. Once the full amplitude is organised in terms of independent partial amplitudes, we can consider the classical limit of each one separately. However, now we have to restore factors of $\hbar$ in both momenta and color coefficients, according to the prescription of [20], where color and non-Abelian theories were studied from a classical perspective.

We now take a moment to consider the partial amplitudes in (4.71). As we show in Table 4.1 – where we list the topologies appearing in the partial amplitudes – A_1 and A_2 involve only diagrams with no non-Abelian (pure-gluon) vertices. We recognise these as the QED amplitude sectors computed in the previous section. The contributions from these sectors can therefore be plugged into the QCD expression simply by dressing them with their given color factor. In this section we therefore focus on the terms which appear for the first time in the case of QCD – namely A_3, A_4 and A_5. As shown in Table 4.1 these partial amplitudes do involve non-Abelian topologies and must be calculated to find the full QCD result. We will refer to A_3 and A_4, A_5 as the *pentagon-* and *maximally non-Abelian* partial amplitudes, respectively.

Color type	A_i	Topologies
$\mathcal{C}$ 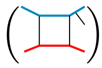	A_1, A_2	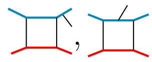
$\mathcal{C}$ 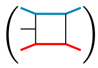	A_3	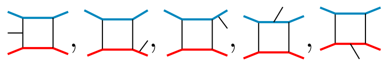
$\mathcal{C}$ 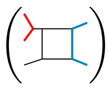	A_4, A_5	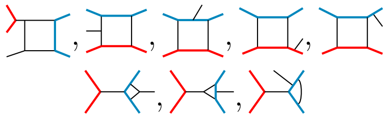

Table 4.1 *Topologies contributing to the partial amplitudes of the color factors* $\mathcal{C}$.

Pentagon

We begin by looking at the partial amplitude A_3. The color factor of this amplitude is simply the color structure of the pentagon topology, given by

$\mathcal{C}$ 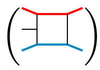 $= f^{Abc} C_1^b \cdot C_1^d \, C_2^c \cdot C_2^d, \qquad (4.72)$

where A is the adjoint index of the emitted gluon and C_i^a is the classical color charge of the massive body i [20]. In this section we will only discuss cutting the p_2 propagator, as remaining cuts can be obtained by relabelling particles. There are two cuts to consider:

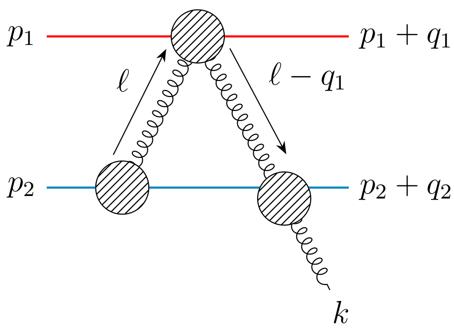

(4.73)

and

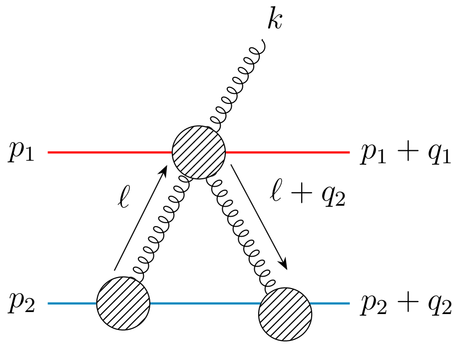

(4.74)

We analyse the cuts along the same lines as in QED, extract the coefficient of the pentagon color factor, and merge the resulting expressions. For instance, the contribution of the first cut to the pentagon involves two Compton amplitudes. Here, the color structure (4.72) is obtained through the following observation. The YM-Compton can be essentially written only in terms of the QED one,[10] which is just $\propto \varepsilon_1 \cdot \varepsilon_2$ in a convenient gauge. In fact, one finds

$$\mathcal{A}_{4,0} = 2ig^2 C_i^a C_i^b \varepsilon_1 \cdot \varepsilon_2 + 2g^2 f^{abc} C_i^c \frac{2p \cdot k_1}{q^2} \varepsilon_1 \cdot \varepsilon_2 \,. \tag{4.75}$$

Then, in the cut 4.73 using the first term above for the upper sub-amplitude and the second for the lower one we reconstruct (4.72). Furthermore, since the polarisation vector structure is the same as in the symmetric-mass QED case, we can reuse our evaluation (4.69) of the quantity K^B in this cut.

The second cut requires parts of the QCD five-point amplitude. We may restrict to those parts of the amplitude which involve a single f^{abc} color structure to match to this pentagon. The relevant terms in the amplitude are

$$i\mathcal{A}_{5,0}^{(1f)} = \frac{4g^3 f^{abd} C_1^c C_1^d}{(k_1 + k_2)^2} \left[\varepsilon_1 \cdot k_2 \, \varepsilon_2 \cdot \varepsilon_3 + \frac{\varepsilon_1 \cdot \varepsilon_2}{p \cdot (k_1 + k_2)} p \cdot k_2 \varepsilon_3 \cdot k_1 - (1 \leftrightarrow 2) \right] + \text{cycles} \,. \tag{4.76}$$

We extract from this contribution terms which are missed by the previous cut. Here, it will be convenient to work in the gauge $p_1 \cdot \varepsilon = 0$ for all external gluons, so we get to use the completeness relation (4.54) with $q = p_1$. At the end, we

[10]The importance of this point was already stressed in [40]. One can verify this explicitly in $D = 4$ or, perhaps even more clearly, by dimensionally reducing the $D = 6$ amplitudes of [248].

find the following expression for the real-part of the pentagon partial amplitude

$$\begin{aligned}\mathrm{Re}\, A_3 = g^5 \int \hat{\mathrm{d}}^D \ell \, \frac{\hat{\delta}(\ell \cdot p_2)}{\ell^2 (\ell + q_2)^2 (\ell - q_1)^2} & \Bigg[\left(\varepsilon^* \cdot p_2 \frac{p_1 \cdot p_2}{p_1 \cdot \ell} + \varepsilon^* \cdot q_2 \frac{(p_1 \cdot p_2)^2}{p_1 \cdot \ell \, p_1 \cdot k} \right) \frac{(\ell - q_1)^2}{2} \\ & - \varepsilon^* \cdot p_2 \left(\frac{(k \cdot p_2)^2}{p_1 \cdot \ell} + \frac{p_1 \cdot \ell \, \ell \cdot k + p_1 \cdot k \, \ell \cdot q_1}{(p_1 \cdot \ell)^2} \right) + \varepsilon^* \cdot \ell \frac{p_1 \cdot p_2 \, p_2 \cdot k}{p_1 \cdot \ell} \\ & + \varepsilon^* \cdot (\ell + q_2) \left(p_2^2 + \frac{p_1 \cdot p_2}{p_1 \cdot \ell} p_2 \cdot q_1 - \left(\frac{p_1 \cdot p_2}{p_1 \cdot \ell} \right)^2 \ell \cdot q_1 \right) \Bigg] .\end{aligned} \tag{4.77}$$

Maximally non-Abelian partial amplitude

Two of the most physically interesting gauge invariant sectors are A_4 and A_5. We will refer to as “maximally non-Abelian” as their color factors involve two structure constants. Noting that these two sectors are related by particle relabelling, we will focus on A_4 only. The color structure corresponding to this partial amplitude is now

$\mathcal{C}\Bigg($ 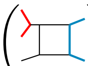 $\Bigg) = C_1^a f^{adb} f^{dAc} C_2^c \cdot C_2^b.$ (4.78)

To compute the real part of A_4 we work along the same lines of 4.4.1 and 4.4.2, so we skip some of the technical steps in this chapter. Furthermore, in order to avoid proliferation of long formulae, we only detail terms which involve a $1/q_1^2$ denominator. In fact, this pole is important for radiation reaction purposes as we will explain later. We find that, for the aforementioned pole

$$\mathrm{Re}\, A_4 \to \frac{16 g^5 m_1 m_2}{q_1^2} \int \hat{\mathrm{d}}^D \ell \, \hat{\delta}(u_2 \cdot \ell) \, \varepsilon_\eta^*(k) \cdot \sum_{i=1}^{4} J_i, \tag{4.79}$$

from cutting line 2. Above, we have conveniently defined the vectors J_i^μ as

$$J_1^\mu = - \frac{\ell^\mu}{(\ell + q_2)^2 (\ell - q_1)^2} \left(\frac{\gamma}{4 \, u_2 \cdot q_1} + \frac{\ell \cdot u_1}{\ell^2} \right), \tag{4.80}$$

$$J_2^\mu = \frac{q_1^\mu}{\ell^2 (\ell + q_2)^2 (\ell - q_1)^2} (\ell \cdot u_1 + \gamma \, u_2 \cdot q_1), \tag{4.81}$$

$$J_3^\mu = \frac{u_1^\mu}{\ell^2}\left(\frac{1}{4(\ell+q_2)^2} - \frac{(u_2\cdot q_1)^{\,2}}{(\ell+q_2)^{\,2}(\ell-q_1)^2}\right), \tag{4.82}$$

$$J_4^\mu = \frac{u_2^\mu}{\ell^2}\left(-\frac{\ell\cdot u_1}{4\,(\ell-q_1)^{\,2}\,u_2\cdot q_1} - \frac{\gamma}{4\,(u_2\cdot q_1)^2} + \frac{(\gamma\, q_1\cdot q_2 - q_1\cdot u_2\, q_2\cdot u_1)}{(\ell+q_2)^{\,2}\,(\ell-q_1)^{\,2}}\right). \tag{4.83}$$

This gauge invariant sector is actually simple enough that it can also be described through Feynman diagrams. Indeed, classically we find that only five diagrams contribute to A_4. These are

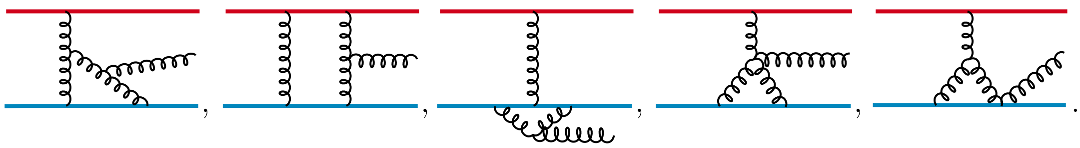

Figure 4.1 *Feynman diagrams contributing classically to* A_4.

Thus, we find it instructive to see how (4.79) can also be derived this way. To this end, and to further ease our narrative, we employ the gauge $\varepsilon\cdot u_2 = 0$ and only look at the propagator structure

$$P^{-1} = \ell^2(\ell+q_2)^2(\ell-q_1)^2. \tag{4.84}$$

Then, it turns out that such pieces arise from the following diagram only

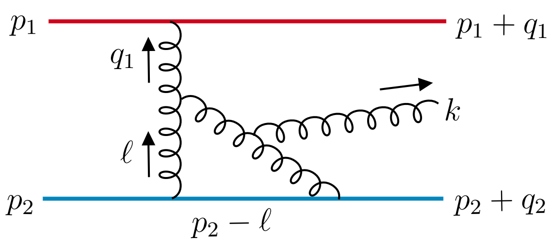

Using usual scalar QCD Feynman rules, this diagram is seen to correspond to

$$\mathrm{Re}\,A_4 \to \frac{4g^5 m_1 m_2}{q_1^2}\int \hat{\mathrm{d}}^D\ell\,\hat{\delta}(u_2\cdot\ell)\frac{N}{\ell^2(\ell+q_2)^2(\ell-q_1)^2}. \tag{4.85}$$

Above, the numerator is found to have the following expression

$$N = u_1^\alpha \, \Pi_{\alpha\beta\gamma}(-q_1, q_1 - \ell, \ell) u_2^\gamma \, \Pi^{\beta\rho\sigma}(\ell - q_1, -k, -\ell - q_2) \varepsilon^*_{\eta,\,\rho}(k) u_{2\,\sigma}, \tag{4.86}$$

where we conveniently defined the three gluon vertex with all incoming momenta as

$$\Pi_{\alpha\beta\gamma}(k, q, r) \equiv (k - q)_\gamma \eta_{\alpha\beta} + (q - r)_\alpha \eta_{\beta\gamma} + (r - k)_\beta \eta_{\alpha\gamma}. \tag{4.87}$$

Let us focus on this numerator then. A little algebra shows that this reduces to

$$N = -4\varepsilon^*_\eta \cdot \ell \, \ell \cdot u_1 + 4\varepsilon^*_\eta \cdot q_1(\ell \cdot u_1 + \gamma q_1 \cdot u_2) - 4\varepsilon^*_\eta \cdot u_1 (q_1 \cdot u_2)^2, \tag{4.88}$$

which is valid on shell of the delta functions and classically. The remaining propagator structures can be confirmed in the same fashion. We omit their derivations since they are straightforward and do not present any new features. Furthermore we have checked (4.79) both against the results of [137] and with our automated code.

We will soon see how this kinematic sector is also responsible for non-Abelian radiation reaction.

4.5 Reaction

As we have seen in section 4.4.1 our amplitude expressions are well able to reproduce conservative classical data. In this part of the chapter we show that the same happens for non conservative effects. For example, such contributions to observables can be explained in terms of the ALD force (after Abraham, Lorentz and Dirac) in classical electrodynamics, see for instance [49]. However, treatment of dissipative forces in both QCD and gravity is, at best, much more challenging. This is why our goal here is to show how these subtle classical effects can be treated in a concise and universal manner through amplitudes. As we will see, it is the imaginary part of amplitudes that has the effect of sourcing dissipation in this context.

Incidentally, as perhaps overlooked until now, we also demonstrate how radiation reaction enters the waveshape already at one loop. In fact, usually one has to deal with it at two loops or higher when computing momentum deflections [49, 249].

4.5.1 QED radiation reaction...

Let us begin with electrodynamics. As elucidated in section 4.2.2, to discuss non conservative dynamics we will only need the imaginary part of the amplitude. To be more precise, we will consider cuts in the channel involving Compton amplitudes. Indeed, we learnt in section 4.3.2 that these are the only ones that are not subtracted classically. Furthermore, as to the the real part of such diagrams, this will be rendered quantum by an appropriate choice of renormalisation scheme [49]. Conveniently for us, $\mathrm{Im}\,\mathcal{A}$ is simply obtained by appropriately cutting all relevant diagrams at this order. For simplicity we will be taking particle 1 to be static: $m_2/m_1 \ll 1$.

We start by considering cuts of diagrams of the following type

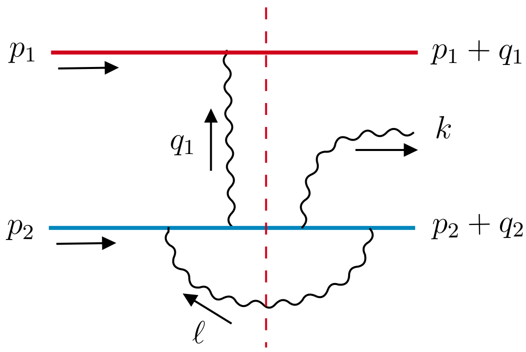

Figure 4.2 *One of the Feynman diagram cuts needed for the radiated waveform calculation. The arrows indicate momentum flow.*

To ease our calculation we will employ another useful trick. This consists of placing the q_1 photon line on-shell too. Being rigorous, we shouldn't be allowed to do so: this cut isolates a tree point amplitude which vanishes on-shell in Minkowski. Nevertheless, it turns out that we can effectively cut this line as well. In fact, multiplying $1/q_1^2$ by q_1^2 does not strictly yield zero, but only gives a contact term which integrates to zero. Thus, for all our purposes $1/q_1^2 \propto \delta(q_1^2)$.

With these considerations in place, we can realise that we only need cuts of the following type

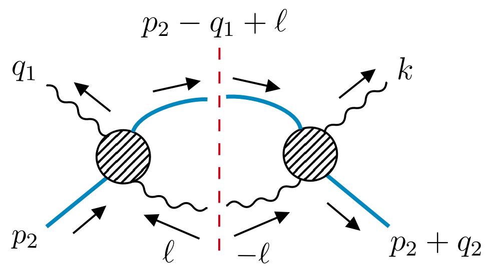

Figure 4.3 *Unitarity cut isolating two tree level Compton amplitudes* (4.89).

which are two particle cuts separating two tree level Compton amplitudes. We write such four point amplitude as

$$\mathcal{A}_{4,0}(p_1, k_1 \to p_2, k_2) = 2iQ^2 \varepsilon^{\mu}_{\eta}(k_1)\varepsilon^{*\nu}_{\eta'}(k_2)\mathcal{J}_{\mu\nu}(p_1, k_1 \to p_2, k_2), \tag{4.89}$$

where we are taking p_1, k_1 incoming and p_2, k_2 outgoing. Above, we have also defined

$$\mathcal{J}_{\mu\nu}(p_1, k_1 \to p_2, k_2) = \frac{p_{1\mu}p_{2\nu}}{p_1 \cdot k_1} + \frac{p_{2\mu}p_{1\nu}}{-p_1 \cdot k_2} - \eta_{\mu\nu}, \quad p_1 + k_1 = p_2 + k_2, \tag{4.90}$$

satisfying

$$\mathcal{J}_{\mu\nu} k_1^{\mu} \varepsilon^{\nu}(k_2) = \mathcal{J}_{\mu\nu}\varepsilon^{\mu}(k_1)k_2^{\nu} = 0. \tag{4.91}$$

Making use of these definitions, the cut is given explicitly by

$$\begin{aligned}\mathrm{Cut}_2 = -4Q^4 \sum_{\eta''} \int & \hat{\mathrm{d}}^D\ell\, \hat{\delta}(2p_2 \cdot (\ell - q_1))\hat{\delta}(\ell^2)\varepsilon^{*\mu}_{\eta}(q_1)\varepsilon^{\nu}_{\eta''}(\ell)\varepsilon^{*\rho}_{\eta''}(\ell)\varepsilon^{*\sigma}_{\eta'}(k) \\ & \times \mathcal{J}_{\mu\nu}(p_2, -q_1 \to p_2 - q_1 + \ell, -\ell)\mathcal{J}_{\rho\sigma}(p_2 - q_1 + \ell, -\ell \to p_2 + q_2, k).\end{aligned} \tag{4.92}$$

We now proceed by using, just as in the previous sections, the gauge where $\varepsilon \cdot p_2 = 0$. This means performing the helicity sum through (4.54) with $q = p_2$. One soon obtains

$$\mathrm{Cut}_2 = \frac{2Q^4}{m_2} \int \hat{\mathrm{d}}^D\ell\, \hat{\delta}(u_2 \cdot (\ell - q_1))\hat{\delta}(\ell^2) \left(\frac{\varepsilon^*_{\eta}(q_1) \cdot \ell\, \varepsilon^*_{\eta'}(k) \cdot \ell}{(u_2 \cdot q_1)^2} + \varepsilon^*_{\eta}(q_1) \cdot \varepsilon^*_{\eta'}(k) \right). \tag{4.93}$$

The loop integrals are easy to do here. The scalar one was first evaluated in [49], taking here $D = 4$

$$\int \hat{\mathrm{d}}^4\ell\, \hat{\delta}(u_2 \cdot (\ell - q_1))\hat{\delta}(\ell^2) = \frac{u_2 \cdot k}{2\pi}\Theta(u_2 \cdot k), \tag{4.94}$$

and the tensor one follows by reduction. We obtain

$$\int \hat{\mathrm{d}}^4\ell\, \hat{\delta}(u_2 \cdot (\ell - q_1))\hat{\delta}(\ell^2)\ell^\mu \ell^\nu = -\frac{(u_2 \cdot k)^3}{6\pi}\left(\eta^{\mu\nu} - 4\, u_2^\mu u_2^\nu\right)\Theta(u_2 \cdot k), \tag{4.95}$$

finally leading to,

$$\begin{aligned}\mathrm{Cut}_2 &= \frac{2Q^4}{m_2}\int \hat{\mathrm{d}}^4\ell\, \hat{\delta}(u_2 \cdot (\ell - q_1))\hat{\delta}(\ell^2)\left(\frac{\varepsilon^*_\eta(q_1)\cdot \ell\, \varepsilon^*_{\eta'}(k)\cdot \ell}{(u_2 \cdot q_1)^2} + \varepsilon^*_\eta(q_1)\cdot \varepsilon^*_{\eta'}(k)\right)\\ &= \frac{2Q^4}{m_2} u_2 \cdot k\, \Theta(u_2 \cdot k)\frac{1}{3\pi}\varepsilon^*_\eta(q_1)\cdot \varepsilon^*_{\eta'}(k).\end{aligned} \tag{4.96}$$

This result is quite simple and remarkable: the cut isolating two Compton amplitudes is proportional to a tree-level Compton amplitude itself (in the $\varepsilon \cdot p_2$ gauge) times a geometric factor $1/6\pi$.

Having computed the two particle cut, we now have to fuse back the three point amplitude we had isolated at the start. To do so we reintroduce polarisation vectors in a generic gauge, getting

$$\varepsilon^*_\eta(q_1)\cdot \varepsilon^*_{\eta'}(k) = \varepsilon^{*\mu}_\eta(q_1)\varepsilon^{*\nu}_{\eta'}(k)\mathcal{J}_{\mu\nu}(p_2, -q_1 \to p_2 + q_2, k). \tag{4.97}$$

This allows us to obtain the total five point cut-amplitude $\mathrm{Cut}_3(q_1, k) \equiv \mathrm{Cut}\,[\mathcal{A}_{5,1}(q_1, k)]$ from tree-level unitarity. At this point we also dress electric couplings with particle labels $Q \to Q_i$

$$\begin{aligned}\mathrm{Cut}_{3,\eta'} &= \frac{iQ_1}{q_1^2}\sum_\eta (2p_1 + q_1)_\rho \varepsilon^\rho_\eta(q_1)\mathrm{Cut}_{2,\eta\eta'}(q_1, k)\\ &= \frac{4iQ_1Q_2^4}{m_2^2}\frac{p_2 \cdot k}{3\pi}\frac{1}{q_1^2}\left(p_1 \cdot \varepsilon^*_{\eta'}(k) - \frac{\varepsilon^*_{\eta'}(k)\cdot p_2\, p_1 \cdot k}{k \cdot p_2}\right.\\ &\qquad\left. + \frac{p_1 \cdot p_2\, \varepsilon^*_{\eta'}(k)\cdot q_1}{p_2 \cdot k} - \frac{p_1 \cdot p_2\, \varepsilon^*_{\eta'}(k)\cdot p_2 k \cdot q_1}{(p_2 \cdot k)^2}\right).\end{aligned} \tag{4.98}$$

Above we have also set $\Theta(u_2 \cdot k) = 1$, which holds on the support of the $\mathrm{d}\Phi(k)$ integral of (4.7). Finally observe that $2i\,\mathrm{Im}\,\mathcal{A} = \mathrm{Disc}\,\mathcal{A}$ where the cutting rules give the latter, thus the imaginary part of the amplitude is

$$\mathrm{Im}\,\mathcal{A}_{5,1} = \frac{4Q_1Q_2^4}{m_2^2}\frac{p_2\cdot k}{6\pi}\frac{1}{q_1^2}\left(p_1\cdot\varepsilon^*_{\eta'}(k) - \frac{\varepsilon^*_{\eta'}(k)\cdot p_2\, p_1\cdot k}{k\cdot p_2}\right.$$
$$\left. + \frac{p_1\cdot p_2\,\varepsilon^*_{\eta'}(k)\cdot q_1}{p_2\cdot k} - \frac{p_1\cdot p_2\,\varepsilon^*_{\eta'}(k)\cdot p_2 k\cdot q_1}{(p_2\cdot k)^2}\right). \tag{4.99}$$

We find the end result of our derivation to be evocative and simple: the classical one-loop five-point amplitude is, up to a factor, the tree level one times $p_2 \cdot k$. To complete the waveform calculation we substitute the amplitude into (4.7), giving

$$F^{\mu\nu}(x) = -i\frac{Q_1Q_2^4}{6\pi m_2^2}\sum_\eta \int \mathrm{d}\Phi(k)\int \hat{\mathrm{d}}^4q_1\hat{\mathrm{d}}^4q_2\,\hat{\delta}(q_1\cdot u_1)\hat{\delta}(q_2\cdot u_2)\hat{\delta}^4(k+q_1+q_2)$$
$$\times\frac{k\cdot u_2}{q_1^2}k^{[\mu}\varepsilon_\eta^{\nu]}\varepsilon^*_\eta\cdot\mathcal{J}(k,q_1)e^{-i(k\cdot x+q_1\cdot b_1+q_2\cdot b_2)} + c.c. \tag{4.100}$$

Where we defined for convenience the classical current

$$\mathcal{J}^\nu(k,q_1) = \left(u_1^\nu + q_1^\nu\frac{u_1\cdot u_2}{k\cdot u_2} - u_2^\nu\frac{k\cdot u_1}{k\cdot u_2} - u_2^\nu\frac{u_1\cdot u_2\,k\cdot q_1}{(k\cdot u_2)^2}\right) = \mathcal{J}^\nu(-k,-q_1). \tag{4.101}$$

We have also checked that an independent computation, which makes judicious use of purely classical ALD forces, correctly reproduces (4.100). These are non-conservative forces (not time invariant) which supplement the usual Lorentz force and which acts on the particle's trajectory through

$$\frac{\mathrm{d}p_2^\mu}{\mathrm{d}\tau} = \frac{Q_2^2}{6\pi m_2}\left(\frac{\mathrm{d}^2p_2^\mu}{\mathrm{d}\tau^2} + \frac{p_2^\mu}{m_2^2}\frac{\mathrm{d}p_2}{\mathrm{d}\tau}\cdot\frac{\mathrm{d}p_2}{\mathrm{d}\tau}\right). \tag{4.102}$$

By solving for $F^{\mu\nu}$ at the desired order one finds a complete match with (4.100).

4.5.2 ...QCD radiation reaction...

We now analyse in some detail the non conservative dynamics of QCD. As it happens, the preparatory work of 4.4.2 will be very convenient for us.

In non-Abelian theories radiation reaction will be present as well, only under a more sophisticated disguise. In fact, from an amplitude standpoint, self force effects can be sourced by every diagram which has a cut isolating a Compton amplitude. As we explained, these cuts will yield an imaginary part of the waveshape that is not subtracted classically. What is more in Yang-Mills, is that we will have QED-like contributions as well as purely non-Abelian ones which involve three or four gluon vertices. We find that the non-Abelian radiation reaction channels are precisely those characterised by A_4 (and A_5) which we studied in section 4.4.2.

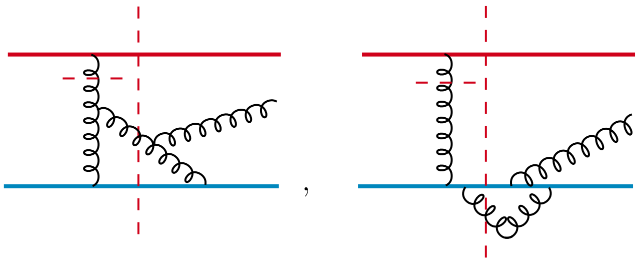

Figure 4.4 *Two cuts contributing to non-Abelian radiation reaction. While the second cut appears in both kinematic sectors A_4 (through a sub-sub-leading $\hbar$ expansion of its color) and A_2 (here with a leading color factor), the first topology belongs in A_4 only. Here, we have also cut the single gluon line as explained in 4.5.1.*

Let us then compute the radiation reaction diagrams of QCD. As before, we consider the following cut diagram

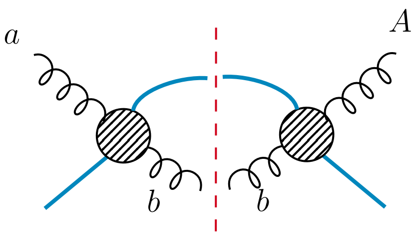

Figure 4.5 *Cut relevant to radiation reaction in QCD. For clarity we have just indicated color indices, momentum routing is the same as in figure 4.3.*

We keep in mind that the gluon a will have to be joined to particle 1. Indicating the full left/right YM Compton amplitudes with $\mathcal{A}^{ab}_{L,R}$ the diagram reads

$$\mathrm{Cut}_2 = \sum_{\text{helicities}} \int \mathrm{d}\Phi(\ell)\, \hat{\delta}(2p_2 \cdot (\ell - q_1))\mathcal{A}^{ab}_L \cdot \mathcal{A}^{bA}_R. \tag{4.103}$$

At this point it is useful to note again that the non-Abelian Compton amplitude $\mathcal{A}^{ab} \equiv \mathcal{A}^{ab}_{4,0}$ can be written as (4.75)

$$\mathcal{A}^{ab} = C^a \cdot C^b A + f^{abc} C^c A', \tag{4.104}$$

where *both* A and A' are abelian Compton amplitudes, which differ only by a factor. Using this piece of knowledge we can expand the integrand in the following manner

$$\begin{aligned} \mathcal{A}^{ab}_L \cdot \mathcal{A}^{bA}_R &= \left(C_2^a \cdot C_2^b A_L + f^{abd} C_2^d A'_L\right) \cdot \left(C_2^b \cdot C_2^A A_R + f^{bAe} C_2^e A'_R\right) \\ &\approx C_2^a \cdot C_2^b \cdot C_2^b \cdot C_2^A A_L A_R + f^{abd} f^{bAe} C_2^d \cdot C_2^e A'_L A'_R, \end{aligned} \tag{4.105}$$

having ignored the cross terms since it's quantum.

Now, the simple relation above makes it very easy to interpret the structure of the cut in non-Abelian gauge theories. The first term in (4.105), the one proportional to $C_2^a \cdot C_2^b \cdot C_2^b \cdot C_2^A$, is exactly the one already encountered in QED in (4.96)! That is to say that

$$\sum_{\text{helicities}} \int \mathrm{d}\Phi(\ell)\, \hat{\delta}(2p_2 \cdot (\ell - q_1)) A_L A_R = \frac{2g^4}{m_2} u_2 \cdot k \frac{1}{3\pi} \varepsilon^*_\eta(q_1) \cdot \varepsilon^*_{\eta'}(k). \tag{4.106}$$

In other words, what we had computed in QED was also part of the QCD story, only now multiplied by a constant color structure. It is immediate to see that the last, non-Abelian, term of (4.105) has (up to relabelling) the structure (4.78). This is precisely the color of the partial amplitude A_4. Then, for the computation of this channel we need precisely the $1/q_1^2$ pole that we described in (4.79), entailing non-Abelian radiation reaction. From (4.79), the imaginary part of the five point amplitude is immediately obtained and it reads

$$\operatorname{Im} A_4 = \frac{8g^5 m_1 m_2}{q_1^2} \varepsilon^*_\mu(k) \int \mathrm{d}\Phi(\ell) \hat{\delta}(u_2 \cdot (\ell - q_1)) \frac{(u_1 \cdot \ell + \gamma q_1 \cdot u_2) q_1^\mu - (u_2 \cdot q_1)^2 u_1^\mu}{(q_1 - \ell)^2 (\ell + k)^2}, \tag{4.107}$$

in a gauge where $\varepsilon \cdot p_2 = 0$.

4.5.3 ...GR radiation reaction

As a final application of this section, we will here tackle gravity self force radiation. This will indeed demonstrate how the dissipative effects are cleanly taken into account by our analytic framework.

Following the examples of QED and QCD we again focus on the 2-particle cut, just involving graviton lines now

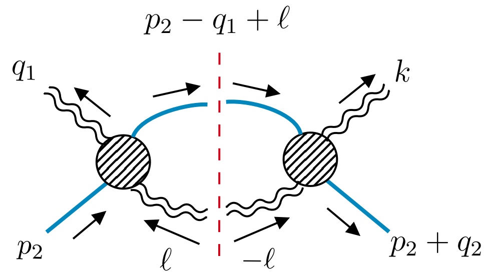

having taken the leg with momentum q_1 to be on-shell as well (as before, we keep in mind that this graviton will have to be reconnected with the worldline of particle 1). The cut-amplitude is given by

$$\mathrm{Cut}_2 = \sum_{\text{helicities}} \int \mathrm{d}\Phi(\ell)\, \hat{\delta}(2p_2 \cdot (\ell - q_1)) \\ \times \mathcal{M}_{4,0}(p_2, -q_1 \to p_2 - q_1 + \ell, -\ell)\mathcal{M}_{4,0}(p_2 - q_1 + \ell, -\ell \to p_2 + q_2, k). \tag{4.108}$$

This quantity can be greatly simplified by choosing, as we did before, a gauge in which graviton polarisations are orthogonal to p_2: $\varepsilon_\mu \varepsilon_\nu p_2^\mu = \varepsilon_\mu \varepsilon_\nu p_2^\nu = 0$. In this case the product of amplitudes becomes proportional to a single contraction [250]

$$\mathcal{M}_{4,0}(p_2, q_1, \ell)\mathcal{M}_{4,0}(p_2, k, \ell) = \frac{\kappa^4}{4} \frac{(p_2 \cdot k)^4}{(\ell + k)^2(\ell - q_1)^2} (\varepsilon^*(q_1) \cdot \varepsilon(\ell)\, \varepsilon^*(\ell) \cdot \varepsilon^*(k))^2. \tag{4.109}$$

At this point we have to evaluate the sum over physical states. Note that we haven't been explicit about helicity assignments since these always come with opposite signs inside the loop. We have

$$\sum_{\text{helicities}} (\varepsilon^*(q_1) \cdot \varepsilon(\ell)\, \varepsilon^*(\ell) \cdot \varepsilon^*(k))^2 = \varepsilon^{*\mu}(q_1)\varepsilon^{*\nu}(k)\varepsilon^{*\rho}(q_1)\varepsilon^{*\sigma}(k)P_{\mu\nu\rho\sigma}(\ell), \tag{4.110}$$

where the projector over physical states reads, for the case of a massive gauge vector p_2

$$P_{\mu\nu\rho\sigma}(\ell) = \sum_{\text{helicities}} \varepsilon_\mu(\ell)\varepsilon^*_\nu(\ell)\varepsilon_\rho(\ell)\varepsilon^*_\sigma(\ell) = \frac{1}{2}\left(P_{\mu\nu}P_{\rho\sigma} + P_{\mu\sigma}P_{\rho\nu} - \frac{2}{D-2}P_{\mu\rho}P_{\sigma\nu}\right). \tag{4.111}$$

Above we have defined

$$P^{\mu\nu}(\ell) = -\left(\eta^{\mu\nu} - \frac{\ell^{(\mu}u_2^{\nu)}}{\ell\cdot u_2} + \frac{\ell^\mu\ell^\nu}{(\ell\cdot u_2)^2}\right), \tag{4.112}$$

which is the projection over on shell states that we had used in the electromagnetic case. The contraction is then straightforward and yields[11]

$$\varepsilon^{*\mu}\varepsilon^{*\nu}\varepsilon^{*\rho}\varepsilon^{*\sigma}P_{\mu\nu\rho\sigma} = \left(\varepsilon^*(q_1)\cdot\varepsilon^*(k) + \frac{\varepsilon^*(q_1)\cdot\ell\,\varepsilon^*(k)\cdot\ell}{(u_2\cdot\ell)^2}\right)^2 - \frac{1}{2}\left(\frac{\varepsilon^*(q_1)\cdot\ell\,\varepsilon^*(k)\cdot\ell}{(u_2\cdot\ell)^2}\right)^2, \tag{4.113}$$

finally giving us a direct expression of the cut

$$\begin{aligned}\mathrm{Cut}_2 = \frac{\kappa^4}{8}(p_2\cdot k)^4\varepsilon^*_\mu(q_1)\varepsilon^*_\nu(q_1)\varepsilon^*_\rho(k)\varepsilon^*_\sigma(k)\int \mathrm{d}\Phi(\ell)\,\hat\delta(p_2\cdot(\ell-q_1))\frac{1}{(\ell+k)^2(\ell-q_1)^2}\\ \times\left(\eta^{\mu\rho}\eta^{\nu\sigma} + \frac{1}{(u_2\cdot\ell)^2}\eta^{\mu\rho}\ell^\nu\ell^\sigma + \frac{1}{2(u_2\cdot\ell)^4}\ell^\mu\ell^\nu\ell^\rho\ell^\sigma\right).\end{aligned} \tag{4.114}$$

The integral is IR divergent; we discuss IR divergences further below.

It is then straightforward to reproduce a very compact expression of the five point amplitude's imaginary part from tree level unitarity

$$\begin{aligned}\mathrm{Im}\,\mathcal{M}_{5,1} = \frac{\kappa^5(p_2\cdot k)^4}{16\,q_1^2}P_{\alpha\beta\mu\nu}(q_1)p_1^\alpha p_1^\beta\varepsilon^*_\rho(k)\varepsilon^*_\sigma(k)\int \mathrm{d}\Phi(\ell)\,\frac{\hat\delta(p_2\cdot(\ell-q_1))}{(\ell+k)^2(\ell-q_1)^2}\\ \times\left(\eta^{\mu\rho}\eta^{\nu\sigma} + \frac{1}{(u_2\cdot\ell)^2}\eta^{\mu\rho}\ell^\nu\ell^\sigma + \frac{1}{2(u_2\cdot\ell)^4}\ell^\mu\ell^\nu\ell^\rho\ell^\sigma\right).\end{aligned} \tag{4.115}$$

We remind the reader that this result was achieved in a gauge where $\varepsilon\cdot p_2 = 0$, but one can still retrieve the explicitly gauge invariant expression substituting in

$$\varepsilon^\mu(k)\to\varepsilon^\mu(k) - \frac{\varepsilon(k)\cdot p_2}{k\cdot p_2}k^\mu. \tag{4.116}$$

It would be interesting to replicate (4.115) using purely classical methods, as we did for QED. One way to do this would be through the "MiSaTaQuWa" equations[12] of [251, 252], which are known to describe linear self force in gravity. However, practical computations based on these (non-local) forces happen to

[11] At this point we have taken $D = 4$.
[12] After Mino, Sasaki, Tanaka, Quinn, Wald.

be subtle. This is because they involve integrals of the (curved space) Green functions over the complete past history of the particle.

As a final remark for this section, we would like to underline the universality of the two-particle cuts of Compton amplitudes (4.92), (4.103) and (4.108). As we hope it is clear by now, this object is crucial for the characterisation of the imaginary part of the full five point amplitude describing the waveform. However, the same object can be used, as was done for instance in [49], to describe $\mathcal{O}(g^6)$ radiation reaction effects that alter the integrated momentum kick of the particle. Classically speaking, the physics of these two situations is different. The radiation reaction $\mathcal{O}(g^5)$ contribution is a transient one[13] that doesn't affect the final trajectory. However, the emitted radiation can still be observed in the waveform. Instead, at $\mathcal{O}(g^6)$, one is able to change the final net trajectory of the particle Δp^μ. Nonetheless, this second (two-loop) process is still entailed by Cut_2: in this case one has to attach both massless states of the cut into the second massive worldline. See the figure below for a graphic depiction of this property of the cut considered

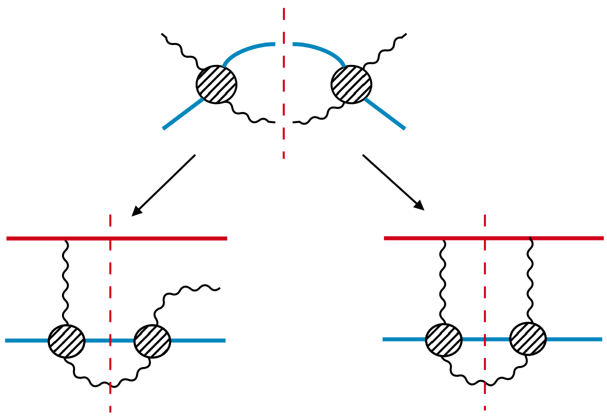

Figure 4.6 *Universality of the Compton amplitude cut. This can be seen as a building block of different phenomena which correspond to distinct classical contributions for the EOM, however both can be generated from the same amplitude entity.*

4.6 Infrared divergences

We will now discuss the effect of infrared divergences arising from soft virtual photons in loop amplitudes. These virtual IR divergences arise from diagrams

[13] In QED this is described by a total derivative Schott term.

where soft photon loops are attached to on-shell external legs of a scattering amplitude in the manner illustrated below.

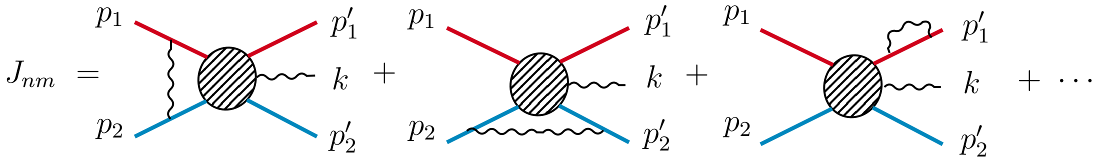

Figure 4.7 *Infrared divergent diagrams in the in the 1-loop amplitude*

IR divergences arise from the region where the virtual loop momentum $|\boldsymbol{\ell}|$ is much smaller than the momenta of of external particle p_i. In this region, it is possible to show that the IR divergent amplitudes take the form [253]:

$$\mathcal{A}^{IR} = \left(\frac{1}{2}\frac{1}{(2\pi)^4}\sum_{nm} e^2 Q_n Q_m \eta_n \eta_m J_{nm}\right) \times \mathcal{A}^{\text{Hard}}, \tag{4.117}$$

where $\mathcal{A}^{\text{Hard}}$ is what is left of the amplitude after removing the virtual photons lines, and the divergent factor J_{nm} is given by[14]

$$J_{nm} \equiv -i\,(p_n \cdot p_m) \int_{\mu \le |\boldsymbol{\ell}| \le \Lambda} \frac{\hat{\mathrm{d}}^4 \ell}{[\ell^2 + i\epsilon]\,[p_n \cdot \ell + i\eta_n \epsilon]\,[-p_m \cdot \ell + i\eta_m \epsilon]} \tag{4.118}$$

where Λ is a scale that defines the soft photons, μ is an IR cutoff and $\eta_n = \pm 1$ for outgoing and incoming particles respectively. In what follows, we will use primed indices to refer to outgoing particles so that $\eta_1 = \eta_2 = -1$ an $\eta_1' = \eta_3' = +1$. Specifically, we will be interested in IR divergences of one-loop five-point amplitudes, so that $\mathcal{A}^{IR} \equiv \mathcal{A}^{IR}_{5,1}$, $\mathcal{A}^{\text{Hard}} \equiv \mathcal{A}^{\text{Hard}}_{5,0}$.

Turning to the integral J_{nm}, we perform the integration over ℓ^0 by residues. In doing so, we will consider two distinct cases. First, we consider the case where one particle is incoming and the other outgoing. Then we consider the same integral when both particles are incoming/outgoing.

Let us start by taking particle n to be outgoing and m to be incoming. In this case the poles are $\ell^0 = \pm|\boldsymbol{\ell}| \pm i\epsilon$, $\ell^0 = \frac{\boldsymbol{p}_n \cdot \boldsymbol{\ell}}{p_n^0} - i\epsilon$ and $\ell^0 = \frac{\boldsymbol{p}_m \cdot \boldsymbol{\ell}}{p_m^0} - i\epsilon$. The important point in this case is that the poles associated with the massive propagators both lie on the same half of the complex ℓ^0 plane, so their contribution can be avoided entirely by closing the contour on the other side of the complex plane. In this

[14] $D = 4$ here.

case, we close the contour on the upper half plane, picking the pole $\ell^0 = |\boldsymbol{\ell}| + i\epsilon$. Evaluating the integral in this manner yields the result[15]

$$\text{Re } J_{nm} = \frac{2\pi^2}{\beta_{nm}} \ln\left(\frac{1+\beta_{nm}}{1-\beta_{nm}}\right) \ln\left(\frac{\Lambda}{\mu}\right), \tag{4.119}$$

where β_{nm} is the relative velocity

$$\beta_{nm} \equiv \sqrt{1 - \frac{m_n^2 m_m^2}{(p_n \cdot p_m)^2}}. \tag{4.120}$$

We now consider the case where both particles are either incoming or outgoing. For definiteness, consider the case where both particles are outgoing so that $\eta_n = \eta_m = 1$. In which case the poles are located at

$$\begin{aligned} \ell^0 &= \pm|\boldsymbol{\ell}| \pm i\epsilon \\ \ell^0 &= \frac{\boldsymbol{p}_n \cdot \boldsymbol{\ell}}{p_n^0} - i\epsilon \\ \ell^0 &= \frac{\boldsymbol{p}_m \cdot \boldsymbol{\ell}}{p_m^0} + i\epsilon \end{aligned} \tag{4.121}$$

In this case, the poles of massive propagators lie on opposite sides of the complex plane, so that we would inevitably pick up one of these poles whichever way the contour is closed. Supposing we close the contour from above, we pick up a pole associated with the photon propagator and one from the massive propagators. The former contribution is identical to the integral above and gives the real part of the integral. The latter pole contributes another term which is [254]

$$\begin{aligned} \text{Im } J_{nm} &= -i\,(p_n \cdot p_m) \int_{\mu \le |\boldsymbol{\ell}| \le \Lambda} \frac{|\boldsymbol{\ell}|^2 \hat{\mathrm{d}}|\boldsymbol{\ell}|\ \hat{\mathrm{d}}\Omega(\boldsymbol{n})}{\left[(\frac{\boldsymbol{p}_m \cdot \boldsymbol{\ell}}{p_m^0})^2 - |\boldsymbol{\ell}|^2 + i\epsilon\right] \left[p_n^0(\boldsymbol{p}_m \cdot \boldsymbol{\ell}) + p_m^0(\boldsymbol{p}_n \cdot \boldsymbol{\ell}) + i\epsilon\right]} \\ &= 2\pi\,(p_n \cdot p_m) \ln\left(\frac{\Lambda}{\mu}\right) \int \frac{\hat{\mathrm{d}}\Omega(\boldsymbol{n})}{\left[(\frac{\boldsymbol{p}_m \cdot \boldsymbol{n}}{p_m^0})^2 - 1 + i\epsilon\right] \left[p_n^0(\boldsymbol{p}_m \cdot \boldsymbol{n}) + p_m^0(\boldsymbol{p}_n \cdot \boldsymbol{n}) + i\epsilon\right]} \end{aligned} \tag{4.122}$$

The last integral is most easily evaluated by going to the rest frame of particle m such that $\boldsymbol{p}_m \cdot \boldsymbol{n} = 0$ and $p_m^0(\boldsymbol{p}_n \cdot \boldsymbol{n}) = m_m m_n \gamma_{nm} \beta_{nm} (\hat{\beta} \cdot \boldsymbol{n})$ where $\gamma_{nm} = p_n \cdot p_m / m_n m_m$ is the Lorentz factor and β_{nm} the relative velocity. In this frame the integral becomes

[15] The same result can be translated to dimreg by replacing $\log(\Lambda/\mu) \to 1/(2\varepsilon)$.

$$4\pi^2 (p_n \cdot p_m) \ln\left(\frac{\Lambda}{\mu}\right) \int_{-1}^{1} \frac{\hat{\mathrm{d}}x}{m_n m_m \gamma_{nm} \beta_{nm} [x+i\epsilon]} \tag{4.123}$$

where we have oriented such that $\hat{\boldsymbol{\beta}} \cdot \boldsymbol{n} = \cos\theta \equiv x$. Finally, we make use of the identity

$$\frac{1}{x+i\varepsilon} = \mathrm{PV}\left(\frac{1}{x}\right) - \frac{i}{2}\hat{\delta}(x) \tag{4.124}$$

and, noting that only the second term contributes to the integral by parity, we arrive at the result

$$\mathrm{Im}\ J_{nm} = -\frac{4i\pi^3}{\beta_{nm}} \ln\left(\frac{\Lambda}{\mu}\right). \tag{4.125}$$

Note that is also possible to recover this imaginary divergence in the spirit of section 4.2.2. It is straightforward to check that cutting the massive propagators attaching to the virtual photon lines recovers the result above. To summarise, we find that the infrared divergences contain both real and imaginary parts. The diagrams where the virtual photons attach to one incoming and one outgoing leg yield purely real IR divergences, while the diagrams in which the virtual photon attaches to two incoming/outgoing legs give both real and imaginary divergences.

We are now ready to address the issue of whether these IR divergences contribute to the classical waveshape. We do so by examining the $\hbar$ expansion of the sum:

$$\frac{1}{2(2\pi)^4} \sum_{nm} Q_n Q_m \eta_n \eta_m J_{nm}. \tag{4.126}$$

Noting that the one-loop amplitude is suppressed by a factor $Q^2/\hbar$ relative to the tree amplitude, we identify the quantum parts of J_{nm} as those of order $\hbar^2$. We denote the incoming and outgoing massive momenta by p_1, p_2 and p_1', p_2' respectively such that $\eta_1 = \eta_2 = -1$ and $\eta_1' = \eta_2' = +1$ and $Q_1 = Q_1'$, $Q_2 = Q_2'$. Using momentum conservation, we write

$$\begin{aligned} p_1' &= p_1 + q \\ p_2' &= p_2 - q - k. \end{aligned} \tag{4.127}$$

Furthermore, from the on-shell conditions we have

$$\begin{aligned} p_1 \cdot q &= \mathcal{O}(\hbar^2) \\ p_2 \cdot q &= -p_2 \cdot k + \mathcal{O}(\hbar^2) \end{aligned} \tag{4.128}$$

Using this it is straightforward to expand J_{nm} in powers of $\hbar$ noting that the

$\hbar$ dependence of follows from expanding the dot products $p_n \cdot p_m$ using the on-shell conditions. We will find it convenient to express our results in terms of the Lorentz factor and relative velocity

$$\gamma \equiv \frac{p_1 \cdot p_2}{m_1 m_2} \quad v \equiv \sqrt{1 - \frac{1}{\gamma^2}}. \tag{4.129}$$

4.6.1 Real divergence

We now examine the $\hbar$ expansion of the real divergences in (4.119). To ensure that these divergences are quantum, we must show that the $\mathcal{O}(\hbar^0)$ and $\mathcal{O}(\hbar)$ terms vanish in the sum over (n, m). Since we are considering real divergences, all values of (n, m) contribute to the sum. Considering the $\mathcal{O}(\hbar^0)$ terms first, it is easy to check the sum of terms cancels exactly. Consider for example the part of the sum proportional to Q_1^2 , we have

$$\frac{1}{2(2\pi)^4} e^2 Q_1^2 \,\mathrm{Re}\,(\eta_1 \eta_1 J_{11} + 2\eta_1 \eta_1' J_{11'} + \eta_1' \eta_1' J_{1'1'}) \tag{4.130}$$

To this order, we have that $p_1 \cdot p_1 = p_1 \cdot p_1' = p_1' \cdot p_1' = m_1^2$ and since J_{nm} is a function of $p_n \cdot p_m$ we conclude that $J_{11} = J_{11'} = J_{1'1'}$ but due to the sign differences arising from the η factors, we find that this sum vanishes. It is easy to verify that a similar cancellation occurs for the terms proportional to Q_1^2 and $Q_1 Q_2$. We conclude that the $O(\hbar^0)$ terms do not contribute to the real IR divergences.

Turning to the $O(\hbar)$ terms, we start by noting that the terms in the sum proportional to Q_i^2 for $i = 1, 2$ still cancel in the same manner as before. This is because the equality $p_i \cdot p_i = p_i \cdot p_i' = p_i' \cdot p_i'$ still holds to this order (they only differ by terms of $\mathcal{O}(\hbar^2)$). We therefore only need to look at the terms proportional to $Q_1 Q_2$. Noting that the terms $J_{12} = J_{21}$ do not contribute powers of $\hbar$, we are left with:

$$\frac{1}{(2\pi)^4} e^2 Q_1 Q_2 \mathrm{Re}\,(\eta_1 \eta_2' J_{12'} + 2\eta_1' \eta_2 J_{1'2} + \eta_1' \eta_2' J_{1'2'}). \tag{4.131}$$

Expanding each term to linear order in $\hbar$ using (4.119) and the kinematics (4.128) we find that

$$\text{Re}\ \eta_1\eta_2' J_{12'} = \frac{2\pi^2 m_1 m_2 k\cdot p_1 \left(2\gamma^2 m_1^2 m_2^2 + m_1^2 m_2^2 \left(v \log\left(\frac{1-v}{1+v}\right) - 2\right)\right)}{\gamma^3 v^4} \tag{4.132}$$

$$\text{Re}\ \eta_1'\eta_2 J_{1'2} = -\frac{2\pi^2 m_1 m_2 k\cdot p_2 \left(2\gamma^2 m_1^2 m_2^2 + m_1^2 m_2^2 \left(v \log\left(\frac{1-v}{1+v}\right) - 2\right)\right)}{\gamma^3 v^4} \tag{4.133}$$

$$\text{Re}\ \eta_1'\eta_2' J_{1'2'} = -\frac{2\pi^2 m_1 m_2 (k\cdot p_1 - k\cdot p_2) \left(2\gamma^2 m_1^2 m_2^2 + m_1^2 m_2^2 \left(v \log\left(\frac{1-v}{1+v}\right) - 2\right)\right)}{\gamma^3 v^4} \tag{4.134}$$

These terms once again cancel in the sum. Having established that the terms of $\hbar$ cancel, we conclude that the real infrared divergences do not contribute classically.

4.6.2 Imaginary part

The $\hbar$ expansion of the imaginary IR divergences proceeds in the manner as in the previous sections, where we now expand:

$$\text{Im}\ J_{nm} = -\frac{4i\pi^3}{\beta_{nm}} \ln\left(\frac{\Lambda}{\mu}\right). \tag{4.135}$$

This time however, the sum does not run over all pairs (n, m) but only those for which $\eta_n = \eta_m$. It is precisely this restriction of the sum which prevents the classical contributions from cancelling. We find that the term $(n, m) = (1', 2')$ in the sum yields a classical contribution which survives the sum due to the absence of the terms $(1, 2')$ and $(1', 2)$ in the imaginary part, so that the imaginary part of the amplitude contains a classical IR divergence. Nevertheless, this divergence drops out of the waveform due to the simplification discussed in section 4.3.2.

4.6.3 QCD and gravity

The analysis of IR divergences in QCD and gravity proceeds broadly in the same manner. Soft divergences arising from graphs where a soft messenger connects two massive lines have the same fate as in QED, and do not contribute to the waveshape.

There are two major differences in QCD and gravity, however. First, in both theories, soft divergences also arise in diagrams where a soft messenger connects a massive to a *massless* line. Imaginary IR divergences in such diagrams do indeed have classical implications, and are discussed in references [77, 78, 255, 256]. Second, in QCD, collinear divergences arise at the level of the amplitude. It would be interesting to explore the classical implications of these collinear divergences in future.

4.7 Discussions

In this chapter we investigated how next-to-leading-order radiation fields can be elegantly computed using the techniques of modern scattering amplitudes.

Building upon the KMOC formalism of [49], we characterised NLO radiation fields in terms of the real and imaginary parts of a waveshape. The real part is extracted by cutting one massive line of a five-point one-loop amplitude, whereas the imaginary part is obtained by a double cut of this amplitude. With this arrangement, all remaining propagators are defined through a principal-value prescription. This propagator structure emerges directly from the Feynman $i\epsilon$ prescription together with the split into real and imaginary parts, with no further intervention by hand.

Our organisation of the observable provides two key benefits. First, it improves computational efficiency: the cancellation of apparently singular inverse powers of $\hbar$ (the "superclassical" terms) can be trivialised. Second, this organisation clarifies the underlying physics. Both real and imaginary parts have separate, gauge invariant, physical meaning.

The real part describes the radiation emitted by a body moving under the influence of essentially conservative forces: for example, a charge accelerated by the Lorentz force in the field of a different charge. In contrast, the imaginary part captures intrinsically dissipative effects: radiation generated under the influence of the particle's self field. In electrodynamics, this can be understood as the portion of radiation generated by the action of the ALD force on the charge. In our description, this aspect of radiation reaction at one loop order is directly related to a simple unitarity cut involving a product of two Compton amplitudes in electrodynamics, Yang-Mills theory and gravity.

An interesting aspect of the waveform is that in electrodynamics, all infrared divergences cancel in the waveshape. However theories with self-interacting massless messengers (Yang-Mills theory and gravity) retain a residual IR divergence [77, 78, 255, 256].

We found scalar QED to be a good guide for the understanding of, more complicated, YM and GR. In fact, although electrodynamics is a comparatively simple theory, it is rich enough to provide a very stimulating laboratory to understand many aspects of the dialogue between amplitudes and classical physics, especially since it is often rather straightforward to pass from electrodynamics to Yang-Mills theory [20, 257, 258].

We will use QED as a guide the upcoming, final, chapter of the thesis too. There, we will look out for exponentiation structures (i.e. eikonal phase and coherence) which are expected to characterise scattering in the classical regime.

Chapter 5

Eikonal and Coherent State Exponentiation

5.1 Introduction

In this final chapter we try to understand what are the structures that arise classically. There are many reasons to be interested in scattering amplitudes besides gravitational wave physics. In fact, we believe amplitudes are fascinating in their own right because of their internal structure. In many theories, including general relativity, amplitudes have uniqueness properties which allow us (in principle) to determine the entire S matrix from basic knowledge of the helicities of the interacting particles [90, 177]. In this way amplitudes provide a way to *define* a quantum field theory. Since amplitudes are intrinsically quantum-mechanical objects this definition hard-wires key aspects of quantum mechanics, such as the uncertainty principle, into the physics.

Taking the viewpoint that scattering amplitudes define the physics, an old question reappears. How do we understand the classical limit? It is more common to define quantum field theories in terms of path integrals: then (thanks to Feynman) it is clear how the classical limit arises: it comes from the stationary phase in the path integral. But amplitudes, as a quantum-first definition of a quantum field theory, do not have as clear a link to classical physics.

Here, we want to focus again on this important point. How is the classical limit encoded in the quantum-first definition of field theory through scattering amplitudes? To answer this question we take another look at the link between amplitudes and classical physics.

As we have already argued and showed, by now there are several methods available for converting amplitudes into classical quantities. It has long been understood that four-point amplitudes are closely connected to classical potentials [40, 101, 179, 180, 259], and it is possible to deduce interaction potentials from four-point multiloop amplitudes. More generally, effective Lagrangians are often used to compute amplitudes — and this procedure can be reversed, allowing Wilson coefficients in effective Lagrangians to be extracted from amplitudes [36–39]. The versatility of effective Lagrangians allows information and the potential, spin effects [6, 257], etc to be readily extracted from amplitudes and applied to bound gravitational systems.

In this chapter we will be particularly interested in two other links between amplitudes and classical physics. We will do this again employing the versatility of the KMOC formalism, which is our first link here. In fact, it is worth emphasising that the methods of KMOC apply equally well to quantum observables which do not make sense in the classical theory (for example, the number of photons radiated during a scattering event). In this sense KMOC is a quantum-first method: it takes the quantum field theory as the basic starting point, making contact with classical physics only at the end of the computation.

The eikonal approximation is the second link between amplitudes and classical physics of particular interest to us. Eikonal physics has a long history, going back to nineteenth century work on the relation between geometric and wave optics. The "eikonal analogy" was a guide in the early development of quantum mechanics. In its long history the precise meaning of the word "eikonal" seems to have undergone some drift. We are interested in the eikonal approximation to (especially four-point) massive amplitudes in quantum field theory [260–267]. In this approximation, the incoming s-channel energy is large compared to momentum transfers. The key fact in this limit is that the amplitude can be separated into two factors. One of these factors is the exponent of an eikonal function which, as we will see, is analogous to a classical action, and is the part of the amplitude which describes classical physics. The remaining terms in the amplitude, which do not exponentiate, are quantum mechanical.

The quintessential difference between classical and quantum physics is uncertainty. Quantum observables naturally have a variance which is absent in classical physics. We begin our study by computing the variance in important classical observables using scattering amplitudes, following the methods of KMOC. In the classical limit the variance must be negligible. We find that this condition of negligible variance can be potentially used to discover infinitely many relations between classical amplitudes[1]. More specifically, in the correspondence regime we can expand our amplitudes in powers of momentum transfer over centre-of-mass energy. This is a semi-classical expansion because the momentum transfers in KMOC are order $\hbar^2$. The zero-variance conditions relate certain terms in this "transfer" expansion between amplitudes with different numbers of loops and legs. For example, five-point amplitudes in the transfer expansion are related to lower loop five-point and four-point amplitudes.

At four points, the zero-variance conditions are very familiar: they are the relations required for eikonal exponentiation. Our work therefore shows that there is a generalisation of the eikonal formula beyond four points. We outline the structure of the generalisation, which involves a coherent radiative state entangled with the four-point dynamics.

As in the previous parts of the thesis, we consider semiclassical scattering events involving two point-like particles. The particles may interact electromagnetically, gravitationally, or via classical Yang-Mills forces. We begin our work in section 5.2 with a discussion of a basic requirement for a successful quantum description of such a classical event: negligible variance in a measurement of the field strength. As we will see, this requirement becomes a non-trivial constraint on scattering amplitudes. The leading obstruction is given by the six-point tree amplitude; this amplitude must be suppressed relative to the corresponding six-point one-loop amplitude. As a check we compute the tree amplitude, demonstrating explicitly that it has the required suppression. We build on this observation in section 5.3 to find an infinite series of constraints on multi-loop, multi-leg scattering amplitudes, verifying the first non-trivial constraint on the five-point one-loop amplitude in section 5.3.2. In section 5.4 we interpret these zero-variance conditions in eikonal terms, arguing that radiation exponentiates in a manner analogous to the conservative terms. We propose a formula for the S matrix acting on our state which is a product of a coherent radiative state entangled with the more

[1]This infinity is meant in the sense that one can consider more and more complicated matrix elements, impose minimal uncertainty, and find relationships between higher loops (and point) amplitude with lower ones. But given a specific amplitude only finitely many relations will exist between it and its easier fragments.

[2]Alternatively one can think of the expansion as a large-mass expansion because the centre-of-mass energy is dominated by the particle masses.

traditional eikonal (conservative) dynamics.

The main body of our chapter concludes in section 5.5 with a discussion.

5.2 Negligible Uncertainty

In classical electrodynamics, a key role is played by the field strength $F_{\mu\nu}(x)$. This object is a complete gauge-invariant characterisation of the field; once it is known, quantities such as the energy-momentum radiated to infinity and the field angular momentum are easily determined. In a quantum description, the field becomes an operator $\mathbb{F}_{\mu\nu}(x)$. In a semiclassical situation, the expectation value of this operator on a state $|\psi\rangle$ should equal the classical field, up to negligible quantum corrections:

$$\langle\psi|\mathbb{F}_{\mu\nu}(x)|\psi\rangle = F_{\mu\nu}(x) + \mathcal{O}(\hbar)\,. \tag{5.1}$$

Note that we have schematically indicated the presence of small, order $\hbar$, quantum corrections. More precisely, these corrections must be suppressed by dimensionless ratios involving Planck's constant; the precise ratios depend on the actual physical context.

Since in the quantum theory a single-valued field is replaced by the expectation value of an operator, we must address the quintessentially quantum mechanical issue of uncertainty. The uncertainty can be characterised by the variance

$$\langle\psi|\mathbb{F}_{\mu\nu}(x)\mathbb{F}_{\rho\sigma}(y)|\psi\rangle - \langle\psi|\mathbb{F}_{\mu\nu}(x)|\psi\rangle\langle\psi|\mathbb{F}_{\rho\sigma}(y)|\psi\rangle\,. \tag{5.2}$$

In the domain of validity of the classical approximation, this variance must be negligible. We have already seen in (2.63) and (2.64) that *initial* coherent states satisfy the conditions (5.1) and (5.2), we will see in this chapter what are the implications for emitted light.

Precisely the same remarks hold in a quantum mechanical approach to GR. The curvature tensor $R_{\mu\nu\rho\sigma}(x)$ in the classical theory is replaced by the expectation value of the curvature operator $\mathbb{R}_{\mu\nu\rho\sigma}(x)$. The variance

$$\langle\psi|\mathbb{R}_{\mu\nu\rho\sigma}(x)\mathbb{R}_{\alpha\beta\gamma\delta}(y)|\psi\rangle - \langle\psi|\mathbb{R}_{\mu\nu\rho\sigma}(x)|\psi\rangle\langle\psi|\mathbb{R}_{\alpha\beta\gamma\delta}(y)|\psi\rangle \tag{5.3}$$

must be negligible.[3]

This section is devoted to an investigation of this condition of negligible uncertainty. Working in the KMOC formalism at lowest order in perturbation theory, we will see that the expectations $\langle\psi|\mathbb{F}_{\mu\nu}(x)\mathbb{F}_{\rho\sigma}(y)|\psi\rangle$ and $\langle\psi|\mathbb{R}_{\mu\nu\rho\sigma}(x)\mathbb{R}_{\alpha\beta\gamma\delta}(y)|\psi\rangle$ are determined by tree-level *six*-point amplitudes while $\langle\psi|\mathbb{F}_{\mu\nu}(x)|\psi\rangle$ together with $\langle\psi|\mathbb{R}_{\mu\nu\rho\sigma}(x)|\psi\rangle$ are determined by *five*-point tree amplitudes. We must then face the question of how it can be that the variance is negligible.

5.2.1 Field strength expectations

We begin by reviewing the evaluation of single field-strength observables in KMOC. The gravitational case is completely analogous to the electromagnetic case, so we only quote key results.

The EM four-potential operator is

$$\mathbb{A}_\mu(x) = \frac{1}{\sqrt{\hbar}}\sum_{\eta=\pm}\int \mathrm{d}\Phi(k)\left[a_\eta(k)\,\varepsilon_\mu^{(\eta)*}(k)\,e^{-i\bar{k}\cdot x} + \text{h.c.}\right]. \tag{5.4}$$

thus the field's strength can be written as

$$\mathbb{F}_{\mu\nu}(x) = \frac{1}{\sqrt{\hbar}}\sum_{\eta=\pm}\int \mathrm{d}\Phi(k)\left[-ia_\eta(k)\,\bar{k}_{[\mu}\varepsilon_{\nu]}^{(\eta)*}(k)\,e^{-i\bar{k}\cdot x} + \text{h.c.}\right]. \tag{5.5}$$

Analogously in gravity, the linearised Riemann tensor operator is, as before

$$\begin{aligned}\mathbb{R}_{\mu\nu\rho\sigma}(x) &= \frac{\kappa}{2}\left(\partial_\sigma\partial_{[\mu}\mathbb{h}_{\nu]\,\rho} - \partial_\rho\partial_{[\mu}\mathbb{h}_{\nu]\,\sigma}\right)\\ &= -\frac{\kappa}{2}\frac{1}{\sqrt{\hbar}}\sum_{\eta=\pm}\int \mathrm{d}\Phi(k)\left[a_\eta(k)\,\bar{k}_{[\mu}\varepsilon_{\nu]}^{(\eta)*}(k)\,\bar{k}_{[\sigma}\varepsilon_{\rho]}^{(\eta)*}(k)\,e^{-i\bar{k}\cdot x} + \text{h.c.}\right].\end{aligned} \tag{5.6}$$

As frequently done in earlier chapters, we still consider KMOC's two-particle states

$$|\psi\rangle = \int \mathrm{d}\Phi(p_1,p_2)\,\phi(p_1,p_2)e^{ib\cdot p_1/\hbar}\,|p_1,p_2\rangle\,, \tag{5.7}$$

as our initial two-particle state to be evolved with the S-matrix.

[3]Here we focus on linearized curvature fields.

In the far future, the expectation value of the field becomes

$$\langle\psi|S^\dagger \mathbb{F}_{\mu\nu}(x)S|\psi\rangle \\ = \frac{1}{\sqrt{\hbar}}\sum_\eta \int \mathrm{d}\Phi(k)\left[-i\langle\psi|S^\dagger a_\eta(k)S|\psi\rangle\,\bar{k}_{[\mu}\varepsilon^{(\eta)*}_{\nu]}(k)\,e^{-i\bar{k}\cdot x} + \text{h.c.}\right]. \tag{5.8}$$

We evaluate it at lowest perturbative order by writing $S = 1 + iT$. Thus we have

$$\begin{aligned}\langle\psi|S^\dagger a_\eta(k)S|\psi\rangle &= i\langle\psi|(a_\eta(k)T - T^\dagger a_\eta(k))|\psi\rangle + \langle\psi|T^\dagger a_\eta(k)T|\psi\rangle \\ &= i\langle\psi|a_\eta(k)T|\psi\rangle + \langle\psi|T^\dagger a_\eta(k)T|\psi\rangle \\ &\simeq i\langle\psi|a_\eta(k)T|\psi\rangle\,.\end{aligned} \tag{5.9}$$

In the middle line above, we used the fact that $a_\eta(k)|\psi\rangle = 0$; in the last line we neglected the term involving two T matrices which does not contribute at lowest order by counting powers of g.

Further expanding the state using eq. (5.7), and taking advantage of the short-hand notation defined the introduction, we may write

$$\langle\psi|S^\dagger \mathbb{F}_{\mu\nu}(x)S|\psi\rangle = 2\,\mathrm{Re}\,\frac{1}{\sqrt{\hbar}}\sum_\eta \int \mathrm{d}\Phi(p_1',p_2',p_1,p_2,k)\phi_b^*(p_1',p_2')\phi_b(p_1,p_2)\times \\ \times \langle k^\eta, p_1', p_2'|T|p_1,p_2\rangle\,\bar{k}_{[\mu}\varepsilon^{(\eta)*}_{\nu]}\,e^{-i\bar{k}\cdot x}\,. \tag{5.10}$$

The matrix element $\langle k^\eta, p_1', p_2'|T|p_1,p_2\rangle$ is, at lowest order, a five-point tree amplitude so it is proportional to g^3. This is consistent with a classical analysis of the outgoing radiation field.

In GR, the equivalent expression is

$$\langle\psi|S^\dagger \mathbb{R}_{\mu\nu\rho\sigma}(x)S|\psi\rangle = 2\,\mathrm{Re}\,\frac{-i}{\sqrt{\hbar}}\frac{\kappa}{2}\sum_\eta \int \mathrm{d}\Phi(p_1',p_2',p_1,p_2,k)\phi_b^*(p_1',p_2')\phi_b(p_1,p_2)\times \\ \times \langle k^\eta, p_1', p_2'|T|p_1,p_2\rangle\,\bar{k}_{[\mu}\varepsilon^{(\eta)*}_{\nu]}\,\bar{k}_{[\sigma}\varepsilon^{(\eta)*}_{\rho]}\,e^{-i\bar{k}\cdot x}\,. \tag{5.11}$$

It will be useful for us to simplify these expressions further, following again the discussions in previous chapters. The matrix element $\langle k^\eta, p_1', p_2'|T|p_1,p_2\rangle$ is the amplitude times a momentum-conserving delta function; our expectation value instructs us to integrate over all momenta in the amplitude. We may relabel these external momenta as shown in fig. 5.1. The measure can then be written

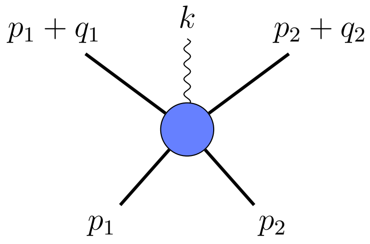

Figure 5.1 *The kinematic configuration we choose for the five-point amplitude which determines the leading-order radiation field.*

as

$$\mathrm{d}\Phi(p_1', p_2', p_1, p_2, k) = \mathrm{d}\Phi(p_1, p_2, k)\hat{\mathrm{d}}^4 q_1 \hat{\mathrm{d}}^4 q_2 \hat{\delta}(2p_1 \cdot q_1 + q_1^2)\hat{\delta}(2p_2 \cdot q_2 + q_2^2)\,. \tag{5.12}$$

In this form, the overall momentum-conserving delta function reads $\hat{\delta}^4(q_1+q_2+k)$. Now, in the classical regime the photon momentum is of order $\hbar$ thus, denoting an n point L loop amplitudes as $\mathcal{A}_{n,L}$ (or $\mathcal{M}_{n,L}$ in gravity), the field strength becomes

$$\begin{aligned}\langle\psi|S^\dagger \mathbb{F}_{\mu\nu}(x) S|\psi\rangle = 2\,\mathrm{Re}\,\hbar^{7/2} \sum_\eta \left\langle\!\!\left\langle \int \mathrm{d}\Phi(\bar{k})\, \hat{\mathrm{d}}^4\bar{q}_1 \hat{\mathrm{d}}^4\bar{q}_2\, \hat{\delta}(2p_1\cdot\bar{q}_1)\hat{\delta}(2p_2\cdot\bar{q}_2) \right.\right.\\ \left.\left. \times\; \mathcal{A}_{5,0}(p_1p_2 \to p_1+q_1, p_2+q_2, k^\eta)\, \hat{\delta}^4(\bar{k}+\bar{q}_1+\bar{q}_2)\, \bar{k}_{[\mu}\varepsilon^{(\eta)*}_{\nu]}\, e^{-i(\bar{k}\cdot x + \bar{q}_1\cdot b)} \right\rangle\!\!\right\rangle\,.\end{aligned} \tag{5.13}$$

Similarly, in gravity, one finds

$$\begin{aligned}\langle\psi|S^\dagger \mathbb{R}_{\mu\nu\rho\sigma}(x) S|\psi\rangle = -2\,\mathrm{Re}\,\hbar^{7/2}\frac{i\kappa}{2} \sum_\eta \left\langle\!\!\left\langle \int \mathrm{d}\Phi(\bar{k})\, \hat{\mathrm{d}}^4\bar{q}_1 \hat{\mathrm{d}}^4\bar{q}_2\, \hat{\delta}(2p_1\cdot\bar{q}_1)\hat{\delta}(2p_2\cdot\bar{q}_2) \right.\right.\\ \left.\left. \times\, \mathcal{M}_{5,0}(p_1p_2 \to p_1+q_1, p_2+q_2, k^\eta)\hat{\delta}^4(\bar{k}+\bar{q}_1+\bar{q}_2)\, \bar{k}_{[\mu}\varepsilon^{(\eta)*}_{\nu]}\, \bar{k}_{[\sigma}\varepsilon^{(\eta)*}_{\rho]}\, e^{-i(\bar{k}\cdot x + \bar{q}_1\cdot b)} \right\rangle\!\!\right\rangle\,.\end{aligned} \tag{5.14}$$

For these expressions to make sense classically, it better be that the overall $\hbar$ dependence of the amplitudes cancels that of the observable. Indeed we may write

$$\begin{aligned}\mathcal{A}_{5,0}(p_1p_2 \to p_1+q_1, p_2+q_2, k^\eta) &= \hbar^{-7/2}\mathcal{A}^{(0)}_{5,0}(p_1p_2 \to p_1+q_1, p_2+q_2, k^\eta) + \mathcal{O}(\hbar)\\ \mathcal{M}_{5,0}(p_1p_2 \to p_1+q_1, p_2+q_2, k^\eta) &= \hbar^{-7/2}\mathcal{M}^{(0)}_{5,0}(p_1p_2 \to p_1+q_1, p_2+q_2, k^\eta) + \mathcal{O}(\hbar)\,,\end{aligned} \tag{5.15}$$

where the quantities $\mathcal{A}^{(0)}_{5,0}$ and $\mathcal{M}^{(0)}_{5,0}$ are independent of $\hbar$, as was noticed in [49]. We will return to this structure below.

The physical interpretation of these expectation values is that they compute the radiative part of the field at large distances. To see this explicitly, the $\bar{k}$ integral needs to be performed taking advantage of the large distance between the point of measurement x and the particles. The integration can be performed using textbook methods and was recently reviewed in detail in ref. [33]. The question of central interest to us in this section, however, is to compute the uncertainty in the field strength; to do so, we turn to computing the expectation of two field strengths.

5.2.2 Expectation of two field strengths

It will be quite straightforward for us to compute expectations of products of operators using precisely the methods of the previous subsection. In electrodynamics, we need to compute

$$\begin{aligned}\langle\psi|S^\dagger \mathbb{F}_{\mu\nu}(x)\mathbb{F}_{\rho\sigma}(y)S|\psi\rangle = -\frac{1}{\hbar}\sum_{\eta,\eta'}\int \mathrm{d}\Phi(k',k)\langle\psi|S^\dagger\left[-ia_\eta(k)\,\bar{k}_{[\mu}\varepsilon^{(\eta)*}_{\nu]}\,e^{-i\bar{k}\cdot x}+\text{h.c.}\right]\\ \times\left[-ia_{\eta'}(k')\,\bar{k}'_{[\rho}\varepsilon'^{(\eta')*}_{\sigma]}\,e^{-i\bar{k}'\cdot y}+\text{h.c.}\right]S|\psi\rangle\,.\end{aligned}\tag{5.16}$$

Working at lowest order, and taking advantage of the fact that $a_\eta(k)|\psi\rangle = 0$, the expectation simplifies to

$$\begin{aligned}\langle\psi|S^\dagger \mathbb{F}_{\mu\nu}(x)\mathbb{F}_{\rho\sigma}(y)S|\psi\rangle = -\frac{2}{\hbar}\,\mathrm{Re}\sum_{\eta,\eta'}\int \mathrm{d}\Phi(k',k)\langle\psi|a_\eta(k)a_{\eta'}(k')iT|\psi\rangle\\ \times\,\bar{k}_{[\mu}\varepsilon^{(\eta)*}_{\nu]}\bar{k}'_{[\rho}\varepsilon'^{(\eta')*}_{\sigma]}\,e^{-i(\bar{k}\cdot x+\bar{k}'\cdot y)}\,,\end{aligned}\tag{5.17}$$

up to a purely quantum single-photon effect [33]. Expanding the wavefunctions, we encounter the matrix element $\langle p_1', p_2'|a_\eta(k)a_{\eta'}(k')T|p_1, p_2\rangle$: a six-point tree amplitude. The classical limit is determined precisely as in the previous section with the result

$$\begin{aligned}\langle\psi|S^\dagger \mathbb{F}_{\mu\nu}(x)\mathbb{F}_{\rho\sigma}(y)S|\psi\rangle = -2\hbar^5\,\mathrm{Re}\sum_{\eta,\eta'}\Big\langle\!\!\Big\langle\int \mathrm{d}\Phi(\bar{k}',\bar{k})\,\hat{\mathrm{d}}^4\bar{q}_1\hat{\mathrm{d}}^4\bar{q}_2\,\hat{\delta}(2p_1\cdot\bar{q}_1)\hat{\delta}(2p_2\cdot\bar{q}_2)\\ \times\,i\mathcal{A}_{6,0}\,\hat{\delta}^4(\bar{k}+\bar{k}'+\bar{q}_1+\bar{q}_2)\,\bar{k}_{[\mu}\varepsilon^{(\eta)*}_{\nu]}\bar{k}'_{[\rho}\varepsilon'^{(\eta')*}_{\sigma]}\,e^{-i(\bar{k}\cdot x+\bar{k}'\cdot y+\bar{q}_1\cdot b)}\Big\rangle\!\!\Big\rangle\,.\end{aligned}\tag{5.18}$$

The amplitude is shown in figure 5.2.

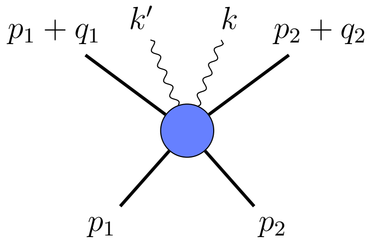

Figure 5.2 *The kinematic configuration we choose for the six-point amplitude appearing at leading-order expectation of a pair of field strength operators.*

Similarly, in gravity, we find

$$\begin{aligned}\langle\psi|S^\dagger \mathbb{R}_{\mu\nu\rho\sigma}(x)\mathbb{R}_{\alpha\beta\gamma\delta}(y)|\psi\rangle \\ &= -2\hbar^5 \,\mathrm{Re}\left(-i\frac{\kappa}{2}\right)^2 \sum_{\eta,\eta'} \left\langle\!\!\left\langle \int \mathrm{d}\Phi(\bar{k}',\bar{k})\, \hat{\mathrm{d}}^4\bar{q}_1 \hat{\mathrm{d}}^4\bar{q}_2\, \hat{\delta}(2p_1\cdot\bar{q}_1)\hat{\delta}(2p_2\cdot\bar{q}_2)\,\mathcal{M}_{6,0}\right.\right. \\ &\quad \times\, \hat{\delta}^4(\bar{k}+\bar{k}'+\bar{q}_1+\bar{q}_2)\, \bar{k}_{[\mu}\varepsilon^{(\eta)*}_{\nu]}\bar{k}_{[\rho}\varepsilon^{(\eta)*}_{\sigma]}\, \bar{k}'_{[\alpha}\varepsilon'^{(\eta')*}_{\beta]}\bar{k}'_{[\gamma}\varepsilon'^{(\eta')*}_{\delta]}\, e^{-i(\bar{k}\cdot x+\bar{k}'\cdot y+\bar{q}_1\cdot b)} \left.\left.\vphantom{\int}\right\rangle\!\!\right\rangle .\end{aligned} \tag{5.19}$$

In both cases, the expectation of two field strengths is given to leading order in g by a tree-level six-point amplitude.

5.2.3 Negligible variance?

We have now seen explicitly that the expectation of a single field strength is determined by a five-point amplitude, while the expectation of two field strengths is a six-point tree amplitude at lowest order in the coupling g. But for the uncertainty in the field strength to be negligible, we need the variance to be negligible. How can this happen?

Let us count powers of the coupling in the electromagnetic variance. The product of two field-strength expectations is

$$\langle\psi|\mathbb{F}_{\mu\nu}(x)|\psi\rangle\langle\psi|\mathbb{F}_{\rho\sigma}(y)|\psi\rangle \sim (\mathcal{A}_{5,0})^2 \sim (g^3)^2 . \tag{5.20}$$

while the expectation of two field strengths is

$$\langle\psi|\mathbb{F}_{\mu\nu}(x)\mathbb{F}_{\rho\sigma}(y)|\psi\rangle \sim \mathcal{A}_{6,0} \sim g^4 . \tag{5.21}$$

Thus the situation seems to very bad: the variance is dominated by the

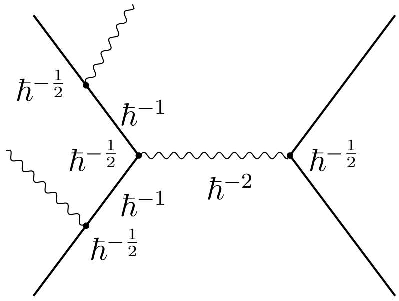

Figure 5.3 *A sample Feynman diagram contributing to the six-point tree amplitude, indicating powers of $\hbar$ assigned by naive power counting to the propagators and vertices.*

expectation of two field-strength operators! For the classical limit to emerge as expected, we need the six-point tree amplitude to be suppressed somehow.

One possibility is that it is suppressed by powers of $\hbar$, but naively that is not the case. Consider, for example, the 6-point Feynman diagram shown in figure 5.3. Counting powers of $\hbar$ we conclude that the six-point tree amplitude contains terms of order $\hbar^{-6}$. Referring back to eq. (5.18) or eq. (5.19) for the expectation of two field strengths, we see that the observables contribute a total of $\hbar^{+5}$. Based on this counting, the observable seems to scale as $\hbar^{-1}$, which would be a serious obstruction to the emergence of a classical limit. Evidently there is more to understand here.

However, it is a familiar story that power counting Feynman diagrams can be misleading: upon combining diagrams to evaluate an amplitude, there can be cancellations. In fact this already happens in the case of the five-point tree; there, naive power counting suggests that the amplitude scales as $\hbar^{-9/2}$ but in fact the leading term in the amplitude is of order $\hbar^{-7/2}$ [48][4]. The question, then, of the fate of the six-point tree amplitude in the expectation value of two field strengths becomes a question of the overall $\hbar$ scaling of six-point tree amplitudes in QED and gravity. We will shortly demonstrate explicitly that the QED amplitude in fact scale as $\hbar^{-4}$; the gravitational case will be discussed in reference [268]. Two powers of $\hbar$ cancel; consequently the contribution of the six-point tree to the variance is entirely at the quantum level.

It is amusing that at next-to-leading order in the perturbative coupling g, namely order g^6, the expectation value of two field strengths is sensitive to one-loop

[4]In reference [48], the analysis of the five-point tree amplitude was performed in gravity using the large mass expansion, which is equivalent to expanding in small $\hbar$.

six-point amplitudes and to products of two tree five-point amplitudes. These products of tree-level five-point amplitudes can be viewed as the cut of a six-point one-loop amplitude. It is easy to check that these scale as $\hbar^{-5}$, so in this sense they are *enhanced* relative to the six-point tree amplitude. This is as desired for negligible uncertainty:

$$\begin{aligned} \langle\psi|\mathbb{F}_{\mu\nu}(x)|\psi\rangle\langle\psi|\mathbb{F}_{\rho\sigma}(y)|\psi\rangle &\sim (\mathcal{A}_{5,0})^2 \sim (g^3)^2\,; \\ \langle\psi|\mathbb{F}_{\mu\nu}(x)\mathbb{F}_{\rho\sigma}(y)|\psi\rangle &\sim \mathcal{A}_{6,1} \sim (\mathcal{A}_{5,0})^2 \sim (g^3)^2\,. \end{aligned} \tag{5.22}$$

5.2.4 Explicit six-point tree amplitudes

We now compute the leading contribution in $\hbar$ of the six-point tree amplitude. We will discuss the computation explicitly in electromagnetism, and explain only the mechanism for cancellation of apparent excess powers of $\hbar$ in gravity (see also [268]).

Suppose particle 1 has charge Q_1 while particle 2 has charge Q_2. Then there are three gauge-invariant six-point tree partial amplitudes:

$$\mathcal{A}_{6,0}(p_1+q_1, p_2+q_2 \to p_1, p_2, k) = Q_1^3 Q_2\, A_{(3,1)} + Q_1^2 Q_2^2\, A_{(2,2)} + Q_1 Q_2^3\, A_{(1,3)}\,. \tag{5.23}$$

The "charge-ordered" partial amplitudes $A_{(3,1)}$, $A_{(2,2)}$, and $A_{(1,3)}$ are analogues of color-ordered amplitudes in gauge theory, which motivates our choice of notation.

Evidently there can be no cancellation of powers of $\hbar$ between these partial amplitudes because of the different powers of the charges. Thus the problem reduces to computing the leading-in-$\hbar$ terms in these amplitudes. There are two partial amplitudes to consider, since $A_{(1,3)}$ can be obtained from $A_{(3,1)}$ by trivially swapping the labels 1 and 2.

Here, we present a computation of the partial amplitudes $A_{(3,1)}$ in a convenient gauge which greatly reduced the labour necessary to see that two powers of $\hbar$ cancel. The gauge we chose (referring to the momentum routing in equation (5.23)) is

$$p_1 \cdot \varepsilon(k_i) = 0 \text{ for } i = 1, 2, \tag{5.24}$$

where p_1 is the momentum of particle 1 while k_i is the outgoing momentum of photon i.

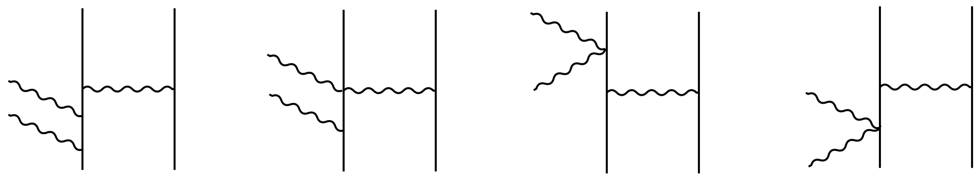

Figure 5.4 *Diagrams in $Q_1^3 Q_2$ sector.*

The effect of this choice is twofold; it removes many diagrams from the calculation and those that remain get an $\hbar$ enhancement from each emission vertex. For example, consider $A_{(3,1)}$: in this case, the emitted photon is radiated from particle 1. With our momentum labelling convention the emission vertices will produce factors of the form $(2p_1 + \hbar\bar{Q})) \cdot \varepsilon(k_i)$, where $\bar{Q}$ is some combination of wavenumbers. The first part vanishes leaving only the $\hbar$ enhanced $\varepsilon(k_i) \cdot \bar{Q}$ term. Any diagram with a photon emitted from the outgoing line of particle 1 vanishes, as it is proportional to $(2p_1 + \hbar\bar{k}_i) \cdot \varepsilon(k_i) = 0$. In what follows we will write $\varepsilon(k_i) = \varepsilon_i$. We will also suppress the $i\epsilon$ factors in the propagators[5]; they all implicitly come with $+i\epsilon$. Finally we will refer to each diagram contributing to the amplitude by, for example, $D(3,1)$ so that

$$iA_{(3,1)} = iD_{(3,1)cubic} + iD_{(3,1)quartic}. \tag{5.25}$$

Some of the sub-amplitudes are given by a single diagram, whereas others are made up of multiple diagrams.

Our gauge choice is most powerful in the case of $A_{(3,1)}$, so we discuss this case in most detail. The Feynman diagrams that constitute this amplitude can be split into 3 classes: the first involves single photon emissions coming from cubic vertices, the second has precisely one photon emitted into the final state from a quartic vertex, while the third class has two photons emitted from the same quartic vertex. These classes are shown in figure 5.4, after removing diagrams which vanish by gauge choice. The first diagram is an example of the first class, the second an example of the second class and the last two diagrams are in the third class.

We choose a particular ordering of k_1 and k_2 for the calculation, and include the permuted case by swapping $k_1 \leftrightarrow k_2$. For the first class there is a single diagram to compute after gauge fixing, and it is trivial to write down the leading term in

[5]The $i\epsilon$ factors are often important — and will play an important role in section 5.3.2 — but in this computation they are spectators.

the amplitude and see that it has the desired scaling. This diagram is

$$
\begin{aligned}
D_{(3,1)}|_{cubic} =& \frac{1}{\hbar^4\bar{q}_2^2}\left[\frac{2(\varepsilon_2\cdot\bar{q}_1)(\varepsilon_1\cdot(2\bar{q}_1-\bar{k}_2))(2p_2+\hbar\bar{q}_2)\cdot(2p_1-\hbar\bar{q}_2)}{(-2p_1\cdot\bar{q}_2+\hbar\bar{q}_2^2)(2p_1\cdot(\bar{q}_1-\bar{k}_1)+\hbar(\bar{q}_1-\bar{k}_1)^2)}\right] \\
=& \frac{1}{\hbar^4\bar{q}_2^2}\left[\frac{4p_1\cdot p_2(\varepsilon_2\cdot\bar{q}_1)(\varepsilon_1\cdot(2\bar{q}_1-\bar{k}_2))}{2(-p_1\cdot\bar{q}_2)(p_1\cdot(\bar{q}_1-\bar{k}_1)}+\mathcal{O}(\hbar)\right] \\
=& \frac{2p_1\cdot p_2}{\hbar^4\bar{q}_2^2}\left[\frac{(\varepsilon_2\cdot\bar{q}_1)(\varepsilon_1\cdot(\bar{q}_1-\bar{q}_2))}{(p_1\cdot(\bar{k}_1+\bar{k}_2))(p_1\cdot\bar{k}_1)}\right]+\mathcal{O}(\hbar^{-3}).
\end{aligned}
\tag{5.26}
$$

We used momentum conservation $q_1 + q_2 = k_1 + k_2$ to write our expressions in terms of just the k_i or the q_i. The choice here is most natural for obtaining a similarly simple expression for the amplitude with k_1 and k_2 swapped.

The second class is actually tractable without fixing a gauge, as there is only a single cancellation to show. However with our gauge fixing this class becomes trivial, and there is only a single diagram to compute. This is

$$
D_{(3,1)}|_{cubic/quartic} = \frac{4(p_2\cdot\varepsilon_2)(\bar{q}_1\cdot\varepsilon_1)}{\hbar^4\bar{q}_2^2 p_1\cdot\bar{k}_1}. \tag{5.27}
$$

The final class is unaffected by our choice of gauge as it is proportional to $\varepsilon_1\cdot\varepsilon_2$. After gauge fixing this is naively $\hbar^{-5}$, so we must find a single cancellation. The mechanism of the cancellation is identical to the case of the five-point tree amplitude. This is done in [48, 269], but we shall review it here for completeness. The key step is to make use of the on-shell conditions

$$
(p_i + q_i)^2 = p_i^2 = m_i^2, \quad i = 1, 2, \tag{5.28}
$$

which allows us, after the $\hbar$ rescaling, to replace $2p_i\cdot\bar{q}_i \to -\hbar\bar{q}_i^2$ in the propagators. Lastly, we Taylor expand. There are two diagrams to compute which are,

$$
\begin{aligned}
D_{(3,1)}|_{quartic,1} =& -\frac{2\varepsilon_1\cdot\varepsilon_2}{\hbar^5\bar{q}_2^2}\left[\frac{(2p_1+\hbar(2\bar{q}_1+\bar{q}_2))\cdot(2p_2+\hbar\bar{q}_2)}{2p_1\cdot(\bar{k}_1+\bar{k}_2)+\hbar(\bar{k}_1+\bar{k}_2)^2}\right] \\
=& -\frac{2\varepsilon_1\cdot\varepsilon_2}{\hbar^5\bar{q}_2^2}\left[\frac{4p_1\cdot p_2}{2p_1\cdot(\bar{k}_1+\bar{k}_2)}\right. \\
&\left.+\hbar\left(\frac{4p_2\cdot\bar{q}_1+2p_1\cdot\bar{q}_2}{2p_1\cdot(\bar{k}_1+\bar{k}_2)}-\frac{4p_1\cdot p_2(\bar{k}_1+\bar{k}_2)^2}{(2p_1\cdot(\bar{k}_1+\bar{k}_2))^2}\right)\right]
\end{aligned}
\tag{5.29}
$$

and

$$D_{(3,1)}|_{quartic,2} = -\frac{2\varepsilon_1\cdot\varepsilon_2}{\hbar^5\bar{q}_2^2}\Bigg[\frac{4p_1\cdot p_2}{-2p_1\cdot(\bar{k}_1+\bar{k}_2)} + \hbar\left(\frac{4p_1\cdot\bar{q}_2}{-2p_1\cdot(\bar{k}_1+\bar{k}_2)}+\frac{4p_1\cdot p_2((\bar{k}_1+\bar{k}_2)^2-\bar{q}_1^2)}{(2p_1\cdot(\bar{k}_1+\bar{k}_2))^2}\right)\Bigg]. \tag{5.30}$$

Notice the most singular terms are equal up to a sign, and so cancel. Combining the remaining terms we obtain

$$D_{(3,1)}|_{quartic} = -\frac{\varepsilon_1\cdot\varepsilon_2}{\hbar^4\bar{q}_2^2}\left[\frac{4(p_1\cdot p_2)(\bar{q}_2\cdot(\bar{k}_1+\bar{k}_2))}{(p_1\cdot(\bar{k}_1+\bar{k}_2))^2}+\frac{4p_2\cdot\bar{q}_1+2p_1\cdot\bar{q}_2}{p_1\cdot(\bar{k}_1+\bar{k}_2)}\right]. \tag{5.31}$$

These can be combined as $A_{(3,1)} = D_{(3,1)cubic} + D_{(3,1)quartic}$ yielding,

$$\begin{aligned}A_{(3,1)} =&\frac{1}{\hbar^4\bar{q}_2^2}\Bigg[\frac{4p_1\cdot p_2(\varepsilon_2\cdot\bar{q}_1)(\varepsilon_1\cdot(\bar{q}_1-\bar{q}_2))}{2(p_1\cdot(\bar{k}_1+\bar{k}_2))(p_1\cdot\bar{k}_1)}+\frac{4p_1\cdot p_2(p_2\cdot\varepsilon_2)(\bar{q}_1\cdot\varepsilon_1)}{p_1\cdot\bar{k}_1}\\ &-(\varepsilon_1\cdot\varepsilon_2)\left(\frac{4(p_1\cdot p_2)(\bar{q}_2\cdot(\bar{k}_1+\bar{k}_2))}{(p_1\cdot(\bar{k}_1+\bar{k}_2))^2}+\frac{4p_2\cdot\bar{q}_1+2p_1\cdot\bar{q}_2}{p_1\cdot(\bar{k}_1+\bar{k}_2)}\right)\Bigg]\\ &+(k_1\leftrightarrow k_2).\end{aligned} \tag{5.32}$$

The story is very similar for $A_{(2,2)}$. We can split into the same 3 classes, use gauge fixing to get rid of one factor of $\hbar$ and then massage using the on-shell constraints to show the final cancellation. Here we just quote the result, the details are in [4]. The result is

$$\begin{aligned}A_{(2,2)} =&\frac{4}{\hbar^4(\bar{q}_2-\bar{k}_2)^2}\Bigg[4\varepsilon_1\cdot\varepsilon_2+\frac{(\varepsilon_1\cdot p_2)(\varepsilon_2\cdot\bar{q}_2)}{p_2\cdot\bar{k}_2}-\frac{(\varepsilon_2\cdot p_2)(\varepsilon_1\cdot(\bar{q}_2+\bar{q}_1))}{2p_2\cdot\bar{k}_2}\\ &\frac{p_1\cdot p_2(\varepsilon_1\cdot\bar{q}_1)(\varepsilon_2\cdot\bar{q}_2)}{(p_2\cdot\bar{k}_2)(p_1\cdot\bar{k}_1)}-\frac{(p_1\cdot\bar{k}_2)(\varepsilon_1\cdot\bar{q}_1)(\varepsilon_2\cdot p_2)}{(p_2\cdot\bar{k}_2)(p_1\cdot\bar{k}_1)}\\ &-\frac{(\varepsilon_1\cdot p_2)(\varepsilon_2\cdot p_2)(\bar{q}_2\cdot\bar{k}_2)}{(p_2\cdot\bar{k}_2)^2}-\frac{p_1\cdot p_2(\varepsilon_1\cdot\bar{q}_1)(\varepsilon_2\cdot p_2)\bar{q}_2\cdot\bar{k}_2}{(p_2\cdot\bar{k}_2)^2(p_1\cdot\bar{k}_1)}\Bigg]\\ &+(k_1\leftrightarrow k_2)\end{aligned} \tag{5.33}$$

Finally $A_{(1,3)}$ can be obtained by swapping the labels $1\leftrightarrow 2$ in the expression for $A_{(3,1)}$ (written in the gauge where $p_2\cdot\varepsilon_i = 0$. Of course the partial amplitudes themselves are gauge-invariant.) In all cases, the $\hbar$ scaling is as required from negligible variance.

5.3 Transfer relations

Our discussion so far reveals that scattering amplitudes, viewed as Laurent series in $\hbar$, obey certain properties which permit the emergence of a classical limit through negligible uncertainty. This Laurent expansion can also be viewed as an expansion in small momentum transfers divided by the centre-of-mass energy $\sqrt{s}$. In fact, the emergence of the classical limit imposes an *infinite* set of these relationships, which we will call "transfer relations" on scattering amplitudes. In this section we will describe the origin of these relations, and explicitly demonstrate a non-trivial example at one loop and five points.

5.3.1 Mixed variances

To see where these relationships are coming from, recall that the double field-strength expectation (5.18) depends on a six-point amplitude. We have seen that the dominant term is actually the six-point one-loop amplitude, occuring at next-to-leading order in the expansion in g. At this order an additional term contributes to the double field-strength expectation; this term is the product of two five-point amplitudes. Now, negligible uncertainty demands that the complete double field-strength expectation must be the product of two single field-strength expectations. At leading order in the coupling, and leading non-trivial order in $\hbar$, we conclude that there must exist a relationship between the leading-in-$\hbar$ six-point one-loop amplitude and the product of two five-point trees.

Further examples of relationships between amplitudes can be obtained by considering expectations of three (or more) field strengths, leading to relationships between seven- (or higher-) point loop amplitudes and products of three (or more) five-point amplitudes.

Yet more relationships occur by considering expectations of products of operators including field strengths and momenta. For example, consider the variance

$$V_{\mu\nu\rho} \equiv \langle\psi|S^\dagger \mathbb{F}_{\nu\rho}(x) S \mathbb{P}_\mu|\psi\rangle - \langle\psi|S^\dagger \mathbb{F}_{\nu\rho}(x) S|\psi\rangle\langle\psi|\mathbb{P}_\mu|\psi\rangle\,. \tag{5.34}$$

This is the variance in a measurement of the initial momentum and the future field strength; it must be negligible in the classical regime. In a quantum-first approach, however, this variance will not vanish. Indeed it need not be real:

$$V^*_{\mu\nu\rho} = \langle\psi|\mathbb{P}_\mu S^\dagger \mathbb{F}_{\nu\rho}(x) S|\psi\rangle - \langle\psi|S^\dagger \mathbb{F}_{\nu\rho}(x) S|\psi\rangle\langle\psi|\mathbb{P}_\mu|\psi\rangle \neq V_{\mu\nu\rho}. \tag{5.35}$$

We can derive an interesting constraint on the five-point one-loop amplitude by demanding that imaginary part of this variance vanishes in the classical approximation. We therefore define

$$\begin{aligned} \mathcal{O}_{\mu\nu\rho} &= i(V^*_{\mu\nu\rho} - V_{\mu\nu\rho}) \\ &= i\langle\psi|\mathbb{P}_\mu S^\dagger \mathbb{F}_{\nu\rho}(x) S - S^\dagger \mathbb{F}_{\nu\rho}(x) S \mathbb{P}_\mu|\psi\rangle \,. \end{aligned} \tag{5.36}$$

Expanding the states as usual, we easily find

$$\begin{aligned} \mathcal{O}_{\mu\nu\rho} = \int \mathrm{d}\Phi(p_1', p_2', p_1, p_2)\, \phi_b^*(p_1', p_2')\phi_b(p_1, p_2) i(p_{1\mu}' - p_{1\mu}) \\ \times \langle p_1' p_2'| i(\mathbb{F}_{\nu\rho}(x) T - T^\dagger \mathbb{F}_{\nu\rho}(x)) + T^\dagger \mathbb{F}_{\nu\rho}(x) T|p_1 p_2\rangle \,. \end{aligned} \tag{5.37}$$

The factor $i(p_{1\mu}' - p_{1\mu})$ is important here: working at leading perturbative order, this factor is of order $\hbar$. It is also worth noting that we may write the expectation of the field strength itself as

$$\begin{aligned} \langle\psi|\mathbb{F}_{\nu\rho}|\psi\rangle = \int \mathrm{d}\Phi(p_1', p_2', p_1, p_2)\, \phi_b^*(p_1', p_2')\phi_b(p_1, p_2) \\ \times \langle p_1' p_2'| i(\mathbb{F}_{\nu\rho}(x) T - T^\dagger \mathbb{F}_{\nu\rho}(x)) + T^\dagger \mathbb{F}_{\nu\rho}(x) T|p_1 p_2\rangle \,. \end{aligned} \tag{5.38}$$

Thus the $i(p_{1\mu}' - p_{1\mu}) \sim \hbar$ factor in the variance is the key distinction between the variance, which vanishes classically, and the field strength which of course should not vanish classically. As we have already seen that the field strength is related to five-point amplitudes, it is now clear that condition of vanishing $\mathcal{O}_{\mu\nu\rho}$ will become a condition on five-point amplitudes.

It is useful to break the variance $\mathcal{O}_{\mu\nu\rho}$ up into two structures:

$$\begin{aligned} \mathcal{O}^{(1)}_{\mu\nu\rho} = \int \mathrm{d}\Phi(p_1', p_2', p_1, p_2)\, \phi_b^*(p_1', p_2')\phi_b(p_1, p_2) i(p_{1\mu}' - p_{1\mu}) \\ \times \langle p_1' p_2'| i(\mathbb{F}_{\nu\rho}(x) T - T^\dagger \mathbb{F}_{\nu\rho}(x))|p_1 p_2\rangle \,, \end{aligned} \tag{5.39}$$

and

$$\begin{aligned} \mathcal{O}^{(2)}_{\mu\nu\rho} = \int \mathrm{d}\Phi(p_1', p_2', p_1, p_2)\, \phi_b^*(p_1', p_2')\phi_b(p_1, p_2) i(p_{1\mu}' - p_{1\mu}) \\ \times \langle p_1' p_2'| T^\dagger \mathbb{F}_{\nu\rho}(x) T|p_1 p_2\rangle \,. \end{aligned} \tag{5.40}$$

Both of these objects are real, which is convenient in terms of keeping the expressions simple.

We may simplify these structures using the explicit expression for the field strength given in equation (5.5). For $\mathcal{O}^{(1)}$ we find

$$\begin{aligned}\mathcal{O}^{(1)}_{\mu\nu\rho} = 2\,\mathrm{Re}\,\frac{1}{\sqrt{\hbar}}\sum_{\eta}\int \mathrm{d}\Phi(p_1', p_2', p_1, p_2, k)\phi_b^*(p_1', p_2')\phi_b(p_1, p_2)\times \\ \times\, i(p'_{1\mu} - p_{1\mu})\langle k^\eta, p_1', p_2'|T|p_1, p_2\rangle\, \bar{k}_{[\nu}\varepsilon^{(\eta)*}_{\rho]}\, e^{-i\bar{k}\cdot x}\,.\end{aligned} \tag{5.41}$$

which should be compared to equation (5.10). Again we see that the crucial new ingredient is a factor $i(p'_{1\mu} - p_{1\mu})$. In the classical regime, we may write this term as

$$\begin{aligned}\mathcal{O}^{(1)}_{\mu\nu\rho} = 2\,\mathrm{Re}\,\hbar^{9/2}\sum_{\eta}\bigg\langle\!\!\bigg\langle \int \mathrm{d}\Phi(\bar{k})\,\hat{\mathrm{d}}^4\bar{q}_1\hat{\mathrm{d}}^4\bar{q}_2\,\hat{\delta}(2p_1\cdot\bar{q}_1)\hat{\delta}(2p_2\cdot\bar{q}_2) \\ \times\, i\bar{q}_\mu\mathcal{A}_5(p_1p_2 \to p_1 + q_1, p_2 + q_2, k^\eta)\,\hat{\delta}^4(\bar{k} + \bar{q}_1 + \bar{q}_2)\,\bar{k}_{[\nu}\varepsilon^{(\eta)*}_{\rho]}\, e^{-i(\bar{k}\cdot x + \bar{q}_1\cdot b)}\bigg\rangle\!\!\bigg\rangle\,.\end{aligned} \tag{5.42}$$

Referring back once more to equation (5.13), the additional $\hbar$ suppression is now manifest.

In order to control the $\hbar$ expansion of scattering amplitudes, it is useful to introduce some further notation. Let us write the amplitudes as explicit Laurent series in $\hbar$ building on equation (5.15). For example, at five-points we may write

$$\begin{aligned}\mathcal{A}_{5,0}(i\to f) &= \hbar^{-7/2}\left(\mathcal{A}^{(0)}_{5,0}(i\to f) + \hbar\mathcal{A}^{(1)}_{5,0}(i\to f) + \cdots\right)\,, \\ \mathcal{A}_{5,1}(i\to f) &= \hbar^{-9/2}\left(\mathcal{A}^{(0)(i\to f)}_{5,1} + \hbar\mathcal{A}^{(1)}_{5,1}(i\to f) + \cdots\right)\,.\end{aligned} \tag{5.43}$$

We have scaled out the dominant (inverse) power of $\hbar$; the quantities $\mathcal{A}^{(p)}_{n,L}$ are $\hbar$-independent gauge-invariant sub-amplitudes; it is precisely these quantities that are related by our reasoning. This expansion defines an infinite set of objects $\mathcal{A}^{(p)}_{n,L}$ which could in principle be reassembled into the full amplitude. They are a kind of partial amplitude, but distinct from the usual use of this term. We will therefore refer to them as "fragmentary amplitudes", or simply as "fragments."

Since $\hbar$ is dimensionful, it is useful to view these fragmentary amplitudes in a slightly different way. Amplitudes are functions of Mandelstam invariants; in the semi-classical region, we are expanding in powers of momentum transfers, such as $q^2 = \hbar^2\bar{q}^2$ at four points, divided by Mandelstam $s = (p_1 + p_2)^2$. The semiclassical expansion is an expansion in powers of $\hbar\sqrt{-\bar{q}^2/s}$. More general amplitudes involve a richer set of momentum transfers $\bar{q}_{ij}^2$; our expansion is in powers of $\hbar\sqrt{-\bar{q}_{ij}^2/s}$. We only consider amplitudes with two incoming massive particles.

We may also view the expansion as being in (inverse) powers of the large mass of the scattering particles [15, 48, 60, 238]. This makes contact with effective field theory, especially heavy quark effective theory or, more generally, heavy particle effective theories as has been emphasised in references [15, 60, 238].

Notice that this expansion is analogous, but different, to a soft expansion. In the soft expansion we take the momentum of an individual particle soft. In this transfer expansion we take the momenta in all messenger lines to be of the same order, and small compared to the incoming centre of mass energy. It is possible to perform the transfer expansion and then, in a second stage, to single out some line, say an outgoing photon, and take its momentum to be softer than all other messenger lines. This yields the soft limit of the transfer expansion. It corresponds to the low-frequency limit in the classical approximation. Interesting classical physics, including memory effects, appear in this region [31, 52, 53, 270–275].

Now at classical order ($\hbar^0$) the tree level amplitude $\mathcal{A}_{5,0}$ does not appear in $\mathcal{O}^{(1)}_{\mu\nu\rho}$ on account of the explicit factor $\hbar^{9/2}$ in equation (5.42). The leading in g, non-trivial, classical contribution arises from the fragment $\mathcal{A}^{(0)}_{5,1}$. We conclude then that

$$\begin{aligned}\mathcal{O}^{(1)}_{\mu\nu\rho} = 2\,\mathrm{Re}\sum_\eta \Bigg\langle\!\!\Bigg\langle \int & \mathrm{d}\Phi(\bar{k})\, \hat{\mathrm{d}}^4\bar{q}_1 \hat{\mathrm{d}}^4\bar{q}_2\, \hat{\delta}(2p_1\cdot\bar{q}_1)\hat{\delta}(2p_2\cdot\bar{q}_2)\times \\ & \times i\bar{q}_\mu \mathcal{A}^{(0)}_{5,1}(p_1p_2\to p_1+q_1, p_2+q_2, k^\eta)\,\hat{\delta}^4(\bar{k}+\bar{q}_1+\bar{q}_2)\,\bar{k}_{[\nu}\varepsilon^{(\eta)*}_{\rho]}\, e^{-i(\bar{k}\cdot x+\bar{q}_1\cdot b)}\Bigg\rangle\!\!\Bigg\rangle\,. \end{aligned} \tag{5.44}$$

The relevant fragmentary amplitude is the leading-in-$\hbar$ five-point one-loop amplitude, sometimes known as the “superclassical” part of the one-loop amplitude. Of course in this context this fragment of the amplitude is contributing precisely at classical order.

Now the full $\mathcal{O}_{\mu\nu\rho}$ should vanish at classical order. Since $\mathcal{O}^{(1)}_{\mu\nu\rho}\neq 0$, it must be that the second structure $\mathcal{O}^{(2)}_{\mu\nu\rho}$ cancels the contribution of equation (5.44). We find that

$$\mathcal{O}^{(2)}_{\mu\nu\rho} = 2\,\mathrm{Re}\sum_\eta \left\langle\!\!\left\langle \int \mathrm{d}\Phi(\bar{k})\,\hat{\mathrm{d}}^4\bar{q}_1\hat{\mathrm{d}}^4\bar{q}_2\hat{\mathrm{d}}^4\bar{w}_1\hat{\mathrm{d}}^4\bar{w}_2\,\hat{\delta}(2p_1\cdot\bar{q}_1)\hat{\delta}(2p_2\cdot\bar{q}_2)\hat{\delta}(2p_1\cdot\bar{w}_1)\hat{\delta}(2p_2\cdot\bar{w}_2) \right.\right.$$
$$\times\,\bar{q}_\mu\,\hat{\delta}^4(\bar{k}+\bar{q}_1+\bar{q}_2)\hat{\delta}^4(\bar{q}_1+\bar{q}_2-\bar{w}_1-\bar{w}_2)\,\bar{k}_{[\nu}\varepsilon^{(\eta)*}_{\rho]}\,e^{-i(\bar{k}\cdot x+\bar{q}_1\cdot b)}$$
$$\left.\left.\times\,\mathcal{A}^{(0)}_{5,0}(p_1p_2\to p_1+w_1,p_2+w_2,k^\eta)\mathcal{A}^{(0)}_{4,0}(p_1+w_1,p_2+w_2\to p_1+q_1,p_2+q_2)\right\rangle\!\!\right\rangle\,. \tag{5.45}$$

Comparing equations (5.44) and (5.45), the condition for vanishing $\mathcal{O}$ is

$$\begin{aligned} &i\mathcal{A}^{(0)}_{5,1}(p_1p_2\to p_1+q_1,p_2+q_2,k^\eta)\\ &\quad=-\int\hat{\mathrm{d}}^4\bar{w}_1\hat{\mathrm{d}}^4\bar{w}_2\,\hat{\delta}(2p_1\cdot\bar{w}_1)\hat{\delta}(2p_2\cdot\bar{w}_2)\hat{\delta}^4(\bar{q}_1+\bar{q}_2-\bar{w}_1-\bar{w}_2)\\ &\qquad\times\mathcal{A}^{(0)}_{5,0}(p_1p_2\to p_1+w_1,p_2+w_2,k^\eta)\mathcal{A}^{(0)}_{4,0}(p_1+w_1,p_2+w_2\to p_1+q_1,p_2+q_2)\,. \end{aligned} \tag{5.46}$$

Thus the dominant part of the five-point one-loop amplitude is given by the tree five-point and tree four-point amplitudes; we will check this relation explicitly in the next subsection. We remark that this relation, together with others one can obtain, only hold for classical amplitudes and on-shell of our integration measures.

Clearly this explicit example is one among an infinite set of relationships. Variances involving one field strength operator and two momenta will lead to relationships among two-loop five-point amplitudes and the product of one five-point tree and two four-point trees. We can continue, in principle, as far as we wish generating similar relations. These negligible uncertainty relations generalise the well-known relations between multiloop four-point amplitudes required for eikonal exponentiation. Indeed consideration of expectations such as

$$\langle\psi|S^\dagger\mathbb{P}_{\mu_1}\mathbb{P}_{\mu_2}\cdots\mathbb{P}_{\mu_n}S|\psi\rangle\simeq\langle\psi|S^\dagger\mathbb{P}_{\mu_1}|\psi\rangle\langle\psi|S^\dagger\mathbb{P}_{\mu_2}|\psi\rangle\cdots\langle\psi|S^\dagger\mathbb{P}_{\mu_n}|\psi\rangle\,, \tag{5.47}$$

shows that there must be a relationship between the $n-1$ loop four-point amplitude and the product of n tree amplitudes.

Thus we find a remarkable abundance of relationships between multiloop, multileg amplitudes, considered as Laurent series in $\hbar$, forced on us by the *absence* of uncertainty in the classical regime. In the next section, we will interpret these relationships in terms of a radiative generalisation of the eikonal exponentiation.

As well as finding explicit relations between different fragmentary amplitudes, we can use similar ideas to determine the $\hbar$ scaling associated with fragments in the transfer expansion. The kinds of multiple cancellations of $\hbar$ powers we saw at six points must continue to occur at higher points. The reason again follows from considering expectations of products of more than two field-strength operators.

The arguments are based simply on counting powers of coupling and $\hbar$. We know that for the single expectation, at leading order, we have

$$\langle \mathbb{F}_{\mu\nu} \rangle \sim g^3. \tag{5.48}$$

This means that we must also have $\langle \mathbb{F}^n \rangle \sim (g^3)^n$. Now we perform the KMOC analysis of $\langle \mathbb{F}^n \rangle$. Following the steps of the calculation earlier in section 5.2.2 we find, schematically, that

$$\langle \mathbb{F}^n \rangle \sim \hbar^{3n/2+2} \int \mathcal{A}_{4+n}. \tag{5.49}$$

These relations allow us to deduce two things. Firstly the relevant fragment of the complete amplitude $\mathcal{A}_{4+n}$ must scale as $\hbar^{-3n/2-2}$. Secondly this fragment must have $3n$ powers of the coupling g — this corresponds to having $n-1$ loops. From this we can also infer the scaling of all other loop and tree amplitudes, in the classical limit, since each loop contributes an extra factor of $\hbar^{-1}$. In particular the tree scaling will be

$$\mathcal{A}_{4+n,0} \sim \hbar^{-n/2-3}. \tag{5.50}$$

This is consistent with the scaling we computed above for six points ($n = 2$), and we have also checked explicitly at seven points. It is interesting to see how these two very simple power counting arguments have completely constrained the $\hbar$ scaling of all $2 \to 2+n$ amplitudes.

5.3.2 One loop factorisation

We now turn to verifying equation (5.46). For simplicity we focus on the case of scalar QED, though the general nature of our arguments indicates that the result should also hold in gravity and in Yang-Mills theory. In order to keep the computational labour to the minimum necessary, we take advantage of lessons we learned in the context of the six-point tree amplitude in section 5.2.4. First, we note that the scalar QED five-point amplitudes can be reduced to gauge-invariant partial amplitudes analogous to colour-ordered amplitudes in Yang-Mills theory.

In particular we write

$$
\begin{aligned}
\mathcal{A}^{(0)}_{4,0}(p_1p_2 \to p_1+w_1, p_2+w_2) &= Q_1Q_2A_{(1,1)}\,, \\
\mathcal{A}^{(0)}_{5,0}(p_1p_2 \to p_1+q_1, p_2+q_2, k) &= Q_1Q_2^2A_{(1,2)} + Q_1^2Q_2A_{(2,1)}\,, \\
\mathcal{A}^{(0)}_{5,1}(p_1p_2 \to p_1+q_1, p_2+q_2, k) &= Q_1^2Q_2^3A_{(2,3)} + Q_1^3Q_2^2A_{(3,2)}\,.
\end{aligned} \tag{5.51}
$$

In view of the symmetry between $A_{2,3}$ and $A_{3,2}$ we may compute just one choice: we choose to focus on the charge sector $Q_1^2Q_2^3$.

Second, we find it useful to choose an explicit gauge, namely

$$\varepsilon_\eta(\bar{k})\cdot p_2 = 0\,. \tag{5.52}$$

This choice drastically reduces the relevant number of terms in the $\hbar$ expansion. It is trivial to determine the tree partial amplitudes in this gauge, which are

$$A_{(1,1)} = e^2\frac{4p_1\cdot p_2}{\bar{w}_1^2}\,, \tag{5.53}$$

and

$$A_{(1,2)} = \frac{4e^3}{\bar{q}_1^2}\left(p_1\cdot\varepsilon_\eta + \frac{p_1\cdot p_2\,\varepsilon_\eta\cdot\bar{q}_1}{p_2\cdot\bar{k}}\right)\,. \tag{5.54}$$

The anatomy of (5.46) is that the leading-in-$\hbar$ fragment of the one-loop five-point amplitude $A_{(2,3)}$ will organise itself into a product of $A_{(1,1)}$ times the four terms that constitute $A_{(1,2)}$. Our strategy will be to isolate these terms one by one. Let us start gathering the relevant diagrams of $A_{(2,3)}$. At one loop, and in the classical limit, we need to consider the transfer expansion of the following five-point diagrams with a photon emitted in the final state:

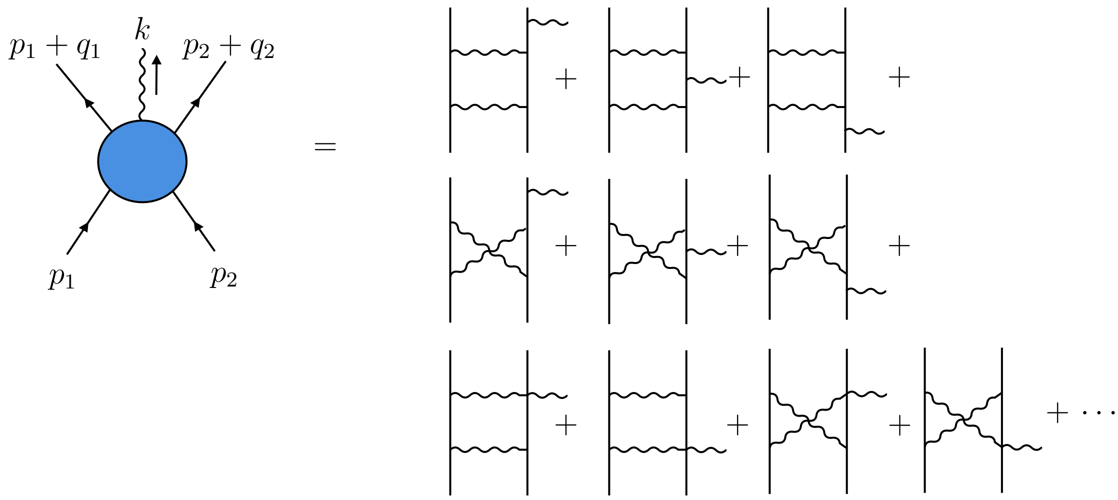

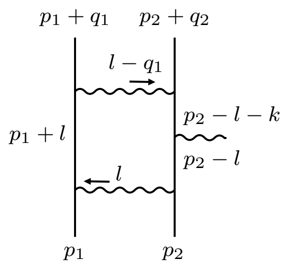

Figure 5.5 *Momentum routing for the pentagon contribution to the five-point one-loop amplitude.*

The ellipsis indicate purely quantum diagrams which are not relevant for us.

As in 5.2.4 we tidy our expressions up by making use of the on-shell conditions. Using the momentum labelling in the figure above these read

$$p_1 \cdot \bar{q}_1 = p_2 \cdot \bar{q}_2 = \mathcal{O}(\hbar). \tag{5.55}$$

Keeping this in mind[6] we start to compute the diagrams. It is helpful to compute the first six diagrams in the figure above, which involve only three-point vertices, separately from the rest of the diagrams (which involved contact four-point vertices). We therefore write

$$A_{(2,3)} = A^{\text{3pt}}_{(2,3)} + A^{\text{4pt}}_{(2,3)} \,. \tag{5.56}$$

We focus first on the six diagrams which constitute $A^{\text{3pt}}_{(2,3)}$. For clarity, let us begin by describing the contribution from the pentagon diagram, in our gauge (5.52) in detail. We choose the momentum routing shown in figure 5.5. On the support of the momentum-conserving delta function $\hat{\delta}^4(q_1 + q_2 + k)$, its contribution to $A_{(2,3)}$ is

$$ie^5 \int \frac{\hat{\mathrm{d}}^4 \bar{l}}{\bar{l}^2 (\bar{l} - \bar{q}_1)^2} \frac{(4p_1 \cdot p_2)^2 (-2\, \varepsilon_\eta \cdot \bar{l})}{(2p_1 \cdot \bar{l})(-2p_2 \cdot \bar{l})(-2p_2 \cdot (\bar{k} + \bar{l}))}. \tag{5.57}$$

The sum of the cubic diagrams yields

[6]Here's a random quote for you: "When two numbers a and b are different, they can only be equal if they are both zero". *Marcel Proust.*

$$
\begin{aligned}
A^{\rm 3pt}_{(2,3)} = ie^5 \int & \frac{\hat{\rm d}^4 \bar{l}}{\bar{l}^2(\bar{l}-\bar{q}_1)^2}(4p_1\cdot p_2)^2 \times \\
& \left(\frac{-2\varepsilon_\eta\cdot\bar{l}}{(2p_1\cdot\bar{l})(-2p_2\cdot\bar{l})(-2p_2\cdot(\bar{k}+\bar{l}))} - \frac{2\varepsilon_\eta\cdot\bar{q}_1}{(2p_1\cdot\bar{l})(-2p_2\cdot\bar{l})(2p_2\cdot\bar{k})} \right. \\
& \left. + \frac{2\varepsilon_\eta\cdot(\bar{l}-\bar{q}_1)}{(2p_1\cdot\bar{l})(2p_2\cdot(\bar{k}+\bar{l}))(2p_2\cdot\bar{l})} - \frac{2\varepsilon_\eta\cdot\bar{q}_1}{(2p_1\cdot\bar{l})(2p_2\cdot(\bar{k}+\bar{l}))(2p_2\cdot\bar{k})} \right).
\end{aligned}
\tag{5.58}
$$

Note that the signs in the linearised propagators are important! We use them to indicate the hidden $i\epsilon$'s,

$$
\frac{1}{\pm p\cdot\bar{l}} \equiv \frac{1}{\pm p\cdot\bar{l}+i\epsilon} \neq \pm\frac{1}{p\cdot\bar{l}} = \frac{1}{\pm p\cdot\bar{l}\pm i\epsilon}. \tag{5.59}
$$

which allows us to make use of the following identity

$$
-i\hat{\delta}(p\cdot\bar{l}) = \frac{1}{p\cdot\bar{l}} + \frac{1}{-p\cdot\bar{l}}. \tag{5.60}
$$

In order to make use of this identity we apply a change of variables $l \to \bar{q}_1 - l$ in the last two terms in (5.58). This, along with the on-shell conditions, allows pairs of terms to take an almost identical form — denominators differ only by a sign in the $p_1\cdot l$ term which is precisely what is needed to apply (5.60). The amplitude then reduces to

$$
A^{\rm 3pt}_{(2,3)} = 4e^5(p_1\cdot p_2)^2 \int \frac{\hat{\rm d}^4\bar{l}}{\bar{l}^2(\bar{l}-\bar{q}_1)^2}\frac{\hat{\delta}(p_1\cdot\bar{l})}{-p_2\cdot\bar{l}}\left(-\frac{\varepsilon_\eta\cdot\bar{q}_1}{p_2\cdot\bar{k}} - \frac{\varepsilon_\eta\cdot\bar{l}}{-p_2\cdot(\bar{k}+\bar{l})} \right). \tag{5.61}
$$

It is possible to expose a second delta function in this expression by writing $-\varepsilon_\eta\cdot\bar{q}_1 = \varepsilon_\eta\cdot(\bar{l}-\bar{q}_1) - \varepsilon_\eta\cdot\bar{l}$. The two terms involving $\varepsilon_\eta\cdot\bar{l}$ under the integral sign can be simplifed by a partial fraction, yielding

$$
\begin{aligned}
A^{\rm 3pt}_{(2,3)} &= 4e^5(p_1\cdot p_2)^2 \int \frac{\hat{\rm d}^4\bar{l}}{\bar{l}^2(\bar{l}-\bar{q}_1)^2}\frac{\hat{\delta}(p_1\cdot\bar{l})}{p_2\cdot\bar{k}}\left(\frac{\varepsilon_\eta\cdot(\bar{l}-\bar{q}_1)}{-p_2\cdot\bar{l}} - \frac{\varepsilon_\eta\cdot\bar{l}}{-p_2\cdot(\bar{l}-\bar{q}_1)} \right) \\
&= 4ie^5(p_1\cdot p_2)^2 \int \frac{\hat{\rm d}^4\bar{l}}{\bar{l}^2(\bar{l}-\bar{q}_1)^2}\hat{\delta}(p_1\cdot\bar{l})\hat{\delta}(p_2\cdot(\bar{l}-\bar{q}_1))\frac{\varepsilon_\eta\cdot\bar{l}}{p_2\cdot\bar{k}}.
\end{aligned}
\tag{5.62}
$$

To obtain the second of these equalities, we redefined the variable of integration to $\bar{l}' = -(\bar{l}-\bar{q}_1)$ in the first term, and dropped the prime.

Next, we address the remaining diagrams contributing to $A_{(2,3)}$ which now involve four-point vertices. After a straightforward computation, we find

$$A^{\text{4pt}}_{(2,3)} = 4ie^5 p_1 \cdot p_2 \, \varepsilon_\eta \cdot p_1 \int \frac{\hat{\mathrm{d}}^4 \bar{l}}{\bar{l}^2 (\bar{l} - \bar{q}_1)^2} \hat{\delta}(p_1 \cdot \bar{l}) \hat{\delta}(p_2 \cdot (\bar{l} - \bar{q}_1)) \,. \tag{5.63}$$

At this stage we can see the structure of the required factorisation — we have exposed the delta functions present in equation (5.46).

Combining the contact terms of equation (5.63) with the rest of the diagrams, equation (5.62), we find that the total expression for the amplitude fragment is

$$A_{(2,3)} = 4ie^5 \, p_1 \cdot p_2 \int \frac{\hat{\mathrm{d}}^4 \bar{l}}{\bar{l}^2 (\bar{l} - \bar{q}_1)^2} \hat{\delta}(p_1 \cdot \bar{l}) \hat{\delta}(p_2 \cdot (\bar{l} - \bar{q}_1)) \left(\varepsilon_\eta \cdot p_1 + p_1 \cdot p_2 \frac{\varepsilon_\eta \cdot \bar{l}}{p_2 \cdot \bar{k}} \right) . \tag{5.64}$$

The final step is to compare this result with the prediction for $A_{(2,3)}$ from equation (5.46). Using the amplitudes of equation (5.51), it is easy to see that the prediction is

$$\begin{aligned} A_{(2,3)} = \int & \hat{\mathrm{d}}^4 \bar{w}_1 \hat{\mathrm{d}}^4 \bar{w}_2 \, \hat{\delta}(2p_1 \cdot \bar{w}_1) \hat{\delta}(2p_2 \cdot \bar{w}_2) \hat{\delta}^4(\bar{q}_1 + \bar{q}_2 - \bar{w}_1 - \bar{w}_2) \\ & \times \frac{4e^3}{\bar{w}_1^2} \left(p_1 \cdot \varepsilon_\eta + \frac{p_1 \cdot p_2 \, \varepsilon_\eta \cdot \bar{w}_1}{p_2 \cdot \bar{k}} \right) \frac{4e^2}{(\bar{q}_1 - \bar{w}_1)^2} p_1 \cdot p_2 \,. \end{aligned} \tag{5.65}$$

Upon performing the integral over $\bar{w}_2$ using the four-fold delta function, relabelling $\bar{w}_1 = \bar{l}$ and recognising that $\bar{k} = -\bar{q}_1 - \bar{q}_2$, we immediately recover equation (5.64).

5.4 Generalising the Eikonal

We have now seen that the uncertainty, or the variance, in the measurement of a scattering observable can be computed in terms of amplitudes and, moreover, that the classical absence of uncertainty leads to an infinite set of relationships among fragments of amplitudes expanded in powers of momentum transfer, which is a Laurent series in $\hbar$. In a purely conservative limit, these relationships can be understood in terms of eikonal exponentiation. Our goal now is to review the eikonal formula, emphasising its connection to final state dynamics. We will then build on this eikonal state to incorporate radiative dynamics as a kind of coherent state so that the variance is naturally small.

5.4.1 Eikonal final state

Eikonal methods have long been used to extract classical physics from quantum mechanics. Recent years have seen a renewed surge of interest in this approach, especially in the context of gravitational scattering [9, 11, 14, 22, 32, 54, 66, 168, 172, 199, 200, 203, 205, 206, 224, 230, 254, 276–282], though this has roots in earlier work [193, 195, 283]. Originally born out of the study of high energy/Regge scattering [260–267] where the Feynman diagrammatics dramatically simplify, eikonal physics now have much wider application. The simplification in this regime allows diagrams, expressed in impact parameter space rather than momentum space, to be summed exactly to an exponential form. This exponential depends on the $2 \to 2$ scattering amplitude, and contains information about classical quantities such as the deflection angle. There are rich connections to soft/IR physics and Wilson lines [196, 198, 284–287] which lead to a formal proof of the exponentiation quite generally [196]. Nowadays the exponentiation is taken as a starting point and applied to various scattering regimes.

In this section our goal is to explain the link between eikonal methods and the KMOC approach. Firstly it is worth noting that the small $\hbar$ expansion in the KMOC formalism is essentially the same as the soft expansion in the eikonal literature; the $\hbar$ scaling counts the order of softness. The key connection is to compute the final state using the methods of KMOC instead of computing observables directly. We will see that this final, outgoing, state is controlled by the usual eikonal function. In this section we restrict to a purely conservative scattering scenario: then eikonal exponentiation is exact. We take two incoming particles and (since the scattering is conservative) assume that the outgoing state is also an element of the two-particle Hilbert space.

We begin with the standard definition of the eikonal as the transverse Fourier transform of the four-point amplitude

$$e^{i\chi(x;\, s)/\hbar}(1 + i\Delta(x;\, s)) - 1 = i \int \hat{\mathrm{d}}^4 q\, \hat{\delta}(2p_1 \cdot q)\hat{\delta}(2p_2 \cdot q) e^{-iq\cdot x/\hbar} \mathcal{A}_4(s, q^2) \,, \quad (5.66)$$

where $\chi(x;\, s)$ is the eikonal function and $\Delta(x;\, s)$ is the so-called quantum remainder which takes into account contributions that do not exponentiate (see for example [9]). This remainder is important for computing the eikonal function — but it will play no role in the remainder of the chapter, so we will omit it.

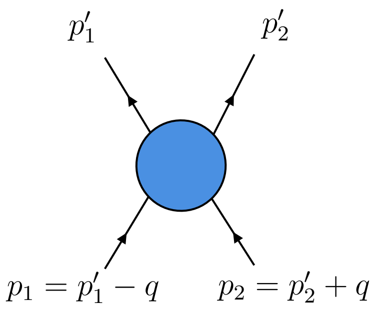

Figure 5.6 *Momentum labelling at four points*

Meanwhile the two Dirac delta functions appearing in equation (5.66) ensure that we integrate only over the components of q transverse to the momenta. This is often just written instead as $\hat{\mathrm{d}}^{D-2}q_\perp$ (times a Jacobian factor). Indeed, the parameter x should be thought of as an element of the $D-2$ dimensional spatial slice perpendicular to p_1 and p_2: this is most evident on the right-hand-side of the equation, where the Dirac delta functions project away any components of q in the (timelike) p_1 and p_2 directions. Consequently no components of x in the space spanned by p_1 and p_2 enter the dot product $q \cdot x$.

The eikonal can be written as an expansion in powers of the generic coupling g

$$\chi(x;\, s) = \sum_{n=0}^{\infty} \chi_n(x;\, s) \quad , \quad \chi_n(x;\, s) \sim g^{2n} \,, \tag{5.67}$$

and we will, as others have (see for example [9, 11, 14, 203, 205, 288]), assume that this holds to all orders. The structure has been formally proven at leading order, (see for example [196, 199]), however an all orders proof has not been given (to the best of our knowledge).

Starting with the in state (5.7) from section 5.2.2, we obtain the final state by acting with the S matrix. Writing $S = 1 + iT$ and inserting a complete set of states, we have

$$\begin{aligned} S|\psi\rangle =& |\psi\rangle + i \int \mathrm{d}\Phi(p_1', p_2', p_1, p_2)\, \phi_b(p_1, p_2) |p_1', p_2'\rangle \langle p_1', p_2'|T|p_1, p_2\rangle \\ =& |\psi\rangle + i \int \mathrm{d}\Phi(p_1', p_2', p_1, p_2)\, \phi_b(p_1, p_2) \mathcal{A}_4(s, q^2) \delta^{(4)}(p_1 + p_2 - p_1' - p_2') |p_1', p_2'\rangle \,. \end{aligned} \tag{5.68}$$

Notice that we made explicit use of our assumption of conservative scattering by restricting the complete set of states to the two-particle Hilbert space.

With the momentum labelling in figure 5.6 we can convert the p_1 and p_2 phase space integrals to integrals over q. Doing so, we may write

$$\begin{aligned} S|\psi\rangle &= |\psi\rangle \\ &+ i\int \mathrm{d}\Phi(p_1',p_2')\,\hat{\mathrm{d}}^4q\,\hat{\delta}(2p_1'\cdot q-q^2)\hat{\delta}(2p_2'\cdot q+q^2)\,\phi_b(p_1'-q,p_2'+q)\mathcal{A}_4(s,q^2)|p_1',p_2'\rangle. \end{aligned} \tag{5.69}$$

At this point, the q integral is tantalising similar to the q integral in the eikonal formula (5.66). However there is a key difference in the nature of the delta functions: those in equation (5.69) involve q^2 terms which are absent in equation (5.66). This issue appeared recently in reference [75]: there the authors proceeded using a “HEFT” phase, which is analogous to yet distinct from the eikonal phase. We will instead continue with the eikonal phase.

It may be worth remarking that the q^2 terms in these delta functions are suppressed in specific examples. One such example is the leading order impulse [49]. Nevertheless the impulse at NLO does indeed involve the full delta functions [49].

To incorporate the full delta functions, we follow the route described in [14]. We introduce new momentum variables $\tilde{p}$ as

$$\tilde{p}_1 = p_1' - \frac{q}{2} \qquad \tilde{p}_2 = p_2' + \frac{q}{2}. \tag{5.70}$$

Now, rather than using the eikonal equation (5.66) directly we can take advantage of its inverse Fourier transform in the following form[7]

$$i\hat{\delta}(2\tilde{p}_1\cdot q)\hat{\delta}(2\tilde{p}_2\cdot q)\mathcal{A}_4(s,q^2) = \frac{1}{\hbar^4}\int \mathrm{d}^4x\, e^{iq\cdot x/\hbar}\left\{e^{i\chi(x_\perp;\,s)/\hbar}-1\right\}, \tag{5.71}$$

where we have written $x_\perp$ as one of the arguments of the eikonal function $\chi(x_\perp;\, s)$ to emphasise that $\chi(x_\perp;\, s)$ only depends on components of x which are orthogonal to the space spanned by $\tilde{p}_1$ and $\tilde{p}_2$. Indeed, integrating over the two components of x which *are* in the space spanned by $\tilde{p}_1$ and $\tilde{p}_2$, one recovers the two Dirac delta functions on the left-hand-side of equation (5.71). In this way, we find that the final state is

$$S|\psi\rangle = \int \mathrm{d}\Phi(p_1',p_2')\,|p_1',p_2'\rangle\frac{1}{\hbar^4}\int \hat{\mathrm{d}}^4q\,\mathrm{d}^4x\, e^{iq\cdot x/\hbar}\, e^{i\chi(x_\perp;\,s)/\hbar}\,\phi_b(p_1'-q,p_2'+q)\,. \tag{5.72}$$

[7]As noted above, we dropped the quantum remainder Δ which plays no role in our analysis.

It is worth emphasising once again that $x_\perp$ is perpendicular to $\tilde{p}_i$, rather than to p_i, so that

$$\tilde{p}_1 \cdot x_\perp = 0 = \tilde{p}_2 \cdot x_\perp . \tag{5.73}$$

In particular, $x_\perp$ depends on q.

5.4.2 The impulse from the eikonal

In this subsection, we will recover one beautiful result from the literature on the eikonal function: the scattering angle can be extracted from the eikonal function using a stationary phase argument. As our interest is not so much in this conservative case but rather in its radiative generalisation (which we discuss below), we wish to emphasise that it is, in fact, possible to extract the *full* final momentum from the eikonal using stationary phase. Later, in section 5.4.4, we will use the same ideas to extract the final momentum in the case of radiation — with radiation, of course, knowledge of the direction of the final momentum is insufficient to recover the full momentum.

The impulse is the observable

$$\begin{aligned} \Delta p_1^\mu &\equiv \langle\psi|S^\dagger \mathbb{P}_1^\mu S|\psi\rangle - \langle\psi|\mathbb{P}_1^\mu|\psi\rangle \\ &= \langle\psi|S^\dagger [\mathbb{P}_1^\mu, S]|\psi\rangle . \end{aligned} \tag{5.74}$$

It is convenient to focus on

$$[\mathbb{P}_1^\mu, S]|\psi\rangle . \tag{5.75}$$

As we shall see, in essence the operator $[\mathbb{P}_1^\mu, S]$ pulls out a factor of the momentum transfer multiplying $S|\psi\rangle$. We will evaluate $[\mathbb{P}_1^\mu, S]|\psi\rangle$ by stationary phase; it is then trivial to determine $\langle\psi|S^\dagger$ in the same way.

We begin our expression for the final-state wavepacket, equation (5.72), quickly finding

$$\begin{aligned} [\mathbb{P}_1^\mu, S]|\psi\rangle = \int \mathrm{d}\Phi(p_1', p_2')\, e^{ib\cdot p_1'/\hbar}\, |p_1', p_2'\rangle \frac{1}{\hbar^4} \int \hat{\mathrm{d}}^4 q\, \mathrm{d}^4 x\, e^{iq\cdot x/\hbar} e^{-ib\cdot q/\hbar} \\ \times e^{i\chi(x_\perp;\, s)/\hbar}\, \phi(p_1' - q, p_2' + q)\, q^\mu . \end{aligned} \tag{5.76}$$

To obtain formulae for the impulse, we apply the stationary phase approximation to the x and q integrals. (Our approach is very similar to that of Ciafaloni and Colferai [289] who previously discussed wavepacket dynamics, the eikonal, and stationary phase.)

The stationary phase condition for x is

$$q_\mu = -\frac{\partial}{\partial x^\mu}\chi(x_\perp, s)\,. \tag{5.77}$$

One thing to note immediately is that this q^μ is *not* of order $\hbar$: it is a classical momentum, of order g^2. Further, it is useful to note that χ is actually a function of $x_\perp^2$ (since the four-point function is a function of s and q^2.) Therefore we may write the momentum transfer as

$$q^\mu = -2\chi'(x_\perp^2, s)x_\perp^\mu\,, \tag{5.78}$$

where $\chi'(x_\perp^2, s)$ is the derivative of χ with respect to its first argument. Since $\tilde{p}_1 \cdot x_\perp = 0 = \tilde{p}_2 \cdot x_\perp$, it now follows that $\tilde{p}_1 \cdot q = 0 = \tilde{p}_2 \cdot q$: thus the on-shell delta functions in equation (5.71) have reappeared, now as "equations of motion" following from the stationary phase conditions[8].

The second stationary phase condition, associated with q, is

$$x^\mu - b^\mu + \frac{\partial}{\partial q_\mu}\chi(x_\perp^2, s) = 0\,. \tag{5.79}$$

The q derivative is non-vanishing because $x_\perp$ depends on q. It is often useful to introduce a particular notation for the variables q and x when they satisfy the stationary phase conditions: we will denote these by q_* and x_*. Armed with this notation, we may use equation (5.77) we may write equation (5.79) as

$$x^\mu = b^\mu + q_{*\nu}\frac{\partial}{\partial q_\mu}x_\perp^\nu\,. \tag{5.80}$$

Performing the derivative is straightforward, but requires some notation which we relegate to appendix A.4. The result may be expressed in the form

$$x_{*\perp}^\mu = b^\mu - \tilde{N}_q(p_1^\mu - p_2^\mu) - \tilde{N}_{0q}(p_1^\mu + p_2^\mu)\,, \tag{5.81}$$

where $\tilde{N}_q$ and $\tilde{N}_{0q}$ can be interpreted as Lagrange multipliers which ensure that $x_\perp \cdot \tilde{p}_1 = 0 = x_\perp \cdot \tilde{p}_2$.

[8]Since some of the x integrations may be performed exactly to yield delta functions, we are slightly abusing terminology by referring to all of the conditions on x and q as "stationary phase conditions". Some of the conditions arise approximately by stationary phase, and some are exact conditions due to the delta functions. Nevertheless it is most convenient to treat all the conditions as one set.

Our result for $x_{*\perp}$ takes a familiar form in the CM frame. Then $x^0_{*\perp} = 0$ and, using, $\boldsymbol{p_2} = -\boldsymbol{p_1}$, we have

$$\begin{aligned} \boldsymbol{x}_{*\perp} &= \boldsymbol{b} - 2N_q \boldsymbol{p} \\ \Rightarrow \boldsymbol{b} \cdot \boldsymbol{x}_{*\perp} &= \boldsymbol{b}^2 \,. \end{aligned} \tag{5.82}$$

Denoting the scattering angle by Ψ, we may write this result[9] as

$$|\boldsymbol{b}| = |\boldsymbol{x}_{*\perp}| \cos(\Psi/2)\,, \tag{5.83}$$

where Ψ is the scattering angle.

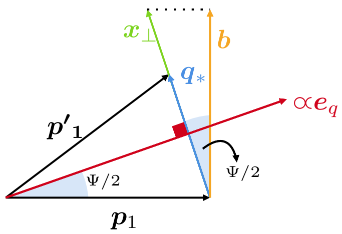

Figure 5.7 *Geometry of eikonal scattering.*

In this way, we have performed the integrals over q and x. The result has been to evaluate the factor q^μ as a derivative of the eikonal function. To obtain the full expectation, we simply evaluate $\langle\psi|S^\dagger$ using stationary phase in precisely the same way: the only difference (apart from the obvious Hermitian conjugation) is the absence of the q^μ factor. We then exploit unitarity to conclude that

$$\Delta p_1^\mu = q^\mu = -\partial^\mu \chi(x_\perp, s)\,, \tag{5.84}$$

where all quantities are defined on using the solution of the stationary phase conditions.

Notice that we have determined the *complete* impulse four-vector, not just the scattering angle. The distinction between these quantities is obviously unimportant at the level of conservative dynamics, but it is important when radiation occurs. The key aspect of our argument which leads to the full impulse rather than the scattering angle is the presence of the perpendicular projector. To see how this works, let us discuss an explicit example: the impulse at next-to-leading order in gravitational fast scattering.

[9] In this context, the quantity $x_\perp$ is sometimes referred to as the "eikonal" impact parameter.

Focusing on the scattering between two massive bodies in general relativity, the eikonal phase at next-to-leading order in G is

$$\chi = -2Gm_1m_2\left(\frac{(2\gamma^2-1)}{\sqrt{\gamma^2-1}}\log|x_\perp| - \frac{3\pi}{8}\frac{(5\gamma^2-1)}{\sqrt{\gamma^2-1}}\frac{G\,(m_1+m_2)}{|x_\perp|}\right)\,, \tag{5.85}$$

where we have defined $\gamma = u_1\cdot u_2$ as the scalar product between the four-velocities of the particles. Using equation (5.84) and straightforward differentiation, we obtain the following expression in terms of $x_\perp^\mu$,

$$\Delta p_1^\mu = \frac{2Gm_1m_2x_\perp^\mu}{|x_\perp^2|}\left(\frac{(2\gamma^2-1)}{\sqrt{\gamma^2-1}} + \frac{3\pi}{8}\frac{(5\gamma^2-1)}{\sqrt{\gamma^2-1}}\frac{G\,(m_1+m_2)}{|x_\perp|}\right)\,, \tag{5.86}$$

where the four-velocities in γ can now be identified with the incoming four-velocities of the particles due to the integrals over the wavepackets that took place to arrive at (5.84). At this point, it is important to remember that $x_\perp^\mu$ is not quite b^μ. It is trivial to show that $x_\perp^\mu$ coincides with b^μ at leading order in the gravitational coupling, but this is no longer the case at next-to-leading order; then instead

$$x_\perp^\mu = b^\mu - \frac{G(2\gamma^2-1)}{(\gamma^2-1)^{3/2}}\left(u_1^\mu(m_2+\gamma m_1) - u_2^\mu(m_1+\gamma m_2)\right)\,, \tag{5.87}$$

where

$$|x_\perp^2| = |b^2|\,. \tag{5.88}$$

We can now express the impulse in terms of the impact parameter b^μ. At the order we are interested in we find,

$$\begin{aligned}\Delta p_1^\mu = &\frac{2Gm_1m_2b^\mu}{|b^2|}\left(\frac{(2\gamma^2-1)}{\sqrt{\gamma^2-1}} + \frac{3\pi}{8}\frac{(5\gamma^2-1)}{\sqrt{\gamma^2-1}}\frac{G\,(m_1+m_2)}{|b|}\right)\\ &-\frac{G^2m_1m_2\,(2\gamma^2-1)^2\left((\gamma m_1+m_2)\,u_1^\mu - (\gamma m_2+m_1)\,u_2^\mu\right)}{(\gamma^2-1)^2\,|b^2|}\,,\end{aligned} \tag{5.89}$$

in perfect agreement with the literature [32].

From the perspective of this chapter, the key achievement of the eikonal resummation is that negligible variance becomes automatic in the stationary phase argument. Indeed since the stationary phase condition (5.77) sets the momentum transfer to a specific, classical, value it is clear that the expectation value of any polynomial in the momentum operator will evaluate to the classical expectation.

5.4.3 Extension with coherent radiation

The exponentiated eikonal final state of equation (5.72) beautifully describes semiclassical conservative dynamics, leading to a transparent method for extracting the impulse (or scattering angle) from amplitudes in a manner which automatically enforces minimal uncertainty. We have also seen that coherent states naturally enforce minimal uncertainty for radiation. Now let us put these two ideas together to form a proposal for an eikonal-type final state in the fully dynamical, radiative, case.

It is very natural to consider a modification of the eikonal formula which includes radiation, and indeed this idea has received attention [278] in the literature. Given that our motivation is to extend the eikonal while maintaining its minimal uncertainty property, an obvious way to proceed is to include an additional factor in the eikonal formula which has the structure of a coherent state, also inspired by the split signature chapter 3. If this radiative part of the state has large occupation number, expectations of products of field-strength operators will naturally factorise into products of expectations of the operators.

We will simply propose one possibility for the structure of this final state, depending on a coherent waveshape parameter $\alpha^{(\eta)}(k)$ (of helicity η) in addition to an eikonal function χ. We believe there is strong evidence in favour of the basic structure of our proposal, and in particular in the idea that two objects χ and $\alpha^{(\eta)}(k)$ suffice to define it; however, it seems possible to implement the idea in somewhat different ways. We will discuss the basic virtues of our proposal in the remainder of this section, leaving it to future work to determine further details. Since we are primarily interested in classical effects, we will continue to neglect the quantum remainder Δ in this discussion[10].

To describe our proposal, we begin with the eikonal final state (5.72). With an eye towards a situation where momentum is lost to radiation, we need a description in which the sum of the momenta of the two final particles differs from the initial momenta. A first step, then, is to Fourier transform the wavepacket to position

[10] Indeed radiative quantum effects will require Δ to be upgraded to an operator.

space:

$$S|\psi\rangle|_{\text{conservative}} = \int \mathrm{d}\Phi(p_1', p_2') \int \hat{\mathrm{d}}^4\bar{q}\, \mathrm{d}^4x\, \mathrm{d}^4x_1\, \mathrm{d}^4x_2\; \tilde{\phi}_b(x_1, x_2)\, e^{i(p_1'\cdot x_1 + p_2'\cdot x_2)/\hbar} \\ \times\, e^{i[q\cdot(x - x_1 + x_2) + \chi(x_\perp; s)]/\hbar}\, |p_1', p_2'\rangle\,. \tag{5.90}$$

Our proposal is now very straightforward: we simply incorporate a coherent state by assuming that

$$S|\psi\rangle = \int \mathrm{d}\Phi(p_1', p_2') \int \hat{\mathrm{d}}^4\bar{q}\, \mathrm{d}^4x\, \mathrm{d}^4x_1\, \mathrm{d}^4x_2\; \tilde{\phi}_b(x_1, x_2)\, e^{i(p_1'\cdot x_1 + p_2'\cdot x_2)/\hbar} \\ \times\; e^{i[q\cdot(x - x_1 + x_2) + \chi(x_\perp; s)]/\hbar} \exp\left[\sum_\eta \int \mathrm{d}\Phi(k)\alpha^{(\eta)}(k, x_1, x_2) a_\eta^\dagger(k)\right] |p_1', p_2'\rangle\,. \tag{5.91}$$

This is a minimal proposal: more generally, one could imagine that the coherent waveshape parameter $\alpha^{(\eta)}$ depends on other variables, for example x or q which appear in the eikonal dynamics. We will nevertheless restrict throughout this chapter to our minimal proposal. However, it is important that the state is not merely an outer product of a conservative eikonal state with a radiative factor. Some entanglement is necessary so that the radiation can backreact on the motion. In the case of the present proposal, the integrals over the variables x_1, x_2 and x perform this role. There is a connection between our proposal here and recent work [281] on the exponential structure of the S matrix.

We know that the waveshape should be proportional to $\hbar^{-3/2}$ so we may also write the state as

$$S|\psi\rangle = \int \mathrm{d}\Phi(p_1', p_2') \int \hat{\mathrm{d}}^4\bar{q}\, \mathrm{d}^4x\, \mathrm{d}^4x_1\, \mathrm{d}^4x_2\; \tilde{\phi}_b(x_1, x_2)\, e^{i(p_1'\cdot x_1 + p_2'\cdot x_2)/\hbar} \\ \times\; e^{i[q\cdot(x - x_1 + x_2) + \chi(x_\perp; s)]/\hbar} \exp\left[\frac{1}{\hbar^{3/2}}\sum_\eta \int \mathrm{d}\Phi(k)\bar{\alpha}^{(\eta)}(k, x_1, x_2) a_\eta^\dagger(k)\right] |p_1', p_2'\rangle\,. \tag{5.92}$$

In this expression, the classical waveshape $\bar{\alpha}^{(\eta)}$ is *independent* of $\hbar$, just as the eikonal function χ is independent of $\hbar$.

In order to determine $\alpha^{(\eta)}$, we follow the same steps as in sections 5.2.2 and 5.4.1; we act on the incoming state with the S matrix, and then expand in terms of integrals of amplitudes. To isolate the waveshape, we consider the overlap of our proposed final state with the bra $\langle p_1'\, p_2'\, k^\eta|$:

$$\langle p_1'\, p_2'\, k^\eta|S|\psi\rangle = \int \hat{\mathrm{d}}^4\bar{q}\, \mathrm{d}^4x\, \mathrm{d}^4x_1\, \mathrm{d}^4x_2\; \tilde{\phi}_b(x_1,x_2)\, e^{i(p_1'\cdot x_1+p_2'\cdot x_2)/\hbar} \\ \times e^{i[q\cdot(x-x_1+x_2)+\chi(x_\perp;s)]/\hbar}\, \alpha^{(\eta)}(k,x_1,x_2)\,. \tag{5.93}$$

Next we expand the S matrix as

$$\begin{aligned}\langle p_1'\, p_2'\, k^\eta|S|\psi\rangle &= \int \mathrm{d}\Phi(p_1,p_2)\, \phi_b(p_1,p_2)\, \langle p_1'\, p_2'\, k^\eta|S|p_1p_2\rangle \\ &= \int \mathrm{d}\Phi(p_1,p_2) \int \mathrm{d}^4x_1\, \mathrm{d}^4x_2\; \tilde{\phi}_b(x_1,x_2)\, e^{i(p_1\cdot x_1+p_2\cdot x_2)/\hbar} \\ &\qquad \times i\mathcal{A}_5(p_1p_2\to p_1'p_2'k^\eta)\, \hat{\delta}^4(p_1+p_2-p_1'-p_2'-k)\,.\end{aligned} \tag{5.94}$$

We note that the five-point amplitude appearing here could in principle include disconnected components beginning at order g. This order g disconnected term would involve exactly zero-energy photons, and does not contribute to observables such as the radiated momentum or the asymptotic Newman-Penrose scalar. We therefore omit this term in the remainder of this chapter.

To continue, it is useful to perform a change of variable in the phase space measures, taking $q_1 \equiv p_1 - p_1'$ and $q_2 \equiv p_2 - p_2'$ as variables of integration. Neglecting Heaviside theta functions (which will always be unity in the domain of validity of our calculation) we find

$$\begin{aligned}\langle p_1'\, p_2'\, k^\eta|S|\psi\rangle = \int & \mathrm{d}^4x_1\, \mathrm{d}^4x_2\; \tilde{\phi}_b(x_1,x_2)\, e^{i(p_1'\cdot x_1+p_2'\cdot x_2)/\hbar} \\ & \times \int \hat{\mathrm{d}}^4q_1\, \hat{\mathrm{d}}^4q_2\, \hat{\delta}(2p_1'\cdot q_1+q_1^2)\hat{\delta}(2p_2'\cdot q_2+q_2^2)\, e^{i(q_1\cdot x_1+q_2\cdot x_2)/\hbar} \\ & \qquad \times i\mathcal{A}_5(p_1'+q_1,p_2'+q_2\to p_1',p_2',k^\eta)\, \hat{\delta}^4(q_1+q_2-k)\,.\end{aligned} \tag{5.95}$$

Requiring equations (5.93) and (5.95) to be equal for any (appropriately classical) initial wavepacket $\tilde{\phi}_b(x_1,x_2)$ we deduce that

$$\begin{aligned}\alpha^{(\eta)}(k,x_1,x_2) =& i\int \hat{\mathrm{d}}^4q_1\, \hat{\mathrm{d}}^4q_2\, \hat{\delta}(2p_1'\cdot q_1+q_1^2)\hat{\delta}(2p_2'\cdot q_2+q_2^2)e^{i(\bar{q}_1\cdot x_1+\bar{q}_2\cdot x_2)} \\ & \times \hat{\delta}^4(q_1+q_2-k)\mathcal{A}_5(p_1'+q_1,p_2'+q_2\to p_1',p_2',k^\eta) \\ & \times \left[\int \hat{\mathrm{d}}^4q\, \mathrm{d}^4x\, e^{iq\cdot x} e^{iq\cdot(x_2-x_1)/\hbar} e^{i\chi(x_\perp;s)/\hbar}\right]^{-1}.\end{aligned} \tag{5.96}$$

It is easy to use the eikonal equation (5.66) to show that equivalently we may write the waveshape as

$$\alpha^{(\eta)}(k,x_1,x_2) = i\int \hat{\mathrm{d}}^4 q_1\, \hat{\mathrm{d}}^4 q_2\, \hat{\delta}(2p_1'\cdot q_1 + q_1^2)\hat{\delta}(2p_2'\cdot q_2 + q_2^2) e^{i(\bar{q}_1\cdot x_1 + \bar{q}_2\cdot x_2)} \\ \times \hat{\delta}^4(q_1+q_2-k)\mathcal{A}_5(p_1'+q_1, p_2'+q_2 \to p_1', p_2', k^\eta) \\ \times \left[1 + \int \hat{\mathrm{d}}^4 q\, \hat{\delta}(2\tilde{p}_1\cdot q)\hat{\delta}(2\tilde{p}_2\cdot q)\, e^{iq\cdot(x_2-x_1)/\hbar} i\mathcal{A}_4(s,q^2)\right]^{-1} . \tag{5.97}$$

This last expression makes the physical meaning transparent: the waveshape is obtained by removing iterated contributions of four-point amplitudes from the five-point amplitude.

To see this in more detail, it is instructive to expand the $\alpha^{(\eta)}(k)$ order-by-order in perturbation theory. We again consider a generic coupling g and expand the waveshape as

$$\alpha^{(\eta)}(k) = \alpha_0^{(\eta)}(k) + \alpha_1^{(\eta)}(k) + \cdots . \tag{5.98}$$

The leading order term, $\alpha_0^{(\eta)}(k)$, follows immediately from equation (5.97):

$$\alpha_0^{(\eta)}(k,x_1,x_2) = i\int \hat{\mathrm{d}}^4 q_1\, \hat{\mathrm{d}}^4 q_2\, \hat{\delta}(2p_1'\cdot q_1 + q_1^2)\hat{\delta}(2p_2'\cdot q_2 + q_2^2)\hat{\delta}^4(q_1+q_2-k) \\ \times e^{i(q_1\cdot(x_1+b)+q_2\cdot x_2)/\hbar}\mathcal{A}_{5,0}(p_1'+q_1, p_2'+q_2 \to p_1', p_2', k^\eta) . \tag{5.99}$$

It is determined by the tree-level five-point amplitude $\mathcal{A}_{5,0}$, so it is of order g^3 in gauge theory and gravity. The fact that the leading-order classical radiation field is intimately related to five-point amplitudes was already discussed in [33, 48, 269, 272]. The basic structure of this leading-order waveshape is strikingly reminiscent of a coherent state which describes the *static* Coulomb/Schwarzschild background on analytic continuation to signature $(+,+,-,-)$ previously seen.

More precisely, $\alpha_0^{(\eta)}(k)$ is really determined by $\mathcal{A}_{5,0}^{(0)}$. This follows by counting powers of $\hbar$. Indeed extracting dominant powers of $\hbar$ using equation (5.43), we find

$$\alpha_0^{(\eta)}(k,x_1,x_2) = \frac{i}{\hbar^{3/2}}\int \hat{\mathrm{d}}^4 \bar{q}_1\, \hat{\mathrm{d}}^4 \bar{q}_2\, \hat{\delta}(2p_1'\cdot \bar{q}_1)\hat{\delta}(2p_2'\cdot \bar{q}_2)\hat{\delta}^4(\bar{q}_1+\bar{q}_2-\bar{k}) \\ \times e^{i(\bar{q}_1\cdot x_1 + \bar{q}_2\cdot x_2)}\mathcal{A}_{5,0}^{(0)}(p_1'+q_1, p_2'+q_2 \to p_1', p_2', k^\eta) . \tag{5.100}$$

Note that the factor $\hbar^{-3/2}$ arises as expected on general grounds. The conclusion is that the leading-in-$\hbar$ part of the five-point tree amplitude determines the radiation. The amplitude itself contains higher order terms in $\hbar$; rather than arising from the radiative factor in our proposal (5.92), these terms arise from a generalised quantum remainder.

The next-to-leading order correction to the waveshape following from equation (5.97) is

$$\begin{aligned}\alpha_1^{(\eta)}(k, x_1, x_2) = i \int &\hat{\mathrm{d}}^4 q_1 \,\hat{\mathrm{d}}^4 q_2 \,\hat{\delta}(2p_1' \cdot q_1 + q_1^2)\hat{\delta}(2p_2' \cdot q_2 + q_2^2)\hat{\delta}^4(q_1 + q_2 - k) \\ &\times e^{i(q_1\cdot x_1 + q_2 \cdot x_2)/\hbar} \mathcal{A}_{5,1}(p_1' + q_1, p_2' + q_2 \to p_1', p_2', k^\eta) \\ - \alpha_0^{(\eta)}(k, x_1, x_2) \int &\hat{\mathrm{d}}^4 q \,\hat{\delta}(2\tilde{p}_1 \cdot q)\hat{\delta}(2\tilde{p}_2 \cdot q)\, e^{iq\cdot(x_2 - x_1)/\hbar} i\mathcal{A}_{4,0}(s, q^2)\,.\end{aligned} \tag{5.101}$$

This correction involves the five-point one-loop amplitude, after subtracting an iteration term. To understand the role of the subtraction, it is instructive to extract the leading-in-$\hbar$ part of $\alpha_1^{(\eta)}(k)$:

$$\begin{aligned}\alpha_1^{(\eta)}(k, x_1, x_2) = \frac{i}{\hbar^{5/2}} \int &\hat{\mathrm{d}}^4 \bar{q}_1 \,\hat{\mathrm{d}}^4 \bar{q}_2 \,\hat{\delta}(2p_1' \cdot \bar{q}_1)\hat{\delta}(2p_2' \cdot \bar{q}_2)\hat{\delta}^4(\bar{q}_1 + \bar{q}_2 - \bar{k}) \\ &\times e^{i(\bar{q}_1\cdot x_1 + \bar{q}_2 \cdot x_2)} \mathcal{A}_{5,1}^{(0)}(p_1' + q_1, p_2' + q_2 \to p_1', p_2', k^\eta) \\ - \frac{1}{\hbar^{5/2}}\bar{\alpha}_0^{(\eta)}(k, x_1, x_2) \int &\hat{\mathrm{d}}^4 \bar{q} \,\hat{\delta}(2p_1' \cdot \bar{q})\hat{\delta}(2p_2' \cdot \bar{q})\, e^{i\bar{q}\cdot(x_2 - x_1)} i\mathcal{A}_{4,0}^{(0)}(s, q^2) \\ + \mathcal{O}(\hbar^{-3/2})\,.&\end{aligned} \tag{5.102}$$

At this stage it seems that there is an unwanted order $\hbar^{-5/2}$ term in the NLO waveshape! Consistency with our proposal therefore demands

$$\begin{aligned}\int \hat{\mathrm{d}}^4 \bar{q}_1 \,\hat{\mathrm{d}}^4 \bar{q}_2 \,\hat{\delta}(2p_1' \cdot \bar{q}_1)\hat{\delta}(2p_2' \cdot \bar{q}_2)\hat{\delta}^4(\bar{q}_1 + \bar{q}_2 - \bar{k}) e^{i(\bar{q}_1\cdot x_1 + \bar{q}_2 \cdot x_2)}& \\ \times \mathcal{A}_{5,1}^{(0)}(p_1' + q_1, p_2' + q_2 \to p_1', p_2', k^\eta)& \\ = -\bar{\alpha}_0^{(\eta)}(k, x_1, x_2) \int \hat{\mathrm{d}}^4 \bar{q} \,\hat{\delta}(2p_1' \cdot \bar{q})\hat{\delta}(2p_2' \cdot \bar{q})\, e^{i\bar{q}\cdot(x_2 - x_1)} \mathcal{A}_{4,0}^{(0)}(s, q^2)\,.&\end{aligned} \tag{5.103}$$

Since $\bar{\alpha}_0^{(\eta)}$ is determined by $\mathcal{A}_{5,0}^{(0)}$, this requirement relates $\mathcal{A}_{5,1}^{(0)}$ to $\mathcal{A}_{5,0}^{(0)}$ and $\mathcal{A}_{4,0}^{(0)}$. The requirement is nothing but a Fourier transform of the zero-variance relation (5.46) which we encountered in section 5.3.1. So we see that the zero-variance relations retain their importance in the context of this eikonal/coherent resummation: their validity admits the possibility of exponentiation.

In the same vein, it is interesting to project our proposal onto a two-photon final state:

$$\langle p_1', p_2', k_1^{\eta_1}, k_2^{\eta_2}|S|\psi\rangle = \int \hat{\mathrm{d}}^4\bar{q}\, \mathrm{d}^4x\, \mathrm{d}^4x_1\, \mathrm{d}^4x_2\; \tilde{\phi}_b(x_1,x_2)\, e^{i(p_1'\cdot x_1 + p_2'\cdot x_2)/\hbar} \\ \times\, e^{i[q\cdot(x-x_1+x_2)+\chi(x_\perp;s)]/\hbar}\, \alpha^{(\eta_1)}(k_1,x_1,x_2)\alpha^{(\eta_2)}(k_2,x_1,x_2)\,. \tag{5.104}$$

Since the waveshape is at least of order g^3, it follows that this overlap begins at order g^6. However by expanding the S matrix out directly, we encounter a six-point amplitude. The conclusion is that our proposal does not populate the (order g^4) tree-level six-point amplitude. Of course this is as it should be: we saw that the six-point tree is suppressed in the classical region in section 5.2.4. Similarly the seven-point tree and one-loop amplitudes are suppressed, etc.

As a final remark, note that we did not introduce any normalisation factor in our proposal. This may be surprising, yet unitarity must already guarantee the normalisation of the final state. As is by now well understood, at two loops the eikonal function χ ceases to be real in the radiative case. Instead the imaginary part of χ is related to $\sum_\eta |\alpha^{(\eta)}(k)|^2$; this supplies the necessary normalisation.

5.4.4 Radiation reaction

Once there is radiation, there must also be radiation reaction: the particle's motion must change in the radiative case relative to the conservative case to account for the loss of momentum to radiation. In this section we will see that the waveshape indeed contributes to the impulse of a particle in the manner required.

We begin by acting on our conjectural final state, equation (5.91), with the momentum operator of the field corresponding to particle 1:

$$\mathbb{P}_1^\mu S|\psi\rangle = \int \mathrm{d}\Phi(p_1',p_2') \int \hat{\mathrm{d}}^4\bar{q}\, \mathrm{d}^4x\, \mathrm{d}^4x_1\, \mathrm{d}^4x_2\; \tilde{\phi}_b(x_1,x_2)\, e^{i(p_1'\cdot x_1 + p_2'\cdot x_2)/\hbar} \\ \times\, e^{i[q\cdot(x-x_1+x_2)+\chi(x_\perp;s)]/\hbar} \exp\left[\sum_\eta \int \mathrm{d}\Phi(k)\alpha^{(\eta)}(k,x_1,x_2)a_\eta^\dagger(k)\right] p_1'^\mu |p_1',p_2'\rangle\,. \tag{5.105}$$

The operator simply inserts a factor $p_1'^\mu$. We proceed by rewriting this factor in terms of a derivative $-i\hbar\partial/\partial x_{1\mu}$ acting on the exponential factor in the first line of equation (5.105), and then integrating by parts. Neglecting the boundary term, the result is

$$\mathbb{P}_1^\mu S|\psi\rangle = \int \mathrm{d}\Phi(p_1', p_2') \int \hat{\mathrm{d}}^4\bar{q}\, \mathrm{d}^4x\, \mathrm{d}^4x_1\, \mathrm{d}^4x_2\;\; e^{i(p_1'\cdot x_1 + p_2'\cdot x_2)/\hbar} e^{i(q\cdot x + \chi(x_\perp;\, s))/\hbar}$$
$$\times\, i\hbar\partial_1^\mu \left(\tilde{\phi}_b(x_1, x_2) e^{iq\cdot(x_2 - x_1)/\hbar} \exp\left[\sum_\eta \int \mathrm{d}\Phi(k)\, \alpha^{(\eta)}(k, x_1, x_2) a_\eta^\dagger(k) \right] \right) |p_1', p_2'\rangle\,. \tag{5.106}$$

Expanding out the derivative, we encounter three terms. In the first, the derivative acts on the spatial wavefunction: as usual in quantum mechanics, this term will evaluate (in the expectation value of the final momentum) to the contribution of the initial momentum. The second term arises when the derivative operator acts on $e^{iq\cdot(x_2-x_1)/\hbar}$, which inserts a factor of q^μ. This term is familiar from equation (5.76) in section 5.4.2, and contributes to the impulse as a (suitably projected) derivative of the eikonal function. Only the final term is new: it involves the waveshape, and must then be the origin of radiation reaction in our approach.

Since we have discussed the conservative impulse in detail in section 5.4.2, we focus on the final (new) term here. In this term, the derivative brings down a factor of

$$\sum_\eta \int \mathrm{d}\Phi(k)\, \partial_1^\mu \alpha^{(\eta)}(k, x_1, x_2) a_\eta^\dagger(k). \tag{5.107}$$

Now to extract the momentum observable we multiply by $\langle\psi|S^\dagger$. Since this will introduce yet more integrals, it is helpful to define a modified KMOC style 'classical average angle brackets' $\left\langle\!\!\left\langle ... \right\rangle\!\!\right\rangle$, defined here by

$$\left\langle\!\!\left\langle ... \right\rangle\!\!\right\rangle = \int \mathrm{d}\Phi(p_1', p_2') \int \hat{\mathrm{d}}^4\bar{q}\, \mathrm{d}^4x\, \hat{\mathrm{d}}^4\bar{Q}\, \mathrm{d}^4y\, \mathrm{d}^4x_1\, \mathrm{d}^4x_2\, \mathrm{d}^4y_1\, \mathrm{d}^4y_2\, \tilde{\phi}_b^*(y_1, y_2)\tilde{\phi}_b(x_1, x_2)$$
$$\times\, e^{i(p_1'\cdot(x_1 - y_1) + p_2'\cdot(x_2 - y_2)/\hbar} e^{i(q\cdot(x_2 - x_1) - Q\cdot(y_2 - y_1))/\hbar} e^{i(q\cdot x + \chi(x_\perp;\, s) - Q\cdot y - \chi^*(y_\perp;\, s))/\hbar}$$
$$\times \exp\left[-\frac{1}{2}\sum_\eta \int \mathrm{d}\Phi(k)\, \left|\alpha^{(\eta)}(k, x_1, x_2) - (\alpha^{(\eta)})^*(k, y_1, y_2)\right|^2 \right] (...)\,. \tag{5.108}$$

The $a^\dagger(k)$ will act on this left state will produce a delta function and α^*. After using the delta function it gives just a factor α^*. Putting this together, and using the angle brackets shorthand we obtain

$$\langle \mathbb{P}_1^\mu \rangle_{\text{reaction}} = \left\langle\!\!\left\langle i \sum_\eta \int \mathrm{d}\Phi(k)\, \alpha^{(\eta),*}(k, x_1, x_2)\partial_1^\mu \alpha^{(\eta)}(k, x_1, x_2) \right\rangle\!\!\right\rangle. \tag{5.109}$$

Notice that the manipulations leading to equation (5.109) were exact (under the assumption of equation (5.91).) However equation (5.109) involves a number of integrals which would need to be performed to arrive at a concrete expression for the impulse. In section 5.4.2, we performed these integrals by stationary phase. In the present (radiative) case a similar approach would be possible, but the stationary phase conditions are significantly more complicated. For example, demanding the phase of the q integral to be stationary leads to a condition involving the variables x_2 and x_1; further demanding that the phases of these x_i integrals should be stationary leads to an equation involving the integral of a quadratic function of the waveshape. In this way the stationary phase conditions involve an intricate interplay of the eikonal and the waveshape. Of course this is as it should be: the complexity of radiation reaction must be captured by the final state.

As a simpler sanity check of our machinery, we evaluate the radiation reaction contribution to the impulse at lowest non-trivial perturbative order. In [49] the leading order radiation reaction term was written as

$$I^{\mu}_{rad} = e^6 \left\langle\!\!\left\langle \int \mathrm{d}\Phi(\bar{k}) \prod_{i=1,2} \hat{\mathrm{d}}^4\bar{q}_i \hat{\mathrm{d}}^4\bar{q}'_i \, \bar{q}_1^{\mu} \, \mathcal{Y}(\bar{q}_1, \bar{q}_2, \bar{k}) \mathcal{Y}^*(\bar{q}'_1, \bar{q}'_2, \bar{k}) \right\rangle\!\!\right\rangle , \tag{5.110}$$

with

$$\mathcal{Y}(\bar{q}_1, \bar{q}_2, \bar{k}) = \delta(p_1 \cdot \bar{q}_1)\delta(p_2 \cdot \bar{q}_2)\hat{\delta}^4(\bar{q}_1 + \bar{q}_2 - k)e^{ib\cdot\bar{q}_1}\mathcal{A}^{(0)}_{5,0}(\bar{q}_1, \bar{k}^{\eta}). \tag{5.111}$$

It is straightforward to verify that this is equivalent to the second term in equation (5.109). In fact, recalling the leading order waveshape formula (5.100), the match between the two expressions (5.110) and (5.109) is immediate, once our definition of average over wave packets (5.108) is taken into account.

We note in passing that the expectation $\langle\psi|S^\dagger \mathbb{F}_{\mu\nu} S|\psi\rangle$ (or $\langle\psi|S^\dagger \mathbb{R}_{\mu\nu\rho\sigma} S|\psi\rangle$) can be determined in a similar way. The annihilation operators in the field strength operator immediately bring down a single power of the waveshape. At leading non-trivial order in g, it is then straightforward to see that the field strength is determined by the five-point tree amplitude (specifically the leading fragment in $\hbar$) consistent with reference [33]. Similarly, the momentum radiated into messengers can be computed as the expectation

$$\langle\psi|S^\dagger \sum_{\eta} \int \mathrm{d}\Phi(k)\, k^{\mu}\, a^{\dagger}_{\eta}(k) a_{\eta}(k) S|\psi\rangle \,. \tag{5.112}$$

In this case, the creation and annihilation operators bring down the waveshape times its conjugate. At leading perturbative order, the momentum radiated is the square of the five-point tree, as observed in [49]. The result is also consistent with classical field theory: in that context, radiation is described the the energy-momentum tensor, which is quadratic in the field strength. Finally, we note that conservation of momentum holds as discussed in [49].

5.5 Discussion

The central theme of this chapter has been that the classical limit emerges from scattering amplitudes via an infinite set of relationships satisfied by multiloop, multileg amplitudes in a transfer expansion. These relationships arise from requiring negligible uncertainty in the measurement of observables computed from amplitudes in the correspondence limit where the classical approximation is valid. One can write scattering amplitudes in an exponential form as a result of these relationships, as has long been recognised in the conservative sector through the eikonal approximation. We have argued that the same holds for radiative physics.

While we focused on the eikonal approach to classical dynamics, it is worth emphasising that we could have phrased our discussion in terms of other, closely related, quantities. Recently the radial action has received particular attention in the literature [7]; this radial action is a classical limit of the usual quantum phase shifts [290], and is a close cousin of the eikonal function [10].

The eikonal and the radial action arise directly in other approaches to gravitational dynamics. While this chapter started with quantum field theory, undergraduate classes start more simply with worldline actions — and indeed pragmatic approaches to gravitational phenomena start with analogous worldline theories [22, 230, 291–294]. Nevertheless there is one inescapable fact about the dynamics that quantum field theory makes blatantly clear: radiation is *not* suppressed in fully relativistic physics. Thus in our approach radiation is encoded in α, fully as important as χ. Similarly the physics of radiation reaction is clear from the outset and is a consequence of a basic principle: conservation of momentum.

One of our central observations was that six-point tree amplitudes are suppressed in the classical region. We showed explicitly that this suppression hold in scalar

QED, but our more general arguments indicate that the suppression should hold in general relativity [268] and in perturbative/classical applications of Yang-Mills theory. This suppression of the six-point tree amplitude is consistent with classical intuition. Classical electrodynamics, for example, involves two main ingredients: knowledge of the electromagnetic field, and knowledge of the particle motion. As our work has focussed on determining the asymptotic properties of particles and waves, the relevant part of the classical field is the radiation field: this is the part which determines the energy and momentum in the field, for example. Similar remarks hold in gravity. In a quantum approach, asymptotic particle motion is captured by the eikonal function (or the radial action.) The radiation field is described at the leading quantum level by the five-point amplitude [33, 48, 269]. Our work generalises this last statement: we have argued that the all-order radiation field is described by the waveshape parameter α, itself determined by the all-order five-point amplitude together with the eikonal function. As the four- and five-point amplitudes are enough to describe the classical dynamics, it makes sense that higher-point amplitudes are classically suppressed.

From a classical perspective, the waveshape α is essentially [33] a Newman-Penrose scalar: either ϕ_2 in gauge theory or ψ_4 in gravity. Our contention is then that a complete description of the classical radiative dynamics is given by knowledge of one of these scalars, and knowledge of the eikonal function χ. It is important for us in this context that the *full* impulse can be deduced by differentiation of χ, not just the scattering angle. Indeed in a radiative context, knowledge of the angle needs to be supplemented by knowledge of the outgoing energy to fully determine the outgoing particle trajectory.

We emphasise that our goal was to provide evidence for an exponential classical structure of the evolved state. It would be certainly fascinating to investigate if and how our proposal can be proved true to all orders. This however appears to be a formidable task. In fact, even just for the eikonal sector, the exponentiation is only verified up to few loop orders. On the other hand, we provided arguments in support of the exponentiation, and indeed at leading non-trivial order it is clear that the radiation is described by a coherent state. Beyond this order much less is known. It certainly seems possible that the waveshape α could depend, in general, on more variables. We leave these fascinating quests to future research.

Chapter 6

Conclusions

In this thesis we have shown how gauge theory amplitudes were secretly holding precious on-shell data that, when properly decoded through the double copy, revealed an impressive effectiveness towards the description of classical black hole scattering. Indeed, the central aim of this work has been to bring advancement in understanding how to carry out such "decoding" efficiently, and what are the structures that can be deduced in the classical regime.

We began our journey in chapter 2 by describing the necessary tools needed: the KMOC formalism [49] for classical observables, the double copy [94] to obtain gravity from gauge theory and coherent states to describe long range radiative waveforms [33].

Then, in chapter 3 we considered a split signature continuation of Minkowski spacetime. This was done in order to describe *real* physical waveforms in terms of the atomic building block of on-shell algorithms [91]: the three-point classical vertex with an on-shell emitted boson. We started from scalar QED and then double copied to obtain gravity radiation emitted by a single scalar particle. This process is obviously impossible when using Minkowskian kinematics, but not in split signatures. Moreover, split signature spacetimes still retained the rich physical interpretation of usual Minkowski, and helped us introduce the concept of coherence in the final state using a minimal set up. We then moved on to discussing how, in this framework, the linearised fields are actually enough to obtain the full gravity solution. This was done through the KS double copy of [95]. We thus obtained for the first time the Schwarzschild metric in (2,2) space, thereby providing the first explicit example of the equivalence between the

BCJ and the KS double copy. Finally, we discussed how additional solutions of axi-dilaton gravity can be sourced by adding spin and magnetic charge to the emitted massless particle.

We then moved on to a thorough study of one-loop waveforms, going back to Minkowski, in chapter 4. Here, in order to interpret the rich physics, we found it wise to divide the waveform kernel (which is essentially the one-loop, five-point amplitude) into its real and imaginary parts. This is a slight rewriting of the usual KMOC cut terms [49]. Doing so allowed us to study separately conservative and radiative contributions. The conservative ones are entailed by the real part: the particle radiates under the acceleration dictated by the Lorentz/geodesic fields of the other body. The imaginary part of the waveshape instead involves radiation reaction: this is the radiation emitted under the particle's own radiation field. This separation is quite useful, since treatment of dissipative terms happens to be quite subtle classically. Instead, from the amplitude standpoint, such effects are clearly connected to two-particle unitarity cut, which in this case involve a product of two tree-level Compton amplitudes. We finally concluded with a discussion of infrared singularities, in the spirit of Weinberg's soft theorems [253].

In the final chapter 5 we used all the gathered knowledge to argue for a general structure that the classical S-matrix should enjoy. This was based on classical considerations, such as factorizations of products of classical observables [49]. The final exponentiated structure that we proposed for the final state has again a dual nature. The conservative part is dictated by an eikonal phase, which is itself specified by a $2 \to 2$ scattering amplitude. The radiation sector is described by a coherent state, whose parameter (or waveshape) is a five-point amplitude. We then tested the consistency of our proposal in two different ways, by making sure that the six-point amplitude (with two massless particles in the final state) is quantum, and by showing that the one-loop five-point one factorises into a product of tree-level amplitudes. Both of these conditions are dictated by the exponentiated structure. Even more, expanding back our exponential state yields an infinity of classical amplitude hierarchies and relations. Finally, we explicitly reproduced some known observables using our developed formalism.

The directions that our research outlines are different. Among some of them, we can readily identify the extension of our calculations to higher loops, the inclusion of spin effects into the waveforms or using split signatures to source new gravity solutions (such as accelerating spacetimes). Another outstanding problem is the one involving bound-state observables, that is to include bound states in our formalism. Indeed, it is believed that a certain analytic continuation can relate scattered data to bounded motion observables [57, 58]. However, current proposals lack a clear understanding of bounded radiation. Perhaps, the exponentiated structure proposed in 5 can take this into account: in the non-relativistic limit the eikonal phase satisfies the Hamilton-Jacobi equations, which are used to discuss bounded motion. Then, it would be interesting to understand what happens to the coherent part of the state, and how bound-motion boundary conditions can be taken into account in this way.

We thus believe there is a wealth of evidence and calculations that prove on-shell amplitudes extremely useful for classical gravity and GW observations, paving the way for many more exciting calculations and research avenues to be pursued.

Appendix A

Spinor conventions and further derivations

A.1 Spinor conventions

In coordinates (t^1, t^2, x^1, x^2), we work with a metric of signature $(+1, +1, -1, -1)$. Since this signature may be unfamiliar, we gather here a list of spinor-helicity conventions appropriate for working in this signature. Our conventions are designed to follow those of reference [34] as closely as possible, while taking advantage of the different reality properties available in split signature.

The Clifford algebra is

$$\sigma^\mu \tilde{\sigma}^\nu + \sigma^\nu \tilde{\sigma}^\mu = 2\eta^{\mu\nu}\mathbb{1}\,. \tag{A.1}$$

In our signature, it is possible to choose a real basis of σ^μ matrices. Our choice is

$$\sigma^\mu = (1, i\sigma_y, \sigma_z, \sigma_x) \tag{A.2}$$

where $\sigma_{x,y,z}$ are the usual Pauli matrices. The $\tilde{\sigma}^\mu$ are obtained by raising spinor indices, as usual:

$$\tilde{\sigma}^{\mu\dot{\alpha}\alpha} = \epsilon^{\alpha\beta}\epsilon^{\dot{\alpha}\dot{\beta}}\sigma^\mu_{\beta\dot{\beta}}\,. \tag{A.3}$$

We define $\epsilon^{12} = +1$, while $\epsilon_{12} = -1$, so that

$$\epsilon_{\alpha\beta}\epsilon^{\beta\gamma} = \delta_\alpha^\gamma\,, \tag{A.4}$$

and choose the same Levi-Civita sign for the opposite chirality,

$$\epsilon_{\dot\alpha\dot\beta} = \epsilon_{\alpha\beta}\,, \quad \epsilon^{\dot\alpha\dot\beta} = \epsilon^{\alpha\beta}\,. \tag{A.5}$$

We raise and lower all spinor indices (of either chirality) by acting from the left:

$$\lambda_\alpha = \epsilon_{\alpha\beta}\lambda^\beta = \epsilon_{\alpha\beta}(\epsilon^{\beta\gamma}\lambda_\gamma)\,. \tag{A.6}$$

It is often helpful to note that

$$\begin{aligned} \sigma_{\alpha\dot\alpha}\cdot\sigma_{\beta\dot\beta} &= 2\epsilon_{\alpha\beta}\epsilon_{\dot\alpha\dot\beta}\,, \\ \sigma_{\alpha\dot\alpha}\cdot\tilde\sigma^{\dot\beta\beta} &= 2\delta^\beta_\alpha\delta^{\dot\beta}_{\dot\alpha}\,. \end{aligned} \tag{A.7}$$

The chiral structure of spinors in split signature is important in our work. This structure is clarified by introducing the $\sigma^{\mu\nu}$ matrices which are proportional to the Lorentz generators in the spinor representations. In particular, we define

$$\begin{aligned} \sigma^{\mu\nu} &= \frac{1}{4}(\sigma^\mu\tilde\sigma^\nu - \sigma^\mu\tilde\sigma^\nu)\,, \\ \tilde\sigma^{\mu\nu} &= \frac{1}{4}(\tilde\sigma^\mu\sigma^\nu - \tilde\sigma^\mu\sigma^\nu)\,. \end{aligned} \tag{A.8}$$

Since these matrices are antisymmetric in μ and ν, there are at most six independent $\sigma^{\mu\nu}$ (and at most six independent $\tilde\sigma^{\mu\nu}$). However, the matrices enjoy the duality properties

$$\begin{aligned} \sigma_{\mu\nu} &= \frac{1}{2}\epsilon_{\mu\nu\rho\sigma}\,\sigma^{\rho\sigma}\,, \\ \tilde\sigma_{\mu\nu} &= -\frac{1}{2}\epsilon_{\mu\nu\rho\sigma}\,\tilde\sigma^{\rho\sigma}\,. \end{aligned} \tag{A.9}$$

Consequently, there are only three independent $\sigma^{\mu\nu}$ matrices, which generate the group $\mathrm{SL}(2,\mathbb{R})$.

To pass between momenta k and spinors λ, $\tilde\lambda$, we define

$$k\cdot\sigma_{\alpha\dot\alpha} = \lambda_\alpha\tilde\lambda_{\dot\alpha}\,. \tag{A.10}$$

We use the symbols $|k\rangle$, $\langle k|$, $[k|$, and $|k]$ to indicate the spinors with the indices in various positions as follows:

$$|k\rangle \leftrightarrow \lambda_\alpha\,, \quad \langle k| \leftrightarrow \lambda^\alpha\,, \quad |k] \leftrightarrow \tilde\lambda^{\dot\alpha}\,, \quad [k| \leftrightarrow \tilde\lambda_{\dot\alpha}\,. \tag{A.11}$$

As usual, we choose a basis of polarisation vectors of definite helicity $\eta = \pm$. Unlike the Minkowski case, these vectors can be chosen to be real, and we make such a choice. Given a momentum k and gauge choice q satisfying $k \cdot q \neq 0$, $k^2 = 0 = q^2$, we define

$$\varepsilon_-^\mu = -\frac{\langle k|\sigma^\mu|q]}{\sqrt{2}[kq]}\,, \qquad \varepsilon_+^\mu = \frac{[k|\tilde{\sigma}^\mu|q\rangle}{\sqrt{2}\langle kq\rangle}\,. \tag{A.12}$$

These polarisation vectors have the properties:

$$\begin{aligned} (\varepsilon_h^\mu(k))^* &= \varepsilon_h^\mu(k)\,, \\ \varepsilon_\pm^2(k) &= 0\,, \\ \varepsilon_+(k)\cdot\varepsilon_-(k) &= -1\,, \end{aligned} \tag{A.13}$$

assuming that both k and q are real.

A plane wave with negative polarisation has a self-dual field strength in our conventions:

$$\begin{aligned} \sigma_{\mu\nu}\, k^{[\mu}\varepsilon_-^{\nu]} &= -\sqrt{2}\,|k\rangle\langle k|\,, \\ \tilde{\sigma}_{\mu\nu}\, k^{[\mu}\varepsilon_-^{\nu]} &= 0\,. \end{aligned} \tag{A.14}$$

Meanwhile, a positive helicity plane wave has anti-self dual field strength given by

$$\begin{aligned} \sigma_{\mu\nu}\, k^{[\mu}\varepsilon_+^{\nu]} &= 0\,, \\ \tilde{\sigma}_{\mu\nu}\, k^{[\mu}\varepsilon_+^{\nu]} &= \sqrt{2}\,|k][k|\,. \end{aligned} \tag{A.15}$$

A.2 The retarded Green's function in $1+2$ dimensions

Because of the translation symmetry in the t^2 direction, much of our discussion really takes place in a three-dimensional space with signature $(+,-,-)$. In this appendix, we compute the retarded Green's function (for the wave operator) in this space. We use the familiar notation $x = (t, \mathbf{x})$ for points in this spacetime, and write wave vectors as $k = (E, \mathbf{k})$.

The Green's function is defined to satisfy

$$\partial^2 G(x) = \delta^{(3)}(x)\,, \tag{A.16}$$

with the boundary condition that

$$G(x) = 0\,, \quad t < 0\,. \tag{A.17}$$

It is easy to express the Green's function in Fourier space as

$$G(x) = -\int \hat{\mathrm{d}}^3 k\, e^{-ik\cdot x} \frac{1}{k^2_{\mathrm{ret}}}\,. \tag{A.18}$$

The instruction 'ret' indicates that we must define the integral to enforce the retarded boundary condition (A.17). As usual, we interpret the integral over the first component E of k^μ as a contour integral, and (as in the main text) we impose the boundary condition by displacing the poles below the real E axis. It is easy to compute the value of the E integral using the residue theorem, with the result that

$$\begin{aligned} G(x) &= \frac{-i}{8\pi^2}\Theta(t) \int \mathrm{d}^2 k\, e^{i\mathbf{k}\cdot\mathbf{x}} \frac{e^{i|\mathbf{k}|t} - e^{-i|\mathbf{k}|t}}{|\mathbf{k}|} \\ &= \frac{-i}{8\pi^2}\Theta(t) \int_0^\infty \mathrm{d}k \int_0^{2\pi} \mathrm{d}\theta\, e^{ikr\cos\theta} \left(e^{ikt} - e^{-ikt}\right)\,, \end{aligned} \tag{A.19}$$

where, in the second equality, we defined $r = |\mathbf{x}|$ and introduced polar coordinates for the $\mathbf{k}$ integration.

Our integral is still not completely well-defined. Notice that if we perform the k integral in equation (A.19) first, we encounter oscillatory factors which do not converge. The solution is again familiar: we introduce $ik\epsilon$ convergence factors in the exponents, adjusting the signs to make the integrals well-defined. The result is

$$G(x) = \frac{-i}{8\pi^2}\Theta(t) \int_0^\infty \mathrm{d}k \int_0^{2\pi} \mathrm{d}\theta\, e^{ikr\cos\theta} \left(e^{ik(t+i\epsilon)} - e^{-ik(t-i\epsilon)}\right)\,. \tag{A.20}$$

Recognising the definition of the Bessel function, it is easy to perform the θ integration next, yielding

$$G(x) = \frac{-i}{4\pi}\Theta(t) \int_0^\infty \mathrm{d}k\, J_0(kr) \left(e^{ik(t+i\epsilon)} - e^{-ik(t-i\epsilon)}\right)\,. \tag{A.21}$$

We can perform the final integral using the result

$$\int_0^\infty \mathrm{d}u\, J_0(u) e^{iuv} = \frac{1}{\sqrt{1-v^2}}\,, \tag{A.22}$$

so that

$$G(x) = \frac{i}{4\pi}\Theta(t)\left(\frac{1}{\sqrt{r^2-t^2+i\epsilon}} - \frac{1}{\sqrt{r^2-t^2-i\epsilon}}\right) . \tag{A.23}$$

At this point, the $i\epsilon$ factors come into their own. Evidently, the Green's function vanishes when we can ignore the ϵ's: this occurs when $r^2 - t^2$ is positive. But when $r^2 - t^2 < 0$, then the ϵ's control which side of the branch cut in the square root function we must choose. We have

$$\begin{aligned} G(x) &= \frac{i}{4\pi}\Theta(t)\Theta(t^2-r^2)\left(\frac{1}{\sqrt{-|t^2-r^2|+i\epsilon}} - \frac{1}{\sqrt{-|t^2-r^2|-i\epsilon}}\right) \\ &= \frac{i}{4\pi}\Theta(t)\Theta(t^2-r^2)\left(\frac{1}{i\sqrt{|t^2-r^2|}} - \frac{1}{(-i)\sqrt{|t^2-r^2|}}\right) \\ &= \frac{1}{2\pi}\Theta(t)\Theta(t^2-r^2)\frac{1}{\sqrt{t^2-r^2}} . \end{aligned} \tag{A.24}$$

As discussed in more detail in section 3.5, this Green's function is a Lorentzian version of the familiar Euclidean Green's function $\sim 1/r$. The theta functions are a result of our boundary conditions.[1]

A.3 A mini recap of NS-NS gravity

The standard notion of geometry in general relativity, a (pseudo-)Riemanian manifold (M, g) endowed with the Levi-Civita connection ∇, can be generalised by relaxing the requirements on the connection. If we allow the connection to have torsion, while insisting on metric-compatibility, the result is called Riemann-Cartan geometry.

Consider a d-dimensional manifold M equipped with a metric $g_{\mu\nu}$ and an affine connection $\mathfrak{D}$. In a coordinate basis, the covariant derivative acts on a vector V as

$$\mathfrak{D}_\nu V^\mu = \partial_\nu V^\mu + \Gamma^\mu{}_{\nu\rho} V^\rho . \tag{A.25}$$

In general, the affine symbols $\Gamma^\mu{}_{\nu\rho}$ do not have to be symmetric. Their anti-symmetric part is the *torsion* tensor, $T^\mu{}_{\nu\rho} \equiv \frac{1}{2}(\Gamma^\mu{}_{\nu\rho} - \Gamma^\mu{}_{\rho\nu}) = \frac{1}{2}\Gamma^\mu{}_{[\nu\rho]}$. We will take $(M, g, \mathfrak{D})$ to be a Riemann-Cartan manifold by requiring that the connection is metric-compatible,

$$\mathfrak{D}_\lambda g_{\mu\nu} = 0 .$$

[1] An equivalent derivation can be found in [295].

This condition constrains the affine symbols to take the form

$$\Gamma^{\mu}{}_{\nu\rho} = \left\{ {}^{\mu}_{\nu\rho} \right\} + K^{\mu}{}_{\nu\rho} \ , \tag{A.26}$$

where the first term denotes the standard Christoffel symbols of the Levi-Civita connection and the second, a tensor called *contorsion*, must satisfy $K_{\mu\nu\rho} = -K_{\rho\nu\mu}$. It can be written uniquely in terms of the torsion as

$$K^{\mu}{}_{\nu\rho} = \frac{1}{2}\, g^{\mu\lambda} \left(g_{\nu\tau}\, T^{\tau}{}_{\lambda\rho} + g_{\rho\tau}\, T^{\tau}{}_{\lambda\nu} + g_{\lambda\tau}\, T^{\tau}{}_{\nu\rho} \right) \ . \tag{A.27}$$

This generalised connection defines a generalised Riemann tensor, which in our conventions we write as

$$\mathfrak{R}_{\mu\nu\rho}{}^{\lambda} = \mathfrak{D}_{\nu}\Gamma^{\lambda}{}_{\mu\rho} - \mathfrak{D}_{\mu}\Gamma^{\lambda}{}_{\nu\rho} + \Gamma^{\lambda}{}_{\nu\tau}\Gamma^{\tau}{}_{\mu\rho} - \Gamma^{\lambda}{}_{\mu\tau}\Gamma^{\tau}{}_{\nu\rho} \ . \tag{A.28}$$

It is important to note that this tensor does not have the symmetries of the usual Riemann tensor. It satisfies $\mathfrak{R}_{\mu\nu\rho\sigma} = \frac{1}{2}\mathfrak{R}_{[\mu\nu]\rho\sigma} = \frac{1}{2}\mathfrak{R}_{\mu\nu[\rho\sigma]}$, but $\mathfrak{R}_{\mu\nu\rho\sigma} \neq \mathfrak{R}_{\rho\sigma\mu\nu}$ due to the lack of symmetry in the last two indices of the contorsion. Using (A.26), it can be shown that

$$\mathfrak{R}_{\mu\nu\rho}{}^{\lambda} = R_{\mu\nu\rho}{}^{\lambda} + \nabla_{\nu}K^{\lambda}{}_{\mu\rho} - \nabla_{\mu}K^{\lambda}{}_{\nu\rho} + K^{\lambda}{}_{\nu\tau}K^{\tau}{}_{\mu\rho} - K^{\lambda}{}_{\mu\tau}K^{\tau}{}_{\nu\rho} \ , \tag{A.29}$$

where ∇ denotes the Levi-Civita connection and $R_{\mu\nu\sigma}{}^{\lambda}$ its Riemann tensor. In general, $\mathfrak{R}$ will denote curvatures with torsion, whereas R is reserved for the standard Riemannian curvatures of the metric.

Riemann-Cartan manifolds have extra geometrical degrees of freedom in the contorsion.[2] These degrees of freedom can be used to accommodate the NS-NS fields, giving them a geometric status similar to the metric. The dilaton is assigned to the trace of the contorsion while the B-field is related to its fully antisymmetric component

$$K^{\mu}{}_{\nu\rho} = \frac{\kappa}{2\sqrt{3}} e^{-\frac{4\kappa\phi}{d-2}}\, H^{\mu}{}_{\nu\rho} - \frac{2\,\kappa}{(d-2)\sqrt{d-1}} \left(\delta^{\mu}{}_{\nu}\, \partial_{\rho}\phi \; - \; g_{\nu\rho}\, g^{\mu\sigma}\, \partial_{\sigma}\phi \right) \ , \tag{A.30}$$

where $H = \mathrm{d}B$ is the curvature of the B-field and κ is the gravitational coupling constant. The contorsion (A.30) was chosen such that the Ricci scalar is

$$\mathfrak{R} = R - \frac{4\kappa^2}{d-2}\nabla_{\mu}\phi\, \nabla^{\mu}\phi - \frac{\kappa^2}{12} e^{-\frac{8\kappa\phi}{d-2}}\, H_{\mu\nu\rho}H^{\mu\nu\rho} + \frac{4\kappa\,\sqrt{d-1}}{d-2}\nabla^{\mu}\nabla_{\mu}\phi \ , \tag{A.31}$$

[2] Thank you for reading this thesis down to the appendix <3.

the motivation being that $\sqrt{|g|}\,\mathfrak{R}$ is equivalent to the usual NS-NS Lagrangian density in the Einstein frame, up to a boundary term:

$$S = \frac{1}{2\kappa^2}\int \mathrm{d}^d x \sqrt{|g|}\left(R - \frac{4\kappa^2}{d-2}\nabla_\mu\phi\,\nabla^\mu\phi - \frac{\kappa^2}{12}e^{-\frac{8\kappa\phi}{d-2}}\,H_{\mu\nu\rho}H^{\mu\nu\rho}\right) , \tag{A.32}$$

$$= \frac{1}{2\kappa^2}\int \mathrm{d}^d x \sqrt{|g|}\;\mathfrak{R}\;. \tag{A.33}$$

In chapter 3, we will be interested in the curvature at linear order in the fields. Starting from $g_{\mu\nu} = \eta_{\mu\nu} + \kappa\, h_{\mu\nu}$, and expanding to linearised order, we obtain

$$\mathfrak{R}_{\mu\nu}{}^{\rho\sigma} = -\frac{\kappa}{2}\partial_{[\mu}\partial^{[\rho}h_{\nu]}{}^{\sigma]} + \frac{\kappa}{(d-2)\sqrt{d-1}}\,\delta_{[\mu}{}^{[\rho}\partial_{\nu]}\partial^{\sigma]}\phi + \frac{\kappa}{2\sqrt{3}}\partial_{[\mu}\partial^{[\rho}B_{\nu]}{}^{\sigma]}\;. \tag{A.34}$$

In $d = 4$, the field redefinitions

$$\phi \to \frac{\sqrt{3}}{2}\phi\;, \qquad\qquad B \to \sqrt{3}B\;, \tag{A.35}$$

simplify the factors to reduce the linearised Riemann tensor to

$$\mathfrak{R}_{\mu\nu}{}^{\rho\sigma} = -\frac{\kappa}{2}\left(\partial_{[\mu}\partial^{[\rho}h_{\nu]}{}^{\sigma]} - \delta_{[\mu}{}^{[\rho}\partial_{\nu]}\partial^{\sigma]}\phi - \partial_{[\mu}\partial^{[\rho}B_{\nu]}{}^{\sigma]}\right)\;. \tag{A.36}$$

At this order, the packaging can be taken one step further by using the 'fat graviton' defined in [105] [3]

$$\mathfrak{H}_{\mu\nu} = \mathfrak{h}_{\mu\nu} - B_{\mu\nu} - P^q_{\mu\nu}\left(2\phi + \mathfrak{h}\right)\;, \tag{A.37}$$

where $\mathfrak{h}_{\mu\nu}$ is the trace-reversed graviton and $P^q_{\mu\nu}$ is a projector

$$\mathfrak{h}_{\mu\nu} = h_{\mu\nu} - \frac{1}{2}\,h\,\eta_{\mu\nu}\;, \qquad P^q_{\mu\nu} = \frac{1}{2}\left(\eta_{\mu\nu} - \frac{q_\mu\partial_\nu + q_\nu\partial_\mu}{q\cdot\partial}\right)\;. \tag{A.38}$$

The constant auxiliary null vector q^μ is related to gauge choices. In fact, the terms involving q^μ drop out of the gauge-invariant curvature, which can be written as the compact expression

$$\mathfrak{R}_{\mu\nu}{}^{\rho\sigma} = -\frac{\kappa}{2}\,\partial_{[\mu}\partial^{[\rho}\mathfrak{H}_{\nu]}{}^{\sigma]}\;. \tag{A.39}$$

In this sense, our generalised curvature is the 'fat Riemann' associated to the 'fat graviton'.

[3] Some factors differ from [105] due to different normalisation conventions.

There is yet another way to rewrite (3.121). In four dimensions, the two-form $B_{\mu\nu}$ can be traded for a pseudoscalar axion σ, defined by

$$H_{\mu\nu\rho} = -e^{2\sqrt{3}\,\phi}\,\epsilon_{\mu\nu\rho\sigma}\partial^{\sigma}\sigma\ . \tag{A.40}$$

At linearised order, the exponential in the expression above is unity, so finally

$$\mathfrak{R}_{\mu\nu}{}^{\rho\sigma} = -\frac{\kappa}{2}\left(\partial_{[\mu}\partial^{[\rho}h_{\nu]}{}^{\sigma]} - \delta_{[\mu}{}^{[\rho}\partial_{\nu]}\partial^{\sigma]}\phi + \epsilon^{\rho\sigma\lambda}{}_{[\mu}\partial_{\nu]}\partial_{\lambda}\sigma\right)\ . \tag{A.41}$$

A.4 Projection in the plane of scattering

The relation between the eikonal impact parameter $x_\perp^\mu$ and b^μ can be stated clearly by first introducing some notation. Let us define the following four-vectors in momentum space

$$\begin{cases} e_0^\mu \equiv N_0(\tilde{p}_1^\mu + \tilde{p}_2^\mu) \\ e_q^\mu \equiv N_q(\tilde{p}_1^\mu - \tilde{p}_2^\mu) - N_{0q}(\tilde{p}_1^\mu + \tilde{p}_2^\mu)\ , \end{cases} \tag{A.42}$$

where the normalization factors N_0, N_q and N_{0q} are fixed by requiring $e_0^2 = 1$, $e_q^2 = -1$ and $e_0 \cdot e_q = 0$. By definition of $x_\perp^\mu$, the following identities hold:

$$e_0 \cdot x_\perp = 0 \quad , \quad e_q \cdot x_\perp = 0\ . \tag{A.43}$$

As a consequence, we can write the projection of x^μ on the plane orthogonal to $\tilde{p}_1^\mu$ and $\tilde{p}_2^\mu$ as

$$x_\perp^\mu = x^\mu - (x\cdot e_0)e_0^\mu + (x\cdot e_q)e_q^\mu\ , \tag{A.44}$$

where the different signs in the the last two terms are a consequence of e_0^μ being time-like while e_q^μ space-like. Using (A.44) we can easily compute some of the derivatives involved in the evaluation of the stationary phase on x^μ such as

$$\frac{\partial x_\perp^2}{\partial x_\mu} = 2x_{\perp,\nu}(\eta^{\mu\nu} - e_0^\mu e_0^\nu + e_q^\mu e_q^\nu) = 2x_\perp^\mu\ . \tag{A.45}$$

Another example where the use of (A.44) is useful is when we apply the stationary phase for the integral over q^μ. In this case, the stationary condition for q^μ can be expressed as

$$x^\mu = b^\mu + q_{\nu,*}\left.\frac{\partial x_\perp^\nu}{\partial q_\mu}\right|_{q=q_*}\ , \tag{A.46}$$

where q_*^μ satisfies the stationary phase condition on x^μ given by $q_*^\mu = -2\chi'(x_\perp)x_\perp^\mu$. One of the advantages in the definition (A.42) of e_0^μ is that it is q^μ independent so that the previous stationary condition can be expressed as

$$x^\mu = b^\mu + q_{\nu,*}\frac{\partial}{\partial q_\mu}\left[(x\cdot e_q)e_q^\nu\right]\Big|_{q=q_*} . \tag{A.47}$$

Since q_*^μ is parallel to $x_\perp^\mu$, we know that $q_*\cdot e_q \propto x_\perp \cdot e_q = 0$, and so equation (A.47) simplifies to

$$x^\mu = b^\mu + q_{\nu,*}(x\cdot e_q)\frac{\partial e_q^\nu}{\partial q_\mu}\Big|_{q=q_*} . \tag{A.48}$$

The remaining derivative can be easily performed using the definition of e_q^μ. The result is

$$q_\nu \frac{\partial e_q^\nu}{\partial q_\mu}\Big|_{q=q_*} = -(N_q\, q^\mu)\Big|_{q=q_*} . \tag{A.49}$$

We can then write the eikonal impact parameter as

$$x_\perp^\mu = b^\mu - (x\cdot e_0)e_0^\mu - \left[(x\cdot e_q)N_q q^\mu\right]\big|_{q=q_*} + \left[(x\cdot e_q)e_q^\mu\right]\big|_{q=q_*} . \tag{A.50}$$

The scalar products $x\cdot e_0$ and $x\cdot e_q$, which can be viewed as Lagrange multipliers for the phase which we are minimizing, are fixed by requiring the eikonal impact parameter to be orthogonal to e_0^μ and e_q^μ. A straightforward calculation gives

$$x_\perp^\mu = b^\mu - \left[(e_q\cdot b)(N_q q^\mu - e_q^\mu)\right]\big|_{q=q_*} . \tag{A.51}$$

Expressing e_q^μ in terms of p_1^μ, p_2^μ and q^μ we obtain

$$x_\perp^\mu = b^\mu - \left[(e_q\cdot b)\left[N_{0q}(p_1^\mu + p_2^\mu) - N_q(p_1^\mu - p_2^\mu)\right]\right]\Big|_{q=q_*} , \tag{A.52}$$

which agrees — when evaluated in the center of mass frame — with the expression for the eikonal impact parameter in (5.82), where $\tilde{N}_q = -(e_q\cdot b)N_q$ and $\tilde{N}_{0q} = (e_q\cdot b)N_{0q}$.

Bibliography

[1] R. Monteiro, D. O'Connell, D. Peinador Veiga and M. Sergola, *Classical solutions and their double copy in split signature*, *JHEP* **05** (2021) 268, [2012.11190].

[2] R. Monteiro, S. Nagy, D. O'Connell, D. Peinador Veiga and M. Sergola, *NS-NS spacetimes from amplitudes*, *JHEP* **06** (2022) 021, [2112.08336].

[3] A. Elkhidir, D. O'Connell, M. Sergola and I. A. Vazquez-Holm, *Radiation and Reaction at One Loop*, 2303.06211.

[4] A. Cristofoli, R. Gonzo, N. Moynihan, D. O'Connell, A. Ross, M. Sergola et al., *The Uncertainty Principle and Classical Amplitudes*, 2112.07556.

[5] G. Menezes and M. Sergola, *NLO deflections for spinning particles and Kerr black holes*, *JHEP* **10** (2022) 105, [2205.11701].

[6] Z. Bern, A. Luna, R. Roiban, C.-H. Shen and M. Zeng, *Spinning black hole binary dynamics, scattering amplitudes, and effective field theory*, *Phys. Rev. D* **104** (2021) 065014, [2005.03071].

[7] Z. Bern, J. Parra-Martinez, R. Roiban, M. S. Ruf, C.-H. Shen, M. P. Solon et al., *Scattering Amplitudes and Conservative Binary Dynamics at $\mathcal{O}(G^4)$*, *Phys. Rev. Lett.* **126** (2021) 171601, [2101.07254].

[8] E. Herrmann, J. Parra-Martinez, M. S. Ruf and M. Zeng, *Gravitational Bremsstrahlung from Reverse Unitarity*, *Phys. Rev. Lett.* **126** (2021) 201602, [2101.07255].

[9] P. Di Vecchia, C. Heissenberg, R. Russo and G. Veneziano, *The eikonal approach to gravitational scattering and radiation at $\mathcal{O}(G^3)$*, *JHEP* **07** (2021) 169, [2104.03256].

[10] Y. F. Bautista, A. Guevara, C. Kavanagh and J. Vines, *From Scattering in Black Hole Backgrounds to Higher-Spin Amplitudes: Part I*, 2107.10179.

[11] Z. Bern, H. Ita, J. Parra-Martinez and M. S. Ruf, *Universality in the classical limit of massless gravitational scattering*, *Phys. Rev. Lett.* **125** (2020) 031601, [2002.02459].

[12] N. Moynihan and J. Murugan, *On-Shell Electric-Magnetic Duality and the Dual Graviton*, 2002.11085.

[13] A. Cristofoli, P. H. Damgaard, P. Di Vecchia and C. Heissenberg, *Second-order Post-Minkowskian scattering in arbitrary dimensions*, *JHEP* **07** (2020) 122, [2003.10274].

[14] J. Parra-Martinez, M. S. Ruf and M. Zeng, *Extremal black hole scattering at $\mathcal{O}(G^3)$: graviton dominance, eikonal exponentiation, and differential equations*, *JHEP* **11** (2020) 023, [2005.04236].

[15] K. Haddad and A. Helset, *The double copy for heavy particles*, 2005.13897.

[16] M. Accettulli Huber, A. Brandhuber, S. De Angelis and G. Travaglini, *Eikonal phase matrix, deflection angle and time delay in effective field theories of gravity*, *Phys. Rev. D* **102** (2020) 046014, [2006.02375].

[17] N. Moynihan, *Scattering Amplitudes and the Double Copy in Topologically Massive Theories*, *JHEP* **12** (2020) 163, [2006.15957].

[18] A. Manu, D. Ghosh, A. Laddha and P. V. Athira, *Soft radiation from scattering amplitudes revisited*, *JHEP* **05** (2021) 056, [2007.02077].

[19] B. Sahoo, *Classical Sub-subleading Soft Photon and Soft Graviton Theorems in Four Spacetime Dimensions*, *JHEP* **12** (2020) 070, [2008.04376].

[20] L. de la Cruz, B. Maybee, D. O'Connell and A. Ross, *Classical Yang-Mills observables from amplitudes*, *JHEP* **12** (2020) 076, [2009.03842].

[21] D. Bonocore, *Asymptotic dynamics on the worldline for spinning particles*, *JHEP* **02** (2021) 007, [2009.07863].

[22] G. Mogull, J. Plefka and J. Steinhoff, *Classical black hole scattering from a worldline quantum field theory*, *JHEP* **02** (2021) 048, [2010.02865].

[23] W. T. Emond, Y.-T. Huang, U. Kol, N. Moynihan and D. O'Connell, *Amplitudes from Coulomb to Kerr-Taub-NUT*, 2010.07861.

[24] C. Cheung, N. Shah and M. P. Solon, *Mining the Geodesic Equation for Scattering Data*, *Phys. Rev. D* **103** (2021) 024030, [2010.08568].

[25] S. Mougiakakos and P. Vanhove, *Schwarzschild-Tangherlini metric from scattering amplitudes in various dimensions*, *Phys. Rev. D* **103** (2021) 026001, [2010.08882].

[26] J. J. M. Carrasco and I. A. Vazquez-Holm, *Loop-Level Double-Copy for Massive Quantum Particles*, 2010.13435.

[27] J.-W. Kim and M. Shim, *Gravitational Dyonic Amplitude at One-Loop and its Inconsistency with the Classical Impulse*, *JHEP* **02** (2021) 217, [2010.14347].

[28] N. E. J. Bjerrum-Bohr, T. V. Brown and H. Gomez, *Scattering of Gravitons and Spinning Massive States from Compact Numerators*, *JHEP* **04** (2021) 234, [2011.10556].

[29] R. Gonzo and A. Pokraka, *Light-ray operators, detectors and gravitational event shapes*, *JHEP* **05** (2021) 015, [2012.01406].

[30] L. de la Cruz, *Scattering amplitudes approach to hard thermal loops*, *Phys. Rev. D* **104** (2021) 014013, [2012.07714].

[31] Y. F. Bautista and A. Laddha, *Soft Constraints on KMOC Formalism*, 2111.11642.

[32] E. Herrmann, J. Parra-Martinez, M. S. Ruf and M. Zeng, *Radiative classical gravitational observables at $\mathcal{O}(G^3)$ from scattering amplitudes*, *JHEP* **10** (2021) 148, [2104.03957].

[33] A. Cristofoli, R. Gonzo, D. A. Kosower and D. O'Connell, *Waveforms from Amplitudes*, 2107.10193.

[34] M.-Z. Chung, Y.-T. Huang, J.-W. Kim and S. Lee, *The simplest massive S-matrix: from minimal coupling to Black Holes*, *JHEP* **04** (2019) 156, [1812.08752].

[35] M.-Z. Chung, Y.-T. Huang and J.-W. Kim, *Classical potential for general spinning bodies*, *JHEP* **09** (2020) 074, [1908.08463].

[36] D. Neill and I. Z. Rothstein, *Classical Space-Times from the S Matrix*, *Nucl. Phys. B* **877** (2013) 177–189, [1304.7263].

[37] C. Cheung, I. Z. Rothstein and M. P. Solon, *From Scattering Amplitudes to Classical Potentials in the Post-Minkowskian Expansion*, *Phys. Rev. Lett.* **121** (2018) 251101, [1808.02489].

[38] Z. Bern, C. Cheung, R. Roiban, C.-H. Shen, M. P. Solon and M. Zeng, *Black Hole Binary Dynamics from the Double Copy and Effective Theory*, *JHEP* **10** (2019) 206, [1908.01493].

[39] Z. Bern, C. Cheung, R. Roiban, C.-H. Shen, M. P. Solon and M. Zeng, *Scattering Amplitudes and the Conservative Hamiltonian for Binary Systems at Third Post-Minkowskian Order*, *Phys. Rev. Lett.* **122** (2019) 201603, [1901.04424].

[40] N. E. J. Bjerrum-Bohr, J. F. Donoghue and P. Vanhove, *On-shell Techniques and Universal Results in Quantum Gravity*, *JHEP* **02** (2014) 111, [1309.0804].

[41] N. E. J. Bjerrum-Bohr, J. F. Donoghue, B. R. Holstein, L. Planté and P. Vanhove, *Bending of Light in Quantum Gravity*, *Phys. Rev. Lett.* **114** (2015) 061301, [1410.7590].

[42] A. Luna, R. Monteiro, I. Nicholson, D. O'Connell and C. D. White, *The double copy: Bremsstrahlung and accelerating black holes*, *JHEP* **06** (2016) 023, [1603.05737].

[43] T. Damour, *Gravitational scattering, post-Minkowskian approximation and Effective One-Body theory*, *Phys. Rev.* **D94** (2016) 104015, [1609.00354].

[44] W. D. Goldberger and A. K. Ridgway, *Radiation and the classical double copy for color charges*, *Phys. Rev. D* **95** (2017) 125010, [1611.03493].

[45] F. Cachazo and A. Guevara, *Leading Singularities and Classical Gravitational Scattering*, *JHEP* **02** (2020) 181, [1705.10262].

[46] A. Guevara, *Holomorphic Classical Limit for Spin Effects in Gravitational and Electromagnetic Scattering*, *JHEP* **04** (2019) 033, [1706.02314].

[47] T. Damour, *High-energy gravitational scattering and the general relativistic two-body problem*, *Phys. Rev.* **D97** (2018) 044038, [1710.10599].

[48] A. Luna, I. Nicholson, D. O'Connell and C. D. White, *Inelastic Black Hole Scattering from Charged Scalar Amplitudes*, *JHEP* **03** (2018) 044, [1711.03901].

[49] D. A. Kosower, B. Maybee and D. O'Connell, *Amplitudes, Observables, and Classical Scattering*, *JHEP* **02** (2019) 137, [1811.10950].

[50] B. Maybee, D. O'Connell and J. Vines, *Observables and amplitudes for spinning particles and black holes*, *JHEP* **12** (2019) 156, [1906.09260].

[51] R. Aoude and A. Ochirov, *Classical observables from coherent-spin amplitudes*, *JHEP* **10** (2021) 008, [2108.01649].

[52] A. Laddha and A. Sen, *Gravity Waves from Soft Theorem in General Dimensions*, *JHEP* **09** (2018) 105, [1801.07719].

[53] A. Laddha and A. Sen, *Observational Signature of the Logarithmic Terms in the Soft Graviton Theorem*, *Phys. Rev. D* **100** (2019) 024009, [1806.01872].

[54] N. E. J. Bjerrum-Bohr, P. H. Damgaard, G. Festuccia, L. Planté and P. Vanhove, *General Relativity from Scattering Amplitudes*, *Phys. Rev. Lett.* **121** (2018) 171601, [1806.04920].

[55] A. Cristofoli, N. E. J. Bjerrum-Bohr, P. H. Damgaard and P. Vanhove, *Post-Minkowskian Hamiltonians in general relativity*, *Phys. Rev. D* **100** (2019) 084040, [1906.01579].

[56] A. Guevara, A. Ochirov and J. Vines, *Black-hole scattering with general spin directions from minimal-coupling amplitudes*, *Phys. Rev. D* **100** (2019) 104024, [1906.10071].

[57] G. Kälin and R. A. Porto, *From Boundary Data to Bound States*, *JHEP* **01** (2020) 072, [1910.03008].

[58] G. Kälin and R. A. Porto, *From boundary data to bound states. Part II. Scattering angle to dynamical invariants (with twist)*, *JHEP* **02** (2020) 120, [1911.09130].

[59] D. Bini, T. Damour and A. Geralico, *Sixth post-Newtonian nonlocal-in-time dynamics of binary systems*, *Phys. Rev. D* **102** (2020) 084047, [2007.11239].

[60] R. Aoude, K. Haddad and A. Helset, *On-shell heavy particle effective theories*, *JHEP* **05** (2020) 051, [2001.09164].

[61] C. Cheung and M. P. Solon, *Classical gravitational scattering at $\mathcal{O}(G^3)$ from Feynman diagrams*, *JHEP* **06** (2020) 144, [2003.08351].

[62] C. Cheung and M. P. Solon, *Tidal Effects in the Post-Minkowskian Expansion*, *Phys. Rev. Lett.* **125** (2020) 191601, [2006.06665].

[63] G. Kälin, Z. Liu and R. A. Porto, *Conservative Dynamics of Binary Systems to Third Post-Minkowskian Order from the Effective Field Theory Approach*, *Phys. Rev. Lett.* **125** (2020) 261103, [2007.04977].

[64] K. Haddad and A. Helset, *Tidal effects in quantum field theory*, *JHEP* **12** (2020) 024, [2008.04920].

[65] G. Kälin, Z. Liu and R. A. Porto, *Conservative Tidal Effects in Compact Binary Systems to Next-to-Leading Post-Minkowskian Order*, *Phys. Rev. D* **102** (2020) 124025, [2008.06047].

[66] P. Di Vecchia, C. Heissenberg, R. Russo and G. Veneziano, *Universality of ultra-relativistic gravitational scattering*, *Phys. Lett. B* **811** (2020) 135924, [2008.12743].

[67] Z. Bern, J. Parra-Martinez, R. Roiban, E. Sawyer and C.-H. Shen, *Leading Nonlinear Tidal Effects and Scattering Amplitudes*, 2010.08559.

[68] M. Accettulli Huber, A. Brandhuber, S. De Angelis and G. Travaglini, *From amplitudes to gravitational radiation with cubic interactions and tidal effects*, *Phys. Rev. D* **103** (2021) 045015, [2012.06548].

[69] LIGO Scientific, Virgo collaboration, B. P. Abbott et al., *GW151226: Observation of Gravitational Waves from a 22-Solar-Mass Binary Black Hole Coalescence*, *Phys. Rev. Lett.* **116** (2016) 241103, [1606.04855].

[70] LIGO Scientific, Virgo collaboration, B. P. Abbott et al., *GW170817: Observation of Gravitational Waves from a Binary Neutron Star Inspiral*, *Phys. Rev. Lett.* **119** (2017) 161101, [1710.05832].

[71] LIGO Scientific, Virgo collaboration, B. P. Abbott et al., *Observation of Gravitational Waves from a Binary Black Hole Merger*, *Phys. Rev. Lett.* **116** (2016) 061102, [1602.03837].

[72] LIGO Scientific, VIRGO, KAGRA collaboration, R. Abbott et al., *GWTC-3: Compact Binary Coalescences Observed by LIGO and Virgo During the Second Part of the Third Observing Run*, 2111.03606.

[73] KAGRA, LIGO Scientific, Virgo, VIRGO collaboration, B. P. Abbott et al., *Prospects for observing and localizing gravitational-wave transients with Advanced LIGO, Advanced Virgo and KAGRA*, *Living Rev. Rel.* **21** (2018) 3, [1304.0670].

[74] A. Brandhuber, G. Chen, G. Travaglini and C. Wen, *A new gauge-invariant double copy for heavy-mass effective theory*, *JHEP* **07** (2021) 047, [2104.11206].

[75] A. Brandhuber, G. Chen, G. Travaglini and C. Wen, *Classical gravitational scattering from a gauge-invariant double copy*, *JHEP* **10** (2021) 118, [2108.04216].

[76] T. Adamo and R. Gonzo, *Bethe-Salpeter equation for classical gravitational bound states*, 2212.13269.

[77] A. Herderschee, R. Roiban and F. Teng, *The sub-leading scattering waveform from amplitudes*, *To appear* (2023) .

[78] A. Brandhuber, G. Brown, G. Chen, S. De Angelis, J. K. Gowdy and G. Travaglini, *One-loop gravitational bremsstrahlung and waveforms from a heavy-mass effective field theory*, *To appear* (2023) .

[79] A. Georgoudis, C. Heissenberg and I. Vazquez-Holm, *One-loop five-point amplitude for classical scattering*, *To appear* (2023) .

[80] A. Antonelli, A. Buonanno, J. Steinhoff, M. van de Meent and J. Vines, *Energetics of two-body Hamiltonians in post-Minkowskian gravity*, *Phys. Rev.* **D99** (2019) 104004, [1901.07102].

[81] V. Kalogera et al., *The Next Generation Global Gravitational Wave Observatory: The Science Book*, 2111.06990.

[82] M. Khalil, A. Buonanno, J. Steinhoff and J. Vines, *Energetics and scattering of gravitational two-body systems at fourth post-Minkowskian order*, *Phys. Rev. D* **106** (2022) 024042, [2204.05047].

[83] A. Buonanno, M. Khalil, D. O'Connell, R. Roiban, M. P. Solon and M. Zeng, *Snowmass White Paper: Gravitational Waves and Scattering Amplitudes*, in *2022 Snowmass Summer Study*, 4, 2022, 2204.05194.

[84] K. G. Chetyrkin and F. V. Tkachov, *Integration by Parts: The Algorithm to Calculate beta Functions in 4 Loops*, *Nucl. Phys. B* **192** (1981) 159–204.

[85] J. M. Henn, *Lectures on differential equations for Feynman integrals*, *J. Phys. A* **48** (2015) 153001, [1412.2296].

[86] J. M. Henn, *Multiloop integrals in dimensional regularization made simple*, *Phys. Rev. Lett.* **110** (2013) 251601, [1304.1806].

[87] Z. Bern and D. A. Kosower, *The Computation of loop amplitudes in gauge theories*, *Nucl. Phys. B* **379** (1992) 451–561.

[88] Z. Bern, L. J. Dixon, D. C. Dunbar and D. A. Kosower, *Fusing gauge theory tree amplitudes into loop amplitudes*, *Nucl. Phys. B* **435** (1995) 59–101, [hep-ph/9409265].

[89] Z. Bern, L. J. Dixon, D. C. Dunbar and D. A. Kosower, *One loop n point gauge theory amplitudes, unitarity and collinear limits*, *Nucl. Phys. B* **425** (1994) 217–260, [hep-ph/9403226].

[90] N. Arkani-Hamed, T.-C. Huang and Y.-t. Huang, *Scattering Amplitudes For All Masses and Spins*, 1709.04891.

[91] R. Britto, F. Cachazo, B. Feng and E. Witten, *Direct proof of tree-level recursion relation in Yang-Mills theory*, *Phys. Rev. Lett.* **94** (2005) 181602, [hep-th/0501052].

[92] Z. Bern, J. Parra-Martinez, R. Roiban, M. S. Ruf, C.-H. Shen, M. P. Solon et al., *Scattering amplitudes and conservative dynamics at the fourth post-Minkowskian order*, *PoS* **LL2022** (2022) 051.

[93] H. Kawai, D. C. Lewellen and S. H. H. Tye, *A Relation Between Tree Amplitudes of Closed and Open Strings*, *Nucl. Phys. B* **269** (1986) 1–23.

[94] Z. Bern, J. J. M. Carrasco and H. Johansson, *New Relations for Gauge-Theory Amplitudes*, *Phys. Rev.* **D78** (2008) 085011, [0805.3993].

[95] R. Monteiro, D. O'Connell and C. D. White, *Black holes and the double copy*, *JHEP* **12** (2014) 056, [1410.0239].

[96] F. Febres Cordero, M. Kraus, G. Lin, M. S. Ruf and M. Zeng, *Conservative Binary Dynamics with a Spinning Black Hole at O(G3) from Scattering Amplitudes*, *Phys. Rev. Lett.* **130** (2023) 021601, [2205.07357].

[97] E. Newman and R. Penrose, *An Approach to gravitational radiation by a method of spin coefficients*, *J. Math. Phys.* **3** (1962) 566–578.

[98] A. Luna, R. Monteiro, I. Nicholson and D. O'Connell, *Type D Spacetimes and the Weyl Double Copy*, *Class. Quant. Grav.* **36** (2019) 065003, [1810.08183].

[99] M. Boyle et al., *The SXS Collaboration catalog of binary black hole simulations*, *Class. Quant. Grav.* **36** (2019) 195006, [1904.04831].

[100] L. D. Landau and E. M. Lifschits, *The Classical Theory of Fields*, vol. Volume 2 of *Course of Theoretical Physics*. Pergamon Press, Oxford, 1975.

[101] B. R. Holstein and J. F. Donoghue, *Classical Physics and Quantum Loops*, *Phys. Rev. Lett.* **93** (2004) 201602, [hep-th/0405239].

[102] Z. Bern, J. J. M. Carrasco and H. Johansson, *Perturbative Quantum Gravity as a Double Copy of Gauge Theory*, *Phys. Rev. Lett.* **105** (2010) 061602, [1004.0476].

[103] H. Kawai, D. Lewellen and S. Tye, *A Relation Between Tree Amplitudes of Closed and Open Strings*, *Nucl. Phys. B* **269** (1986) 1–23.

[104] J. J. M. Carrasco and I. A. Vazquez-Holm, *Extracting Einstein from the loop-level double-copy*, *JHEP* **11** (2021) 088, [2108.06798].

[105] A. Luna, R. Monteiro, I. Nicholson, A. Ochirov, D. O'Connell, N. Westerberg et al., *Perturbative spacetimes from Yang-Mills theory*, *JHEP* **04** (2017) 069, [1611.07508].

[106] H. Johansson and A. Ochirov, *Pure Gravities via Color-Kinematics Duality for Fundamental Matter*, *JHEP* **11** (2015) 046, [1407.4772].

[107] N. Arkani-Hamed, Y.-t. Huang and D. O'Connell, *Kerr black holes as elementary particles*, *JHEP* **01** (2020) 046, [1906.10100].

[108] Z. Bern, J. J. Carrasco, M. Chiodaroli, H. Johansson and R. Roiban, *The Duality Between Color and Kinematics and its Applications*, 1909.01358.

[109] M. Ben-Shahar and H. Johansson, *Off-shell color-kinematics duality for Chern-Simons*, *JHEP* **08** (2022) 035, [2112.11452].

[110] R. Monteiro and D. O'Connell, *The Kinematic Algebra From the Self-Dual Sector*, *JHEP* **07** (2011) 007, [1105.2565].

[111] H. Stephani, D. Kramer, M. A. H. MacCallum, C. Hoenselaers and E. Herlt, *Exact solutions of Einstein's field equations.* Cambridge Monographs on Mathematical Physics. Cambridge Univ. Press, Cambridge, 2003, 10.1017/CBO9780511535185.

[112] A. Luna, R. Monteiro, D. O'Connell and C. D. White, *The classical double copy for Taub–NUT spacetime*, *Phys. Lett.* **B750** (2015) 272–277, [1507.01869].

[113] G. Cardoso, S. Nagy and S. Nampuri, *A double copy for $\mathcal{N} = 2$ supergravity: a linearised tale told on-shell*, *JHEP* **10** (2016) 127, [1609.05022].

[114] T. Adamo, E. Casali, L. Mason and S. Nekovar, *Scattering on plane waves and the double copy*, *Class. Quant. Grav.* **35** (2018) 015004, [1706.08925].

[115] A. Anastasiou, L. Borsten, M. J. Duff, S. Nagy and M. Zoccali, *Gravity as Gauge Theory Squared: A Ghost Story*, *Phys. Rev. Lett.* **121** (2018) 211601, [1807.02486].

[116] K. Lee, *Kerr-Schild Double Field Theory and Classical Double Copy*, *JHEP* **10** (2018) 027, [1807.08443].

[117] J. Plefka, J. Steinhoff and W. Wormsbecher, *Effective action of dilaton gravity as the classical double copy of Yang-Mills theory*, *Phys. Rev. D* **99** (2019) 024021, [1807.09859].

[118] W. Cho and K. Lee, *Heterotic Kerr-Schild Double Field Theory and Classical Double Copy*, *JHEP* **07** (2019) 030, [1904.11650].

[119] H. Godazgar, M. Godazgar and C. Pope, *Taub-NUT from the Dirac monopole*, *Phys. Lett. B* **798** (2019) 134938, [1908.05962].

[120] I. Bah, R. Dempsey and P. Weck, *Kerr-Schild Double Copy and Complex Worldlines*, *JHEP* **02** (2020) 180, [1910.04197].

[121] R. Alawadhi, D. S. Berman, B. Spence and D. Peinador Veiga, *S-duality and the double copy*, *JHEP* **03** (2020) 059, [1911.06797].

[122] W. D. Goldberger and J. Li, *Strings, extended objects, and the classical double copy*, *JHEP* **02** (2020) 092, [1912.01650].

[123] A. Luna, S. Nagy and C. D. White, *The convolutional double copy: a case study with a point*, 2004.11254.

[124] A. Cristofoli, *Gravitational shock waves and scattering amplitudes*, *JHEP* **11** (2020) 160, [2006.08283].

[125] T. Adamo, A. Cristofoli and A. Ilderton, *Classical physics from amplitudes on curved backgrounds*, *JHEP* **08** (2022) 281, [2203.13785].

[126] L. Borsten and S. Nagy, *The pure BRST Einstein-Hilbert Lagrangian from the double-copy to cubic order*, *JHEP* **07** (2020) 093, [2004.14945].

[127] E. Chacón, H. García-Compeán, A. Luna, R. Monteiro and C. D. White, *New heavenly double copies*, 2008.09603.

[128] H. Godazgar, M. Godazgar, R. Monteiro, D. Peinador Veiga and C. Pope, *The Weyl Double Copy for Gravitational Waves*, 2010.02925.

[129] C. D. White, *Twistorial Foundation for the Classical Double Copy*, *Phys. Rev. Lett.* **126** (2021) 061602, [2012.02479].

[130] D. S. Berman, K. Kim and K. Lee, *The classical double copy for M-theory from a Kerr-Schild ansatz for exceptional field theory*, *JHEP* **04** (2021) 071, [2010.08255].

[131] E. Lescano and J. A. Rodríguez, *$\mathcal{N} = 1$ supersymmetric Double Field Theory and the generalized Kerr-Schild ansatz*, *JHEP* **10** (2020) 148, [2002.07751].

[132] A. K. Ridgway and M. B. Wise, *Static Spherically Symmetric Kerr-Schild Metrics and Implications for the Classical Double Copy*, *Phys. Rev.* **D94** (2016) 044023, [1512.02243].

[133] C. D. White, *Exact solutions for the biadjoint scalar field*, *Phys. Lett. B* **763** (2016) 365–369, [1606.04724].

[134] W. D. Goldberger, S. G. Prabhu and J. O. Thompson, *Classical gluon and graviton radiation from the bi-adjoint scalar double copy*, *Phys. Rev.* **D96** (2017) 065009, [1705.09263].

[135] W. D. Goldberger and A. K. Ridgway, *Bound states and the classical double copy*, *Phys. Rev. D* **97** (2018) 085019, [1711.09493].

[136] N. Bahjat-Abbas, A. Luna and C. D. White, *The Kerr-Schild double copy in curved spacetime*, *JHEP* **12** (2017) 004, [1710.01953].

[137] C.-H. Shen, *Gravitational Radiation from Color-Kinematics Duality*, *JHEP* **11** (2018) 162, [1806.07388].

[138] A. Ilderton, *Screw-symmetric gravitational waves: a double copy of the vortex*, *Phys. Lett. B* **782** (2018) 22–27, [1804.07290].

[139] D. S. Berman, E. Chacón, A. Luna and C. D. White, *The self-dual classical double copy, and the Eguchi-Hanson instanton*, *JHEP* **01** (2019) 107, [1809.04063].

[140] N. Bahjat-Abbas, R. Stark-Muchão and C. D. White, *Biadjoint wires*, *Phys. Lett. B* **788** (2019) 274–279, [1810.08118].

[141] M. Gurses and B. Tekin, *Classical Double Copy: Kerr-Schild-Kundt metrics from Yang-Mills Theory*, *Phys. Rev. D* **98** (2018) 126017, [1810.03411].

[142] A. Luna, R. Monteiro, I. Nicholson and D. O'Connell, *Type D Spacetimes and the Weyl Double Copy*, *Class. Quant. Grav.* **36** (2019) 065003, [1810.08183].

[143] G. Cardoso, S. Nagy and S. Nampuri, *Multi-centered $\mathcal{N} = 2$ BPS black holes: a double copy description*, *JHEP* **04** (2017) 037, [1611.04409].

[144] K. Andrzejewski and S. Prencel, *From polarized gravitational waves to analytically solvable electromagnetic beams*, *Phys. Rev. D* **100** (2019) 045006, [1901.05255].

[145] J. Plefka, C. Shi, J. Steinhoff and T. Wang, *Breakdown of the classical double copy for the effective action of dilaton-gravity at NNLO*, *Phys. Rev. D* **100** (2019) 086006, [1906.05875].

[146] M. Carrillo González, B. Melcher, K. Ratliff, S. Watson and C. D. White, *The classical double copy in three spacetime dimensions*, 1904.11001.

[147] S. Sabharwal and J. W. Dalhuisen, *Anti-Self-Dual Spacetimes, Gravitational Instantons and Knotted Zeros of the Weyl Tensor*, *JHEP* **07** (2019) 004, [1904.06030].

[148] L. Borsten, I. Jubb, V. Makwana and S. Nagy, *Gauge $\times$ gauge on spheres*, *JHEP* **06** (2020) 096, [1911.12324].

[149] L. Borsten, H. Kim, B. Jur**c**o, T. Macrelli, C. Saemann and M. Wolf, *Double Copy from Homotopy Algebras*, *Fortsch. Phys.* **69** (2021) 2100075, [2102.11390].

[150] L. Borsten, I. Jubb, V. Makwana and S. Nagy, *Gauge $\times$ gauge = gravity on homogeneous spaces using tensor convolutions*, *JHEP* **06** (2021) 117, [2104.01135].

[151] N. Bahjat-Abbas, R. Stark-Muchão and C. D. White, *Monopoles, shockwaves and the classical double copy*, *JHEP* **04** (2020) 102, [2001.09918].

[152] G. Elor, K. Farnsworth, M. L. Graesser and G. Herczeg, *The Newman-Penrose Map and the Classical Double Copy*, 2006.08630.

[153] T. Adamo and A. Ilderton, *Classical and quantum double copy of back-reaction*, *JHEP* **09** (2020) 200, [2005.05807].

[154] L. Alfonsi, C. D. White and S. Wikeley, *Topology and Wilson lines: global aspects of the double copy*, *JHEP* **07** (2020) 091, [2004.07181].

[155] C. Keeler, T. Manton and N. Monga, *From Navier-Stokes to Maxwell via Einstein*, *JHEP* **08** (2020) 147, [2005.04242].

[156] D. A. Easson, C. Keeler and T. Manton, *Classical double copy of nonsingular black holes*, *Phys. Rev. D* **102** (2020) 086015, [2007.16186].

[157] D. A. Easson, T. Manton and A. Svesko, *Sources in the Weyl double copy*, 2110.02293.

[158] O. Pasarin and A. A. Tseytlin, *Generalised Schwarzschild metric from double copy of point-like charge solution in Born-Infeld theory*, *Phys. Lett. B* **807** (2020) 135594, [2005.12396].

[159] M. K. Gumus and G. Alkac, *More on the classical double copy in three spacetime dimensions*, *Phys. Rev. D* **102** (2020) 024074, [2006.00552].

[160] R. Alawadhi, D. S. Berman, C. D. White and S. Wikeley, *The single copy of the gravitational holonomy*, *JHEP* **10** (2021) 229, [2107.01114].

[161] E. Lescano and J. A. Rodríguez, *Higher-derivative heterotic Double Field Theory and classical double copy*, *JHEP* **07** (2021) 072, [2101.03376].

[162] S. Angus, K. Cho and K. Lee, *The classical double copy for half-maximal supergravities and T-duality*, *JHEP* **10** (2021) 211, [2105.12857].

[163] C. Cheung and J. Mangan, *Covariant color-kinematics duality*, *JHEP* **11** (2021) 069, [2108.02276].

[164] G. Alkac, M. K. Gumus and M. A. Olpak, *Kerr-Schild double copy of the Coulomb solution in three dimensions*, *Phys. Rev. D* **104** (2021) 044034, [2105.11550].

[165] P. Ferrero and D. Francia, *On the Lagrangian formulation of the double copy to cubic order*, *JHEP* **02** (2021) 213, [2012.00713].

[166] G. Alkac, M. K. Gumus and M. Tek, *The Kerr-Schild Double Copy in Lifshitz Spacetime*, *JHEP* **05** (2021) 214, [2103.06986].

[167] R. Gonzo and C. Shi, *Geodesics from classical double copy*, *Phys. Rev. D* **104** (2021) 105012, [2109.01072].

[168] R. Saotome and R. Akhoury, *Relationship Between Gravity and Gauge Scattering in the High Energy Limit*, *JHEP* **01** (2013) 123, [1210.8111].

[169] L. Borsten, B. Jur**c**o, H. Kim, T. Macrelli, C. Saemann and M. Wolf, *Becchi-Rouet-Stora-Tyutin-Lagrangian Double Copy of Yang-Mills Theory*, *Phys. Rev. Lett.* **126** (2021) 191601, [2007.13803].

[170] M. Campiglia and S. Nagy, *A double copy for asymptotic symmetries in the self-dual sector*, *JHEP* **03** (2021) 262, [2102.01680].

[171] H. Godazgar, M. Godazgar, R. Monteiro, D. Peinador Veiga and C. N. Pope, *Asymptotic Weyl double copy*, *JHEP* **11** (2021) 126, [2109.07866].

[172] C. Shi and J. Plefka, *Classical Double Copy of Worldline Quantum Field Theory*, 2109.10345.

[173] N. Moynihan, *Massive Covariant Colour-Kinematics in 3D*, 2110.02209.

[174] T. Adamo, A. Cristofoli, A. Ilderton and S. Klisch, *All-order waveforms from amplitudes*, 2210.04696.

[175] R. M. Wald, *General Relativity.* Chicago Univ. Pr., Chicago, USA, 1984, 10.7208/chicago/9780226870373.001.0001.

[176] R. J. Glauber, *Coherent and incoherent states of the radiation field*, *Phys. Rev.* **131** (1963) 2766–2788.

[177] P. Benincasa and F. Cachazo, *Consistency Conditions on the S-Matrix of Massless Particles*, 0705.4305.

[178] N. Arkani-Hamed, T.-C. Huang and Y.-t. Huang, *Scattering Amplitudes For All Masses and Spins*, 1709.04891.

[179] J. F. Donoghue, *Leading quantum correction to the Newtonian potential*, *Phys. Rev. Lett.* **72** (1994) 2996–2999, [gr-qc/9310024].

[180] J. F. Donoghue, *General relativity as an effective field theory: The leading quantum corrections*, *Phys. Rev.* **D50** (1994) 3874–3888, [gr-qc/9405057].

[181] R. Sachs, *Gravitational waves in general relativity. 6. The outgoing radiation condition*, *Proc. Roy. Soc. Lond. A* **264** (1961) 309–338.

[182] Z. Bern, J. J. Carrasco, M. Chiodaroli, H. Johansson and R. Roiban, *The Duality Between Color and Kinematics and its Applications*, 1909.01358.

[183] A. Anastasiou, L. Borsten, M. Duff, L. Hughes and S. Nagy, *Yang-Mills origin of gravitational symmetries*, *Phys. Rev. Lett.* **113** (2014) 231606, [1408.4434].

[184] Y. F. Bautista and A. Guevara, *On the Double Copy for Spinning Matter*, 1908.11349.

[185] K. Kim, K. Lee, R. Monteiro, I. Nicholson and D. Peinador Veiga, *The Classical Double Copy of a Point Charge*, *JHEP* **02** (2020) 046, [1912.02177].

[186] A. Banerjee, E. Colgáin, J. Rosabal and H. Yavartanoo, *Ehlers as EM duality in the double copy*, *Phys. Rev. D* **102** (2020) 126017, [1912.02597].

[187] R. Alawadhi, D. S. Berman and B. Spence, *Weyl doubling*, *JHEP* **09** (2020) 127, [2007.03264].

[188] S. G. Prabhu, *The classical double copy in curved spacetimes: Perturbative Yang-Mills from the bi-adjoint scalar*, 2011.06588.

[189] D. Amati, M. Ciafaloni and G. Veneziano, *Superstring Collisions at Planckian Energies*, *Phys. Lett. B* **197** (1987) 81.

[190] G. 't Hooft, *Graviton Dominance in Ultrahigh-Energy Scattering*, *Phys. Lett. B* **198** (1987) 61–63.

[191] I. Muzinich and M. Soldate, *High-Energy Unitarity of Gravitation and Strings*, *Phys. Rev. D* **37** (1988) 359.

[192] D. Amati, M. Ciafaloni and G. Veneziano, *Classical and Quantum Gravity Effects from Planckian Energy Superstring Collisions*, *Int. J. Mod. Phys. A* **3** (1988) 1615–1661.

[193] D. Amati, M. Ciafaloni and G. Veneziano, *Higher Order Gravitational Deflection and Soft Bremsstrahlung in Planckian Energy Superstring Collisions*, *Nucl. Phys. B* **347** (1990) 550–580.

[194] D. Amati, M. Ciafaloni and G. Veneziano, *Planckian scattering beyond the semiclassical approximation*, *Phys. Lett. B* **289** (1992) 87–91.

[195] D. N. Kabat and M. Ortiz, *Eikonal quantum gravity and Planckian scattering*, *Nucl. Phys. B* **388** (1992) 570–592, [hep-th/9203082].

[196] E. Laenen, G. Stavenga and C. D. White, *Path integral approach to eikonal and next-to-eikonal exponentiation*, *JHEP* **03** (2009) 054, [0811.2067].

[197] G. D'Appollonio, P. Di Vecchia, R. Russo and G. Veneziano, *High-energy string-brane scattering: Leading eikonal and beyond*, *JHEP* **11** (2010) 100, [1008.4773].

[198] S. Melville, S. G. Naculich, H. J. Schnitzer and C. D. White, *Wilson line approach to gravity in the high energy limit*, *Phys. Rev. D* **89** (2014) 025009, [1306.6019].

[199] R. Akhoury, R. Saotome and G. Sterman, *High Energy Scattering in Perturbative Quantum Gravity at Next to Leading Power*, *Phys. Rev. D* **103** (2021) 064036, [1308.5204].

[200] A. Luna, S. Melville, S. G. Naculich and C. D. White, *Next-to-soft corrections to high energy scattering in QCD and gravity*, *JHEP* **01** (2017) 052, [1611.02172].

[201] N. E. J. Bjerrum-Bohr, B. R. Holstein, J. F. Donoghue, L. Planté and P. Vanhove, *Illuminating Light Bending*, *PoS* **CORFU2016** (2017) 077, [1704.01624].

[202] A. K. Collado, P. Di Vecchia, R. Russo and S. Thomas, *The subleading eikonal in supergravity theories*, *JHEP* **10** (2018) 038, [1807.04588].

[203] A. Koemans Collado, P. Di Vecchia and R. Russo, *Revisiting the second post-Minkowskian eikonal and the dynamics of binary black holes*, *Phys. Rev. D* **100** (2019) 066028, [1904.02667].

[204] N. E. J. Bjerrum-Bohr, A. Cristofoli and P. H. Damgaard, *Post-Minkowskian Scattering Angle in Einstein Gravity*, *JHEP* **08** (2020) 038, [1910.09366].

[205] P. Di Vecchia, A. Luna, S. G. Naculich, R. Russo, G. Veneziano and C. D. White, *A tale of two exponentiations in $\mathcal{N} = 8$ supergravity*, *Phys. Lett. B* **798** (2019) 134927, [1908.05603].

[206] P. Di Vecchia, S. G. Naculich, R. Russo, G. Veneziano and C. D. White, *A tale of two exponentiations in $\mathcal{N} = 8$ supergravity at subleading level*, *JHEP* **03** (2020) 173, [1911.11716].

[207] A. Parnachev and K. Sen, *Notes on AdS-Schwarzschild eikonal phase*, 2011.06920.

[208] M. J. Duff, *Quantum Tree Graphs and the Schwarzschild Solution*, *Phys. Rev.* **D7** (1973) 2317–2326.

[209] G. U. Jakobsen, *Schwarzschild-Tangherlini Metric from Scattering Amplitudes*, *Phys. Rev. D* **102** (2020) 104065, [2006.01734].

[210] K. Cho, K. Kim and K. Lee, *The Off-Shell Recursion for Gravity and the Classical Double Copy for currents*, 2109.06392.

[211] F. Diaz-Jaramillo, O. Hohm and J. Plefka, *Double Field Theory as the Double Copy of Yang-Mills*, 2109.01153.

[212] R. Penrose, *Spinors and torsion in general relativity*, *Found. Phys.* **13** (1983) 325–339.

[213] Y.-T. Huang, U. Kol and D. O'Connell, *Double copy of electric-magnetic duality*, *Phys. Rev. D* **102** (2020) 046005, [1911.06318].

[214] A. Guevara, B. Maybee, A. Ochirov, D. O'Connell and J. Vines, *A worldsheet for Kerr*, *JHEP* **03** (2021) 201, [2012.11570].

[215] A. I. Janis, E. T. Newman and J. Winicour, *Reality of the Schwarzschild Singularity*, *Phys. Rev. Lett.* **20** (1968) 878–880.

[216] J. Vines, *Scattering of two spinning black holes in post-Minkowskian gravity, to all orders in spin, and effective-one-body mappings*, *Class. Quant. Grav.* **35** (2018) 084002, [1709.06016].

[217] C. P. Burgess, R. C. Myers and F. Quevedo, *On spherically symmetric string solutions in four-dimensions*, *Nucl. Phys. B* **442** (1995) 75–96, [hep-th/9410142].

[218] I. Bogush and D. Gal'tsov, *Generation of rotating solutions in Einstein-scalar gravity*, *Phys. Rev. D* **102** (2020) 124006, [2001.02936].

[219] N. E. J. Bjerrum-Bohr, J. F. Donoghue and P. Vanhove, *On-shell Techniques and Universal Results in Quantum Gravity*, *JHEP* **02** (2014) 111, [1309.0804].

[220] N. E. J. Bjerrum-Bohr, J. F. Donoghue, B. R. Holstein, L. Plante and P. Vanhove, *Light-like Scattering in Quantum Gravity*, *JHEP* **11** (2016) 117, [1609.07477].

[221] N. E. J. Bjerrum-Bohr, P. H. Damgaard, G. Festuccia, L. Planté and P. Vanhove, *General Relativity from Scattering Amplitudes*, *Phys. Rev. Lett.* **121** (2018) 171601, [1806.04920].

[222] A. Guevara, A. Ochirov and J. Vines, *Scattering of Spinning Black Holes from Exponentiated Soft Factors*, *JHEP* **09** (2019) 056, [1812.06895].

[223] N. E. J. Bjerrum-Bohr, P. H. Damgaard, L. Planté and P. Vanhove, *Classical gravity from loop amplitudes*, *Phys. Rev. D* **104** (2021) 026009, [2104.04510].

[224] N. E. J. Bjerrum-Bohr, P. H. Damgaard, L. Planté and P. Vanhove, *The Amplitude for Classical Gravitational Scattering at Third Post-Minkowskian Order*, 2105.05218.

[225] A. Brandhuber, G. Chen, H. Johansson, G. Travaglini and C. Wen, *Kinematic Hopf Algebra for Bern-Carrasco-Johansson Numerators in Heavy-Mass Effective Field Theory and Yang-Mills Theory*, *Phys. Rev. Lett.* **128** (2022) 121601, [2111.15649].

[226] G. Cho, R. A. Porto and Z. Yang, *Gravitational radiation from inspiralling compact objects: Spin effects to fourth Post-Newtonian order*, 2201.05138.

[227] Z. Bern, D. Kosmopoulos, A. Luna, R. Roiban and F. Teng, *Binary Dynamics Through the Fifth Power of Spin at $\mathcal{O}(G^2)$*, 2203.06202.

[228] W.-M. Chen, M.-Z. Chung, Y.-t. Huang and J.-W. Kim, *The 2PM Hamiltonian for binary Kerr to quartic in spin*, 2111.13639.

[229] F. Alessio and P. Di Vecchia, *Radiation reaction for spinning black-hole scattering*, 2203.13272.

[230] G. U. Jakobsen, G. Mogull, J. Plefka and J. Steinhoff, *Classical Gravitational Bremsstrahlung from a Worldline Quantum Field Theory*, *Phys. Rev. Lett.* **126** (2021) 201103, [2101.12688].

[231] G. Travaglini et al., *The SAGEX Review on Scattering Amplitudes*, 2203.13011.

[232] D. A. Kosower, R. Monteiro and D. O'Connell, *The SAGEX Review on Scattering Amplitudes, Chapter 14: Classical Gravity from Scattering Amplitudes*, 2203.13025.

[233] N. Isgur and M. B. Wise, *Weak Decays of Heavy Mesons in the Static Quark Approximation*, *Phys. Lett. B* **232** (1989) 113–117.

[234] H. Georgi, *An Effective Field Theory for Heavy Quarks at Low-energies*, *Phys. Lett. B* **240** (1990) 447–450.

[235] M. E. Luke and A. V. Manohar, *Reparametrization invariance constraints on heavy particle effective field theories*, *Phys. Lett. B* **286** (1992) 348–354, [hep-ph/9205228].

[236] M. Neubert, *Heavy quark symmetry*, *Phys. Rept.* **245** (1994) 259–396, [hep-ph/9306320].

[237] A. V. Manohar and M. B. Wise, *Heavy quark physics*, vol. 10. 2000.

[238] P. H. Damgaard, K. Haddad and A. Helset, *Heavy Black Hole Effective Theory*, *JHEP* **11** (2019) 070, [1908.10308].

[239] G. 't Hooft and M. J. G. Veltman, *DIAGRAMMAR*, *NATO Sci. Ser. B* **4** (1974) 177–322.

[240] G. F. Sterman, *An Introduction to quantum field theory*. Cambridge University Press, 8, 1993.

[241] M. Srednicki, *Quantum field theory*. Cambridge University Press, 1, 2007.

[242] M. D. Schwartz, *Quantum Field Theory and the Standard Model*. Cambridge University Press, 3, 2014.

[243] R. Aoude, K. Haddad and A. Helset, *Searching for Kerr in the 2PM amplitude*, *JHEP* **07** (2022) 072, [2203.06197].

[244] N. E. J. Bjerrum-Bohr, G. Chen and M. Skowronek, *Classical Spin Gravitational Compton Scattering*, 2302.00498.

[245] L. Cangemi, M. Chiodaroli, H. Johansson, A. Ochirov, P. Pichini and E. Skvortsov, *Kerr Black Holes Enjoy Massive Higher-Spin Gauge Symmetry*, 2212.06120.

[246] Z. Bern, D. Kosmopoulos, A. Luna, R. Roiban and F. Teng, *Binary Dynamics Through the Fifth Power of Spin at $\mathcal{O}(G^2)$*, 2203.06202.

[247] Y. F. Bautista, A. Guevara, C. Kavanagh and J. Vinese, *Scattering in Black Hole Backgrounds and Higher-Spin Amplitudes: Part II*, 2212.07965.

[248] C. Cheung and D. O'Connell, *Amplitudes and Spinor-Helicity in Six Dimensions*, *JHEP* **07** (2009) 075, [0902.0981].

[249] C. Dlapa, G. Kälin, Z. Liu, J. Neef and R. A. Porto, *Radiation Reaction and Gravitational Waves at Fourth Post-Minkowskian Order*, 2210.05541.

[250] Z. Bern, *Perturbative quantum gravity and its relation to gauge theory*, *Living Rev. Rel.* **5** (2002) 5, [gr-qc/0206071].

[251] Y. Mino, M. Sasaki and T. Tanaka, *Gravitational radiation reaction to a particle motion*, *Phys. Rev. D* **55** (1997) 3457–3476, [gr-qc/9606018].

[252] T. C. Quinn and R. M. Wald, *An Axiomatic approach to electromagnetic and gravitational radiation reaction of particles in curved space-time*, *Phys. Rev. D* **56** (1997) 3381–3394, [gr-qc/9610053].

[253] S. Weinberg, *Infrared photons and gravitons*, *Phys. Rev.* **140** (1965) B516–B524.

[254] C. Heissenberg, *Infrared divergences and the eikonal exponentiation*, *Phys. Rev. D* **104** (2021) 046016, [2105.04594].

[255] W. D. Goldberger and A. Ross, *Gravitational radiative corrections from effective field theory*, *Phys. Rev. D* **81** (2010) 124015, [0912.4254].

[256] R. A. Porto, A. Ross and I. Z. Rothstein, *Spin induced multipole moments for the gravitational wave amplitude from binary inspirals to 2.5 Post-Newtonian order*, *JCAP* **09** (2012) 028, [1203.2962].

[257] L. de la Cruz, A. Luna and T. Scheopner, *Yang-Mills observables: from KMOC to eikonal through EFT*, *JHEP* **01** (2022) 045, [2108.02178].

[258] Z. Bern, J. P. Gatica, E. Herrmann, A. Luna and M. Zeng, *Scalar QED as a toy model for higher-order effects in classical gravitational scattering*, *JHEP* **08** (2022) 131, [2112.12243].

[259] N. E. J. Bjerrum-Bohr, J. F. Donoghue and B. R. Holstein, *Quantum corrections to the Schwarzschild and Kerr metrics*, *Phys. Rev. D* **68** (2003) 084005, [hep-th/0211071].

[260] R. Torgerson, *Field-theoretic formulation of the optical model at high energies*, *Phys. Rev.* **143** (Mar, 1966) 1194–1215.

[261] H. D. I. Abarbanel and C. Itzykson, *Relativistic eikonal expansion*, *Phys. Rev. Lett.* **23** (1969) 53.

[262] H. Cheng and T. T. Wu, *High-energy elastic scattering in quantum electrodynamics*, *Phys. Rev. Lett.* **22** (1969) 666.

[263] H. Cheng and T. T. Wu, *Impact factor and exponentiation in high-energy scattering processes*, *Phys. Rev.* **186** (Oct, 1969) 1611–1618.

[264] S. J. Wallace, *Eikonal expansion*, *Annals of Physics* **78** (1973) 190–257.

[265] M. Lévy and J. Sucher, *Eikonal approximation in quantum field theory*, *Phys. Rev.* **186** (Oct, 1969) 1656–1670.

[266] S. J. Wallace and J. A. McNeil, *Relativistic Eikonal Expansion*, *Phys. Rev. D* **16** (1977) 3565.

[267] H. Cheng, J. Dickinson, P. Yeung and K. Olaussen, *Consequences of the eikonal formula*, *Physical Review D* **23** (1981) 1411–1420.

[268] R. Britto, R. Gonzo and G. Jehu, *Graviton particle statistics and coherent states from classical scattering amplitudes*, .

[269] D. A. Kosower, B. Maybee and D. O'Connell, *Amplitudes, Observables, and Classical Scattering*, *JHEP* **02** (2019) 137, [1811.10950].

[270] A. Laddha and A. Sen, *Logarithmic Terms in the Soft Expansion in Four Dimensions*, *JHEP* **10** (2018) 056, [1804.09193].

[271] B. Sahoo and A. Sen, *Classical and Quantum Results on Logarithmic Terms in the Soft Theorem in Four Dimensions*, *JHEP* **02** (2019) 086, [1808.03288].

[272] Y. F. Bautista and A. Guevara, *From Scattering Amplitudes to Classical Physics: Universality, Double Copy and Soft Theorems*, 1903.12419.

[273] A. Laddha and A. Sen, *Classical proof of the classical soft graviton theorem in D>4*, *Phys. Rev. D* **101** (2020) 084011, [1906.08288].

[274] A. P. Saha, B. Sahoo and A. Sen, *Proof of the classical soft graviton theorem in $D = 4$*, *JHEP* **06** (2020) 153, [1912.06413].

[275] B. Sahoo and A. Sen, *Classical Soft Graviton Theorem Rewritten*, 2105.08739.

[276] M. Ciafaloni, D. Colferai, F. Coradeschi and G. Veneziano, *Unified limiting form of graviton radiation at extreme energies*, *Phys. Rev. D* **93** (2016) 044052, [1512.00281].

[277] N. E. J. Bjerrum-Bohr, J. F. Donoghue, B. R. Holstein, L. Plante and P. Vanhove, *Light-like Scattering in Quantum Gravity*, *JHEP* **11** (2016) 117, [1609.07477].

[278] M. Ciafaloni, D. Colferai and G. Veneziano, *Infrared features of gravitational scattering and radiation in the eikonal approach*, *Phys. Rev. D* **99** (2019) 066008, [1812.08137].

[279] P. Di Vecchia, C. Heissenberg, R. Russo and G. Veneziano, *Radiation Reaction from Soft Theorems*, *Phys. Lett. B* **818** (2021) 136379, [2101.05772].

[280] K. Haddad, *Exponentiation of the leading eikonal with spin*, 2109.04427.

[281] P. H. Damgaard, L. Plante and P. Vanhove, *On an exponential representation of the gravitational S-matrix*, *JHEP* **11** (2021) 213, [2107.12891].

[282] W. T. Emond, N. Moynihan and L. Wei, *Quantization Conditions and the Double Copy*, 2109.11531.

[283] D. Amati, M. Ciafaloni and G. Veneziano, *Towards an S-matrix description of gravitational collapse*, *JHEP* **02** (2008) 049, [0712.1209].

[284] I. A. Korchemskaya and G. P. Korchemsky, *High-energy scattering in QCD and cross singularities of Wilson loops*, *Nucl. Phys. B* **437** (1995) 127–162, [hep-ph/9409446].

[285] E. Laenen, L. Magnea, G. Stavenga and C. D. White, *Next-to-Eikonal Corrections to Soft Gluon Radiation: A Diagrammatic Approach*, *JHEP* **01** (2011) 141, [1010.1860].

[286] C. D. White, *Factorization Properties of Soft Graviton Amplitudes*, *JHEP* **05** (2011) 060, [1103.2981].

[287] C. D. White, *An Introduction to Webs*, *J. Phys. G* **43** (2016) 033002, [1507.02167].

[288] A. Koemans Collado, P. Di Vecchia, R. Russo and S. Thomas, *The subleading eikonal in supergravity theories*, *JHEP* **10** (2018) 038, [1807.04588].

[289] M. Ciafaloni and D. Colferai, *Rescattering corrections and self-consistent metric in Planckian scattering*, *JHEP* **10** (2014) 085, [1406.6540].

[290] U. Kol, D. O'Connell and O. Telem, *The radial action from probe amplitudes to all orders*, *JHEP* **03** (2022) 141, [2109.12092].

[291] W. D. Goldberger and I. Z. Rothstein, *An Effective field theory of gravity for extended objects*, *Phys. Rev. D* **73** (2006) 104029, [hep-th/0409156].

[292] S. Mougiakakos, M. M. Riva and F. Vernizzi, *Gravitational Bremsstrahlung in the post-Minkowskian effective field theory*, *Phys. Rev. D* **104** (2021) 024041, [2102.08339].

[293] G. U. Jakobsen, G. Mogull, J. Plefka and J. Steinhoff, *Gravitational Bremsstrahlung and Hidden Supersymmetry of Spinning Bodies*, 2106.10256.

[294] G. U. Jakobsen, G. Mogull, J. Plefka and J. Steinhoff, *SUSY in the Sky with Gravitons*, 2109.04465.

[295] K. Watanabe, *Integral transform techniques for green's function.* Springer.